OCS Study
BOEM 2022-029

Characteristics and Contributions of Noise Generated by Mechanical Cutting During Conductor Removal Operations

Volume 3: Appendices B – F

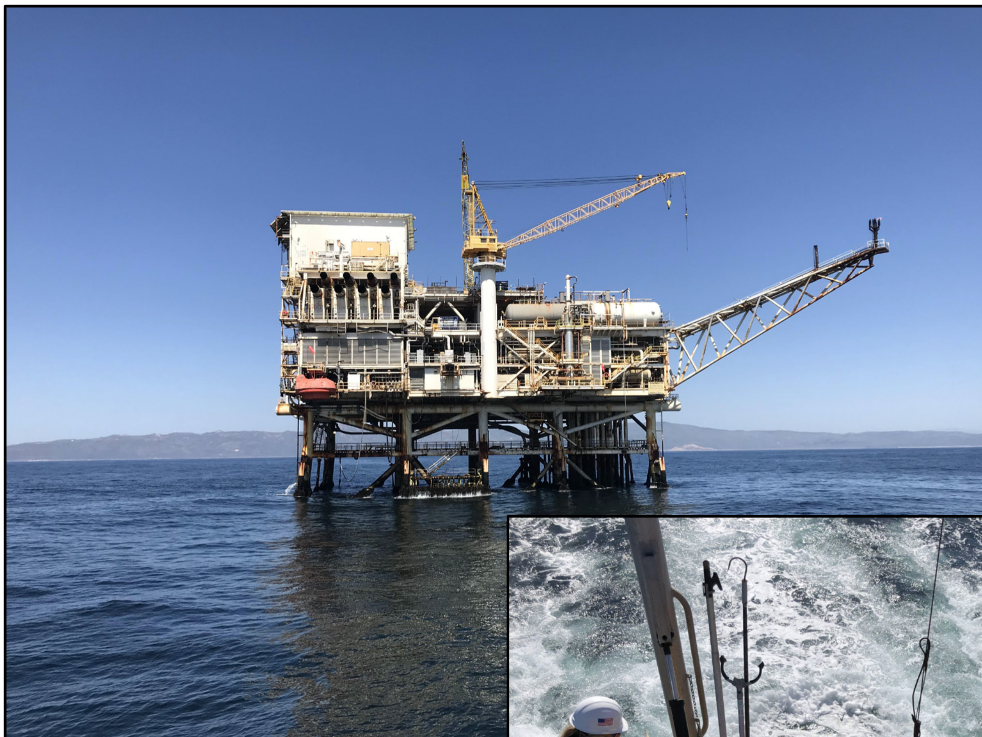

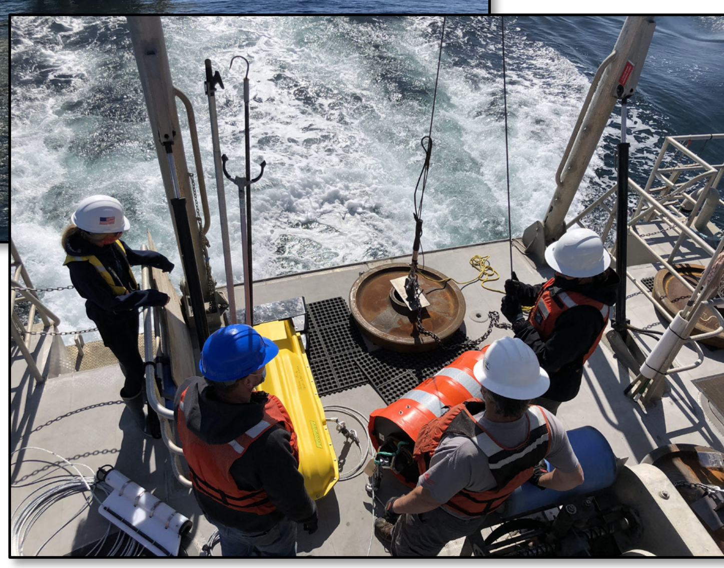

U.S. Department of the Interior
Bureau of Ocean Energy Management
Pacific OCS Region, Camarillo, CA

BOEM
Bureau of Ocean Energy Management

OCS Study
BOEM 2022-029

Characteristics and Contributions of Noise Generated by Mechanical Cutting During Conductor Removal Operations

Volume 3: Appendices B – F

June 2022

Authors:
Kevin Fowler
Patricia Pellerin
Ann Zoidis

Prepared under Contract No. 140M0120C0011
By:
Tetra Tech, Inc.
10 Post Office Square
Suite 1100
Boston, MA 02109

With support from Subcontractors:

Ocean Science Analytics	Integral Consulting Inc.
13328 Sparren Avenue	200 Washington Street, Suite 201
San Diego, CA 92129	Santa Cruz, CA 95060

U.S. Department of the Interior
Bureau of Ocean Energy Management
Pacific OCS Region, Camarillo, CA

DISCLAIMER

Study concept, oversight, and funding were provided by the U.S. Department of the Interior, Bureau of Ocean Energy Management (BOEM), Environmental Studies Program, Washington D.C., under Contract Number 140M0120C0011. Additional funding was provided by the BOEM Pacific OCS Region and Gulf of Mexico OCS Region. This report has been technically reviewed by BOEM, and it has been approved for publication. The views and conclusions contained in this document are those of the authors and should not be interpreted as representing the opinions or policies of BOEM, nor does mention of trade names or commercial products constitute endorsement or recommendation for use.

REPORT AVAILABILITY

To download a PDF file of this report, go to the U.S. Department of the Interior, Bureau of Ocean Energy Management Data and Information Systems webpage (http://www.boem.gov/Environmental-Studies-EnvData/), click on the link for the Environmental Studies Program Information System (ESPIS), and search on 2022-029.

CITATION

Fowler K, Pellerin P, Zoidis A (Tetra Tech, Inc., Boston, MA). 2022. Characteristics and contributions of noise generated by mechanical cutting during conductor removal operations; Volume 3: Appendices B ─ F. Camarillo (CA): U.S. Department of the Interior, Bureau of Ocean Energy Management. 252 p. Report No.: OCS Study BOEM 2022-029. Contract No.: 140M0120C0011.

ABOUT THE COVER

Left photo: Photo of Platform Hermosa was taken by Kevin Fowler, Tetra Tech, Inc., during the deployment of the monitoring equipment on March 21, 2021. Right photo: Photo was taken by Kaus Raghukumar, Integral Consulting Inc., of the field team preparing to deploy the hydrophone moorings on March 21, 2021.

REPORT ORGANIZATION

Report OCS Study BOEM 2022-029 consists of three volumes:

Volume 1: Final Report
Volume 2: Appendix A: Final Field Plan
Volume 3: Appendices B ─ F
- Appendix B: Supplementary Acoustic Data
- Appendix C: Acoustic Analysis: Study Report A, Determination of Periods of Vocally Active Marine Mammals and Evaluation of Acoustic Indices
- Appendix D: Marine Mammal Acoustic Analysis: Study Report B, Development of a Deep Neural Network for Humpback Whales and Delphinids
- Appendix E: Noise Study Photo Log
- Appendix F: Hydrophone - Ocean Instruments Calibration Data

Volume 3: Appendices B – F

Contents

Appendix B: Supplementary Acoustic Data

Contents

List of Figures

List of Tables

B.1 Supplementary Acoustic Data

A total of 25 wells and empty conductors were cut with 40 cutting events. Tables B-1 and B-2 provide a summary of the measured sound levels from each of the mechanical cutting event measured during the study period. This appendix also provides measurement results for each individual cutting event. The SPL, SEL and Lpk are provide for the full duration of each event. The Max SPL and Min SPL are the maximum and minimum SPL levels that occurred during the event.

Table B-1. Mechanical Cutting Events Noise Data Summary

Conductor	Start Time	End Time	Direction	Monitor Station Name	Distance to Conductor (m)	L_p	Max L_p	Min L_p	$L_{p,pk}$	L_E
B-1	4/1/2021 17:06	4/1/2021 17:25	North	5362	156.31	121.8	124.6	112.7	144.5	150.7
			North	5363	156.31	121.3	126.3	111.6	143.4	152.1
			East	5366	114.62	123.8	127.9	107.9	149.8	154.5
			South	5365	116.82	122.1	126.6	108.3	149.4	152.8
			West	5356	141.16	120.6	124.8	110.2	143.8	151.4
			South	5353	274.72	116.9	120.3	107.4	141.2	147.6
	4/1/2021 18:01	4/1/2021 18:54	North	5362	156.31	123.9	130.8	111.7	154.0	158.9
			North	5363	156.31	124.2	130.2	111.4	155.8	159.2
			East	5366	114.62	128.0	135.2	108.5	156.5	163.0
			South	5365	116.82	126.5	133.3	108.4	156.5	161.6
			West	5356	141.16	124.6	131.6	110.3	152.9	159.7
			South	5353	274.72	120.5	126.5	106.7	147.4	155.6
	4/1/2021 22:05	4/2/2021 4:08	North	5362	156.31	124.8	143.8	108.5	160.8	168.2
			North	5363	156.31	126.0	145.0	109.9	165.7	169.4
			East	5366	114.62	126.7	143.3	106.4	166.4	170.1
			South	5365	116.82	124.5	141.7	106.8	162.9	167.9
			West	5356	141.16	124.4	141.1	109.2	166.0	167.8
			South	5353	274.72	122.1	137.9	106.2	157.6	165.5
B-9	4/2/2021 17:42	4/2/2021 19:18	North	5362	152.9	123.1	129.0	117.7	150.7	160.7
			North	5363	152.9	123.6	129.3	111.2	147.0	161.3
			East	5366	116.78	126.2	133.5	108.7	155.6	163.9
			South	5365	119.26	124.1	130.3	108.2	153.1	161.7
			West	5356	139.5	123.7	129.6	110.4	147.6	161.3
			South	5353	275.73	119.1	124.6	107.0	144.4	156.8
	4/2/2021 23:37	4/3/2021 6:28	North	5362	152.9	128.4	146.6	111.2	164.0	172.3
			North	5363	152.9	129.7	147.7	112.5	169.3	173.6
			East	5366	116.78	128.5	142.3	109.5	164.0	172.4
			South	5365	119.26	128.6	142.7	111.0	162.2	172.5
			West	5356	139.5	129.7	144.5	112.4	167.7	173.6
			South	5353	275.73	124.2	137.0	110.4	161.1	168.1
	4/3/2021 15:35	4/3/2021 21:42	North	5362	152.9	129.6	143.5	110.9	164.4	173.0
			North	5363	152.9	131.8	144.6	111.3	169.9	175.2
			East	5366	116.78	128.1	140.2	109.9	162.6	171.5
			South	5365	119.26	126.9	141.3	109.8	162.2	170.4
			West	5356	139.5	129.1	145.0	111.8	167.3	172.5
			South	5353	275.73	122.4	138.0	108.9	161.3	165.8
B-16	4/4/2021 14:19	4/4/2021 16:37	North	5362	149.69	128.5	142.5	112.4	161.7	167.7
			North	5363	149.69	130.6	145.7	113.2	165.3	169.8
			East	5366	115.23	127.8	143.0	110.2	159.2	167.0
			South	5365	123.11	125.5	139.9	112.3	155.9	164.7

Conductor	Start Time	End Time	Direction	Monitor Station Name	Distance to Conductor (m)	L_p	Max L_p	Min L_p	$L_{p,pk}$	L_E
			West	5356	141.64	127.1	140.3	113.4	160.2	166.3
			South	5353	279.47	121.0	135.9	110.0	153.8	160.2
	4/4/2021 19:00	4/5/2021 8:03	North	5362	149.69	124.1	144.2	109.5	163.1	170.8
			North	5363	149.69	125.3	145.1	113.7	166.3	172.1
			East	5366	115.23	125.2	140.6	109.4	162.3	171.9
			South	5365	123.11	122.8	138.7	108.8	156.5	169.4
			West	5356	141.64	123.8	142.7	110.3	159.8	170.5
			South	5353	279.47	118.3	137.2	107.5	154.4	165.1
	4/5/2021 11:58	4/5/2021 23:32	North	5362	149.69	120.6	127.5	110.2	154.6	166.8
			North	5363	149.69	121.3	136.3	111.0	154.4	167.5
			East	5366	115.23	123.3	130.3	109.0	159.4	169.5
			South	5365	123.11	120.9	131.3	109.9	154.8	167.1
			West	5356	141.64	121.4	132.2	110.7	156.2	165.1
			South	5353	279.47	116.9	123.9	107.2	148.7	163.1
B-3	4/6/2021 8:00	4/6/2021 9:36	North	5362	151.45	120.5	127.7	111.4	153.3	158.1
			North	5363	151.45	120.8	128.1	114.1	151.2	158.4
			East	5366	112.26	123.8	132.1	112.8	156.0	161.4
			South	5365	122.72	121.2	129.0	109.6	150.0	158.9
			West	5356	144.32	121.0	128.8	111.7	151.5	158.6
			South	5353	280.45	116.4	122.9	108.4	141.8	154.1
	4/6/2021 13:02	4/6/2021 15:33	North	5362	151.45	129.7	145.2	114.5	164.0	169.3
			North	5363	151.45	132.7	146.5	114.1	163.8	172.2
			East	5366	112.26	126.9	142.5	111.7	160.8	166.5
			South	5365	122.72	125.3	141.2	113.5	155.8	164.8
			West	5356	144.32	127.2	141.6	115.0	166.7	166.9
			South	5353	280.45	120.8	135.2	111.6	161.3	160.4
S-25	4/7/2021 9:51	4/7/2021 10:53	North	5362	154.62	125.9	134.1	110.6	157.3	161.6
			North	5363	154.62	126.4	136.0	111.5	159.2	162.1
			East	5366	107.34	131.2	140.1	108.6	168.4	166.9
			South	5365	122.16	128.4	136.9	108.8	161.2	164.1
			West	5356	148.85	125.9	133.7	110.7	154.7	161.6
			South	5353	282.1	121.3	129.6	107.4	160.2	157.1
S-29	4/7/2021 18:35	4/7/2021 19:17	North	5362	157.7	127.5	135.9	109.2	160.8	161.6
			North	5363	157.7	127.5	135.9	110.2	162.8	161.6
			East	5366	109.05	132.4	140.9	107.8	165.2	166.5
			South	5365	118.21	130.3	139.2	108.4	166.2	164.4
			West	5356	146.7	127.1	135.2	109.6	156.2	161.2
			South	5353	278.29	123.7	132.8	106.4	155.7	157.8
S-33	4/8/2021 4:06	4/8/2021 5:44	North	5362	160.86	122.6	129.1	113.1	153.9	160.2
			North	5363	160.86	123.2	130.2	113.2	157.6	160.9
			East	5366	110.81	128.7	136.2	108.7	160.0	166.4

Conductor	Start Time	End Time	Direction	Monitor Station Name	Distance to Conductor (m)	L_p	Max L_p	Min L_p	$L_{p,pk}$	L_E
			South	5365	114.33	127.8	135.1	109.7	160.4	165.5
			West	5356	144.68	123.8	130.3	112.1	154.2	161.5
			South	5353	274.53	121.3	132.0	108.0	153.6	159.1
S-46	4/8/2021 12:49	4/8/2021 15:45	North	5362	156.22	123.6	129.0	111.8	153.8	163.9
			North	5363	156.22	124.6	129.6	111.5	158.9	164.9
			East	5366	118.51	126.6	131.9	112.9	157.7	166.8
			South	5365	115.34	125.4	131.5	111.3	157.8	165.7
			West	5356	137.28	125.0	130.7	111.8	152.7	165.3
			South	5353	271.87	119.7	126.6	108.9	146.7	160.0
S-47	4/9/2021 0:20	4/9/2021 1:43	North	5362	159.48	120.2	129.3	111.5	153.9	157.2
			North	5363	159.48	120.7	129.4	110.7	155.8	157.7
			East	5366	116.54	124.0	133.9	108.8	161.4	161.0
			South	5365	112.97	122.8	133.0	109.2	161.0	159.9
			West	5356	138.96	121.2	130.4	110.2	157.8	158.3
			South	5353	270.95	116.7	126.1	107.9	150.2	153.7
S-36	4/9/2021 7:08	4/9/2021 7:59	North	5362	160.75	124.0	128.9	110.9	151.3	158.9
			North	5363	160.75	124.6	129.6	112.5	153.4	159.5
			East	5366	114.59	129.2	134.5	112.2	158.8	164.1
			South	5365	112.6	127.6	134.1	113.1	163.8	162.5
			West	5356	140.89	125.5	130.9	112.6	154.0	160.4
			South	5353	271.57	121.8	127.6	109.1	157.5	156.7
S-34	4/9/2021 15:07	4/9/2021 16:45	North	5362	159.11	119.5	126.1	110.8	152.0	157.2
			North	5363	159.11	119.9	126.1	111.8	152.3	157.7
			East	5366	113.6	124.5	131.8	111.6	164.9	162.2
			South	5365	114.63	122.6	130.5	111.8	155.1	160.3
			West	5356	141.96	120.2	126.8	111.1	147.9	157.9
			South	5353	273.55	116.2	123.4	107.6	147.7	153.9
B-17	4/10/2021 22:41	4/11/2021 1:10	North	5362	155.82	117.7	125.2	112.1	147.2	157.2
			North	5363	155.82	118.5	125.6	113.5	151.4	158.0
			East	5366[1]	111.89	--	--	--	--	--
			South	5365	118.56	119.5	127.6	110.3	150.6	159.0
			West	5356	144.03	118.1	125.7	111.7	146.1	157.6
			South	5353	277.33	114.9	121.8	108.7	147.7	154.4
	4/11/2021 4:40	4/11/2021 15:51	North	5362	155.82	122.0	128.9	108.7	156.9	168.0
			North	5363	155.82	123.2	129.2	109.0	159.0	168.2
			East	5366	111.89	125.8	133.3	108.5	161.4	171.8
			South	5365	118.56	124.1	131.4	109.2	159.2	170.1
			West	5356	144.03	122.0	130.8	110.3	156.3	168.1
			South	5353	277.33	118.9	125.2	106.9	150.8	164.1
S-41	4/11/2021 21:06	4/11/2021 23:00	North	5362	154.65	118.6	127.7	110.2	152.3	157.0
			North	5363	154.65	120.3	129.1	111.9	153.6	157.4

Conductor	Start Time	End Time	Direction	Monitor Station Name	Distance to Conductor (m)	L_p	Max L_p	Min L_p	$L_{p,pk}$	L_E
			East	5366	113.9	122.6	132.2	107.6	156.9	160.9
			South	5365	118.8	120.6	130.7	108.8	157.3	159.0
			West	5356	142.11	119.7	137.5	111.2	155.4	158.1
			South	5353	276.63	114.9	123.2	108.4	144.6	153.3
S-28	4/12/2021 9:48	4/12/2021 15:35	North	5362	154.3	127.6	146.1	109.8	165.2	170.7
			North	5363	154.3	129.2	148.8	110.6	169.4	172.3
			East	5366	111.08	130.1	141.5	107.9	163.7	173.4
			South	5365	120.46	126.7	139.0	109.0	157.9	169.9
			West	5356	145.03	126.3	141.8	110.6	162.8	169.5
			South	5353	279.19	120.8	133.7	106.2	154.1	163.8
S-12	4/13/2021 11:50	4/13/2021 12:47	North	5362	145.46	123.3	133.0	109.4	161.9	158.4
			North	5363	145.46	123.3	133.1	110.4	163.3	158.7
			East	5366	106.92	128.6	139.0	108.6	164.1	163.8
			South	5365	131.57	123.7	133.9	108.3	161.5	159.1
			West	5356	151.48	122.6	134.0	110.1	158.3	158.0
			South	5353	289.93	117.6	127.5	105.7	149.4	153.5
S-23	4/13/2021 21:05	4/13/2021 22:29	North	5362	144.1	115.4	128.6	109.8	151.6	152.4
			North	5363	144.1	116.5	128.3	112.4	154.5	153.5
			East	5366	109.04	117.7	131.9	109.7	157.8	153.9
			South	5365	131.82	127.3	142.8	108.9	162.4	168.1
			West	5356	149.65	115.3	128.3	111.4	157.2	152.3
			South	5353	289.29	111.3	122.6	106.7	143.0	148.4
S-21	4/14/2021 7:44	4/11/2021 10:48	North	5362	142.52	128.9	145.3	119.5	163.5	169.3
			North	5363	142.52	130.2	147.1	115.0	164.7	170.6
			East	5366	108.42	128.6	141.1	115.9	163.4	169.0
			South	5365	133.81	130.0	146.9	114.5	166.1	170.4
			West	5356	150.86	130.3	144.6	112.4	164.7	170.8
			South	5353	291.21	124.6	137.3	112.6	162.6	165.1
B-14	4/14/2021 17:06	4/14/2021 19:05	North	5362	143.97	125.3	132.9	112.9	156.9	163.8
			North	5363	143.97	125.1	136.0	113.4	159.4	163.7
			East	5366	106.27	129.7	137.1	117.3	161.3	168.2
			South	5365	133.52	125.1	132.9	109.5	158.9	163.6
			West	5356	152.65	124.5	133.0	110.5	157.3	163.1
			South	5353	291.82	119.6	129.0	106.9	149.9	158.2
	4/15/2021 1:05	4/15/2021 10:59	North	5362	143.97	118.7	129.5	109.5	151.5	164.2
			North	5363	143.97	118.7	127.4	112.4	149.7	164.3
			East	5366	106.27	122.6	133.3	107.1	158.0	168.2
			South	5365	133.52	118.4	127.8	109.8	148.2	163.9
			West	5356	152.65	118.2	127.4	110.7	153.2	163.7
			South	5353	291.82	114.3	121.7	107.6	144.3	159.8
S-9			North	5362	145.87	131.7	145.3	116.5	165.8	169.4

Conductor	Start Time	End Time	Direction	Monitor Station Name	Distance to Conductor (m)	L_p	Max L_p	Min L_p	$L_{p,pk}$	L_E
	4/15/2021 18:23	4/15/2021 20:01	North	5363	145.87	133.7	149.0	119.7	171.6	171.2
			East	5366	103.26	131.5	142.5	123.7	165.9	168.9
			South	5365	133.35	128.3	139.2	116.3	158.5	166.0
			West	5356	155.25	129.5	140.6	118.1	165.5	167.2
			South	5353	292.83	122.7	133.9	114.4	155.0	160.4
B-08	4/16/2021 8:33	4/16/2021 10:21	North	5362	140.59	123.9	129.8	115.3	158.7	162.0
			North	5363	140.59	124.2	130.3	115.8	154.0	162.4
			East	5366	111.45	124.9	130.4	114.5	158.0	163.0
			South	5365	134.21	122.1	127.9	113.2	152.7	160.3
			West	5356	148.34	122.8	128.5	113.5	155.8	161.0
			South	5353	290.33	118.7	123.8	111.1	149.1	156.9
	4/16/2021 13:07	4/16/2021 18:32	North	5362	140.59	124.2	133.2	111.3	159.5	167.1
			North	5363	140.59	124.4	132.1	113.0	157.1	167.3
			East	5366	111.45	125.0	132.9	107.7	161.7	167.9
			South	5365	134.21	122.4	129.7	109.2	155.6	165.3
			West	5356	148.34	123.1	130.9	111.9	154.5	166.0
			South	5353	290.33	119.0	126.0	109.4	151.2	161.9
B-13	4/17/2021 1:54	4/17/2021 3:41	North	5362	139.12	126.6	144.6	112.1	162.4	164.7
			North	5363	139.12	127.7	147.1	113.1	168.5	165.6
			East	5366	110.9	127.8	143.9	112.2	163.9	165.8
			South	5365	136.11	125.1	141.4	112.4	165.2	163.2
			West	5356	149.57	125.0	139.9	112.6	162.4	163.1
			South	5353	292.2	120.2	132.2	109.9	160.3	158.3
	4/17/2021 7:02	4/17/2021 15:48	North	5362	139.12	120.6	127.5	116.7	150.8	165.5
			North	5363	139.12	120.9	129.8	116.1	150.2	165.9
			East	5366	110.9	121.8	128.6	113.1	157.0	166.8
			South	5365	136.11	119.2	126.7	111.9	148.6	164.2
			West	5356	149.57	119.9	126.0	113.8	148.2	164.9
			South	5353	292.2	116.4	130.8	112.2	144.4	161.4
	4/17/2021 17:09	4/18/2021 3:56	North	5362	139.12	126.1	145.6	110.2	163.1	172.0
			North	5363	139.12	127.2	147.9	111.8	167.7	173.1
			East	5366	110.9	127.0	143.8	109.5	162.5	172.8
			South	5365	136.11	123.8	139.9	109.6	157.8	169.6
			West	5356	149.57	127.4	141.2	115.0	162.1	167.4
			South	5353	292.2	119.5	132.8	108.1	153.9	165.4
B-10	4/18/2021 12:47	4/18/2021 14:30	North	5362	141.03	118.6	130.5	112.9	154.4	156.4
			North	5363	141.03	118.9	129.9	110.5	150.0	156.8
			East	5366	107.83	119.9	132.6	110.9	154.0	157.8
			South	5365	135.74	117.1	127.5	110.0	145.2	155.0
			West	5356	152.13	117.8	128.4	112.7	147.0	155.7
			South	5353	293.12	114.4	123.4	107.9	144.3	152.3

Conductor	Start Time	End Time	Direction	Monitor Station Name	Distance to Conductor (m)	L_p	Max L_p	Min L_p	$L_{p,pk}$	L_E
	4/18/2021 15:58	4/18/2021 17:17	North	5362	141.03	122.2	130.5	111.4	158.2	159.0
			North	5363	141.03	122.1	128.4	112.2	153.1	158.9
			East	5366	107.83	124.6	132.1	110.9	159.7	161.4
			South	5365	135.74	120.0	128.1	110.7	155.7	156.8
			West	5356	152.13	120.7	127.9	111.5	156.6	157.5
			South	5353	293.12	116.3	122.4	108.9	148.7	153.1
	4/18/2021 21:06	4/18/2021 23:02	North	5362	141.03	120.4	130.3	111.6	156.2	157.7
			North	5363	141.03	120.6	129.9	112.6	153.3	158.9
			East	5366	107.83	122.3	133.1	108.5	158.5	160.8
			South	5365	135.74	118.3	127.0	109.8	148.9	156.7
			West	5356	152.13	118.7	127.3	111.7	153.2	157.1
			South	5353	293.12	114.6	122.5	109.0	145.3	153.0
	4/18/2021 23:22	4/19/2021 1:52	North	5362	141.03	124.1	131.0	110.4	162.5	163.7
			North	5363	141.03	124.3	130.7	114.0	159.0	163.9
			East	5366	107.83	126.8	133.4	109.1	163.0	166.3
			South	5365	135.74	122.1	128.4	110.0	150.8	161.7
			West	5356	152.13	122.7	129.8	112.0	158.1	162.2
			South	5353	293.12	117.9	124.2	108.6	150.3	157.4
S-7	4/19/2021 7:41	4/19/2021 10:20	North	5362	144.47	129.1	145.9	112.1	174.0	168.8
			North	5363	144.47	130.5	146.8	112.9	173.7	170.2
			East	5366	102.61	129.0	141.9	111.3	163.6	168.8
			South	5365	135.26	127.8	141.5	112.1	164.1	167.6
			West	5356	156.46	130.4	146.0	114.4	163.2	170.1
			South	5353	294.72	124.0	137.4	111.4	159.3	163.9
S-6	4/19/2021 15:47	4/19/2021 21:37	North	5362	140.94	129.1	145.9	112.1	174.0	168.8
			North	5363	140.94	131.1	149.7	116.7	165.8	172.9
			East	5366	105.12	128.6	141.0	114.6	170.9	176.6
			South	5365	137.48	125.3	138.2	112.1	160.2	169.9
			West	5356	155.09	126.1	140.5	115.8	167.9	170.6
			South	5353	295.64	119.8	133.1	113.5	162.8	164.3
S-4	4/20/2021 11:30	4/20/2021 12:55	North	5362	139.45	130.1	138.2	122.3	165.3	167.2
			North	5363	139.45	130.2	137.9	120.5	164.3	167.3
			East	5366	104.59	133.0	141.6	115.9	174.5	170.1
			South	5365	139.43	127.8	134.2	117.5	157.3	165.0
			West	5356	156.36	127.7	135.9	118.7	162.4	164.9
			South	5353	297.56	123.2	131.8	115.6	156.3	160.4

[1] Data were not collected during this event due to the equipment time adjustment.

L_p and $L_{p,pk}$ = (dB re 1 μPa); L_E = (dB re 1 μPa^2·s)

Table B-2. Mechanical Cutting Events Noise Data with Marine Mammal Hearing Group Weightings

Conductor	Start Time	End Time	Monitor Station Name	L_p				L_E			
				LF	MF	HF	PP	LF	MF	HF	PP
B-1	4/1/2021 17:06	4/1/2021 17:25	5362	118.6	99.5	95.4	111.1	149.2	130.1	126.0	141.7
			5363	119.1	103.2	99.5	113.0	149.8	133.8	130.1	143.6
			5366	123.9	95.0	90.9	113.7	153.0	124.1	120.0	142.8
			5365	120.7	97.9	94.6	111.7	151.5	128.7	125.4	142.5
			5356	119.1	100.1	96.5	111.4	149.7	130.7	127.1	142.0
			5353	115.3	99.1	95.4	109.0	146.0	129.8	126.1	139.7
	4/1/2021 18:01	4/1/2021 18:54	5362	122.7	98.7	94.5	114.1	157.7	133.7	129.5	149.1
			5363	122.9	101.4	97.6	114.9	157.9	136.4	132.6	149.9
			5366	126.8	98.3	93.1	117.8	161.9	133.4	128.2	152.8
			5365	125.5	99.9	95.4	117.3	160.6	134.9	130.5	152.3
			5356	123.4	99.5	95.5	115.0	158.5	134.6	130.5	150.1
			5353	119.4	97.5	93.6	111.4	154.4	132.5	128.6	146.4
	4/1/2021 22:05	4/2/2021 4:08	5362	121.3	98.7	94.6	113.4	163.0	140.4	136.2	155.1
			5363	121.7	101.6	97.8	114.4	163.3	143.2	139.4	156.1
			5366	125.5	98.0	93.0	116.9	167.3	139.8	134.7	158.7
			5365	122.7	99.9	96.1	115.1	166.1	143.3	139.5	158.5
			5356	122.2	100.6	96.9	114.3	165.5	143.9	140.2	157.7
			5353	117.9	97.5	93.8	110.5	159.6	139.2	135.5	152.2
B-9	4/2/2021 17:42	4/2/2021 19:18	5362	122.3	99.7	95.3	115.4	160.0	137.3	100.4	153.0
			5363	122.7	101.8	97.9	115.6	160.3	139.4	135.5	153.3
			5366	125.6	100.0	94.4	118.7	163.3	137.7	132.1	156.3
			5365	123.2	99.5	95.4	115.9	160.8	137.1	133.0	153.5
			5356	122.9	99.7	95.6	115.5	160.5	137.3	133.2	153.1
			5353	118.2	97.2	93.4	111.1	155.8	134.9	131.1	148.7
	4/2/2021 23:37	4/3/2021 6:28	5362	125.4	105.1	101.5	118.2	169.3	149.0	145.4	162.1
			5363	126.7	107.6	104.3	119.7	170.7	151.5	148.2	163.6
			5366	126.0	103.0	98.8	118.7	169.9	146.9	142.7	162.7
			5365	125.1	105.4	102.2	117.7	169.1	149.4	146.2	161.8
			5356	126.6	105.2	101.6	118.7	170.5	149.1	145.5	162.6
			5353	121.4	101.9	98.5	114.0	165.3	145.8	142.4	157.9
	4/3/2021 15:35	4/3/2021 21:42	5362	126.3	105.4	101.7	118.7	169.7	148.9	145.1	162.2
			5363	128.6	108.8	105.3	121.3	172.0	152.2	148.7	164.7
			5366	125.0	104.1	100.6	117.7	168.4	147.5	144.0	161.1
			5365	123.4	104.7	101.4	115.9	166.9	148.2	144.9	159.4
			5356	125.8	104.8	101.3	117.9	169.2	148.3	144.7	161.4
			5353	119.7	101.1	97.9	112.4	163.2	144.5	141.3	155.9
B-16	4/4/2021 14:19	4/4/2021 16:37	5362	125.3	103.0	99.1	117.5	164.5	142.2	138.3	156.7
			5363	127.5	106.2	102.5	119.9	166.5	145.2	141.6	159.0
			5366	125.3	102.3	98.3	117.8	164.6	141.5	137.5	157.1
			5365	122.2	100.5	97.1	114.2	161.4	139.7	136.3	153.4

Conductor	Start Time	End Time	Monitor Station Name	L_p				L_E			
				LF	MF	HF	PP	LF	MF	HF	PP
			5356	124.3	102.9	99.3	116.5	163.5	142.1	138.5	155.7
			5353	118.4	98.0	94.6	110.6	157.6	137.2	133.8	149.8
	4/4/2021 19:00	4/5/2021 8:03	5362	121.8	100.7	96.8	114.4	167.8	146.7	142.8	160.4
			5363	122.7	103.6	100.1	115.6	169.4	150.3	146.8	162.3
			5366	123.0	100.0	95.6	115.6	169.8	146.7	142.3	162.3
			5365	119.9	99.1	95.8	112.0	166.5	145.6	142.4	158.6
			5356	121.3	100.6	97.0	113.7	168.1	147.3	143.8	160.4
			5353	116.2	97.5	94.1	109.1	162.9	144.2	140.8	155.8
	4/5/2021 11:58	4/5/2021 23:32	5362	119.1	98.4	94.4	111.6	165.3	144.6	140.6	157.8
			5363	119.7	101.0	97.3	112.7	165.9	147.2	143.5	158.9
			5366	122.0	97.6	92.7	114.3	168.2	143.8	138.9	160.4
			5365	118.9	97.4	94.1	110.5	165.1	143.6	140.3	156.7
			5356	119.9	98.8	95.0	112.2	166.1	145.0	141.2	158.3
			5353	115.3	96.4	92.8	108.1	161.4	142.5	138.9	154.3
B-3	4/6/2021 8:00	4/6/2021 9:36	5362	119.1	98.4	94.5	111.4	156.7	136.0	132.1	149.0
			5363	119.3	101.2	97.6	112.3	156.9	138.8	135.2	149.9
			5366	122.4	97.2	92.6	113.9	160.1	134.8	130.2	151.6
			5365	119.7	97.9	94.6	111.1	157.3	135.5	132.2	148.8
			5356	119.6	99.1	95.4	111.5	157.2	136.6	133.0	149.1
			5353	114.8	96.7	93.3	107.3	152.5	134.5	131.0	145.1
	4/6/2021 13:02	4/6/2021 15:33	5362	126.0	103.3	99.4	118.1	165.6	142.9	138.9	157.6
			5363	129.0	106.6	102.8	121.3	168.6	146.2	142.3	160.9
			5366	123.8	101.7	98.1	116.1	163.3	141.2	137.7	155.6
			5365	121.3	100.3	97.1	112.9	160.8	139.9	136.7	152.5
			5356	123.8	103.8	100.3	116.3	163.4	143.4	139.9	155.9
			5353	117.8	99.4	96.0	110.5	157.4	138.9	135.6	150.0
S-25	4/7/2021 9:51	4/7/2021 10:53	5362	124.9	103.9	99.7	119.0	160.6	139.6	135.4	154.7
			5363	125.4	105.5	101.7	119.8	161.1	141.2	137.4	155.5
			5366	130.6	109.0	104.0	125.5	166.3	144.7	139.7	161.2
			5365	127.5	106.5	102.1	121.9	163.2	142.1	137.8	157.5
			5356	125.0	103.4	99.0	119.0	160.6	139.1	134.7	154.7
			5353	120.4	100.6	96.4	114.9	156.1	136.3	132.1	150.6
S-29	4/7/2021 18:35	4/7/2021 19:17	5362	126.6	108.1	104.4	121.0	160.7	142.1	138.4	155.0
			5363	126.5	108.9	105.6	121.0	160.5	142.9	139.6	155.0
			5366	131.7	111.3	107.3	126.1	165.7	145.3	141.3	160.1
			5365	129.5	110.5	107.1	123.8	163.5	144.6	141.1	157.9
			5356	125.9	105.7	102.0	119.5	159.9	139.7	136.0	153.5
			5353	122.8	105.0	101.5	117.4	156.8	139.0	135.5	151.4
S-33	4/8/2021 4:06	4/8/2021 5:44	5362	121.4	100.8	96.5	115.3	159.1	138.5	134.2	153.0
			5363	122.0	102.8	98.9	116.2	159.7	140.5	136.6	153.9
			5366	128.0	105.9	100.6	122.7	165.8	143.7	138.4	160.5

Conductor	Start Time	End Time	Monitor Station Name	L_p				L_E			
				LF	MF	HF	PP	LF	MF	HF	PP
			5365	127.2	105.8	101.4	121.6	164.9	143.5	139.1	159.3
			5356	122.7	102.1	97.9	116.8	160.4	139.8	135.6	154.5
			5353	120.7	101.1	96.9	115.4	158.4	138.8	134.6	153.1
S-46	4/8/2021 12:49	4/8/2021 15:45	5362	122.8	101.3	96.5	117.1	163.0	141.5	136.8	157.3
			5363	123.7	103.2	98.7	118.3	164.0	143.4	139.0	158.6
			5366	125.8	102.3	96.5	120.2	166.0	142.5	136.7	160.4
			5365	124.6	102.6	97.7	118.9	164.8	142.8	138.0	159.2
			5356	124.3	102.5	97.7	118.7	164.5	142.7	138.0	158.9
			5353	118.8	98.7	94.4	113.2	159.0	138.9	134.6	153.5
S-47	4/9/2021 0:20	4/9/2021 1:43	5362	118.8	100.0	95.9	113.3	155.8	136.9	132.9	150.3
			5363	119.4	102.2	98.5	114.1	156.4	139.2	135.4	151.1
			5366	123.2	101.7	96.9	117.5	160.0	138.5	133.7	154.3
			5365	121.9	102.8	98.9	116.7	158.8	139.7	135.8	153.5
			5356	120.0	101.4	97.4	114.6	157.0	138.3	134.4	151.6
			5353	115.4	98.5	94.8	110.5	152.4	135.5	131.7	147.4
S-36	4/9/2021 7:08	4/9/2021 7:59	5362	122.8	100.5	96.2	115.8	157.6	135.3	131.0	150.6
			5363	123.4	102.3	95.4	116.5	158.2	137.1	133.2	151.3
			5366	128.8	105.2	99.8	122.4	163.3	140.1	134.7	157.2
			5365	126.7	105.9	101.4	120.9	161.6	140.8	136.2	155.8
			5356	124.4	102.9	98.5	118.1	159.3	137.8	133.4	153.0
			5353	120.9	100.6	96.1	115.2	155.8	135.4	131.0	150.1
S-34	4/9/2021 15:07	4/9/2021 16:45	5362	117.7	97.2	93.1	112.0	155.4	134.9	130.8	149.7
			5363	118.1	99.4	95.7	112.5	155.8	137.1	133.4	150.2
			5366	123.4	101.4	95.8	118.5	161.1	139.1	133.5	156.2
			5365	121.0	99.7	95.5	115.1	158.8	137.4	133.2	128.8
			5356	111.2	99.1	95.8	107.7	148.9	136.9	133.5	145.5
			5353	114.6	95.9	92.2	109.2	152.3	133.6	129.9	146.9
B-17	4/10/2021 22:41	4/11/2021 1:10	5362	115.9	97.0	93.5	108.8	155.5	136.6	133.0	148.3
			5363	116.6	99.6	96.3	110.2	156.1	139.1	135.8	149.7
			5366	--[1]	--[1]	--[1]	--[1]	--[1]	--[1]	--[1]	--[1]
			5365	117.8	97.3	94.2	109.9	157.3	136.8	133.7	149.4
			5356	116.2	97.8	94.5	109.0	155.7	137.3	134.0	148.5
			5353	113.1	95.3	92.0	106.2	152.6	134.8	131.5	145.7
	4/11/2021 4:40	4/11/2021 15:51	5362	120.8	100.4	96.1	114.1	166.8	146.5	142.2	160.2
			5363	122.2	103.1	99.0	115.9	166.9	147.9	143.8	160.7
			5366	124.7	102.1	97.1	118.1	170.8	148.2	143.1	164.2
			5365	123.4	102.0	97.8	116.6	168.6	147.2	143.0	161.8
			5356	120.7	100.2	96.3	113.6	166.7	146.2	142.3	159.6
			5353	117.7	98.3	94.3	111.3	162.9	143.4	139.4	156.5
S-41	4/11/2021 21:06	4/11/2021 23:00	5362	117.1	99.5	95.6	111.7	155.5	137.9	134.0	150.0
			5363	119.7	102.0	98.3	114.3	154.9	137.2	133.4	149.4

Conductor	Start Time	End Time	Monitor Station Name	L_p				L_E			
				LF	MF	HF	PP	LF	MF	HF	PP
			5366	122.3	101.0	96.2	116.7	159.7	138.3	133.6	154.0
			5365	119.2	99.9	96.3	113.5	157.6	138.3	134.6	151.9
			5356	118.1	100.1	96.3	112.6	156.5	138.5	134.7	151.0
			5353	115.1	97.7	94.1	109.4	150.2	132.9	129.2	144.5
S-28	4/12/2021 9:48	4/12/2021 15:35	5362	125.9	106.0	101.5	120.4	168.3	148.4	143.9	162.7
			5363	127.4	108.6	104.5	121.8	169.8	151.0	146.9	164.3
			5366	129.1	110.3	104.7	125.6	172.3	153.5	147.9	168.8
			5365	125.1	107.3	102.6	121.0	168.3	150.5	145.8	164.2
			5356	124.4	105.9	101.6	119.5	167.6	149.1	144.8	162.7
			5353	119.0	101.1	96.6	114.5	162.1	144.3	139.8	157.7
S-12	4/13/2021 11:50	4/13/2021 12:47	5362	122.1	102.8	98.8	116.5	157.5	138.2	134.3	152.0
			5363	122.3	103.9	100.3	116.7	157.7	139.3	135.7	152.1
			5366	127.9	107.2	102.4	123.0	163.4	142.6	137.8	158.4
			5365	122.8	103.7	100.3	116.9	158.2	139.1	135.7	152.3
			5356	121.6	103.0	99.2	116.5	157.3	138.7	134.8	152.1
			5353	117.0	98.5	94.9	111.3	152.4	133.9	130.2	146.6
S-23	4/13/2021 21:05	4/13/2021 22:29	5362	114.1	98.6	94.5	110.0	151.1	135.6	131.6	147.0
			5363	115.2	102.5	98.8	112.2	152.2	139.5	135.8	149.2
			5366	115.8	96.5	92.2	110.5	152.8	133.6	129.2	147.6
			5365	122.7	102.8	99.8	114.6	163.6	143.7	140.7	155.5
			5356	113.7	100.0	96.4	110.0	150.8	137.0	133.4	147.0
			5353	109.8	98.0	94.4	107.0	146.9	135.1	131.4	144.1
S-21	4/14/2021 7:44	4/11/2021 10:48	5362	125.2	104.7	101.1	117.2	165.7	145.1	141.5	157.6
			5363	127.1	107.9	104.5	119.5	167.5	148.4	145.0	160.0
			5366	124.8	104.7	101.5	117.0	165.2	145.1	141.9	157.4
			5365	125.9	107.2	104.1	118.6	166.3	147.6	144.5	159.1
			5356	127.2	107.3	103.9	119.8	167.6	147.8	144.3	160.2
			5353	121.7	104.0	100.8	115.1	162.2	144.5	141.3	155.5
B-14	4/14/2021 17:06	4/14/2021 19:05	5362	124.5	100.8	96.2	117.3	163.1	139.4	134.8	155.9
			5363	124.3	103.2	99.2	117.2	162.9	141.7	137.8	155.7
			5366	129.0	102.6	96.8	121.7	167.6	141.2	135.4	160.3
			5365	124.2	100.1	96.0	116.8	162.8	138.7	134.6	155.4
			5356	123.8	101.0	96.8	116.7	162.4	139.5	135.3	155.3
			5353	118.7	98.3	94.5	111.5	157.3	136.9	133.1	150.0
	4/15/2021 1:05	4/15/2021 10:59	5362	117.4	98.2	94.5	110.4	162.9	143.8	140.0	155.9
			5363	117.2	101.2	97.8	106.5	162.8	146.8	143.3	157.0
			5366	121.4	95.4	91.0	113.0	167.0	140.9	136.6	158.5
			5365	116.6	97.3	94.3	108.8	162.2	142.8	139.8	154.3
			5356	116.6	98.7	95.2	110.0	162.2	144.2	140.7	155.6
			5353	112.3	96.6	93.3	106.3	157.9	142.2	138.8	151.8
S-9			5362	128.3	107.8	104.1	120.4	166.0	145.5	141.9	158.1

Conductor	Start Time	End Time	Monitor Station Name	Lp				LE			
				LF	MF	HF	PP	LF	MF	HF	PP
	4/15/2021 18:23	4/15/2021 20:01	5363	130.3	111.1	107.7	122.8	168.0	148.8	145.4	160.5
			5366	127.7	106.6	103.0	120.1	165.4	144.3	140.7	157.8
			5365	124.0	103.9	101.0	115.5	161.7	141.6	138.7	153.2
			5356	126.1	106.9	103.6	118.3	163.8	144.6	141.4	156.1
			5353	119.4	100.6	97.6	111.4	157.1	138.3	135.3	149.1
B-08	4/16/2021 8:33	4/16/2021 10:21	5362	122.8	100.2	95.9	115.6	160.9	138.3	134.0	153.7
			5363	123.1	102.5	98.6	116.0	161.2	140.7	136.8	154.2
			5366	123.6	96.7	91.8	115.4	161.7	134.8	129.9	153.5
			5365	120.5	98.1	94.7	112.3	158.7	136.3	132.8	150.4
			5356	121.6	100.3	96.4	114.2	159.8	138.4	134.5	152.4
			5353	117.5	98.0	94.3	110.5	155.6	136.1	132.4	148.6
	4/16/2021 13:07	4/16/2021 18:32	5362	123.5	100.3	95.8	116.2	166.0	142.8	138.4	158.7
			5363	123.3	102.2	98.3	116.1	166.2	145.1	141.2	159.0
			5366	123.7	96.9	91.9	115.6	166.6	139.8	134.8	158.5
			5365	120.8	98.1	94.5	112.6	163.7	141.0	137.4	155.5
			5356	121.9	99.9	95.8	114.5	164.8	142.8	138.7	157.4
			5353	117.7	97.5	93.7	110.6	160.6	140.4	136.6	153.5
B-13	4/17/2021 1:54	4/17/2021 3:41	5362	122.8	104.5	101.9	115.4	160.8	142.5	140.0	153.4
			5363	123.9	107.2	104.7	116.9	161.9	145.2	142.8	155.0
			5366	100.7	124.3	127.8	116.7	138.8	162.3	165.8	154.7
			5365	121.1	103.9	102.1	113.1	159.1	142.0	140.1	151.1
			5356	121.4	104.2	102.0	113.8	159.5	142.3	140.1	151.9
			5353	117.4	101.1	99.1	110.0	155.5	139.1	137.2	148.0
	4/17/2021 7:02	4/17/2021 15:48	5362	119.0	98.3	94.3	111.5	164.0	143.3	139.3	156.5
			5363	119.2	100.5	96.9	112.3	164.2	145.5	141.9	157.3
			5366	120.3	95.6	91.2	112.2	165.3	140.7	136.2	157.2
			5365	117.2	97.1	94.0	108.6	162.2	142.1	139.0	153.6
			5356	118.1	98.5	94.9	110.7	163.1	143.5	139.9	155.7
			5353	114.1	96.2	92.7	107.1	159.1	141.2	137.7	152.1
	4/17/2021 17:09	4/18/2021 3:56	5362	124.0	102.7	98.6	116.8	169.9	148.6	144.5	162.7
			5363	124.8	104.8	101.2	117.7	170.6	150.7	147.1	163.5
			5366	125.4	101.6	96.9	117.9	171.2	147.4	142.7	163.7
			5365	121.3	100.1	96.8	113.1	167.1	146.0	142.7	159.0
			5356	122.6	102.2	98.5	115.3	168.5	148.0	144.4	161.1
			5353	117.6	98.6	95.2	110.4	163.5	144.5	141.1	156.3
B-10	4/18/2021 12:47	4/18/2021 14:30	5362	117.3	97.6	93.6	110.2	155.2	135.5	131.5	148.1
			5363	117.5	102.0	98.3	111.9	155.4	139.9	136.2	149.8
			5366	118.6	93.8	90.1	110.1	156.5	131.7	128.0	148.0
			5365	114.7	96.3	93.3	106.6	152.7	134.2	131.2	144.5
			5356	116.0	99.1	95.5	109.5	153.9	137.0	133.4	147.4
			5353	112.3	97.5	93.9	106.9	149.9	135.2	131.5	144.5
			5362	121.2	98.0	94.1	113.5	158.0	134.8	130.9	150.3

Conductor	Start Time	End Time	Monitor Station Name	L_p				L_E			
				LF	MF	HF	PP	LF	MF	HF	PP
	4/18/2021 15:58	4/18/2021 17:17	5363	121.0	101.0	97.4	113.9	157.8	137.8	134.2	150.7
			5366	123.6	97.8	93.0	116.1	160.4	134.6	129.8	152.9
			5365	118.4	97.5	94.3	110.5	155.2	134.3	131.1	147.3
			5356	119.4	98.3	94.6	112.2	156.2	135.1	131.4	149.0
			5353	114.7	96.1	92.7	107.8	151.5	132.9	129.5	144.6
	4/18/2021 21:06	4/18/2021 23:02	5362	119.2	99.5	96.1	112.2	157.7	138.0	134.6	150.7
			5363	119.3	102.5	99.2	113.2	157.7	140.8	137.6	151.6
			5366	121.5	97.4	93.5	114.3	159.8	135.7	131.8	152.6
			5365	116.5	98.3	95.6	109.1	155.0	136.7	134.0	147.5
			5356	117.4	99.1	95.9	110.9	155.8	137.4	134.3	149.2
			5353	113.1	97.8	94.6	107.5	151.5	136.2	133.1	145.9
	4/18/2021 23:22	4/19/2021 1:52	5362	123.2	100.3	96.1	115.7	162.7	139.8	135.7	155.2
			5363	123.3	102.4	98.7	116.0	162.8	142.0	138.2	155.5
			5366	125.8	100.4	95.3	118.3	165.3	139.9	134.9	157.8
			5365	120.6	98.7	95.5	112.5	160.2	138.2	135.0	152.1
			5356	121.5	99.9	96.2	114.1	161.0	139.4	135.7	153.6
			5353	116.6	97.5	94.0	109.7	156.1	137.0	133.5	149.2
S-7	4/19/2021 7:41	4/19/2021 10:20	5362	126.0	108.0	104.5	119.6	165.8	147.8	144.3	159.4
			5363	127.4	109.7	106.4	120.8	167.2	149.5	146.2	160.6
			5366	127.1	106.1	101.7	121.6	166.9	145.9	141.5	161.4
			5365	124.6	106.0	102.9	117.6	164.4	145.8	142.7	157.4
			5356	127.0	106.1	102.2	119.6	166.8	145.9	142.0	159.4
			5353	121.3	102.7	99.2	114.4	161.1	142.5	139.0	154.2
S-6	4/19/2021 15:47	4/19/2021 21:37	5362	125.9	104.7	100.8	118.9	174.0	152.8	148.9	167.0
			5363	127.5	108.6	105.2	121.0	170.7	151.8	148.4	164.2
			5366	126.3	105.6	101.4	120.5	174.4	153.7	149.5	168.6
			5365	122.5	103.0	99.8	115.7	166.4	146.9	143.7	159.6
			5356	123.3	104.6	101.1	117.1	167.9	149.2	145.7	161.7
			5353	117.5	99.7	96.3	111.3	161.4	143.6	140.2	155.2
S-4	4/20/2021 11:30	4/20/2021 12:55	5362	128.6	110.9	107.5	123.4	165.7	148.0	144.6	160.5
			5363	128.5	112.3	109.6	123.3	165.6	149.5	146.8	160.5
			5366	132.2	113.1	108.9	127.8	169.3	150.2	146.1	164.9
			5365	126.0	106.7	103.4	120.0	163.2	143.9	140.5	157.1
			5356	126.0	107.7	104.2	120.3	163.2	144.8	141.4	157.5
			5353	121.3	102.1	98.7	115.2	158.4	139.2	135.7	152.3

[1] Data were not collected during this event due to the equipment time adjustment.
L_p and $L_{p,pk}$ = (dB re 1 μPa); L_E = (dB re 1 μPa^2·s)
LF – low frequency; MF – mid-frequency; HF – high frequency; PP – phocid pinnipeds

Table B-3. Wellbore Conductor B-1
(17:06 April 1, 2021 – 4:08 April 2, 2021)

Conductor	Start Time	End Time	Total Duration of Cut (minutes)	Overall Wall Thickness (inches)	Cut Depth Below Mudline (Feet)	Cutter RPM
B-1	4/1/2021 17:06	4/1/2021 17:25	16	1.857	25	60
	4/1/2021 18:01	4/1/2021 18:54	53			
	4/1/2021 22:05	4/2/2021 4:08	363			

Conductor	Start Time	End Time	Direction	Monitor Station Name	Distance to Conductor (m)	L_p	Max L_p	Min L_p	$L_{p,pk}$	L_E
B-1	4/1/2021 17:06	4/1/2021 17:25	North	5362	156.31	121.8	124.6	112.7	144.5	150.7
			North	5363	156.31	121.3	126.3	111.6	143.4	152.1
			East	5366	114.62	123.8	127.9	107.9	149.8	154.5
			South	5365	116.82	122.1	126.6	108.3	149.4	152.8
			West	5356	141.16	120.6	124.8	110.2	143.8	151.4
			South	5353	274.72	116.9	120.3	107.4	141.2	147.6
	4/1/2021 18:01	4/1/2021 18:54	North	5362	156.31	123.9	130.8	111.7	154.0	158.9
			North	5363	156.31	124.2	130.2	111.4	155.8	159.2
			East	5366	114.62	128.0	135.2	108.5	156.5	163.0
			South	5365	116.82	126.5	133.3	108.4	156.5	161.6
			West	5356	141.16	124.6	131.6	110.3	152.9	159.7
			South	5353	274.72	120.5	126.5	106.7	147.4	155.6
	4/1/2021 22:05	4/2/2021 4:08	North	5362	156.31	124.8	143.8	108.5	160.8	168.2
			North	5363	156.31	126.0	145.0	109.9	165.7	169.4
			East	5366	114.62	126.7	143.3	106.4	166.4	170.1
			South	5365	116.82	124.5	141.7	106.8	162.9	167.9
			West	5356	141.16	124.4	141.1	109.2	166.0	167.8
			South	5353	274.72	122.1	137.9	106.2	157.6	165.5

L_p and$L_{p.pk}$ = (dB re 1 μPa); L_E = (dB re 1 μPa²·s)

Conductor	Start Time	End Time	Monitor Station Name	L_p				L_E			
				LF	MF	HF	PP	LF	MF	HF	PP
B-1	4/1/2021 17:06	4/1/2021 17:25	5362	118.6	99.5	95.4	111.1	149.2	130.1	126.0	141.7
			5363	119.1	103.2	99.5	113.0	149.8	133.8	130.1	143.6
			5366	123.9	95.0	90.9	113.7	153.0	124.1	120.0	142.8
			5365	120.7	97.9	94.6	111.7	151.5	128.7	125.4	142.5
			5356	119.1	100.1	96.5	111.4	149.7	130.7	127.1	142.0
			5353	115.3	99.1	95.4	109.0	146.0	129.8	126.1	139.7
	4/1/2021 18:01	4/1/2021 18:54	5362	122.7	98.7	94.5	114.1	157.7	133.7	129.5	149.1
			5363	122.9	101.4	97.6	114.9	157.9	136.4	132.6	149.9
			5366	126.8	98.3	93.1	117.8	161.9	133.4	128.2	152.8
			5365	125.5	99.9	95.4	117.3	160.6	134.9	130.5	152.3
			5356	123.4	99.5	95.5	115.0	158.5	134.6	130.5	150.1
			5353	119.4	97.5	93.6	111.4	154.4	132.5	128.6	146.4
	4/1/2021 22:05	4/2/2021 4:08	5362	121.3	98.7	94.6	113.4	163.0	140.4	136.2	155.1
			5363	121.7	101.6	97.8	114.4	163.3	143.2	139.4	156.1
			5366	125.5	98.0	93.0	116.9	167.3	139.8	134.7	158.7
			5365	122.7	99.9	96.1	115.1	166.1	143.3	139.5	158.5
			5356	122.2	100.6	96.9	114.3	165.5	143.9	140.2	157.7
			5353	117.9	97.5	93.8	110.5	159.6	139.2	135.5	152.2

L_p and$L_{p,pk}$ = (dB re 1 μPa); L_E = (dB re 1 $\mu Pa^2 \cdot s$)
LF – low frequency; MF – mid-frequency; HF – high frequency; PP – phocid pinnipeds

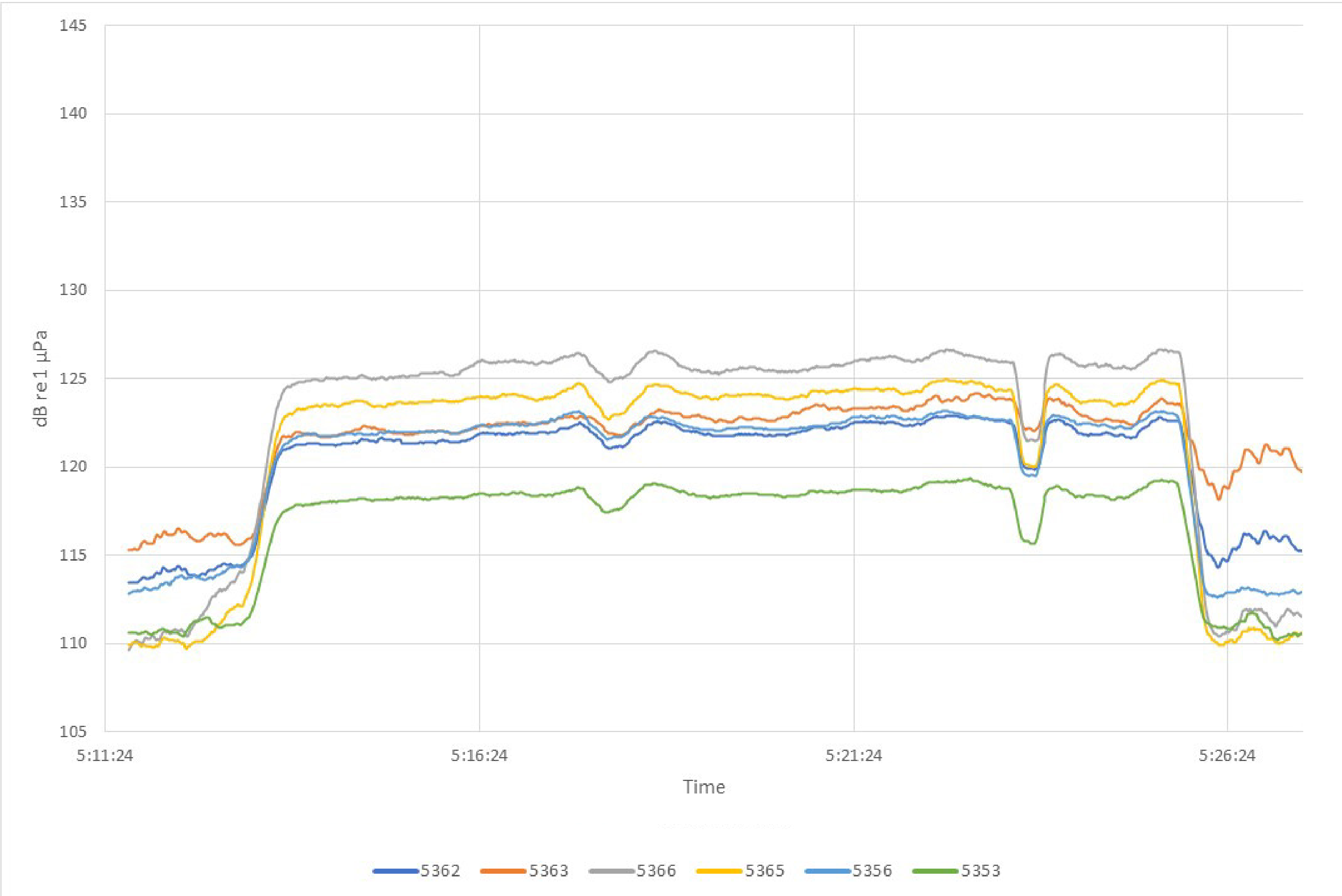

Figure B-1. Time History Plot of B-1 Mechanical Cut from April 1, 2021, 17:06 to 17:25 (20-second sample interval)

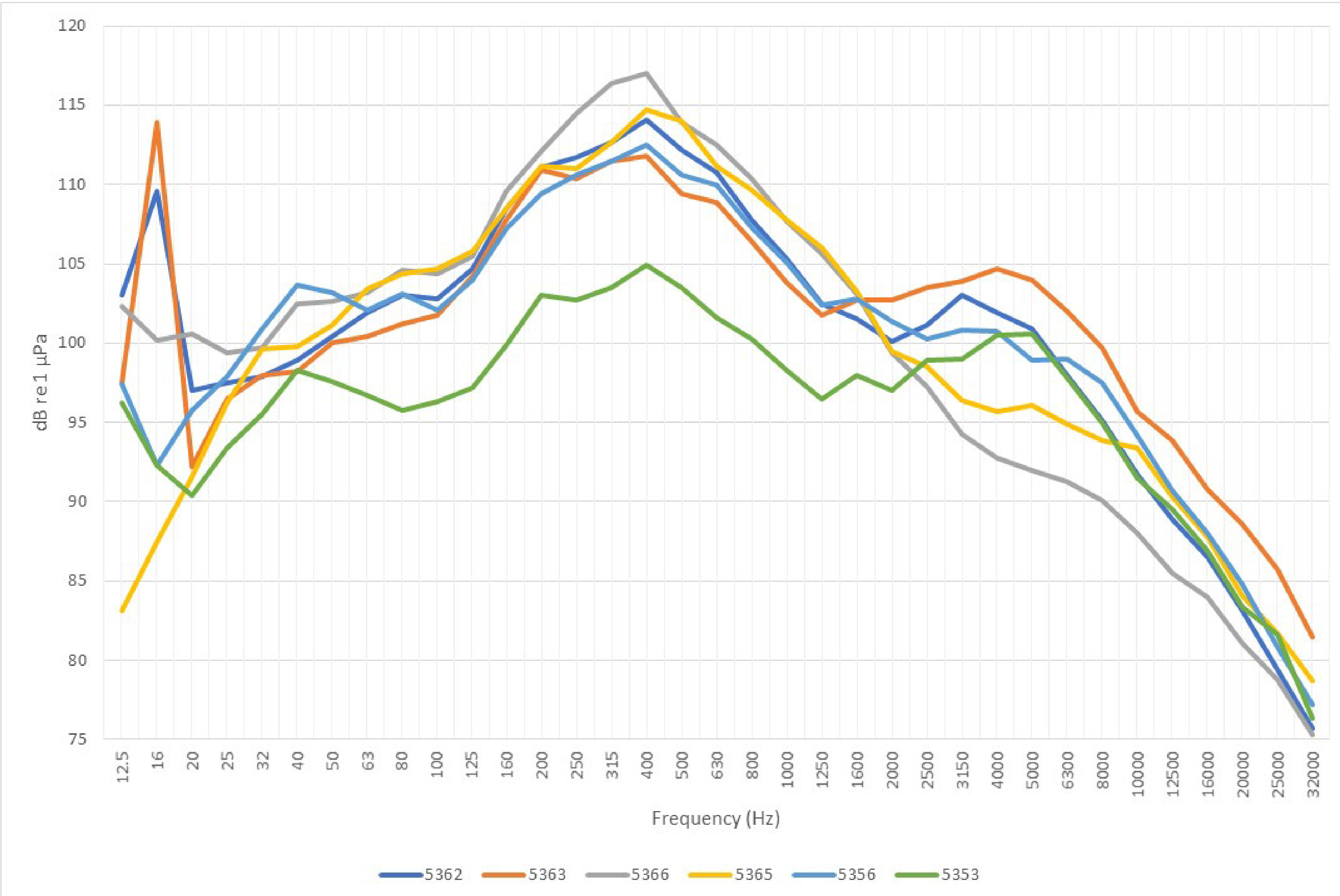

Figure B-2. SPL RMS 1/3 Octave Band Plot of B-1 Mechanical Cut from April 1, 2021, 17:06 to 17:25

Figure B-3. Time History Plot of B-1 Mechanical Cut from April 1, 2021, 18:01 to 18:54 (20-second sample interval)

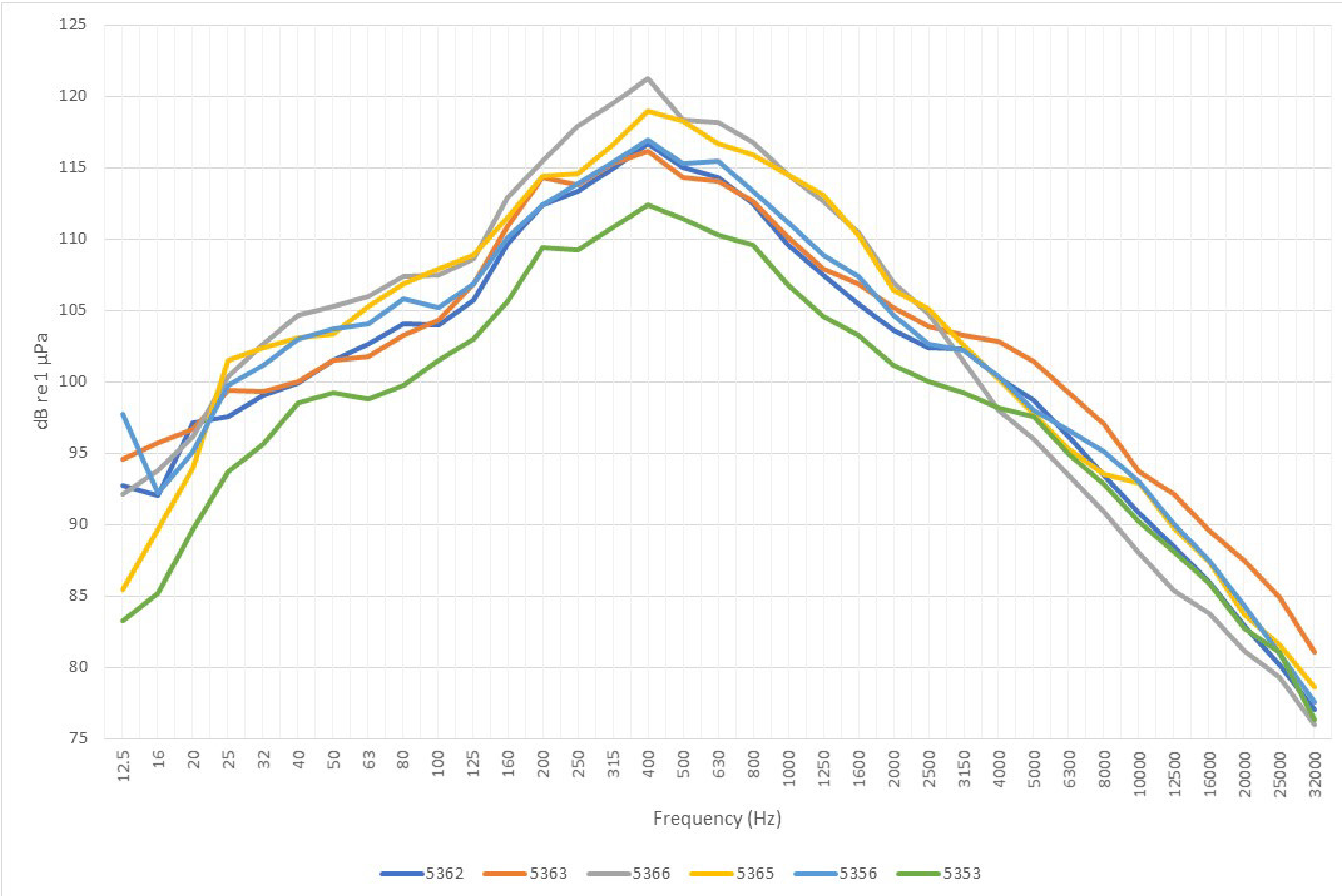

Figure B-4. SPL RMS 1/3 Octave Band Plot of B-1 Mechanical Cut from April 1, 2021, 18:01 to 18:54

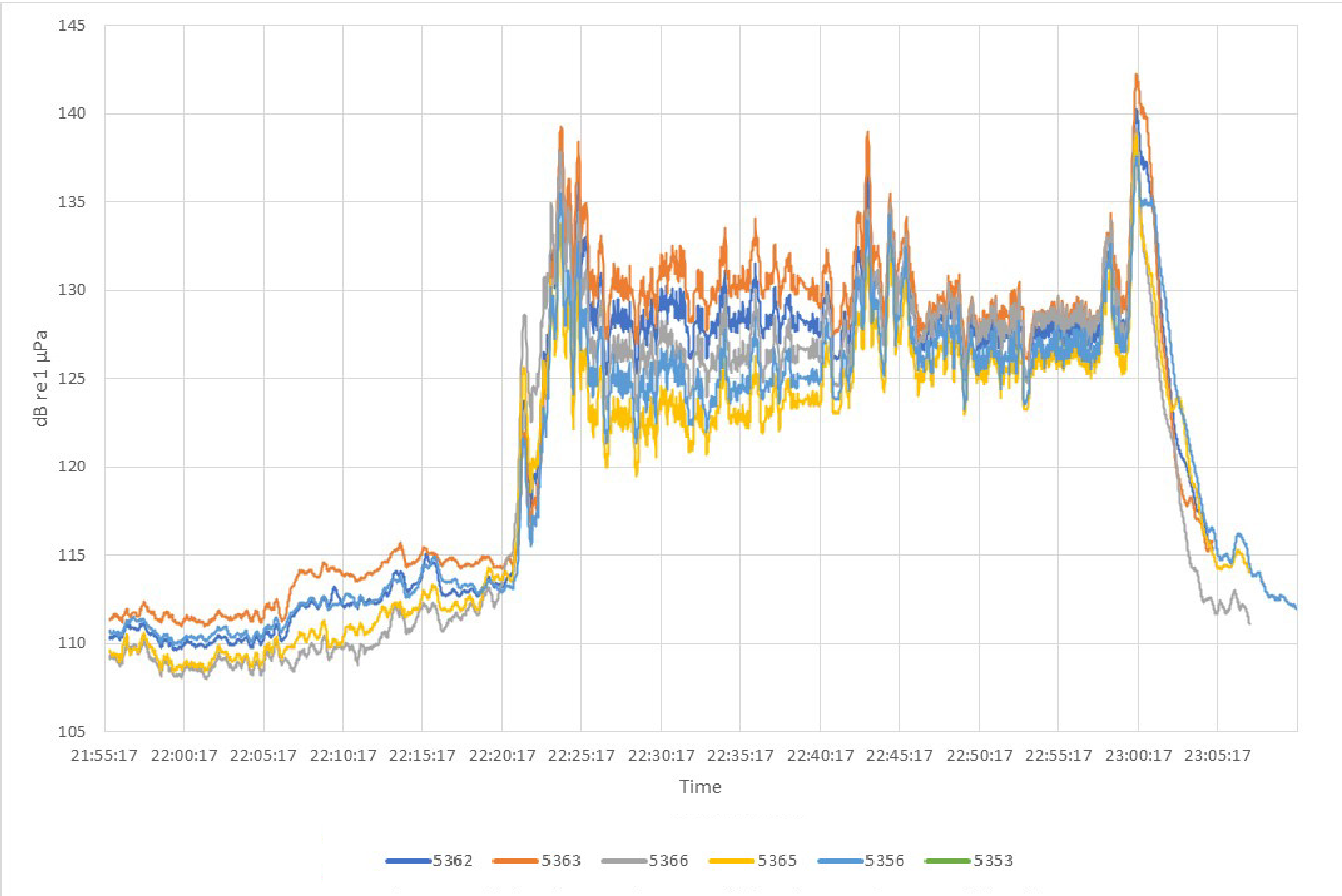

Figure B-5. Time History Plot of B-1 Mechanical Cut from April 1, 2021, 22:05 to 4:08 (20-second sample interval)

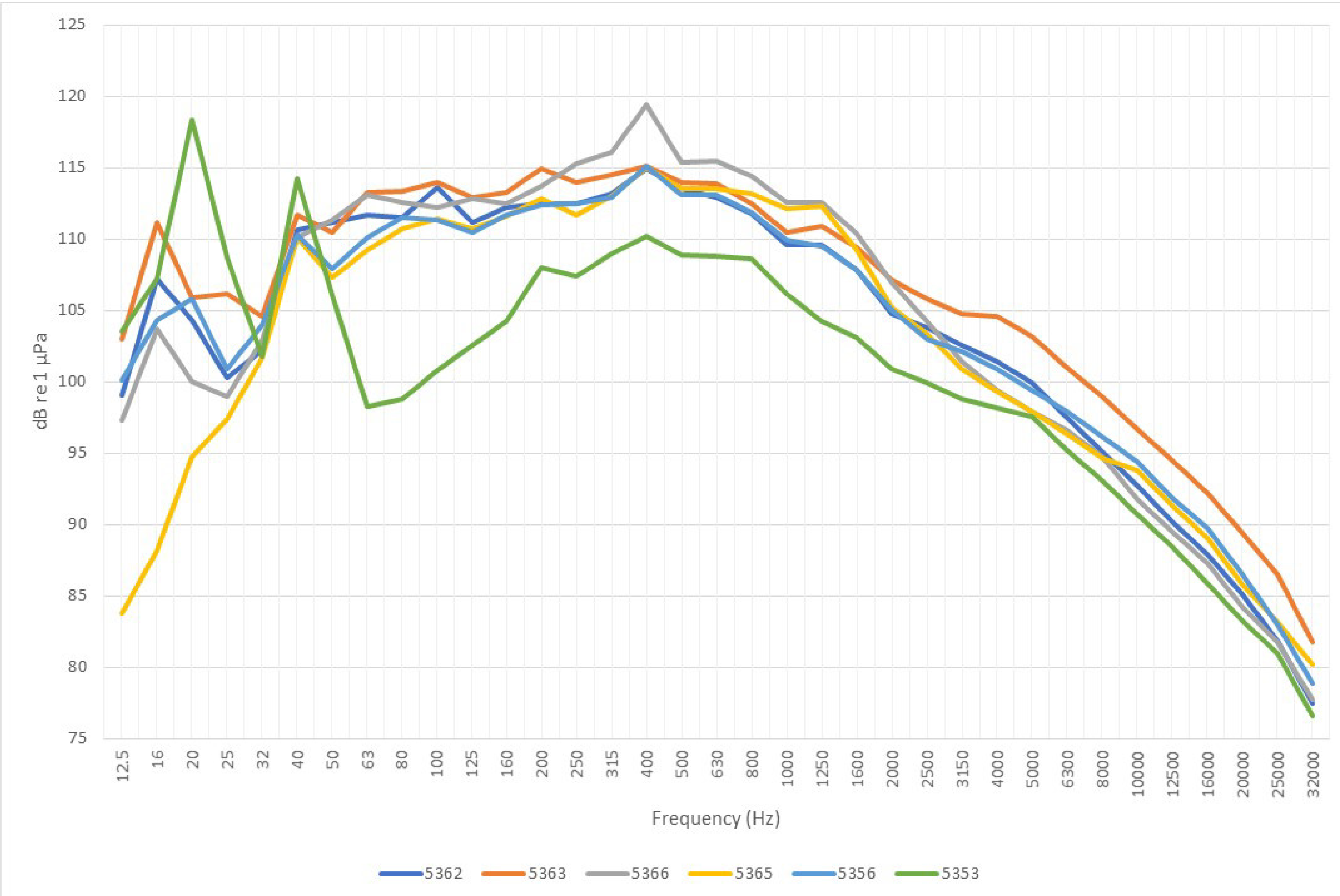

Figure B-6. SPL RMS 1/3 Octave Band Plot of B-1 Mechanical Cut from April 1, 2021, 22:05 to 4:08

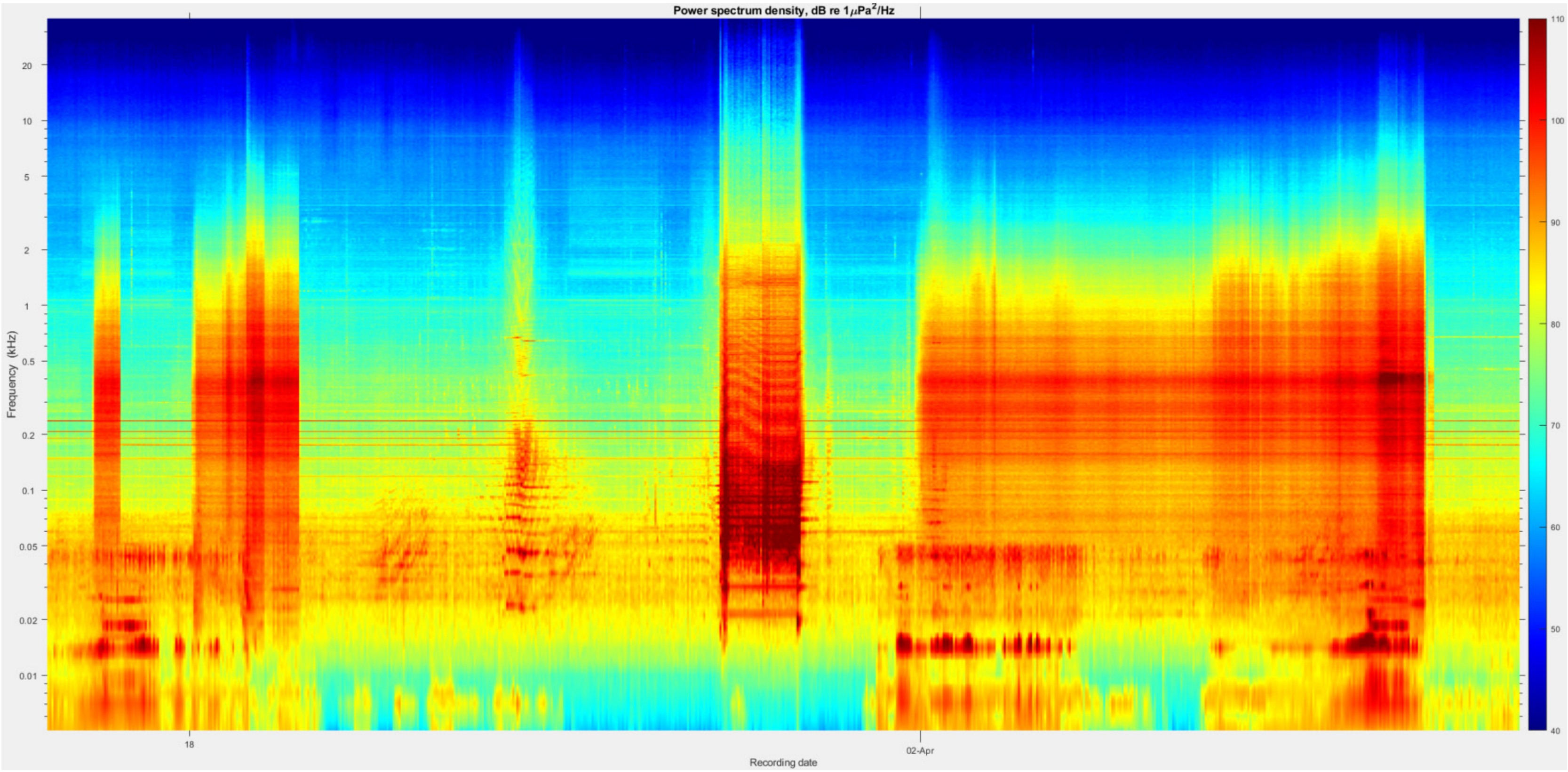

Figure B-7. PSD Spectrogram Plot of B-1 Mechanical Cut from 17:06 April 1, 2021 to 4:08 April 2, 2021

Table B-4. Wellbore Conductor B-9
(17:42 April 2, 2021 – 21:42 April 3, 2021)

Conductor	Start Time	End Time	Total Duration of Cut (minutes)	Overall Wall Thickness (inches)	Cut Depth Below Mudline (Feet)	Cutter RPM
B-9	4/2/2021 17:42	4/2/2021 19:18	96	1.542	22	68
	4/2/2021 23:37	4/3/2021 6:28	411			
	4/3/2021 15:35	4/3/2021 21:42	367			

Conductor	Start Time	End Time	Direction	Monitor Station Name	Distance to Conductor (m)	L_p	Max L_p	Min L_p	$L_{p,pk}$	L_E
B-9	4/2/2021 17:42	4/2/2021 19:18	North	5362	152.9	123.1	129	117.7	150.7	160.7
			North	5363	152.9	123.6	129.3	111.2	147	161.3
			East	5366	116.78	126.2	133.5	108.7	155.6	163.9
			South	5365	119.26	124.1	130.3	108.2	153.1	161.7
			West	5356	139.5	123.7	129.6	110.4	147.6	161.3
			South	5353	275.73	119.1	124.6	107	144.4	156.8
	4/2/2021 23:37	4/3/2021 6:28	North	5362	152.9	128.4	146.6	111.2	164	172.3
			North	5363	152.9	129.7	147.7	112.5	169.3	173.6
			East	5366	116.78	128.5	142.3	109.5	164	172.4
			South	5365	119.26	128.6	142.7	111	162.2	172.5
			West	5356	139.5	129.7	144.5	112.4	167.7	173.6
			South	5353	275.73	124.2	137	110.4	161.1	168.1
	4/3/2021 15:35	4/3/2021 21:42	North	5362	152.9	129.6	143.5	110.9	164.4	173
			North	5363	152.9	131.8	144.6	111.3	169.9	175.2
			East	5366	116.78	128.1	140.2	109.9	162.6	171.5
			South	5365	119.26	126.9	141.3	109.8	162.2	170.4
			West	5356	139.5	129.1	145	111.8	167.3	172.5
			South	5353	275.73	122.4	138	108.9	161.3	165.8

L_p and$L_{p,pk}$ = (dB re 1 μPa); L_E = (dB re 1 μPa^2·s)

Conductor	Start Time	End Time	Monitor Station Name	L_p				L_E			
				LF	MF	HF	PP	LF	MF	HF	PW
B-9	4/2/2021 17:42	4/2/2021 19:18	5362	122.3	99.7	95.3	115.4	160	137.3	100.4	153
			5363	122.7	101.8	97.9	115.6	160.3	139.4	135.5	153.3
			5366	125.6	100	94.4	118.7	163.3	137.7	132.1	156.3
			5365	123.2	99.5	95.4	115.9	160.8	137.1	133	153.5
			5356	122.9	99.7	95.6	115.5	160.5	137.3	133.2	153.1
			5353	118.2	97.2	93.4	111.1	155.8	134.9	131.1	148.7
	4/2/2021 23:37	4/3/2021 6:28	5362	125.4	105.1	101.5	118.2	169.3	149	145.4	162.1
			5363	126.7	107.6	104.3	119.7	170.7	151.5	148.2	163.6
			5366	126	103	98.8	118.7	169.9	146.9	142.7	162.7
			5365	125.1	105.4	102.2	117.7	169.1	149.4	146.2	161.8
			5356	126.6	105.2	101.6	118.7	170.5	149.1	145.5	162.6
			5353	121.4	101.9	98.5	114	165.3	145.8	142.4	157.9
	4/3/2021 15:35	4/3/2021 21:42	5362	126.3	105.4	101.7	118.7	169.7	148.9	145.1	162.2
			5363	128.6	108.8	105.3	121.3	172	152.2	148.7	164.7
			5366	125	104.1	100.6	117.7	168.4	147.5	144	161.1
			5365	123.4	104.7	101.4	115.9	166.9	148.2	144.9	159.4
			5356	125.8	104.8	101.3	117.9	169.2	148.3	144.7	161.4
			5353	119.7	101.1	97.9	112.4	163.2	144.5	141.3	155.9

L_p and$L_{p,pk}$ = (dB re 1 μPa); L_E = (dB re 1 μPa²·s)
LF – low frequency; MF – mid-frequency; HF – high frequency; PP – phocid pinnipeds

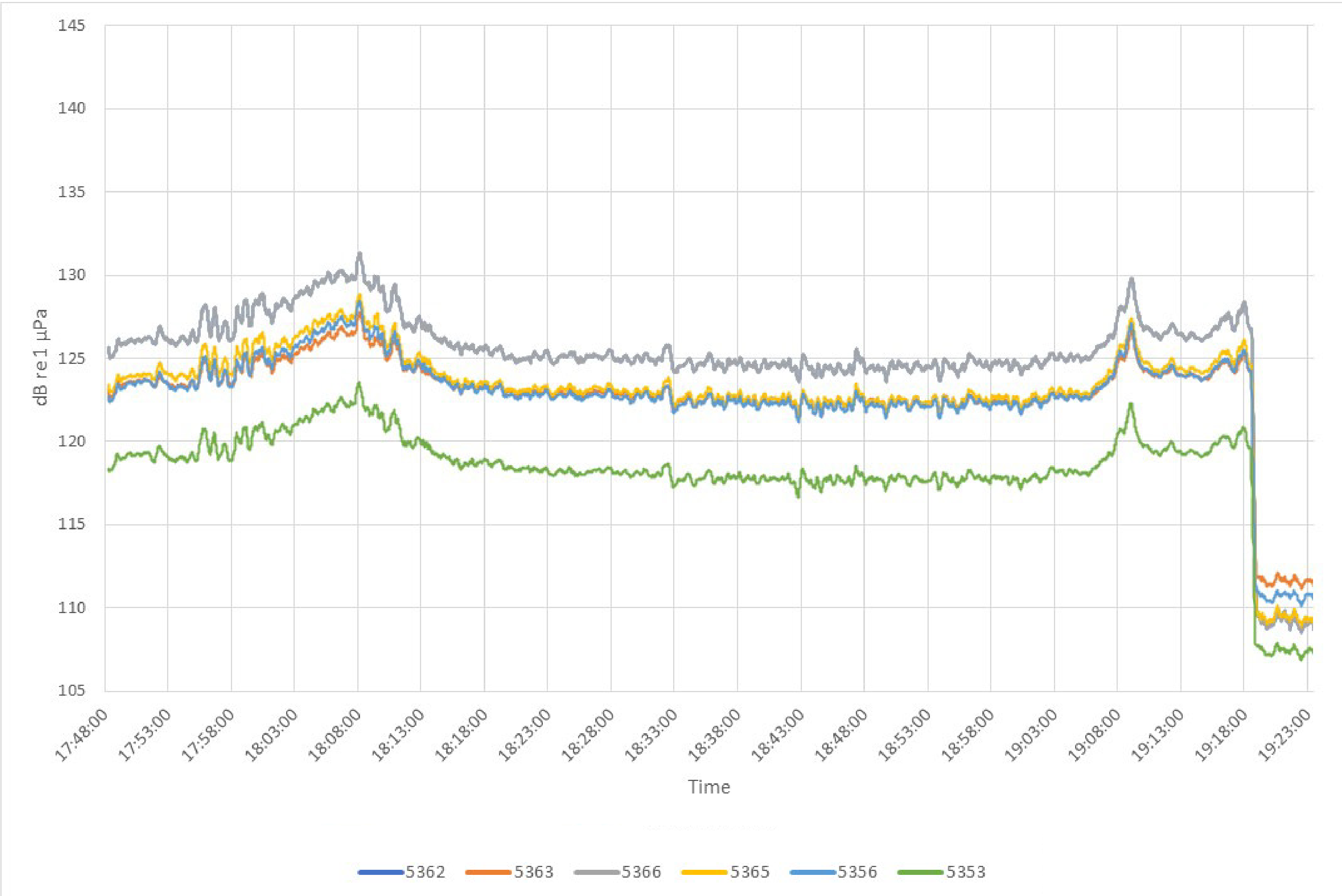

Figure B-8. Time History Plot of B-9 Mechanical Cut from April 2, 2021, 17:42 to 19:18 (20-second sample interval)

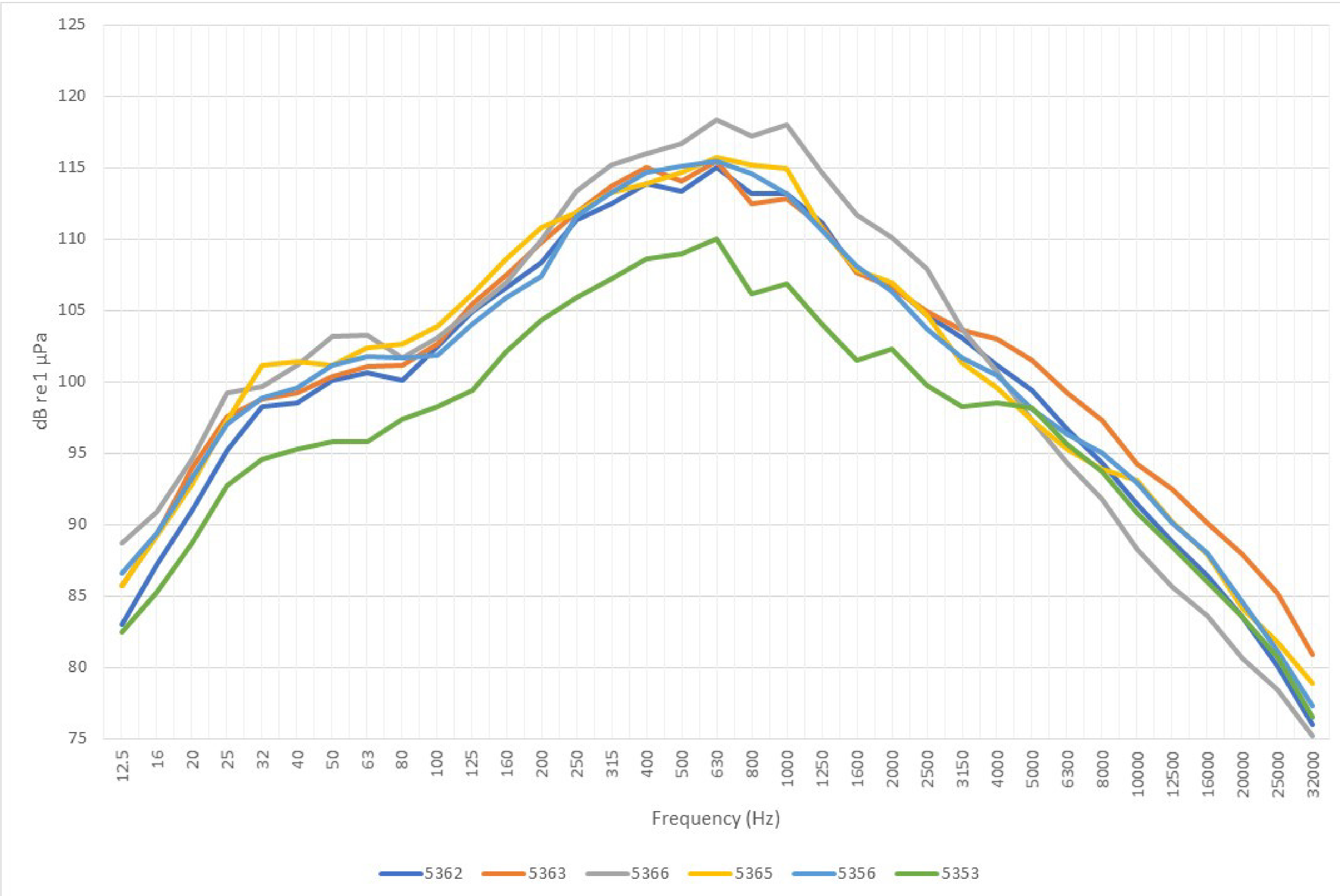

Figure B-9. SPL RMS 1/3 Octave Band Plot of B-9 Mechanical Cut from April 2, 2021, 17:42 to 19:18

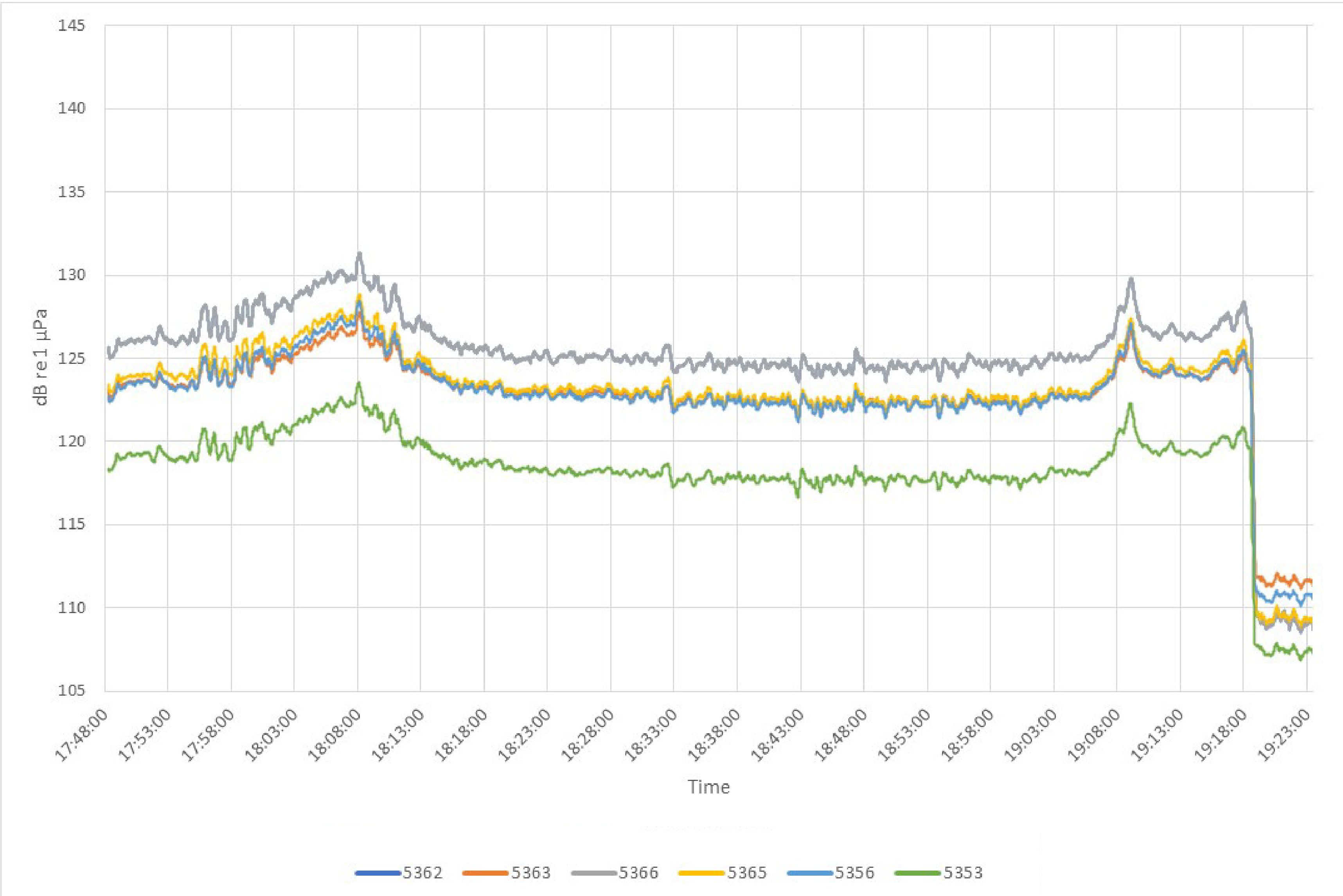

Figure B-10. Time History Plot of B-9 Mechanical Cut from April 2, 2021, 23:37 to April 3, 2021, 6:28 (20-second sample interval)

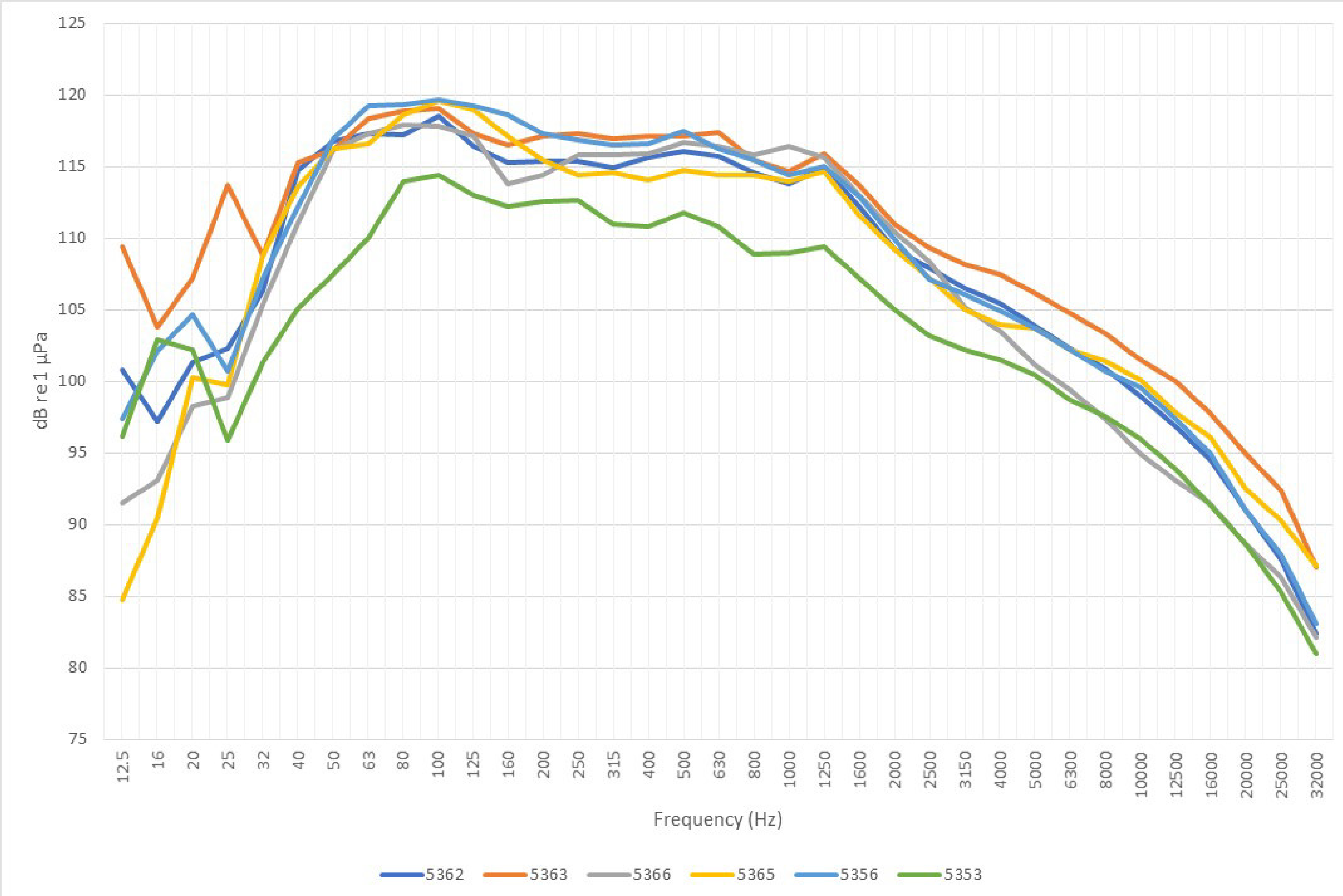

Figure B-11. SPL RMS 1/3 Octave Band Plot of B-9 Mechanical Cut from April 2, 2021, 23:37 to April 3, 2021, 6:28

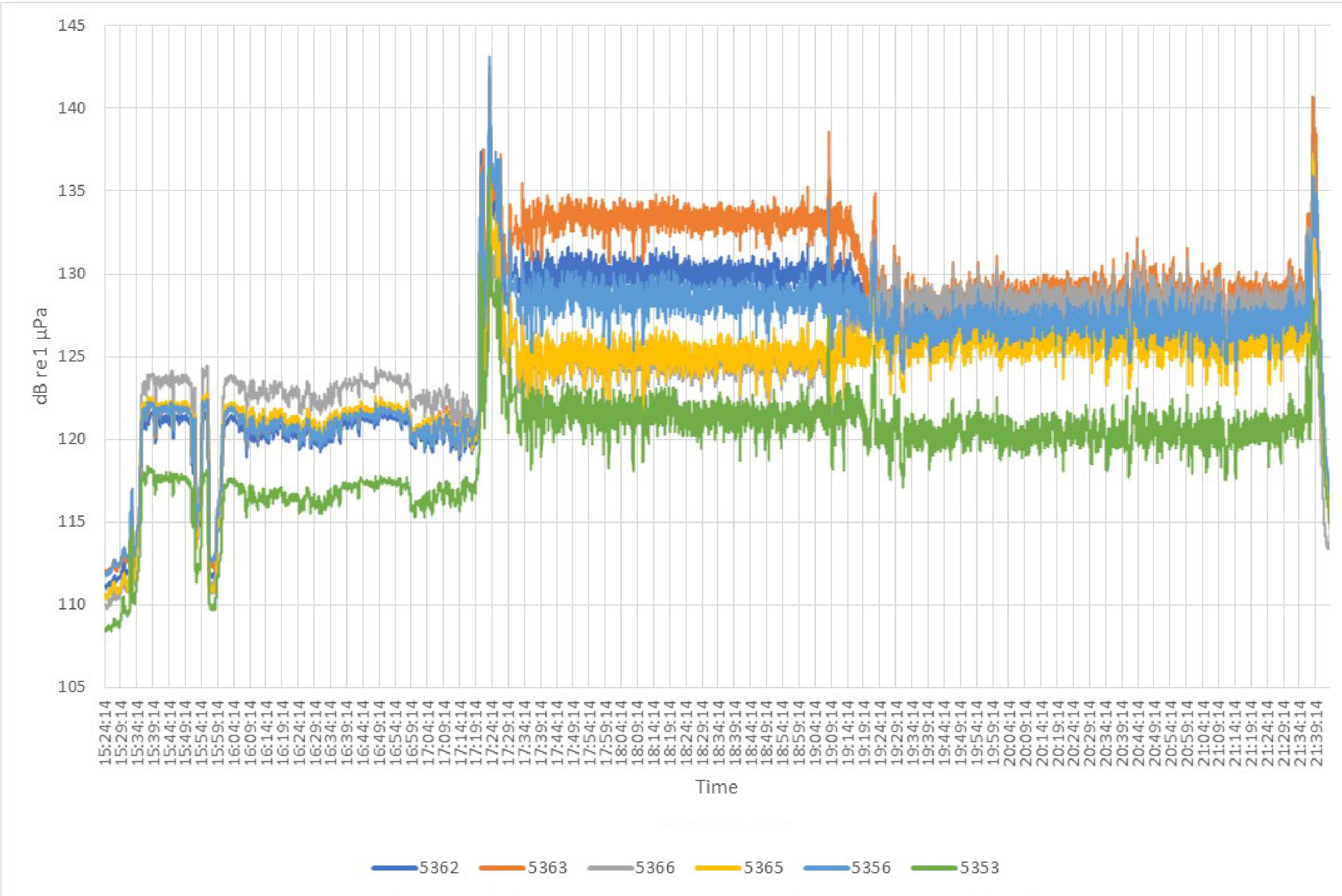

Figure B-12. Time History Plot of B-9 Mechanical Cut from April 3, 2021, 15:35 to 21:42 (20-second sample interval)

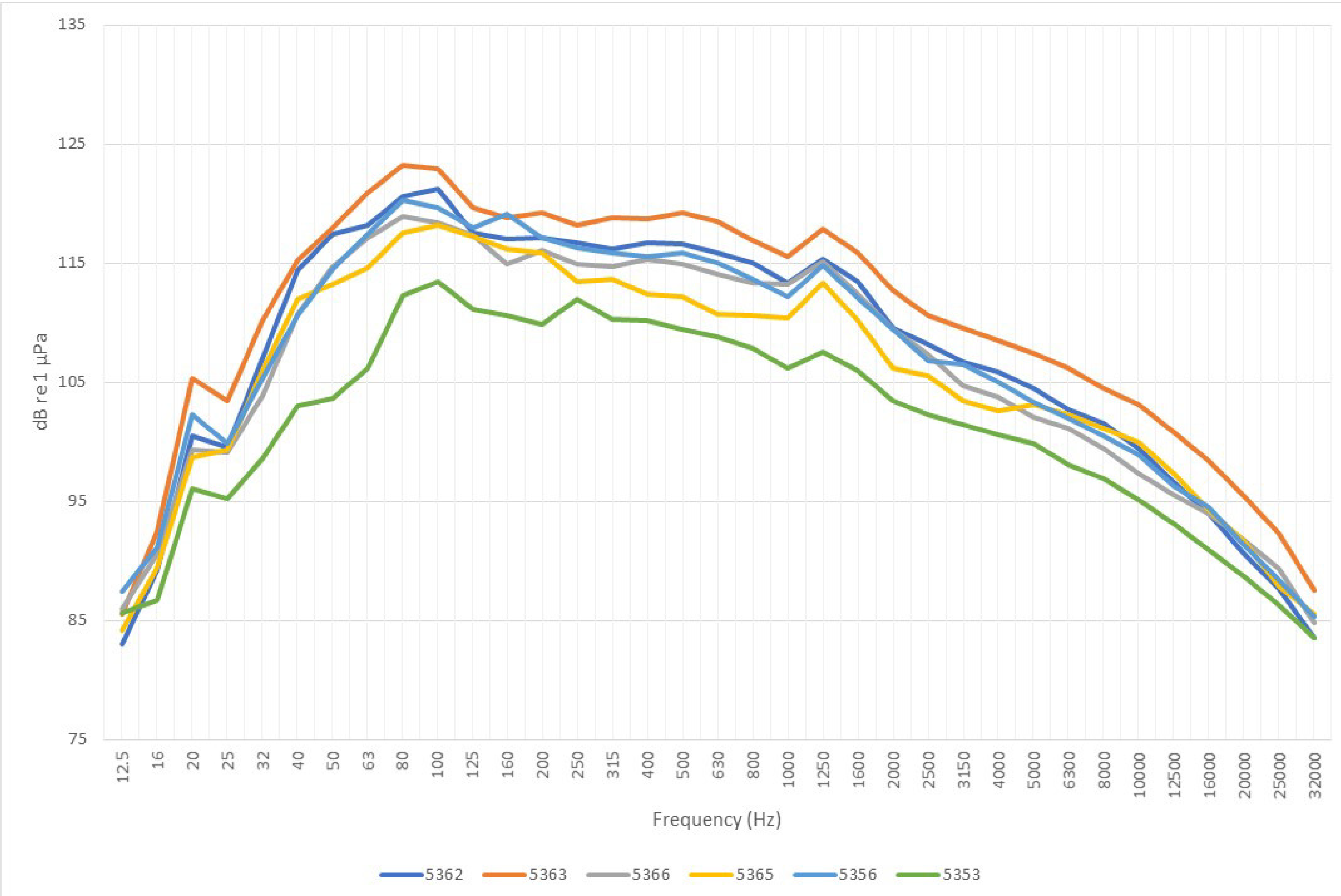

Figure B-13. SPL RMS 1/3 Octave Band Plot of B-9 Mechanical Cut from April 3, 2021, 15:35 to 21:42

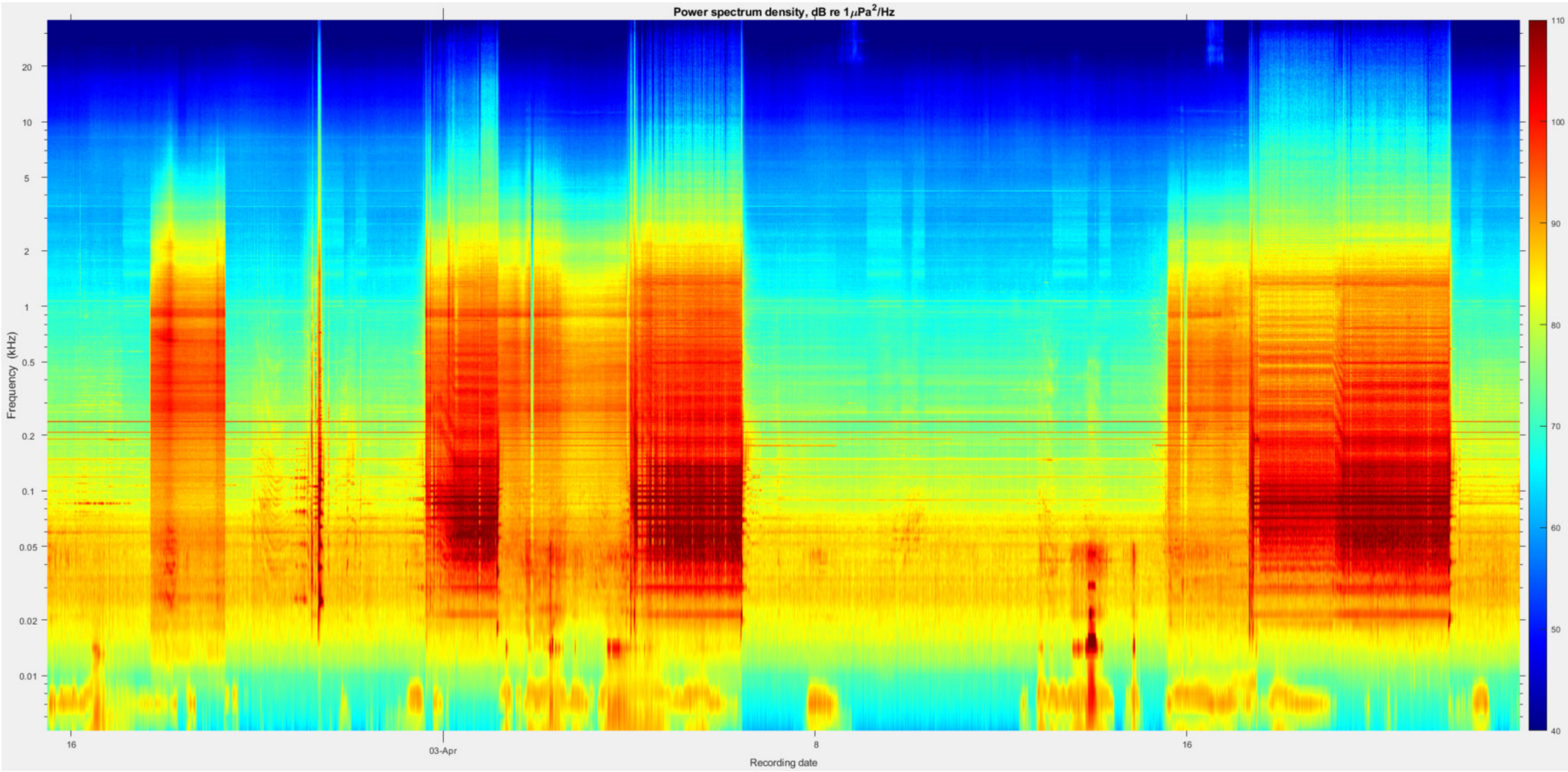

Figure B-14. PSD Spectrogram Plot of B-9 Mechanical Cut from 17:42 April 2, 2021 – 21:42 April 3, 2021

Table B-5. Conductor B-16 Noise Monitoring Results Summary
(14:19 April 4, 2021 – 23:02 April 5, 2021)

Conductor	Start Time	End Time	Total Duration of Cut (minutes)	Overall Wall Thickness (inches)	Cut Depth Below Mudline (Feet)	Cutter RPM
B-16	4/4/2021 14:19	4/4/2021 16:37	138	1.919	25	72
	4/4/2021 19:00	4/5/2021 8:03	783			
	4/5/2021 11:58	4/5/2021 23:32	694			

Conductor	Start Time	End Time	Direction	Monitor Station Name	Distance to Conductor (m)	L_p	Max L_p	Min L_p	$L_{p,pk}$	L_E
B-16	4/4/2021 14:19	4/4/2021 16:37	North	5362	149.69	128.5	142.5	112.4	161.7	167.7
			North	5363	149.69	130.6	145.7	113.2	165.3	169.8
			East	5366	115.23	127.8	143.0	110.2	159.2	167.0
			South	5365	123.11	125.5	139.9	112.3	155.9	164.7
			West	5356	141.64	127.1	140.3	113.4	160.2	166.3
			South	5353	279.47	121.0	135.9	110.0	153.8	160.2
	4/4/2021 19:00	4/5/2021 8:03	North	5362	149.69	124.1	144.2	109.5	163.1	170.8
			North	5363	149.69	125.3	145.1	113.7	166.3	172.1
			East	5366	115.23	125.2	140.6	109.4	162.3	171.9
			South	5365	123.11	122.8	138.7	108.8	156.5	169.4
			West	5356	141.64	123.8	142.7	110.3	159.8	170.5
			South	5353	279.47	118.3	137.2	107.5	154.4	165.1
	4/5/2021 11:58	4/5/2021 23:32	North	5362	149.69	120.6	127.5	110.2	154.6	166.8
			North	5363	149.69	121.3	136.3	111.0	154.4	167.5
			East	5366	115.23	123.3	130.3	109.0	159.4	169.5
			South	5365	123.11	120.9	131.3	109.9	154.8	167.1
			West	5356	141.64	121.4	132.2	110.7	156.2	165.1
			South	5353	279.47	116.9	123.9	107.2	148.7	163.1

L_p and $L_{p,pk}$ = (dB re 1 μPa); L_E = (dB re 1 μPa^2·s)

Conductor	Start Time	End Time	Monitor Station Name	L_p				L_E			
				LF	MF	HF	PP	LF	MF	HF	PP
B-16	4/4/2021 14:19	4/4/2021 16:37	5362	125.3	103.0	99.1	117.5	164.5	142.2	138.3	156.7
			5363	127.5	106.2	102.5	119.9	166.5	145.2	141.6	159.0
			5366	125.3	102.3	98.3	117.8	164.6	141.5	137.5	157.1
			5365	122.2	100.5	97.1	114.2	161.4	139.7	136.3	153.4
			5356	124.3	102.9	99.3	116.5	163.5	142.1	138.5	155.7
			5353	118.4	98.0	94.6	110.6	157.6	137.2	133.8	149.8
	4/4/2021 19:00	4/5/2021 8:03	5362	121.8	100.7	96.8	114.4	167.8	146.7	142.8	160.4
			5363	122.7	103.6	100.1	115.6	169.4	150.3	146.8	162.3
			5366	123.0	100.0	95.6	115.6	169.8	146.7	142.3	162.3
			5365	119.9	99.1	95.8	112.0	166.5	145.6	142.4	158.6
			5356	121.3	100.6	97.0	113.7	168.1	147.3	143.8	160.4
			5353	116.2	97.5	94.1	109.1	162.9	144.2	140.8	155.8
	4/5/2021 11:58	4/5/2021 23:32	5362	119.1	98.4	94.4	111.6	165.3	144.6	140.6	157.8
			5363	119.7	101.0	97.3	112.7	165.9	147.2	143.5	158.9
			5366	122.0	97.6	92.7	114.3	168.2	143.8	138.9	160.4
			5365	118.9	97.4	94.1	110.5	165.1	143.6	140.3	156.7
			5356	119.9	98.8	95.0	112.2	166.1	145.0	141.2	158.3
			5353	115.3	96.4	92.8	108.1	161.4	142.5	138.9	154.3

L_p and $L_{p,pk}$ = (dB re 1 μPa); L_E = (dB re 1 μPa^2·s)
LF – low frequency; MF – mid-frequency; HF – high frequency; PP – phocid pinnipeds

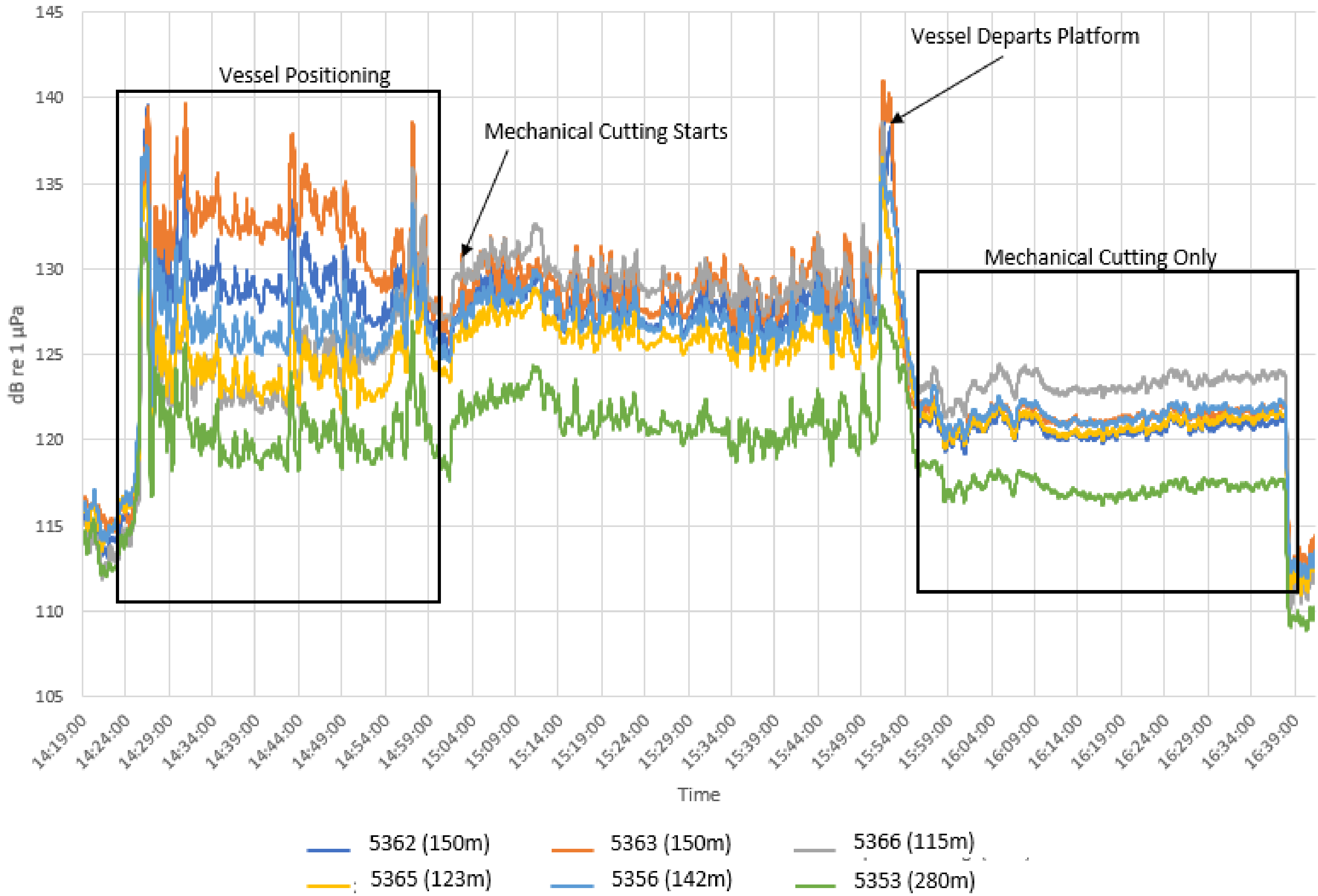

Figure B-15. Time History Plot of B-16 Mechanical Cut from April 4, 2021, 14:19 to 16:37 (20-second sample interval)

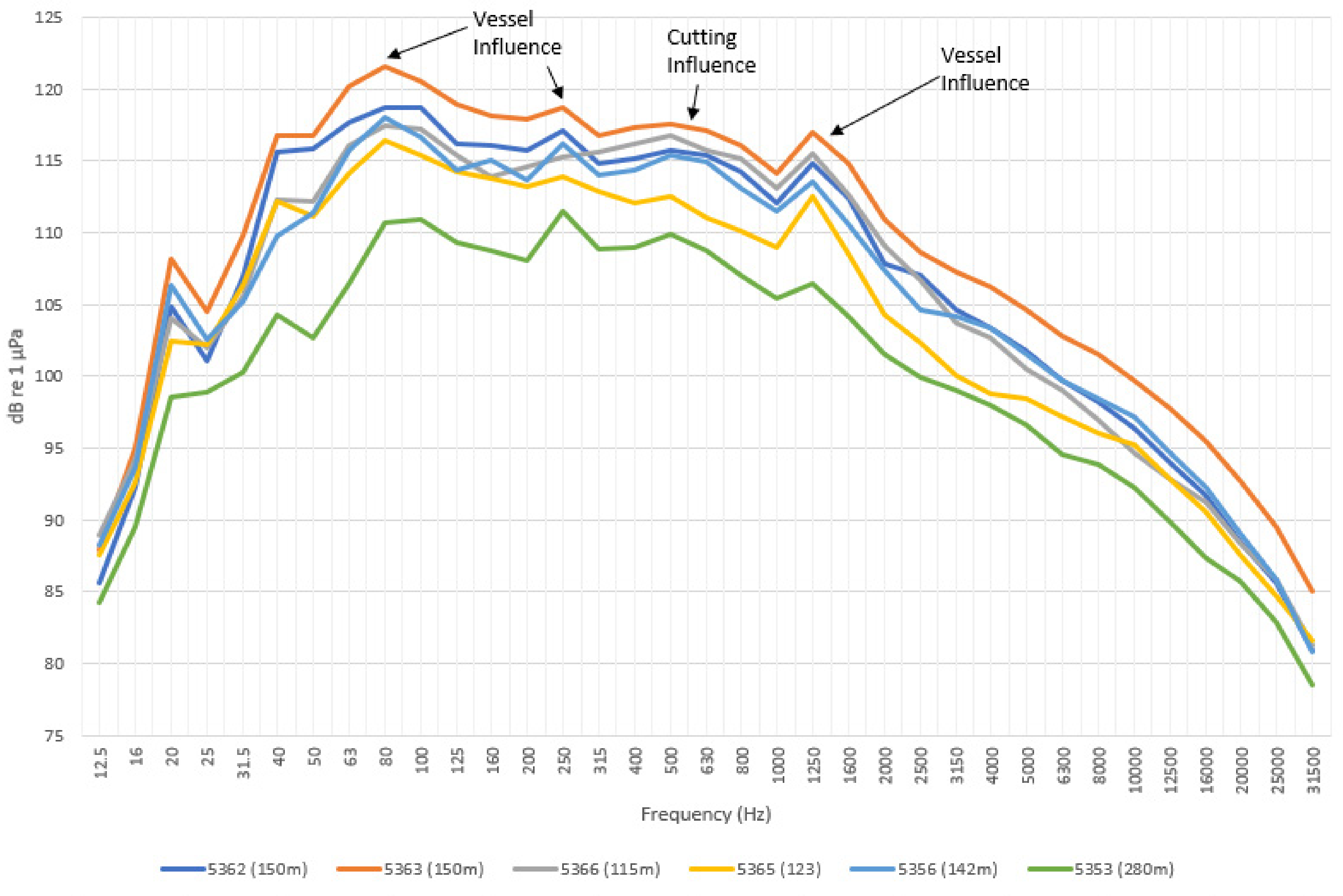

Figure B-16. SPL RMS 1/3 Octave Band Plot of B-16 Mechanical Cut from April 4, 2021, 14:19 to 16:37

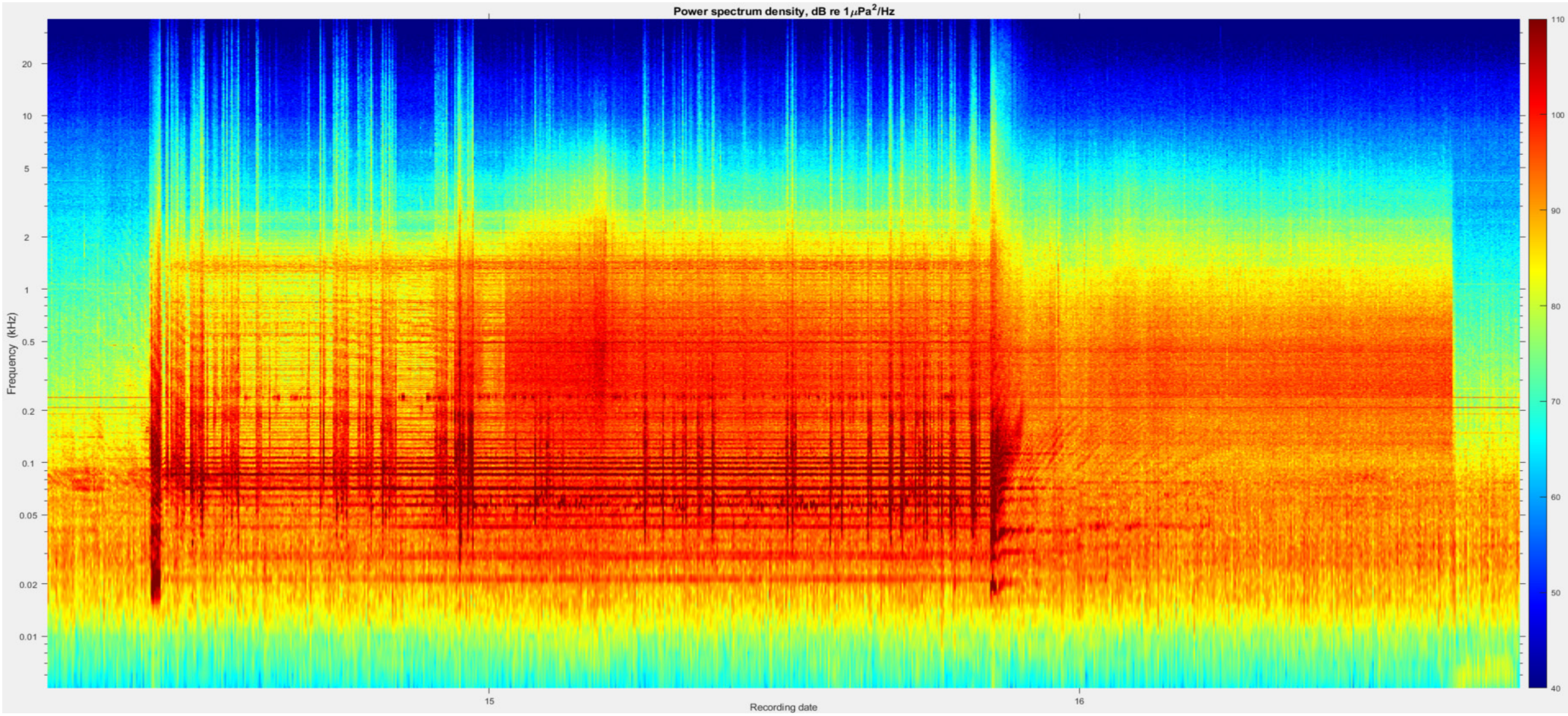

Figure B-17. PSD Spectrogram Plot of B-16 Mechanical Cut from 14:19 to 16:37 (SoundTrap 5366)

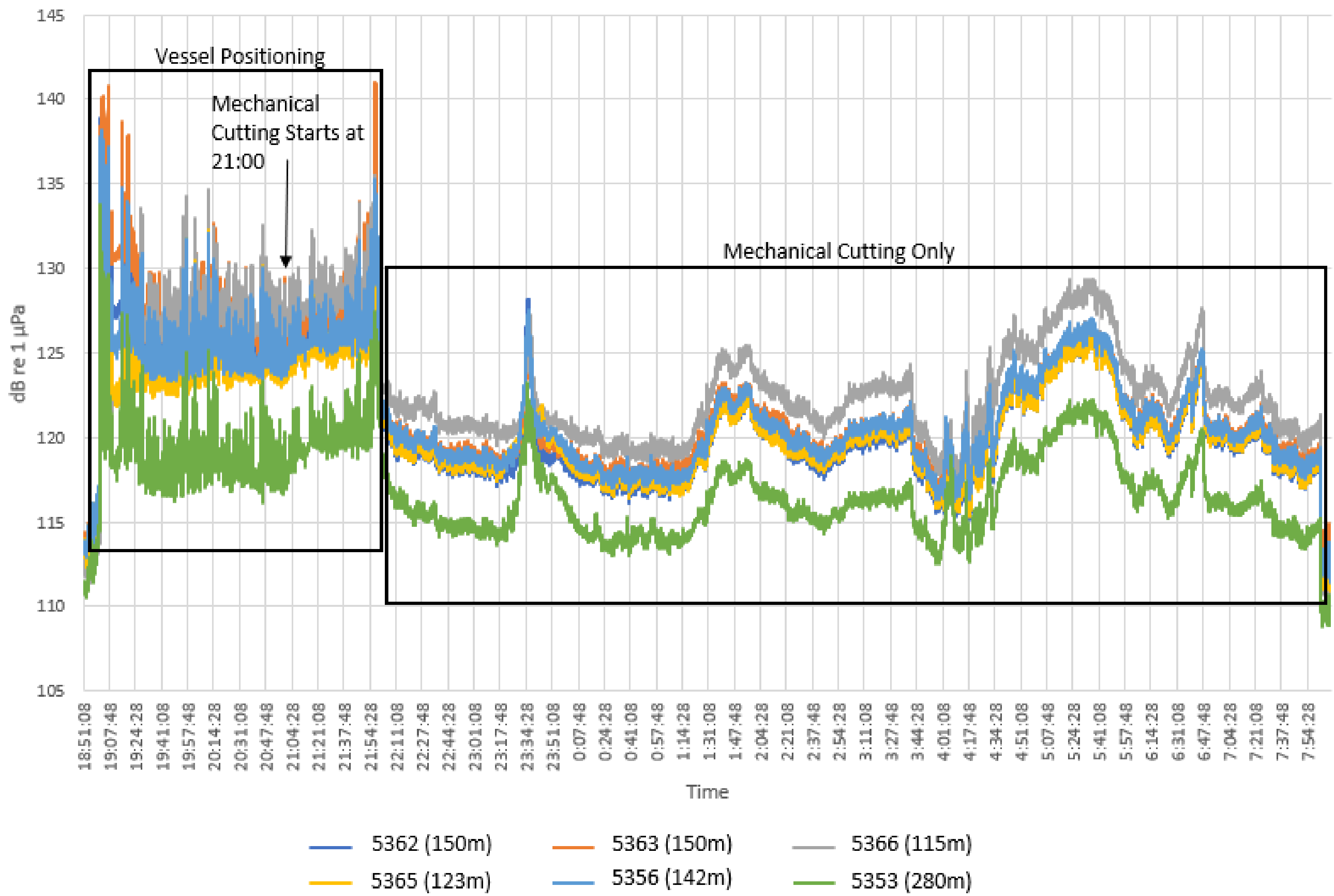

Figure B-18. Time History Plot of B-16 Mechanical Cut from April 4, 2021, 19:00 to April 5, 2021, 8:03 (20-second sample interval)

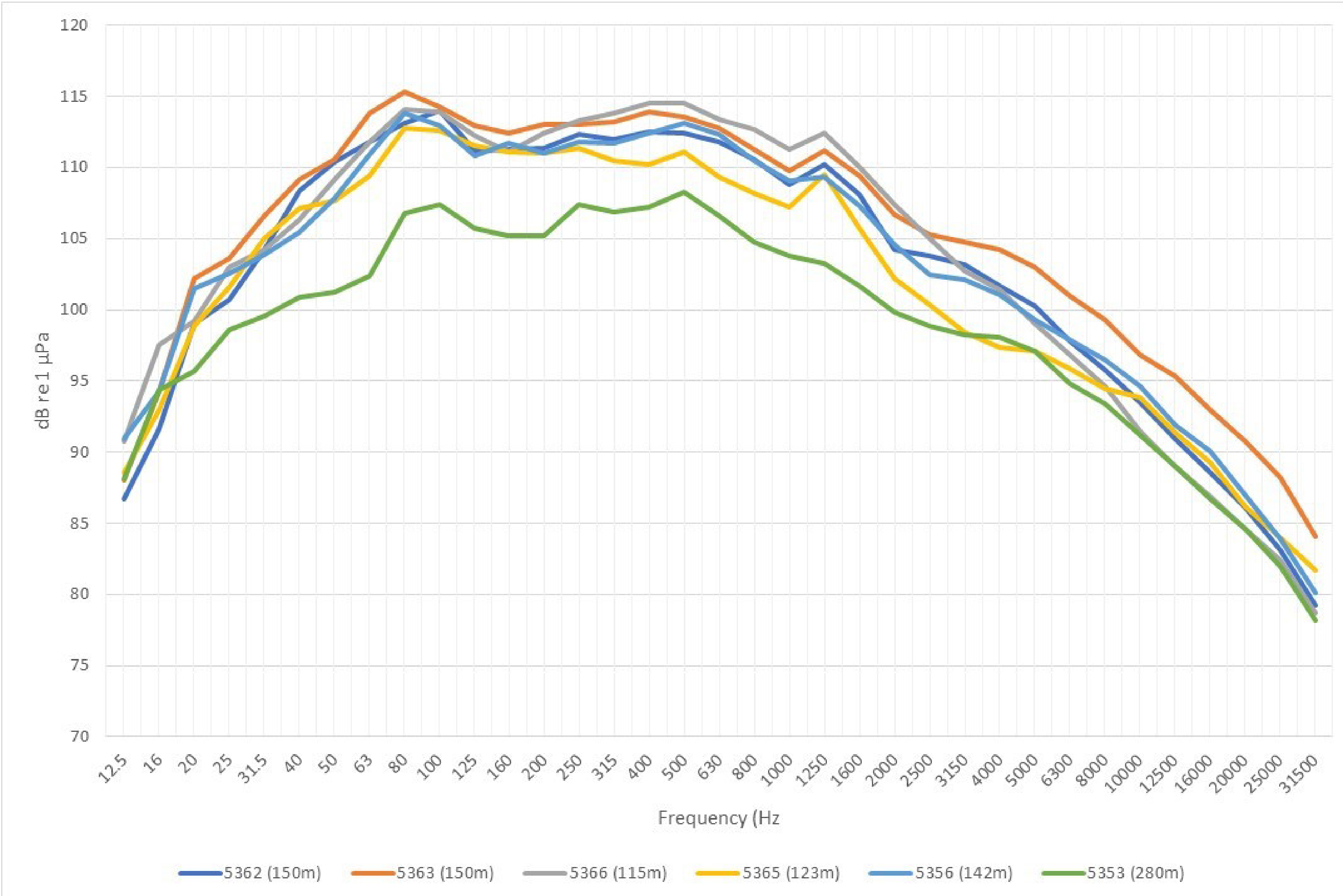

Figure B-19. SPL RMS 1/3 Octave Band Plot of B-16 Mechanical Cut from April 4, 2021, 19:00 to April 5, 2021, 8:03

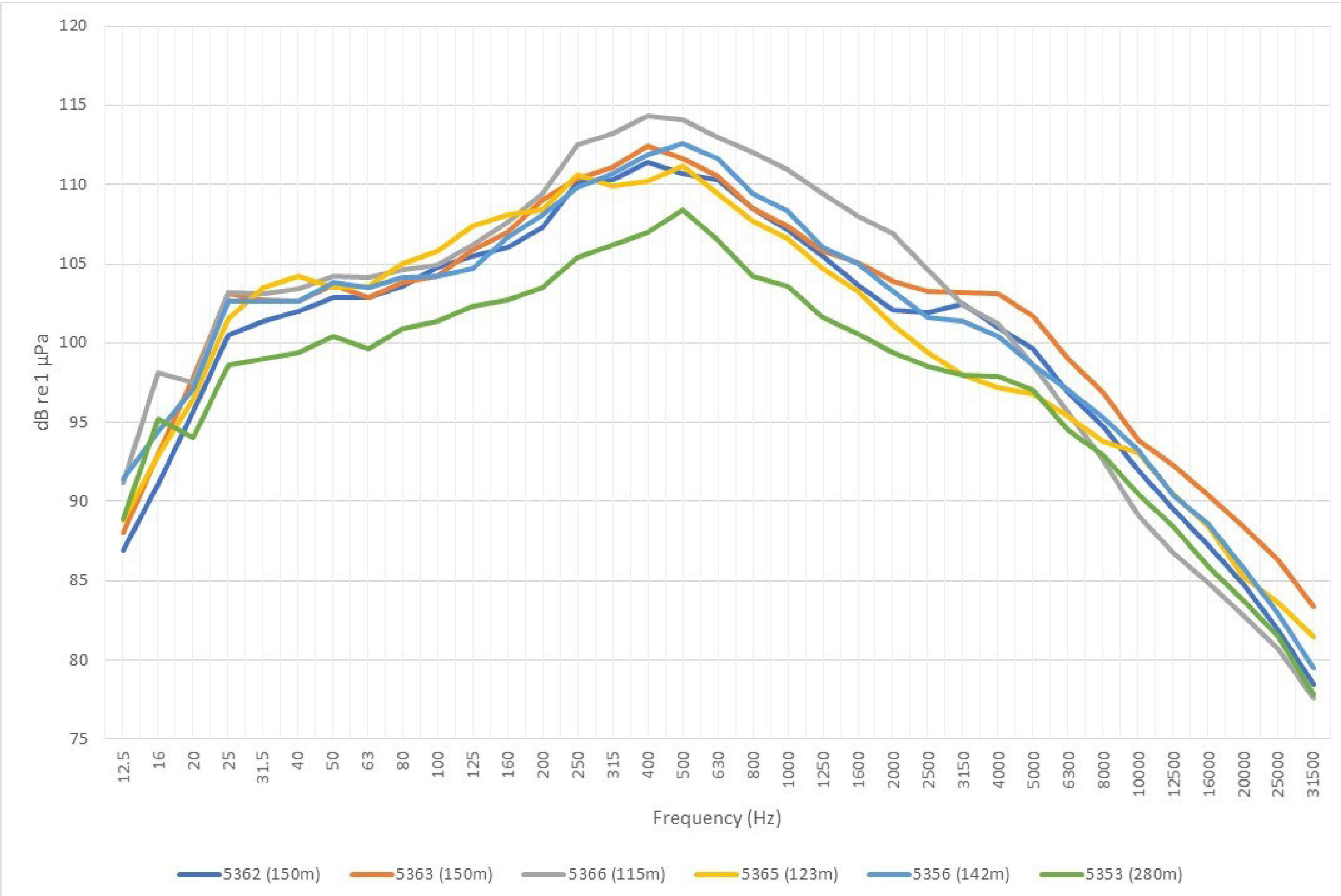

Figure B-20. SPL RMS 1/3 Octave Band Plot of B-16 Mechanical Cut from April 4, 2021, 19:00 to April 5, 2021, 8:03 (Mechanical Cutting Only)

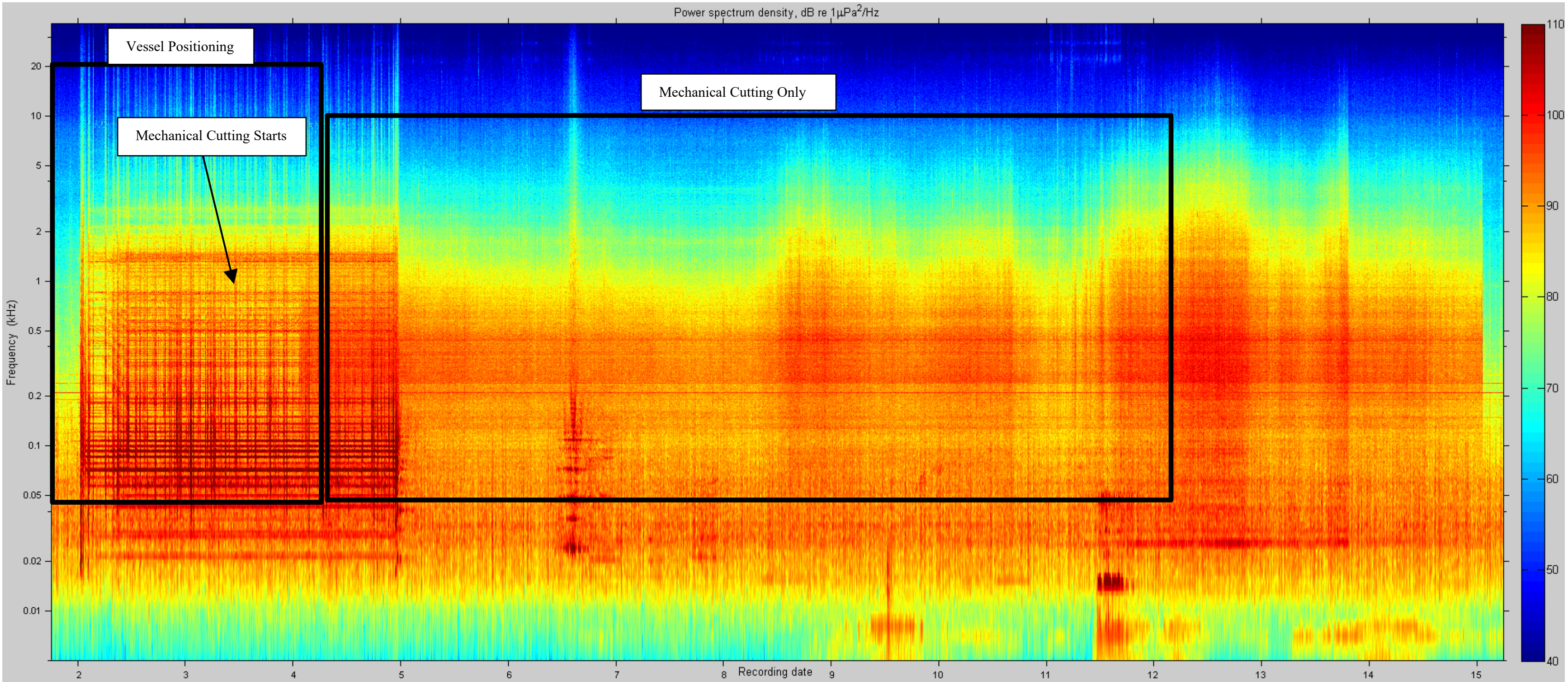

Figure B-21. PSD Spectrogram Plot of B-16 Mechanical Cut from April 4, 2021, 19:00 to April 5, 2021, 8:03

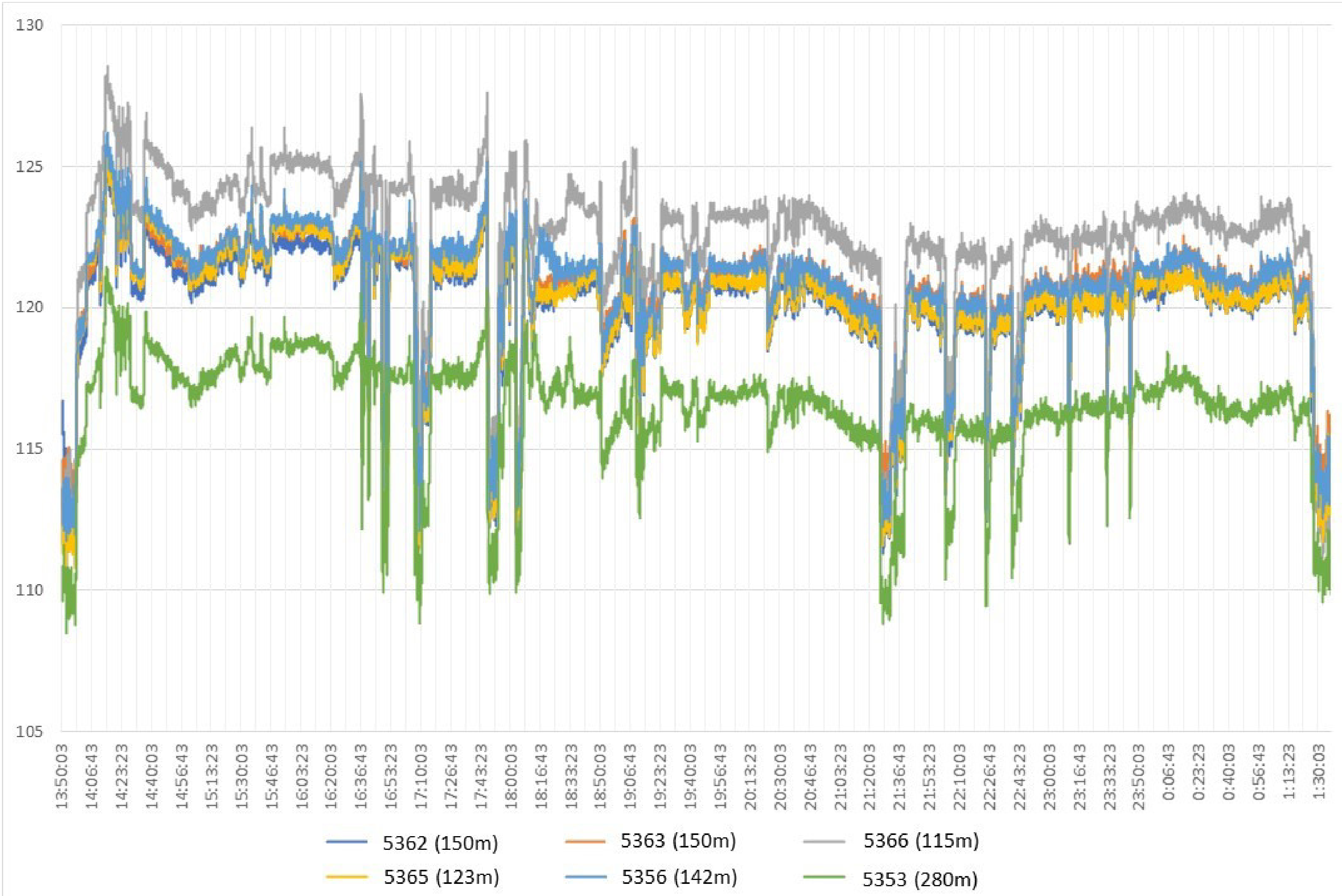

Figure B-22. Time History Plot of B-16 Mechanical Cut from April 5, 2021, 11:58 to 23:32 (20-second sample interval)

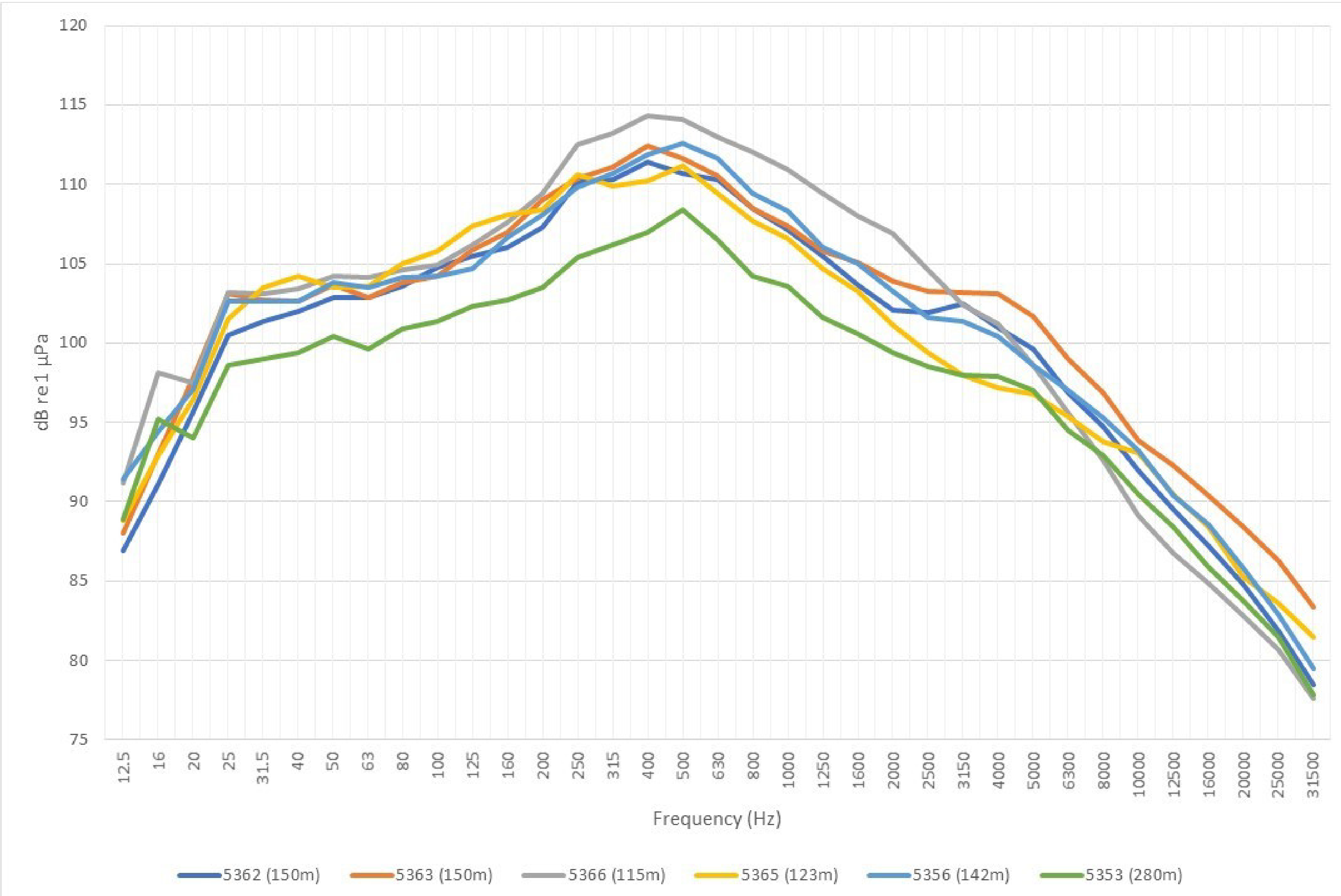

Figure B-23. SPL RMS 1/3 Octave Band Plot of B-16 Mechanical Cut from April 5, 2021 11:58 to 23:32

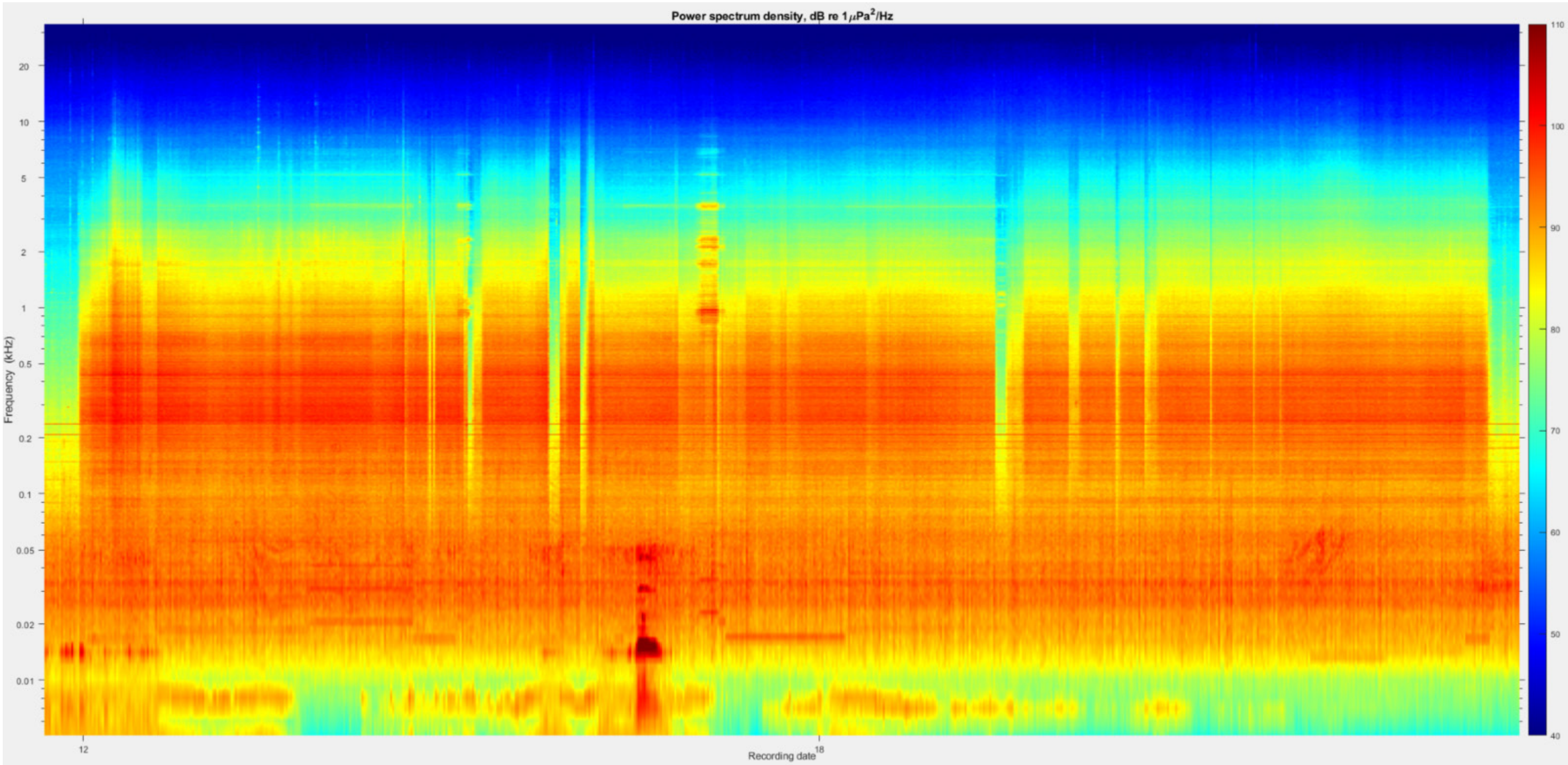

Figure B-24. PSD Spectrogram Plot of B-16 Mechanical Cut from April 5, 2021, 11:58 to 23:32 (SoundTrap 5366)

Table B-6. Conductor B-3 Noise Monitoring Results Summary
(8:00 April 6, 2021 – 20:32 April 6, 2021)

Conductor	Start Time	End Time	Total Duration of Cut (minutes)	Overall Wall Thickness (inches)	Cut Depth Below Mudline (Feet)	Cutter RPM
B-3	4/6/2021 8:00	4/6/2021 9:36	96	1.919	20	60
	4/6/2021 16:30	4/6/2021 20:32	151			

Conductor	Start Time	End Time	Direction	Monitor Name	Distance to Conductor (m)	L_p	Max L_p	Min L_p	$L_{p,pk}$	L_E
B-3	4/6/2021 8:00	4/6/2021 9:36	North	5362	151.45	120.5	127.7	111.4	153.3	158.1
			North	5363	151.45	120.8	128.1	114.1	151.2	158.4
			East	5366	112.26	123.8	132.1	112.8	156.0	161.4
			South	5365	122.72	121.2	129.0	109.6	150.0	158.9
			West	5356	144.32	121.0	128.8	111.7	151.5	158.6
			South	5353	280.45	116.4	122.9	108.4	141.8	154.1
	4/6/2021 16:30	4/6/2021 20:32	North	5362	151.45	125.9	131.8	109.3	158.3	167.5
			North	5363	151.45	125.8	131.0	111.0	159.2	167.5
			East	5366	112.26	129.8	135.9	108.5	164.0	171.4
			South	5365	122.72	126.6	132.2	108.4	158.0	168.2
			West	5356	144.32	126.4	132.4	110.7	157.4	168.0
			South	5353	280.45	121.2	126.5	107.7	147.9	162.9

L_p and $L_{p.pk}$ = (dB re 1 μPa); L_E = (dB re 1 μPa^2·s)

Conductor	Start Time	End Time	Monitor Station Name	Lp				LE			
				LF	MF	HF	PP	LF	MF	HF	PP
B-3	4/6/2021 8:00	4/6/2021 9:36	5362	119.1	98.4	94.5	111.4	156.7	136.0	132.1	149.0
			5363	119.3	101.2	97.6	112.3	156.9	138.8	135.2	149.9
			5366	122.4	97.2	92.6	113.9	160.1	134.8	130.2	151.6
			5365	119.7	97.9	94.6	111.1	157.3	135.5	132.2	148.8
			5356	119.6	99.1	95.4	111.5	157.2	136.6	133.0	149.1
			5353	114.8	96.7	93.3	107.3	152.5	134.5	131.0	145.1
	4/6/2021 13:02	4/6/2021 15:33	5362	126.0	103.3	99.4	118.1	165.6	142.9	138.9	157.6
			5363	129.0	106.6	102.8	121.3	168.6	146.2	142.3	160.9
			5366	123.8	101.7	98.1	116.1	163.3	141.2	137.7	155.6
			5365	121.3	100.3	97.1	112.9	160.8	139.9	136.7	152.5
			5356	123.8	103.8	100.3	116.3	163.4	143.4	139.9	155.9
			5353	117.8	99.4	96.0	110.5	157.4	138.9	135.6	150.0

L_p and $L_{p,pk}$ = (dB re 1 μPa); L_E = (dB re 1 μPa²·s)
LF – low frequency; MF – mid-frequency; HF – high frequency; PP – phocid pinnipeds

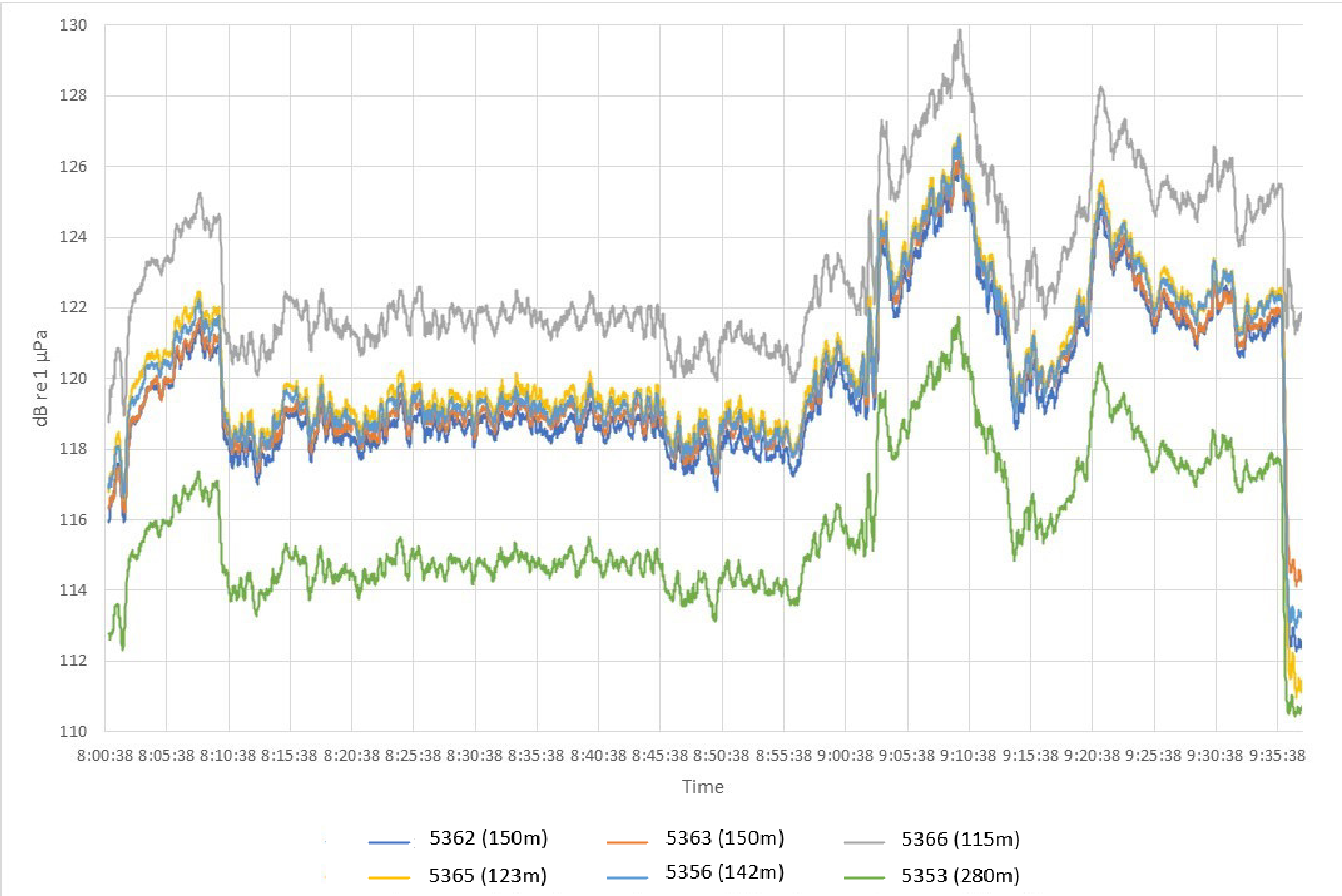

Figure B-25. Time History Plot of B-3 Mechanical Cut from April 6, 2021, 8:00 to 9:36 (20 second sample interval)

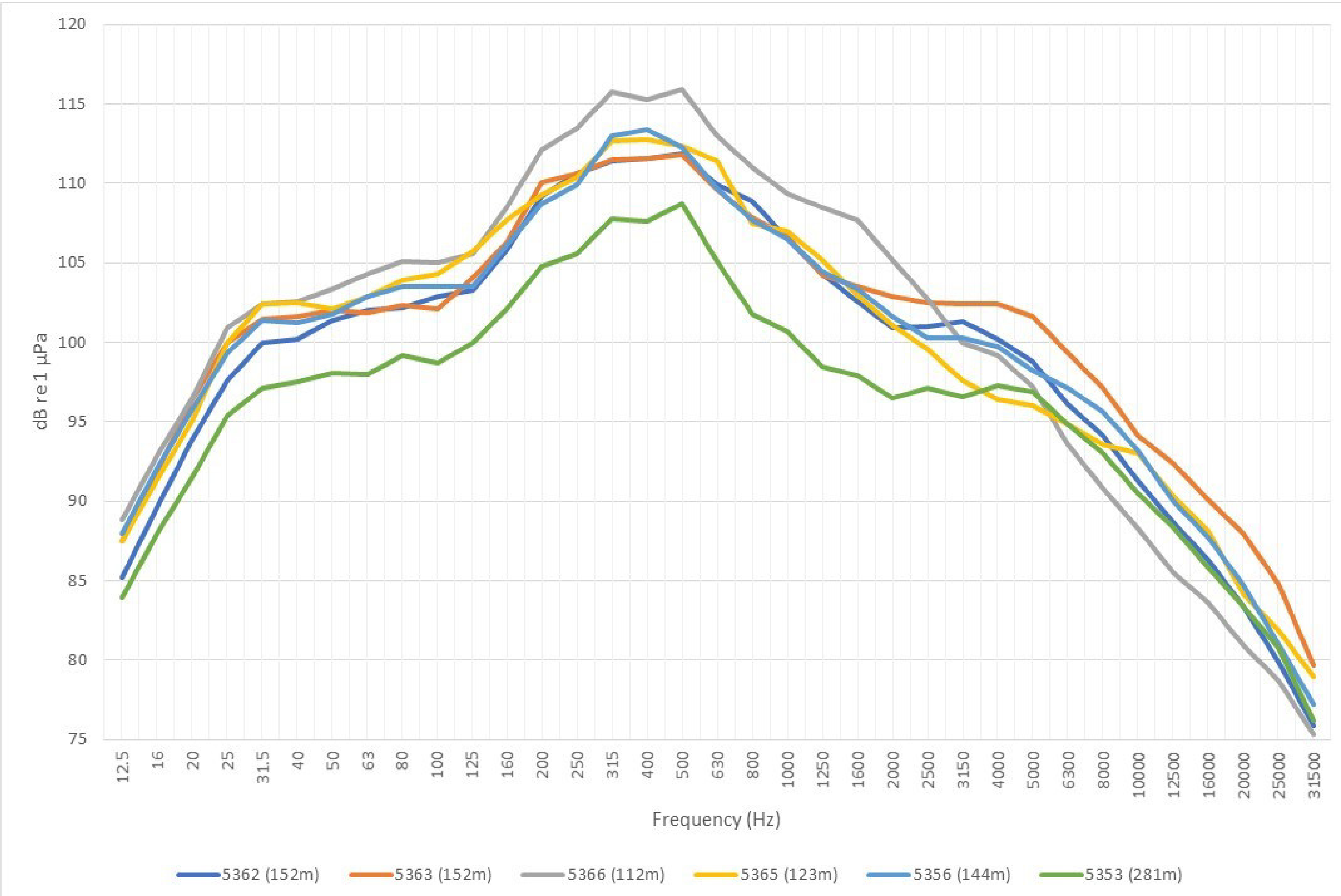

Figure B-26. SPL RMS 1/3 Octave Band Plot of B-3 Mechanical Cut from April 6, 2021, 8:00 to 9:36

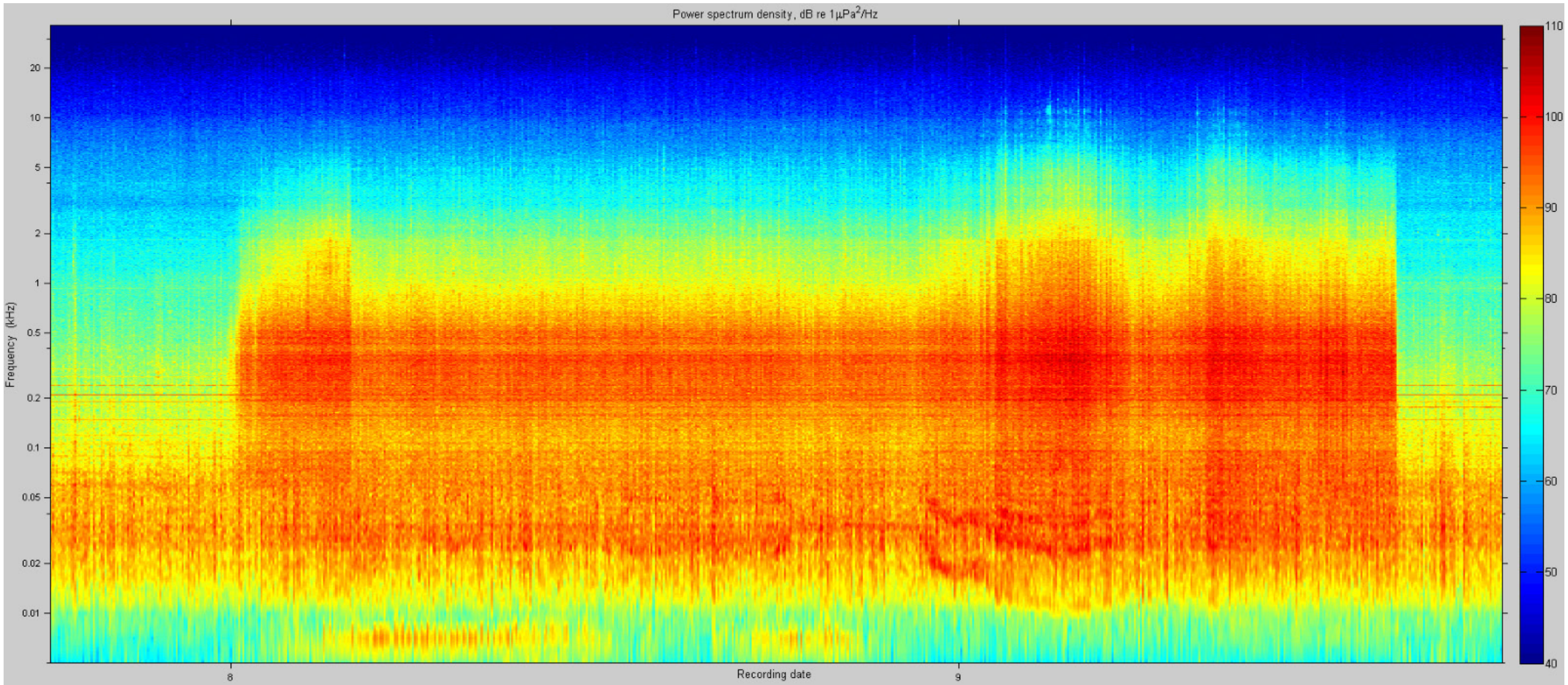

Figure B-27. PSD Spectrogram Plot of B-3 Mechanical Cut from April 6, 2021 8:00 to 9:36 (SoundTrap 5366)

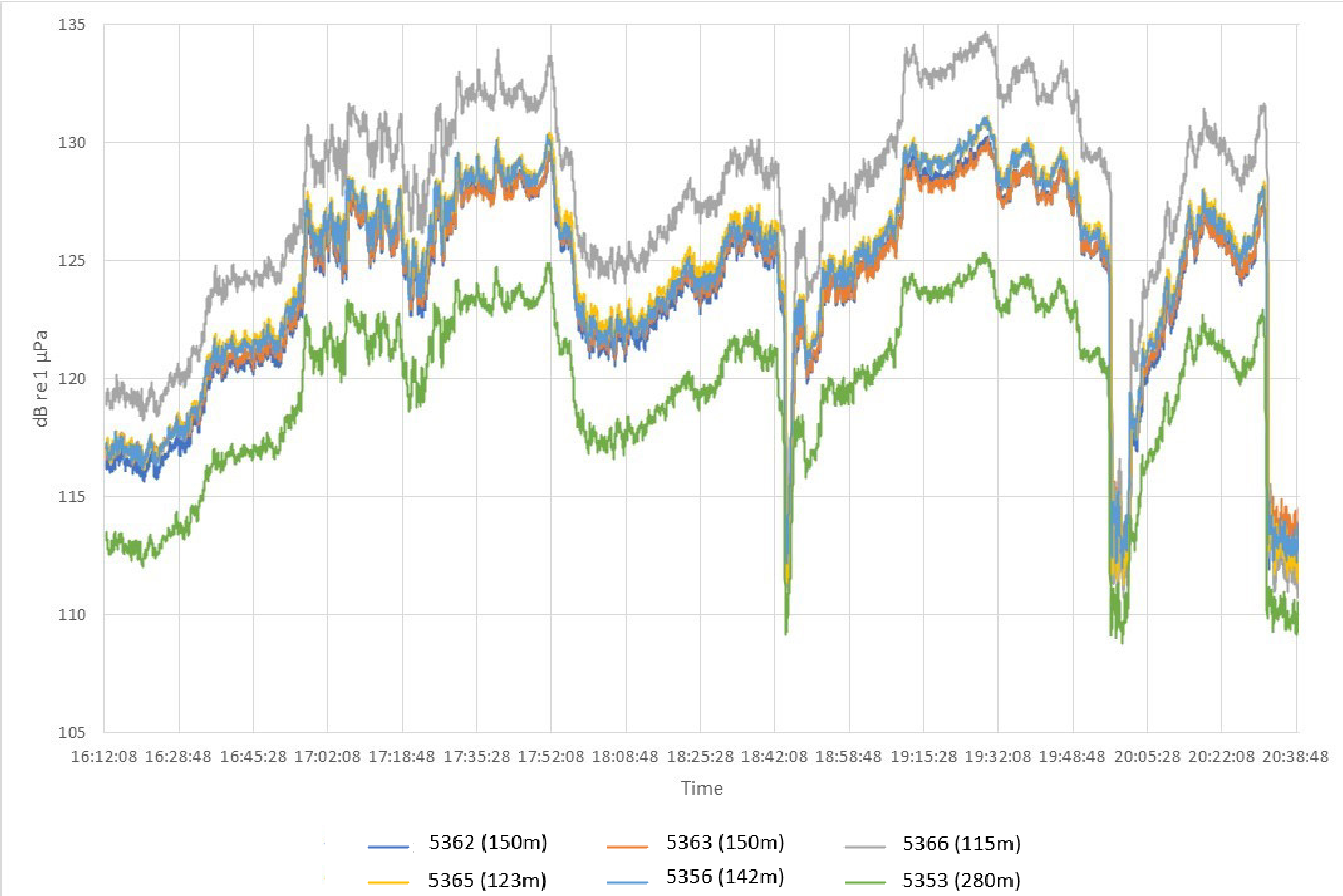

Figure B-28. Time History Plot of B-3 Mechanical Cut from April 6, 2021, 16:30 to 20:32 (20-second sample interval)

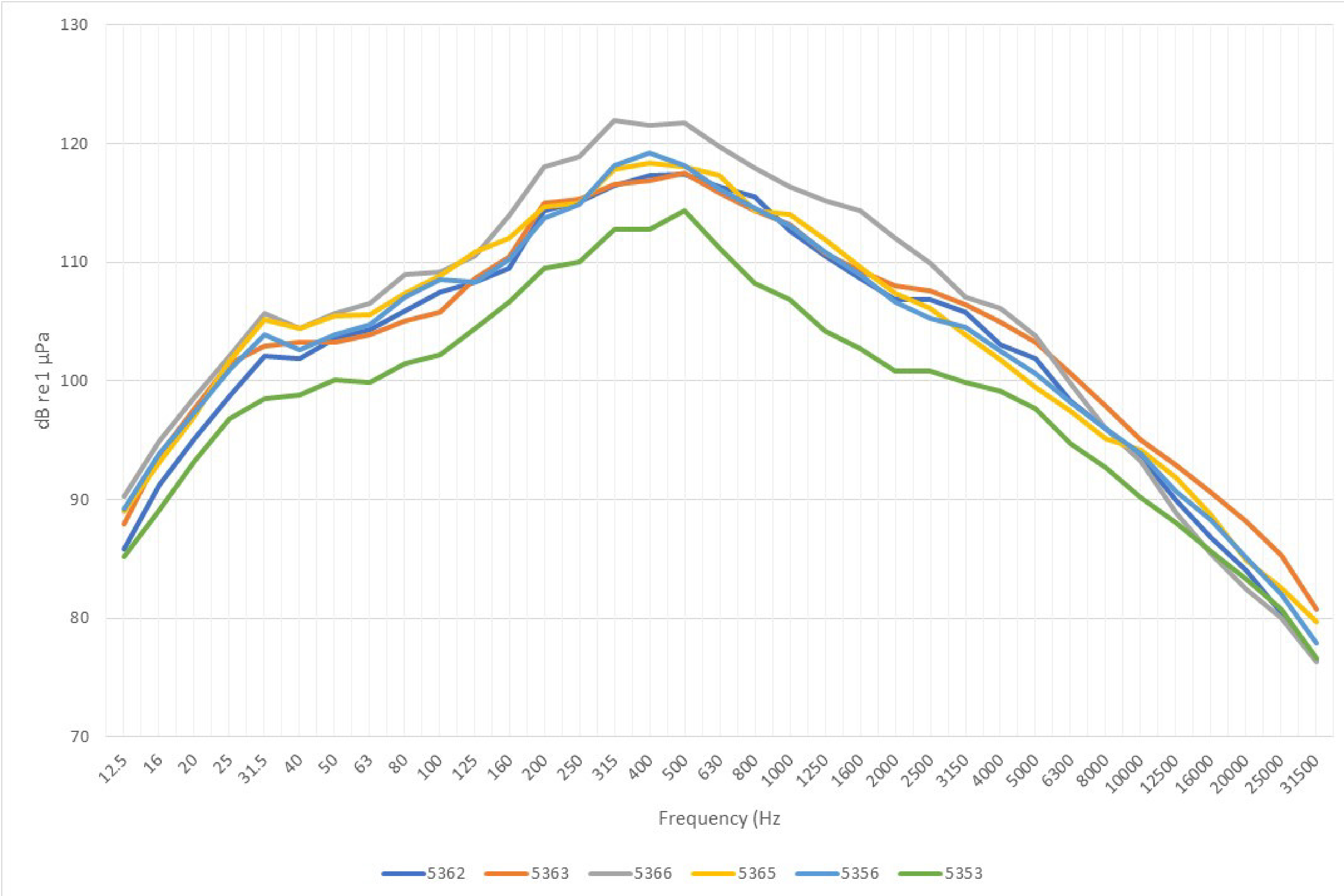

Figure B-29. SPL RMS 1/3 Octave Band Plot of B-3 Mechanical Cut from April 6, 2021, 16:30 to 20:32

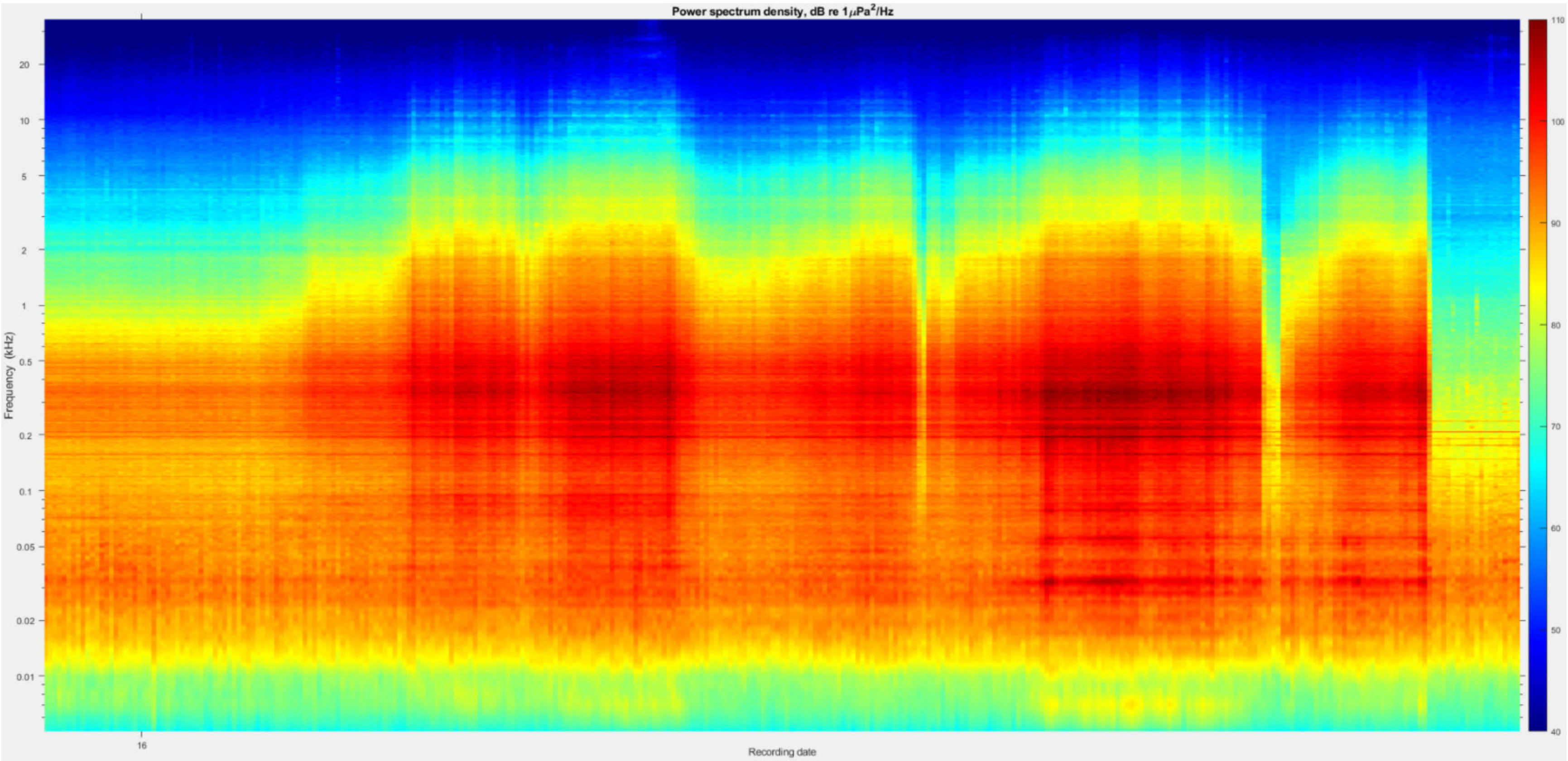

Figure B-30. PSD Spectrogram Plot of B-3 Mechanical Cut from April 6, 2021, 16:30 to 20:32

Table B-7. Empty Conductor S-25
(9:51 April 7, 2021 – 10:53 April 7, 2021)

Conductor	Start Time	End Time	Total Duration of Cut (minutes)	Overall Wall Thickness (inches)	Cut Depth Below Mudline (Feet)	Cutter RPM
S-25	4/7/2021 9:51	4/7/2021 10:53	62	0.812	20	60

Conductor	Start Time	End Time	Direction	Monitor Station Name	Distance to Conductor (m)	L_p	Max L_p	Min L_p	$L_{p,pk}$	L_E
S-25	4/7/2021 9:51	4/7/2021 10:53	North	5362	154.62	125.9	134.1	110.6	157.3	161.6
			North	5363	154.62	126.4	136	111.5	159.2	162.1
			East	5366	107.34	131.2	140.1	108.6	168.4	166.9
			South	5365	122.16	128.4	136.9	108.8	161.2	164.1
			West	5356	148.85	125.9	133.7	110.7	154.7	161.6
			South	5353	282.1	121.3	129.6	107.4	160.2	157.1

L_p and $L_{p.pk}$ = (dB re 1 μPa); L_E = (dB re 1 μPa²·s)

Conductor	Start Time	End Time	Monitor Station Name	L_p				L_E			
				LF	MF	HF	PP	LF	MF	HF	PP
S-25	4/7/2021 9:51	4/7/2021 10:53	5362	124.9	103.9	99.7	119	160.6	139.6	135.4	154.7
			5363	125.4	105.5	101.7	119.8	161.1	141.2	137.4	155.5
			5366	130.6	109	104	125.5	166.3	144.7	139.7	161.2
			5365	127.5	106.5	102.1	121.9	163.2	142.1	137.8	157.5
			5356	125	103.4	99	119	160.6	139.1	134.7	154.7
			5353	120.4	100.6	96.4	114.9	156.1	136.3	132.1	150.6

L_p and$L_{p.pk}$ = (dB re 1 μPa); L_E = (dB re 1 μPa²·s)
LF – low frequency; MF – mid-frequency; HF – high frequency; PP – phocid pinnipeds

Figure B-31. Time History Plot of S-25 Mechanical Cut from April 7, 2021, 9:51 to 10:53 (20-second sample interval)

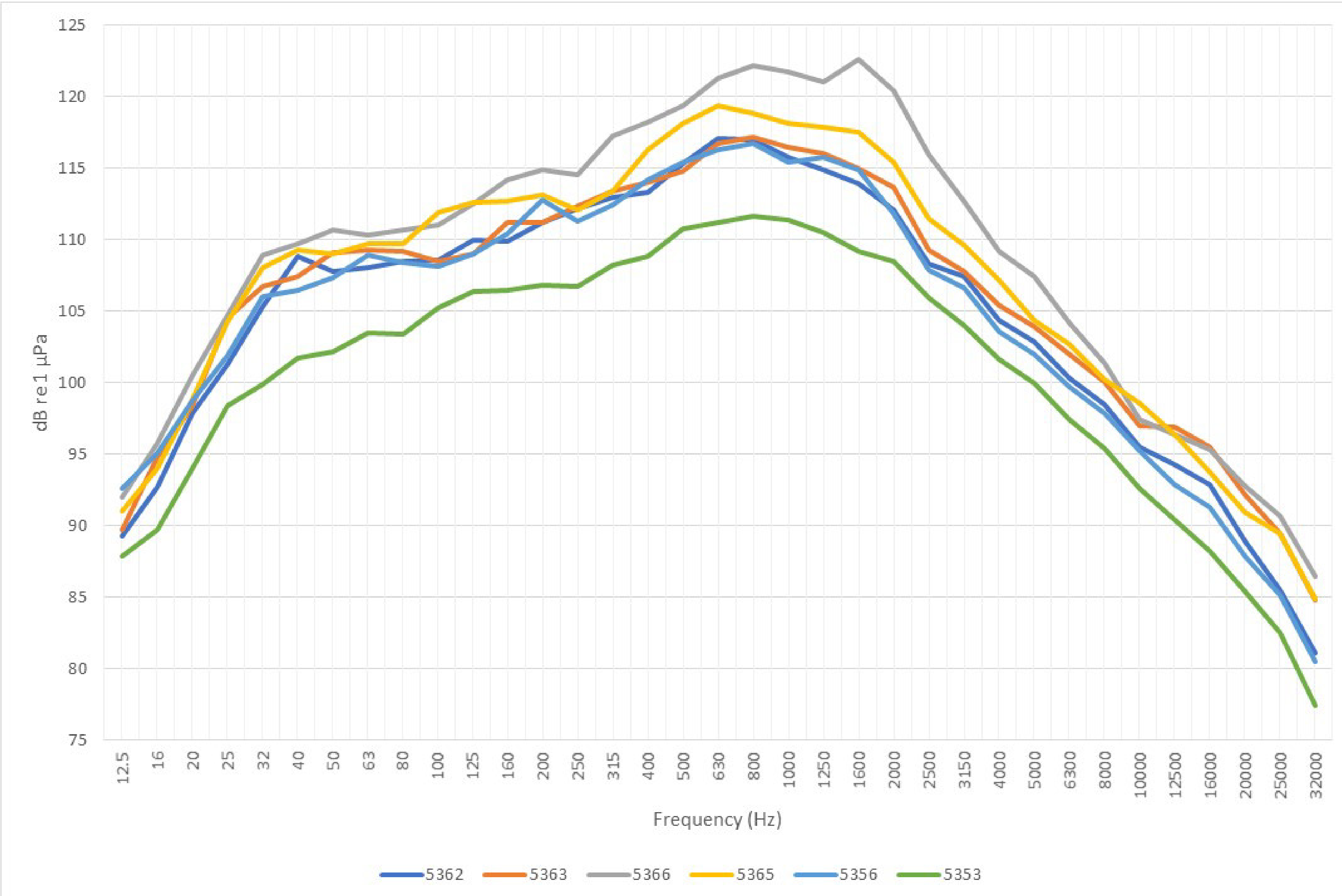

Figure B-32. SPL RMS 1/3 Octave Band Plot of S-25 Mechanical Cut from April 7, 2021, 9:51 to 10:53

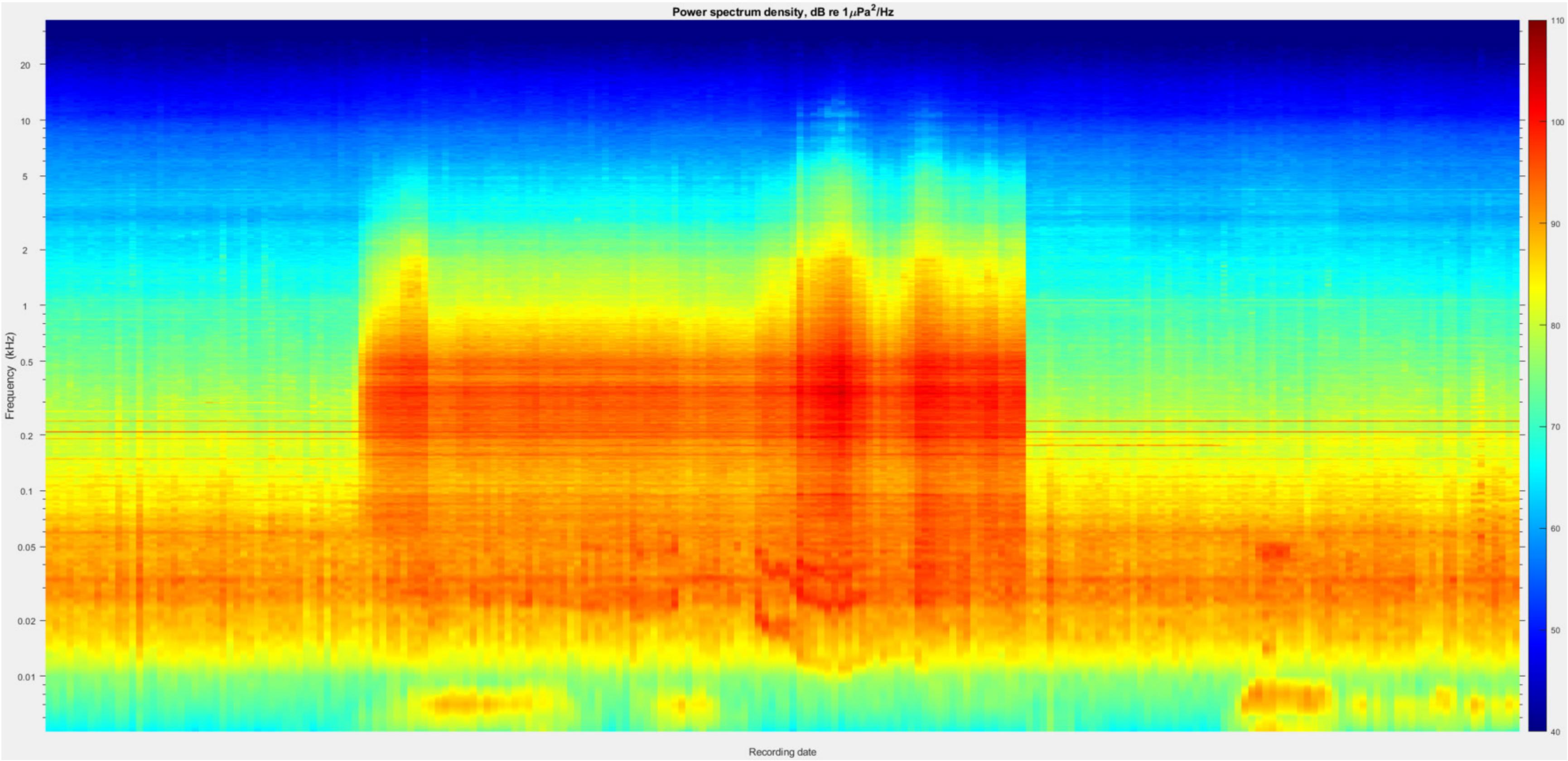

Figure B-33. PSD Spectrogram Plot of S-25 Mechanical Cut from 9:51 April 7, 2021 – 10:53 April 7, 2021

Table B-8. Conductor S-29 Noise Monitoring Results Summary
(18:35 April 7, 2021 – 19:17 April 7, 2021)

Conductor	Start Time	End Time	Total Duration of Cut (minutes)	Overall Wall Thickness (inches)	Cut Depth Below Mudline (Feet)	Cutter RPM
S-29	4/7/2021 18:35	4/7/2021 19:17	42	0.812	20	60

Conductor	Start Time	End Time	Direction	Monitor Name	Distance to Conductor (m)	L_p	Max L_p	Min L_p	$L_{p,pk}$	L_E
S-29	4/7/2021 18:35	4/7/2021 19:17	North	5362	157.7	127.5	135.9	109.2	160.8	161.6
			North	5363	157.7	127.5	135.9	110.2	162.8	161.6
			East	5366	109.05	132.4	140.9	107.8	165.2	166.5
			South	5365	118.21	130.3	139.2	108.4	166.2	164.4
			West	5356	146.7	127.1	135.2	109.6	156.2	161.2
			South	5353	278.29	123.7	132.8	106.4	155.7	157.8

L_p and $L_{p.pk}$ = (dB re 1 μPa); L_E = (dB re 1 μPa²·s)

Conductor	Start Time	End Time	Monitor Station Name	L_p				L_E			
				LF	MF	HF	PP	LF	MF	HF	PP
S-29	4/7/2021 18:35	4/7/2021 19:17	5362	126.6	108.1	104.4	121.0	160.7	142.1	138.4	155.0
			5363	126.5	108.9	105.6	121.0	160.5	142.9	139.6	155.0
			5366	131.7	111.3	107.3	126.1	165.7	145.3	141.3	160.1
			5365	129.5	110.5	107.1	123.8	163.5	144.6	141.1	157.9
			5356	125.9	105.7	102.0	119.5	159.9	139.7	136.0	153.5
			5353	122.8	105.0	101.5	117.4	156.8	139.0	135.5	151.4

L_p and$L_{p.pk}$ = (dB re 1 μPa); L_E = (dB re 1 μPa²·s)
LF – low frequency; MF – mid-frequency; HF – high frequency; PP – phocid pinnipeds

Figure B-34. Time History Plot of S-29 Mechanical Cut from April 7, 2021, 18:35 to 19:17 (20-second sample interval)

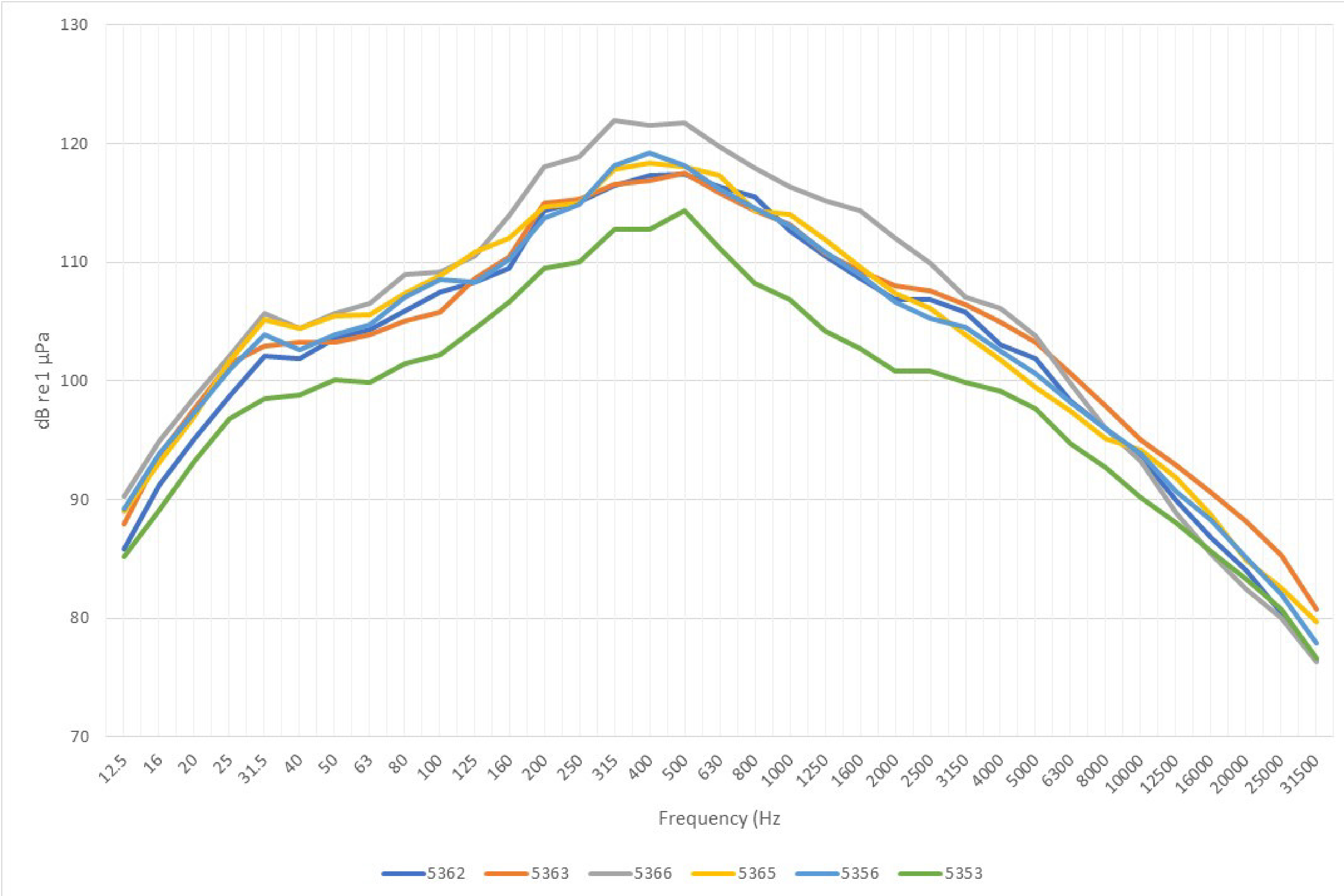

Figure B-35. SPL RMS 1/3 Octave Band Plot of S-29 Mechanical Cut from April 7, 2021, 18:35 to 19:17

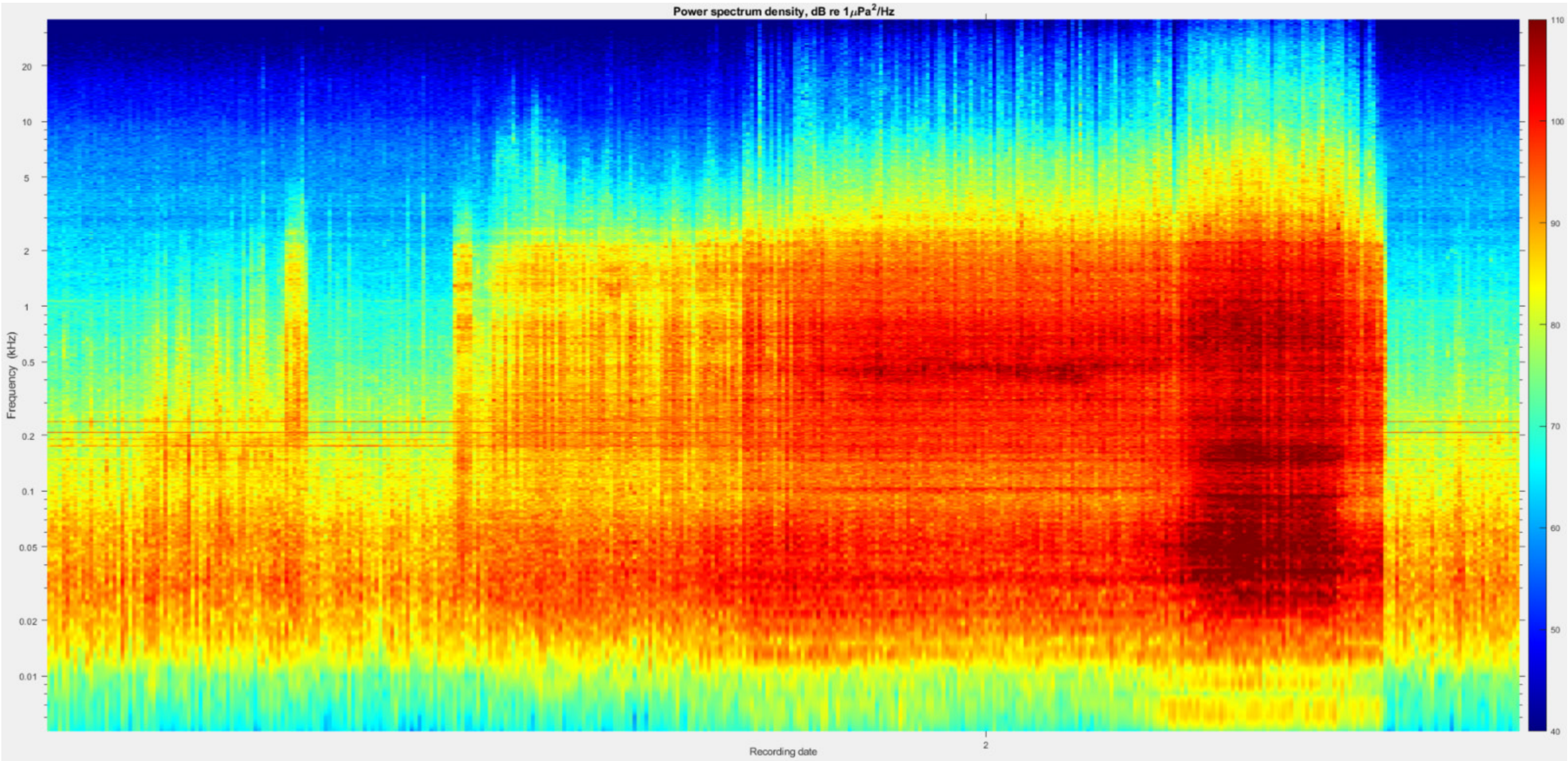

Figure B-36. PSD Spectrogram Plot of S-29 Mechanical Cut from April 7, 2021, 18:35 to 19:17 (SoundTrap 5366)

Table B-9. Empty Conductor S-33
(4:06 April 8, 2021 – 5:44 April 8, 2021)

Conductor	Start Time	End Time	Total Duration of Cut (minutes)	Overall Wall Thickness (inches)	Cut Depth Below Mudline (Feet)	Cutter RPM
S-33	4/8/2021 4:06	4/8/2021 5:44	98	0.812	20	60

Conductor	Start Time	End Time	Direction	Monitor Station Name	Distance to Conductor (m)	L_p	Max L_p	Min L_p	$L_{p,pk}$	L_E
S-33	4/8/2021 4:06	4/8/2021 5:44	North	5362	160.86	122.6	129.1	113.1	153.9	160.2
			North	5363	160.86	123.2	130.2	113.2	157.6	160.9
			East	5366	110.81	128.7	136.2	108.7	160	166.4
			South	5365	114.33	127.8	135.1	109.7	160.4	165.5
			West	5356	144.68	123.8	130.3	112.1	154.2	161.5
			South	5353	274.53	121.3	132.0	108.0	153.6	159.1

L_p and $L_{p.pk}$ = (dB re 1 μPa); L_E = (dB re 1 μPa²·s)

Conductor	Start Time	End Time	Monitor Station Name	L_p				L_E			
				LF	MF	HF	PP	LF	MF	HF	PP
S-33	4/8/2021 4:06	4/8/2021 5:44	5362	121.4	100.8	96.5	115.3	159.1	138.5	134.2	153
			5363	122	102.8	98.9	116.2	159.7	140.5	136.6	153.9
			5366	128	105.9	100.6	122.7	165.8	143.7	138.4	160.5
			5365	127.2	105.8	101.4	121.6	164.9	143.5	139.1	159.3
			5356	122.7	102.1	97.9	116.8	160.4	139.8	135.6	154.5
			5353	120.7	101.1	96.9	115.4	158.4	138.8	134.6	153.1

L_p and$L_{p.pk}$ = (dB re 1 μPa); L_E = (dB re 1 μPa²·s)
LF – low frequency; MF – mid-frequency; HF – high frequency; PP – phocid pinnipeds

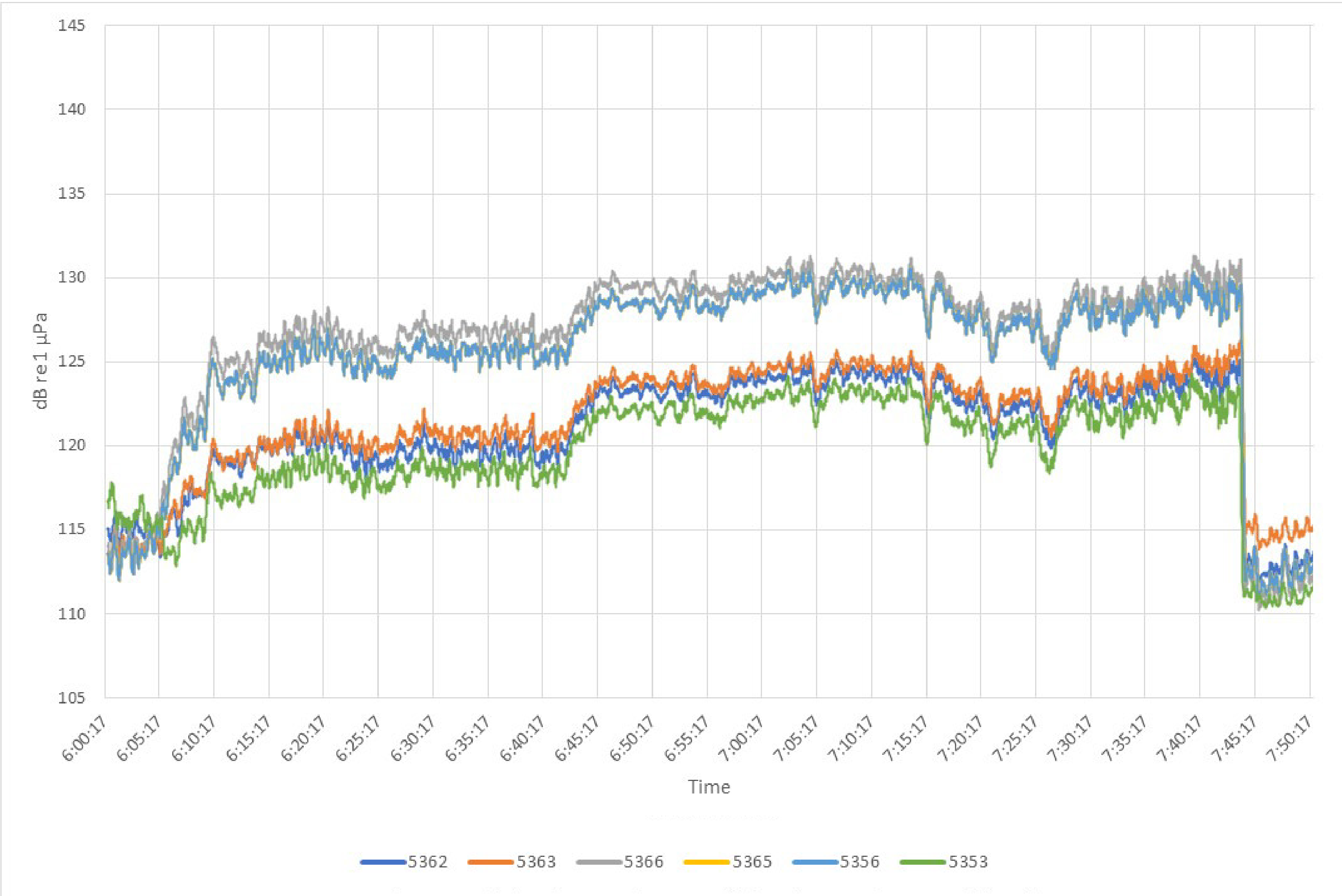

Figure B-37. Time History Plot of S-33 Mechanical Cut from April 8, 2021, 4: 06 to 5:44 (20-second sample interval)

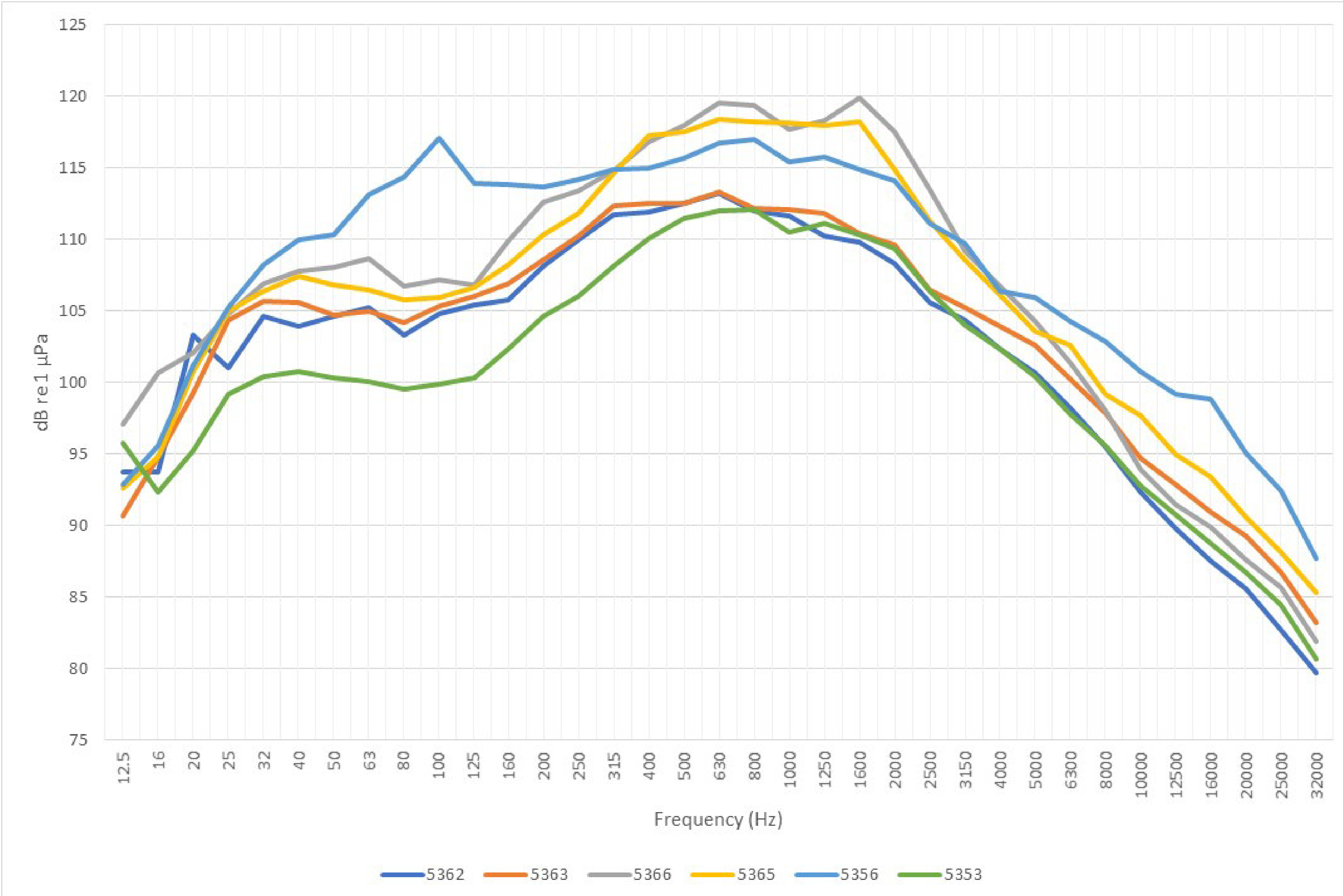

Figure B-38. SPL RMS 1/3 Octave Band Plot of S-33 Mechanical Cut from April 8, 2021, 4:06 to 5:44

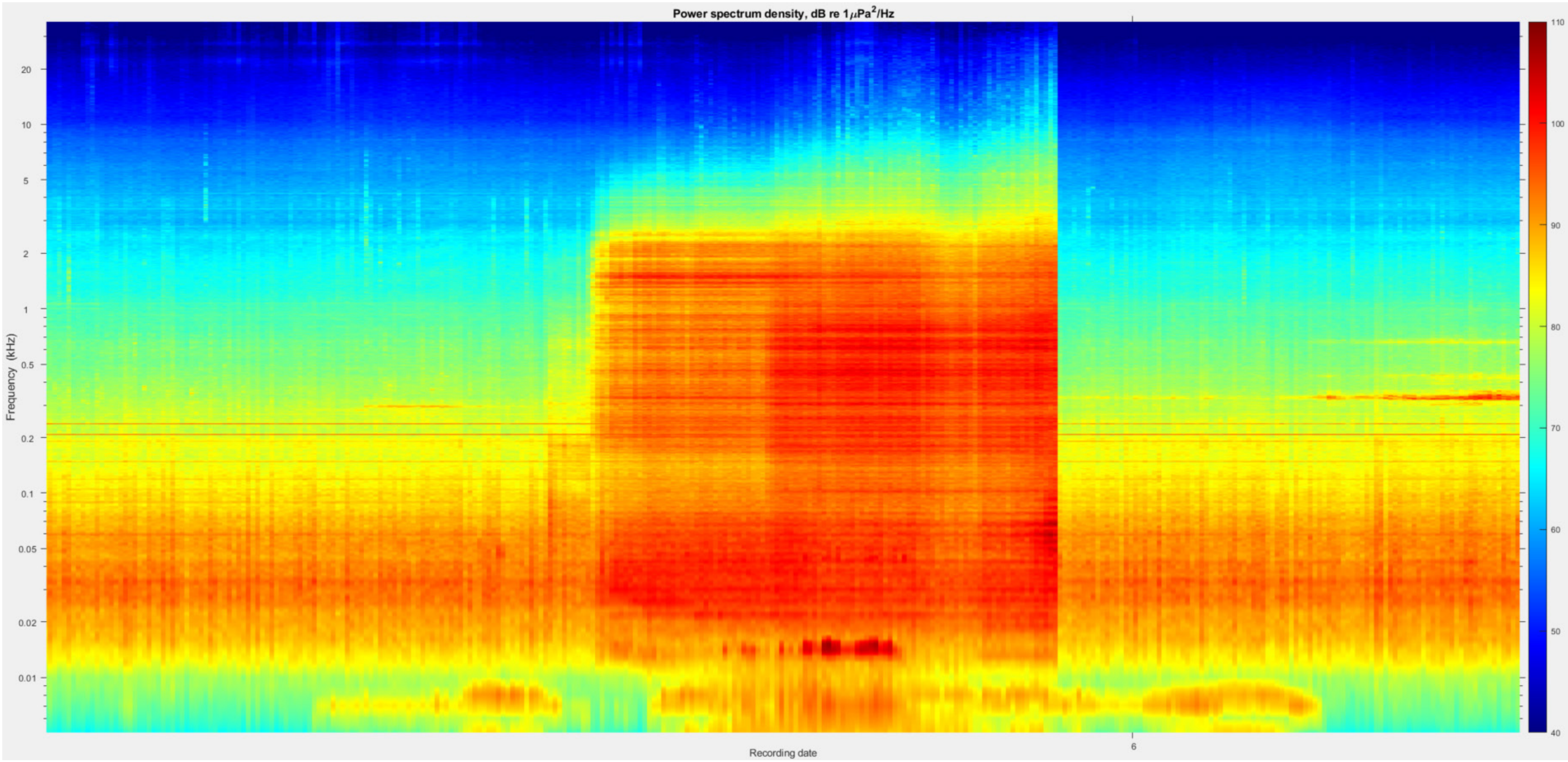

Figure B-39. PSD Spectrogram Plot of S-33 Mechanical Cut from 4:06 April 8, 2021 – 5:44 April 8, 2021

Table B-10. Empty Conductor S-46
(12:49 April 8, 2021 – 15:45 April 8, 2021)

Conductor	Start Time	End Time	Total Duration of Cut (minutes)	Overall Wall Thickness (inches)	Cut Depth Below Mudline (Feet)	Cutter RPM
S-46	4/8/2021 12:49	4/8/2021 15:45	176	0.812	20	60

Conductor	Start Time	End Time	Direction	Monitor Station Name	Distance to Conductor (m)	L_p	Max L_p	Min L_p	$L_{p,pk}$	L_E
S-46	4/8/2021 12:49	4/8/2021 15:45	North	5362	156.22	123.6	129	111.8	153.8	163.9
			North	5363	156.22	124.6	129.6	111.5	158.9	164.9
			East	5366	118.51	126.6	131.9	112.9	157.7	166.8
			South	5365	115.34	125.4	131.5	111.3	157.8	165.7
			West	5356	137.28	125	130.7	111.8	152.7	165.3
			South	5353	271.87	119.7	126.6	108.9	146.7	160

L_p and $L_{p.pk}$ = (dB re 1 μPa); L_E = (dB re 1 μPa²·s)

Conductor	Start Time	End Time	Monitor Station Name	L_p				L_E			
				LF	MF	HF	PP	LF	MF	HF	PP
S-46	4/8/2021 12:49	4/8/2021 15:45	5362	122.8	101.3	96.5	117.1	163	141.5	136.8	157.3
			5363	123.7	103.2	98.7	118.3	164	143.4	139	158.6
			5366	125.8	102.3	96.5	120.2	166	142.5	136.7	160.4
			5365	124.6	102.6	97.7	118.9	164.8	142.8	138	159.2
			5356	124.3	102.5	97.7	118.7	164.5	142.7	138	158.9
			5353	118.8	98.7	94.4	113.2	159	138.9	134.6	153.5

L_p and$L_{p.pk}$ = (dB re 1 μPa); L_E = (dB re 1 μPa²·s)
LF – low frequency; MF – mid-frequency; HF – high frequency; PP – phocid pinnipeds

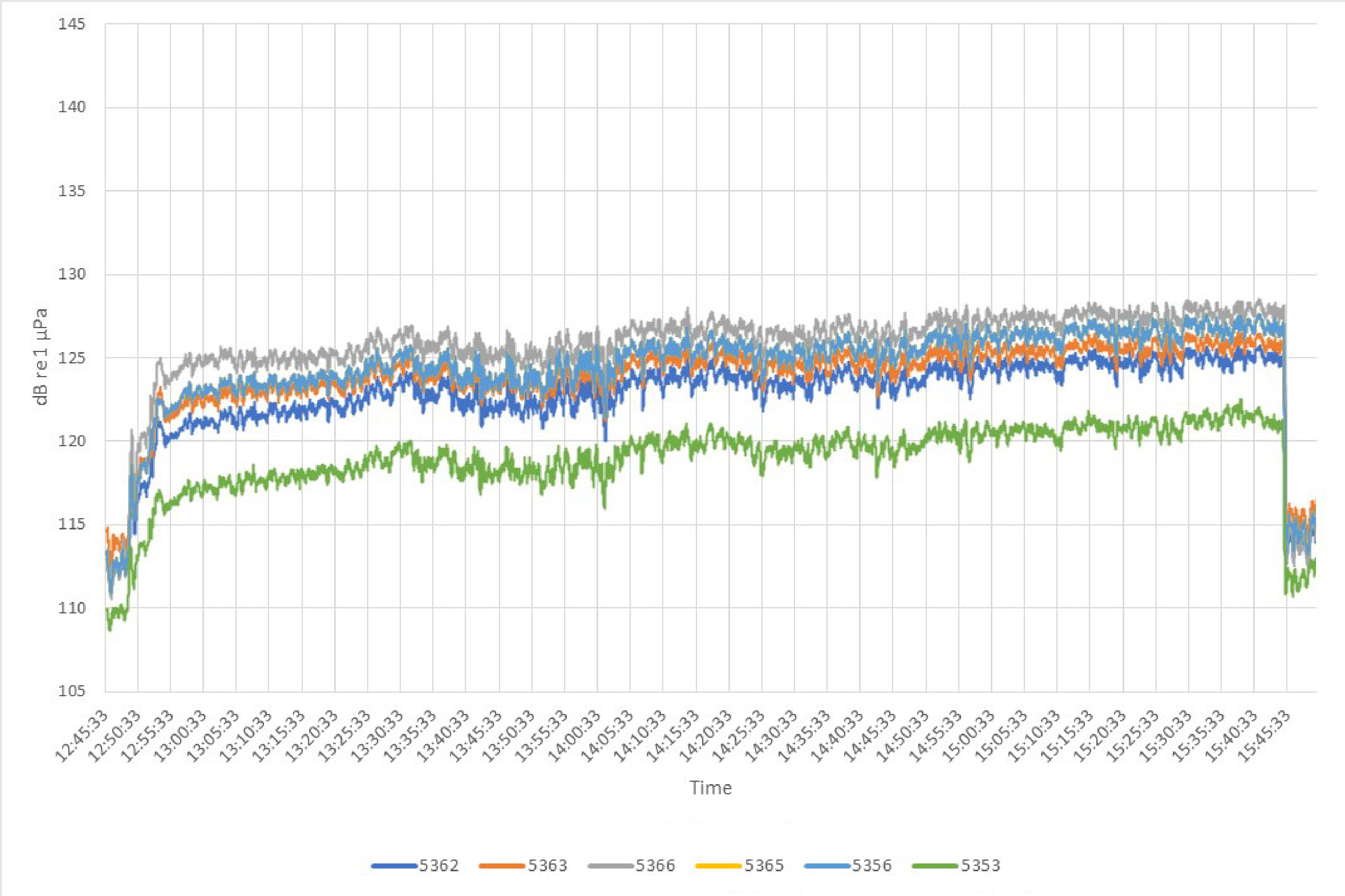

Figure B-40. Time History Plot of S-46 Mechanical Cut from April 8, 2021, 12:49 to 15:45 (20-second sample interval)

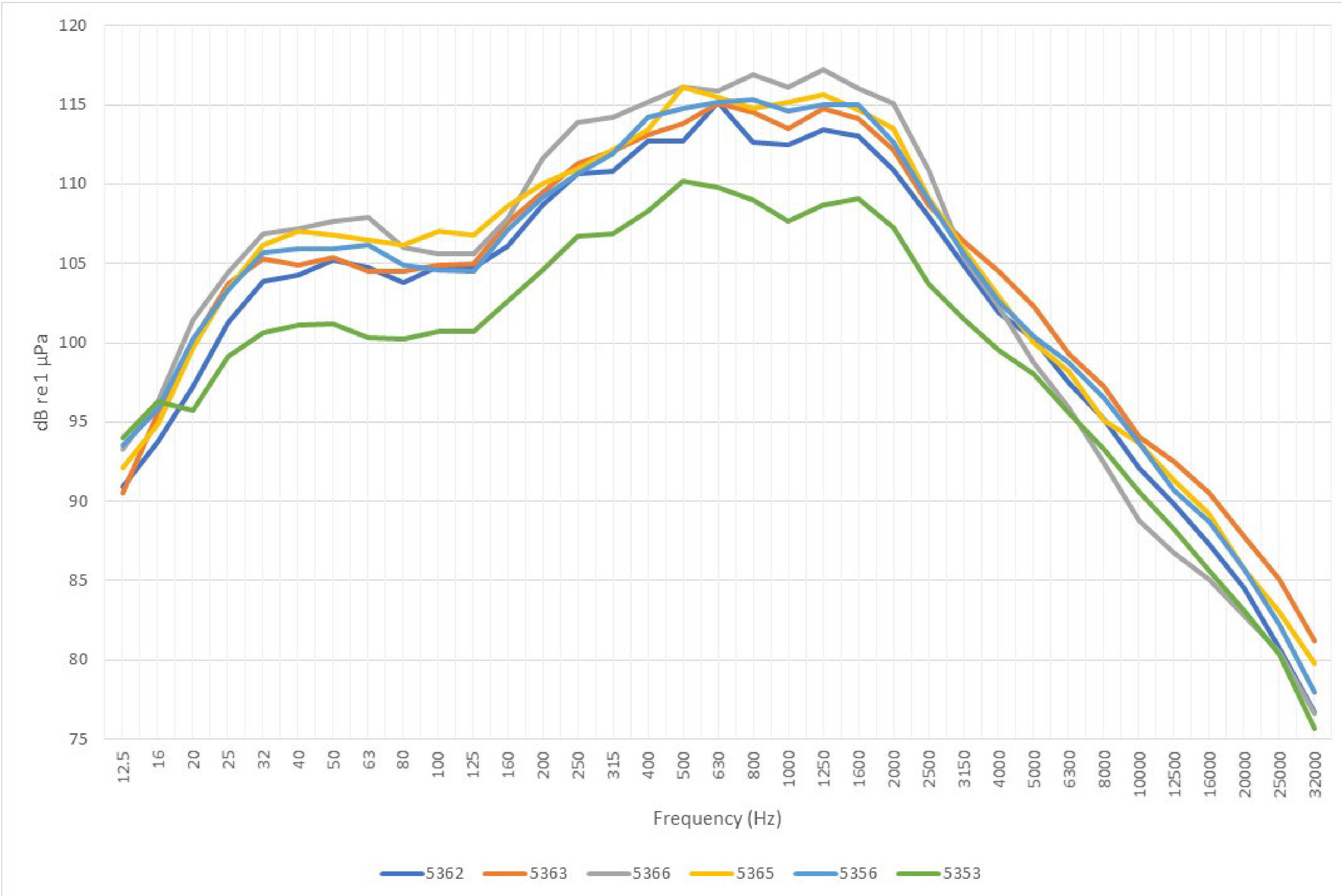

Figure B-41. SPL RMS 1/3 Octave Band Plot of S-46 Mechanical Cut from April 8, 2021, 12:49 to 15:45

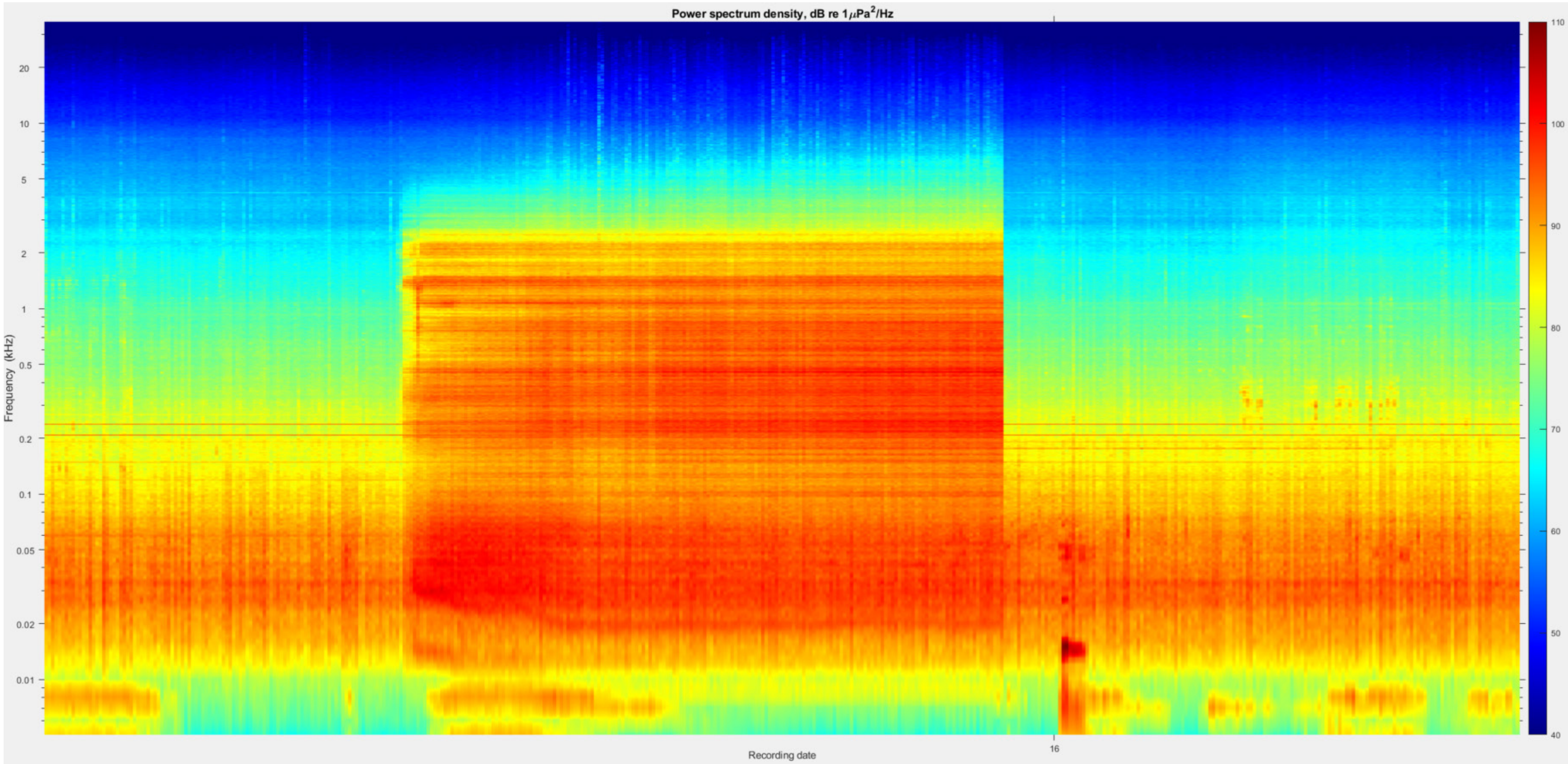

Figure B-42. PSD Spectrogram Plot of S-46 Mechanical Cut from 12:49 April 8, 2021 – 15:45 April 8, 2021

Table B-11. Empty Conductor S-47
(0:20 April 9, 2021 – 1:43 April 9, 2021)

Conductor	Start Time	End Time	Total Duration of Cut (minutes)	Overall Wall Thickness (inches)	Cut Depth Below Mudline (Feet)	Cutter RPM
S-47	4/9/2021 0:20	4/9/2021 1:43	83	0.812	20	60

Conductor	Start Time	End Time	Direction	Monitor Station Name	Distance to Conductor (m)	L_p	Max L_p	Min L_p	$L_{p,pk}$	L_E
S-47	4/9/2021 0:20	4/9/2021 1:43	North	5362	159.48	120.2	129.3	111.5	153.9	157.2
			North	5363	159.48	120.7	129.4	110.7	155.8	157.7
			East	5366	116.54	124	133.9	108.8	161.4	161
			South	5365	112.97	122.8	133	109.2	161	159.9
			West	5356	138.96	121.2	130.4	110.2	157.8	158.3
			South	5353	270.95	116.7	126.1	107.9	150.2	153.7

L_p and $L_{p.pk}$ = (dB re 1 μPa); L_E = (dB re 1 μPa²·s)

Conductor	Start Time	End Time	Monitor Station Name	L_p				L_E			
				LF	MF	HF	PP	LF	MF	HF	PP
S-47	4/9/2021 0:20	4/9/2021 1:43	5362	118.8	100	95.9	113.3	155.8	136.9	132.9	150.3
			5363	119.4	102.2	98.5	114.1	156.4	139.2	135.4	151.1
			5366	123.2	101.7	96.9	117.5	160	138.5	133.7	154.3
			5365	121.9	102.8	98.9	116.7	158.8	139.7	135.8	153.5
			5356	120	101.4	97.4	114.6	157	138.3	134.4	151.6
			5353	115.4	98.5	94.8	110.5	152.4	135.5	131.7	147.4

L_p and$L_{p.pk}$ = (dB re 1 μPa); L_E = (dB re 1 μPa²·s)
LF – low frequency; MF – mid-frequency; HF – high frequency; PP – phocid pinnipeds

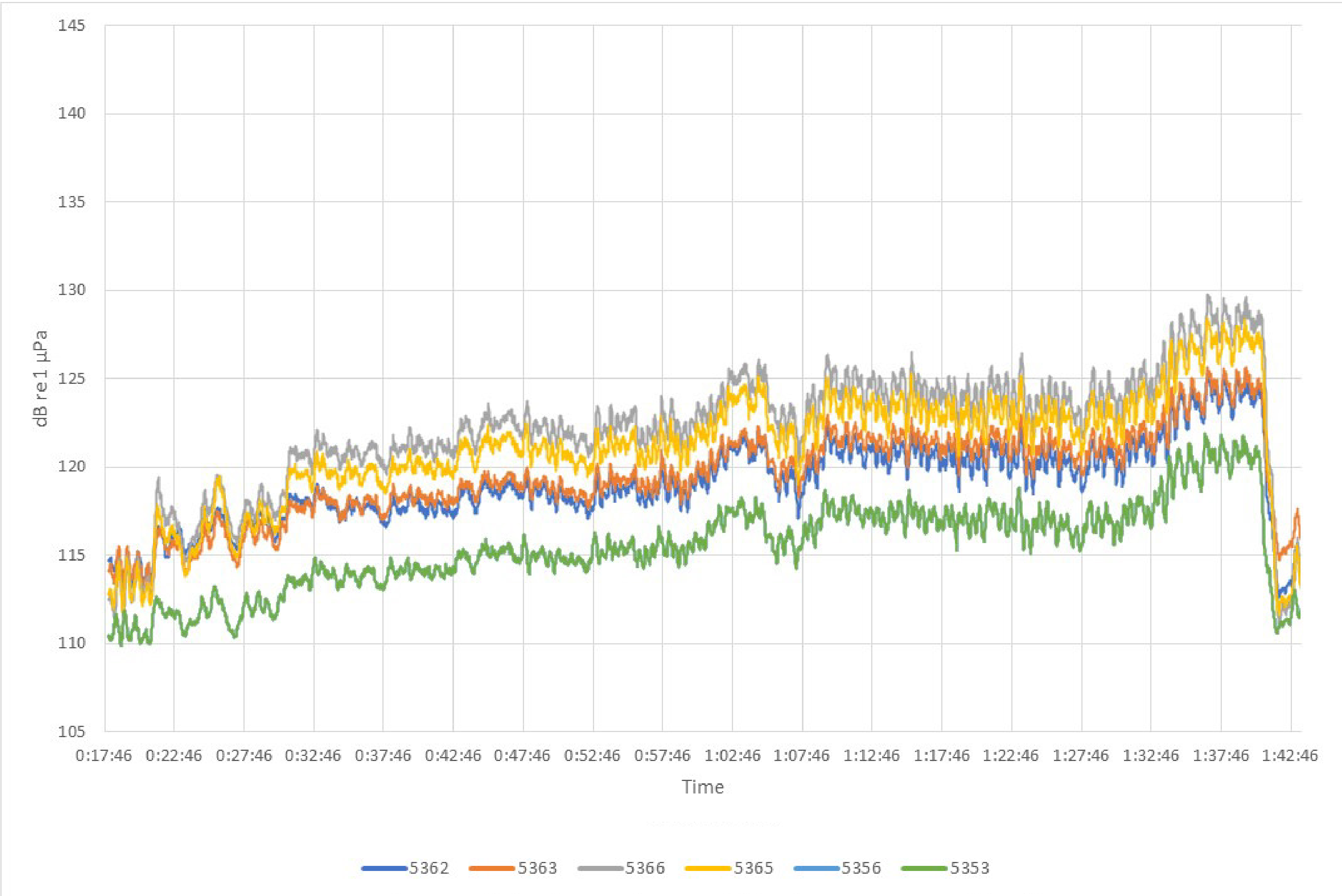

Figure B-43. Time History Plot of S-47 Mechanical Cut from April 8, 2021, 0:20 to 1:43 (20-second sample interval)

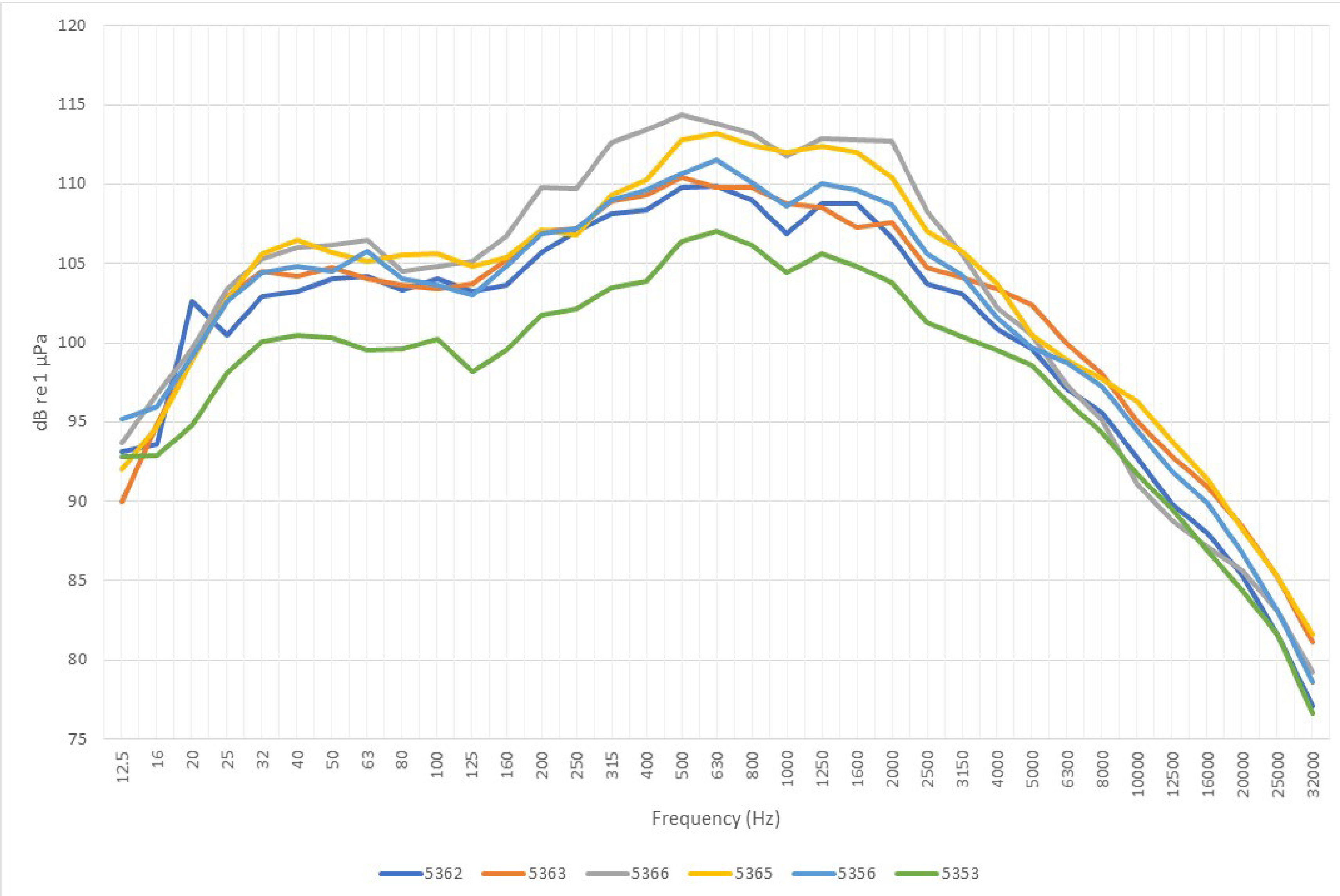

Figure B-44. SPL RMS 1/3 Octave Band Plot of S-47 Mechanical Cut from April 8, 2021, 0:20 to 1:43

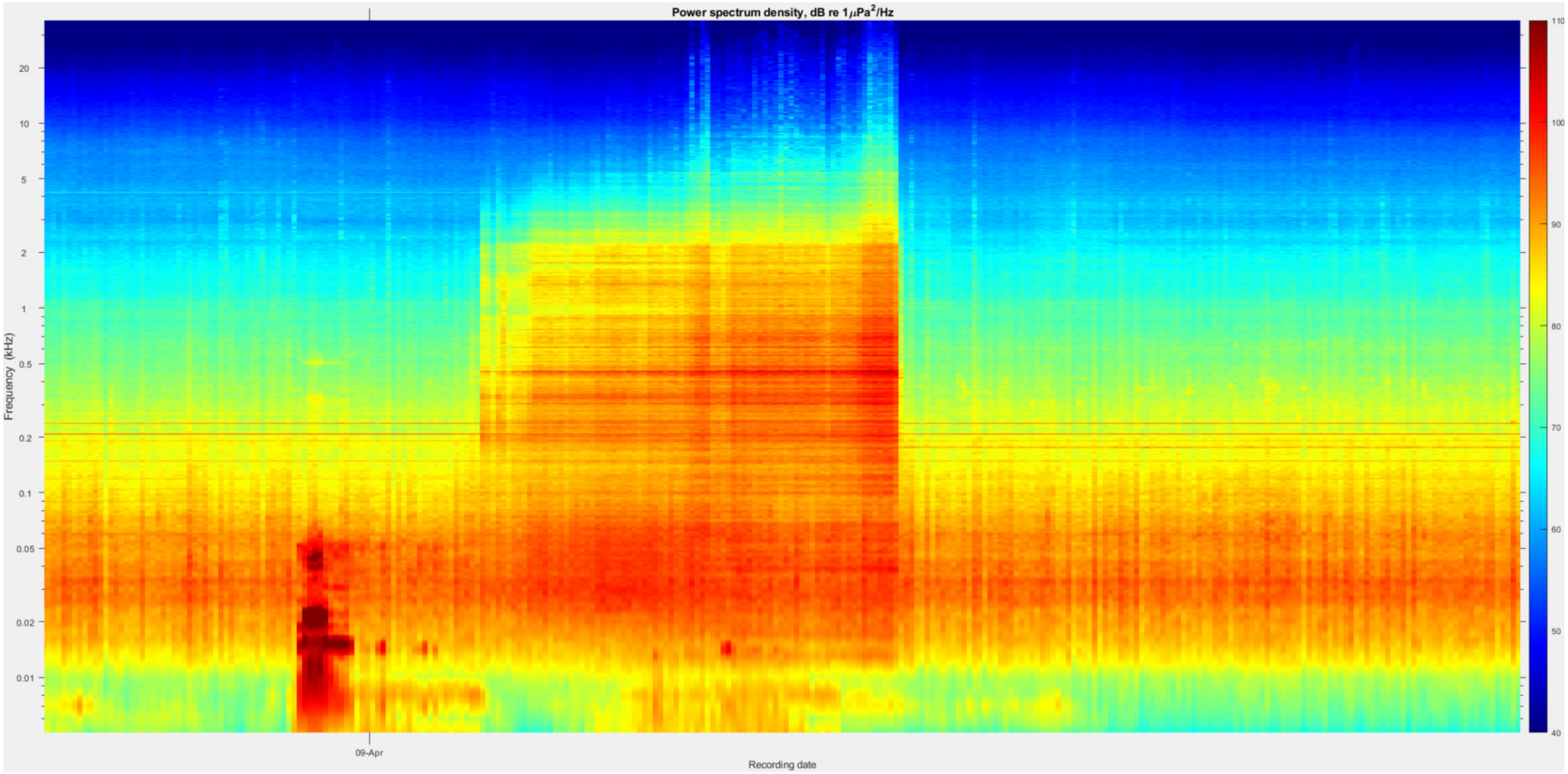

Figure B-45. PSD Spectrogram Plot of S-47 Mechanical Cut from 0:20 April 9, 2021 – 1:43 April 9, 2021

Table B-12. Empty Conductor S-36
(7:08 April 9, 2021 – 7:59 April 9, 2021)

Conductor	Start Time	End Time	Total Duration of Cut (minutes)	Overall Wall Thickness (inches)	Cut Depth Below Mudline (Feet)	Cutter RPM
S-36	4/9/2021 7:08	4/9/2021 7:59	51	0.812	20	60

Conductor	Start Time	End Time	Direction	Monitor Station Name	Distance to Conductor (m)	L_p	Max L_p	Min L_p	$L_{p,pk}$	L_E
S-36	4/9/2021 7:08	4/9/2021 7:59	North	5362	160.75	124	128.9	110.9	151.3	158.9
			North	5363	160.75	124.6	129.6	112.5	153.4	159.5
			East	5366	114.59	129.2	134.5	112.2	158.8	164.1
			South	5365	112.6	127.6	134.1	113.1	163.8	162.5
			West	5356	140.89	125.5	130.9	112.6	154	160.4
			South	5353	271.57	121.8	127.6	109.1	157.5	156.7

L_p and $L_{p.pk}$ = (dB re 1 μPa); L_E = (dB re 1 μPa²·s)

Conductor	Start Time	End Time	Monitor Station Name	L_p				L_E			
				LF	MF	HF	PP	LF	MF	HF	PP
S-36	4/9/2021 7:08	4/9/2021 7:59	5362	122.8	100.5	96.2	115.8	157.6	135.3	131	150.6
			5363	123.4	102.3	95.4	116.5	158.2	137.1	133.2	151.3
			5366	128.8	105.2	99.8	122.4	163.3	140.1	134.7	157.2
			5365	126.7	105.9	101.4	120.9	161.6	140.8	136.2	155.8
			5356	124.4	102.9	98.5	118.1	159.3	137.8	133.4	153
			5353	120.9	100.6	96.1	115.2	155.8	135.4	131	150.1

L_p and$L_{p.pk}$ = (dB re 1 μPa); L_E = (dB re 1 μPa²·s)
LF – low frequency; MF – mid-frequency; HF – high frequency; PP – phocid pinnipeds

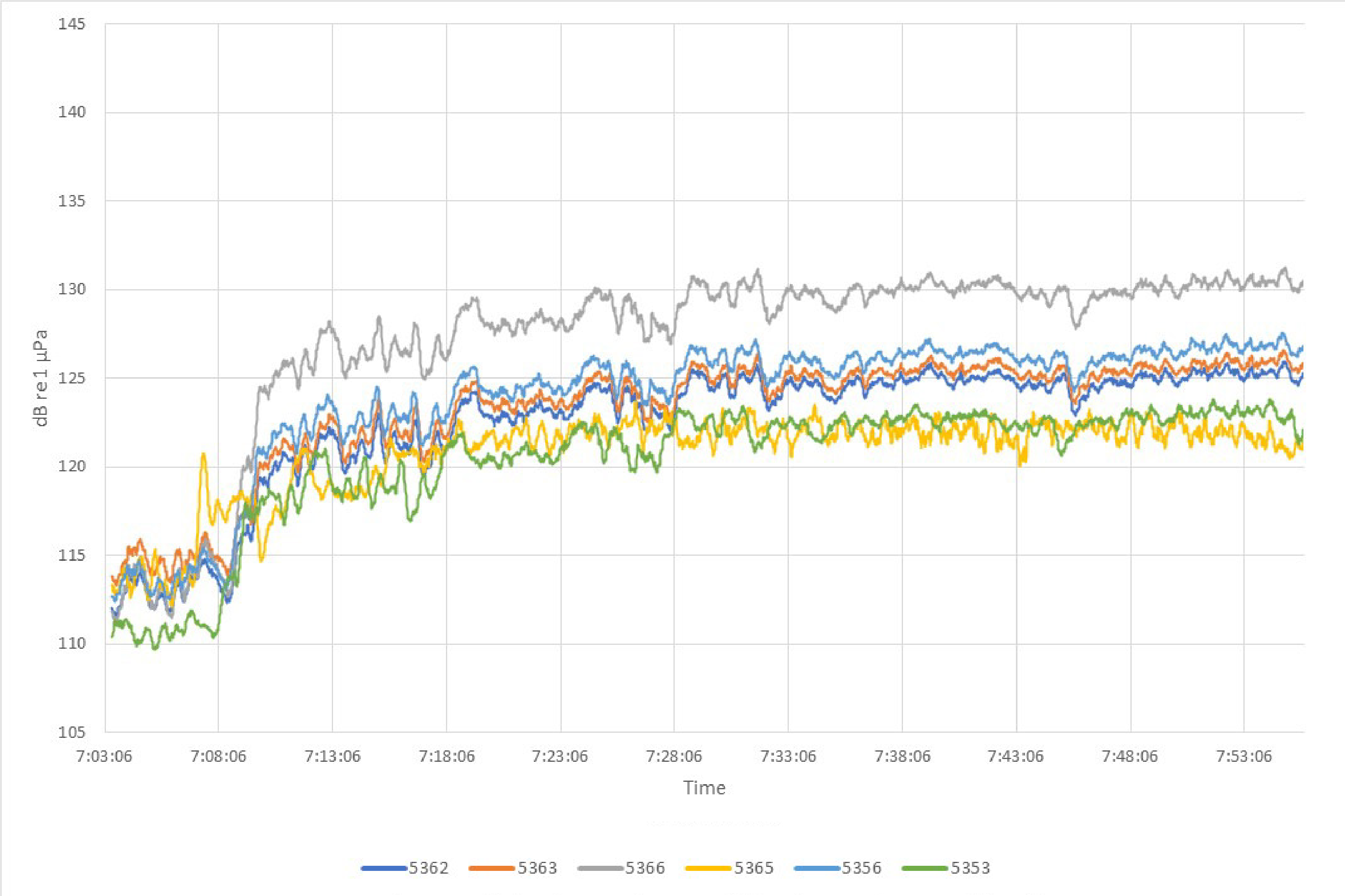

Figure B-46. Time History Plot of S-36 Mechanical Cut from April 9, 2021, 7:08 to 7:59 (20-second sample interval)

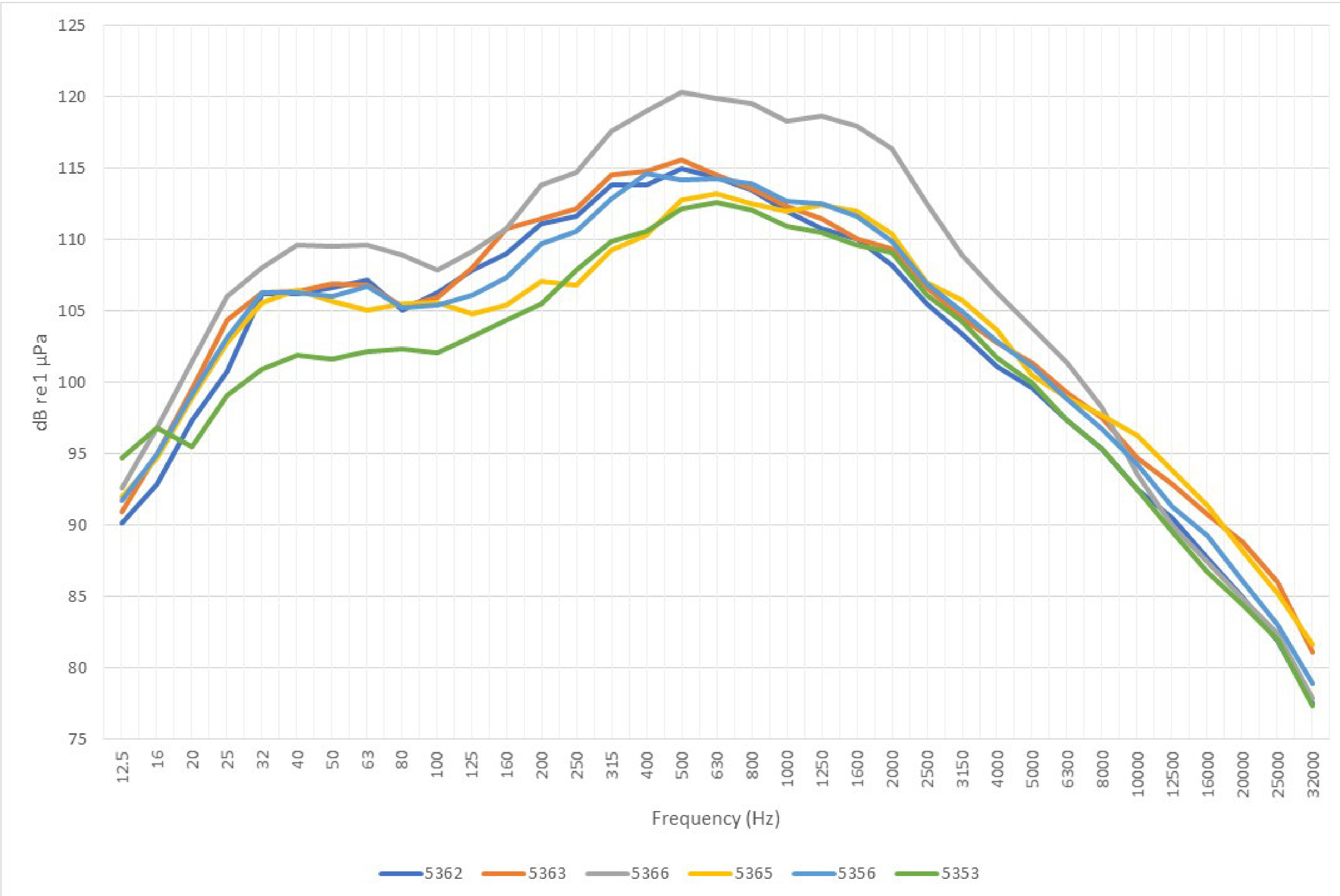

Figure B-47. SPL RMS 1/3 Octave Band Plot of S-36 Mechanical Cut from April 9, 2021, 7:08 to 7:59

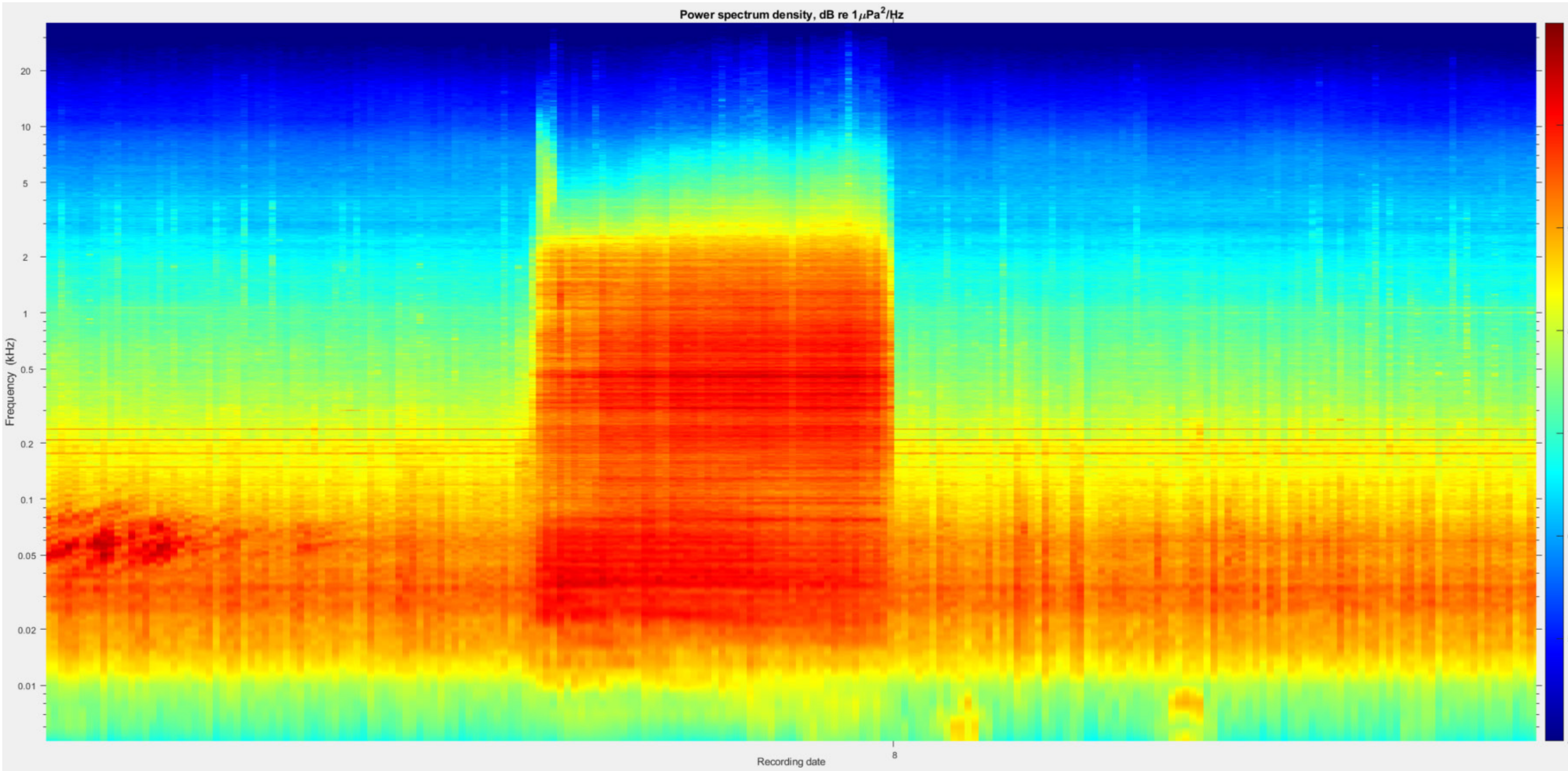

Figure B-48. PSD Spectrogram Plot of S-36 Mechanical Cut from 7:08 April 9, 2021 – 7:59 April 9, 2021

Table B-13. Empty Conductor S-34
(15:07 April 9, 2021 – 16:45 April 9, 2021)

Conductor	Start Time	End Time	Total Duration of Cut (minutes)	Overall Wall Thickness (inches)	Cut Depth Below Mudline (Feet)	Cutter RPM
S-34	4/9/2021 15:07	4/9/2021 16:45	98	0.812	20	60

Conductor	Start Time	End Time	Direction	Monitor Station Name	Distance to Conductor (m)	L_p	Max L_p	Min L_p	$L_{p,pk}$	L_E
S-34	4/9/2021 15:07	4/9/2021 16:45	North	5362	159.11	119.5	126.1	110.8	152.0	157.2
			North	5363	159.11	119.9	126.1	111.8	152.3	157.7
			East	5366	113.6	124.5	131.8	111.6	164.9	162.2
			South	5365	114.63	122.6	130.5	111.8	155.1	160.3
			West	5356	141.96	120.2	126.8	111.1	147.9	157.9
			South	5353	273.55	116.2	123.4	107.6	147.7	153.9

L_p and $L_{p.pk}$ = (dB re 1 μPa); L_E = (dB re 1 μPa^2·s)

Conductor	Start Time	End Time	Monitor Station Name	L_p				L_E			
				LF	MF	HF	PP	LF	MF	HF	PP
S-34	4/9/2021 15:07	4/9/2021 16:45	5362	117.7	97.2	93.1	112.0	155.4	134.9	130.8	149.7
			5363	118.1	99.4	95.7	112.5	155.8	137.1	133.4	150.2
			5366	123.4	101.4	95.8	118.5	161.1	139.1	133.5	156.2
			5365	121	99.7	95.5	115.1	158.8	137.4	133.2	128.8
			5356	111.2	99.1	95.8	107.7	148.9	136.9	133.5	145.5
			5353	114.6	95.9	92.2	109.2	152.3	133.6	129.9	146.9

L_p and$L_{p.pk}$ = (dB re 1 μPa); L_E = (dB re 1 μPa^2·s)
LF – low frequency; MF – mid-frequency; HF – high frequency; PP – phocid pinnipeds

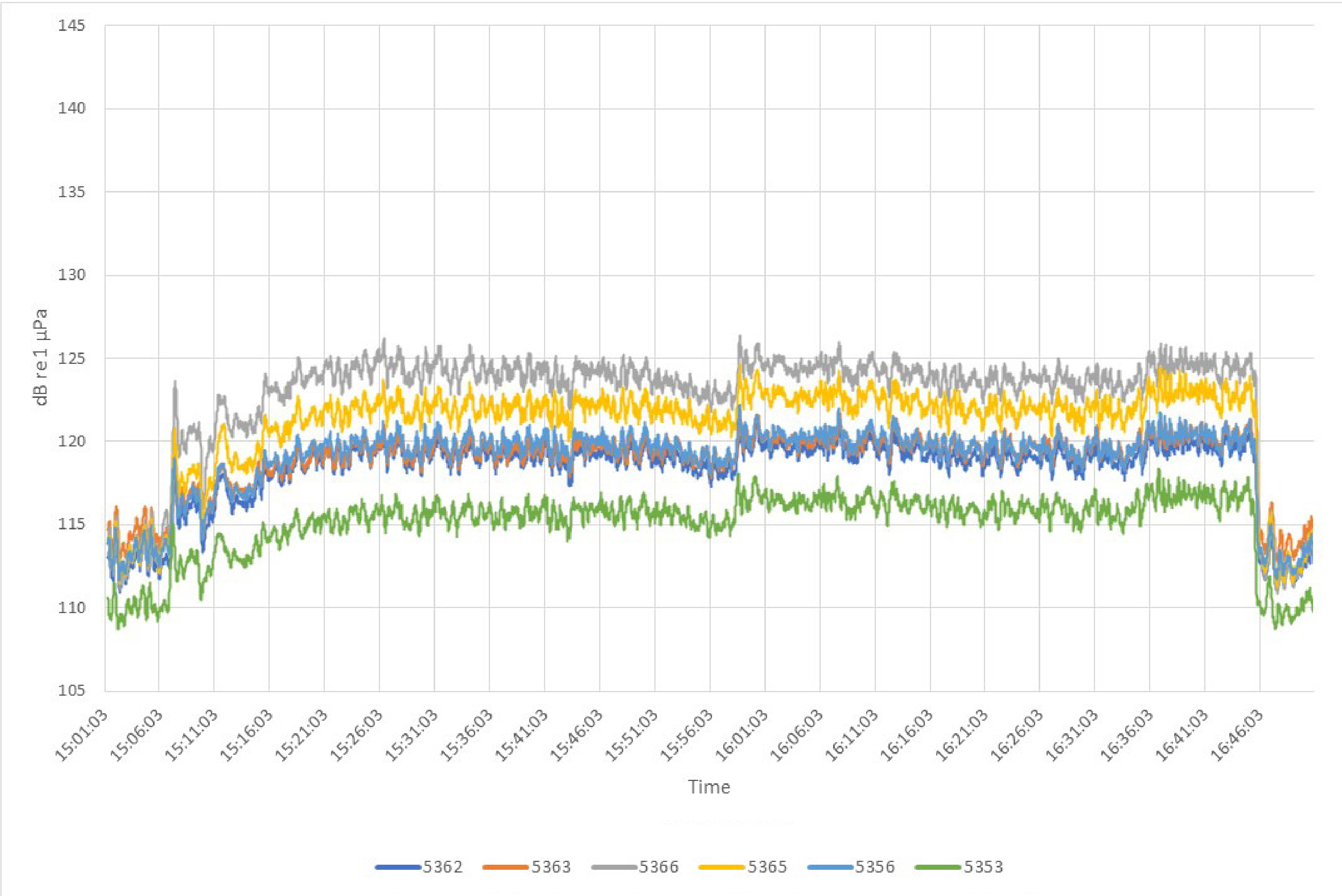

Figure B-49. Time History Plot of S-34 Mechanical Cut from April 9, 2021, 15:07 to 16:45 (20-second sample interval)

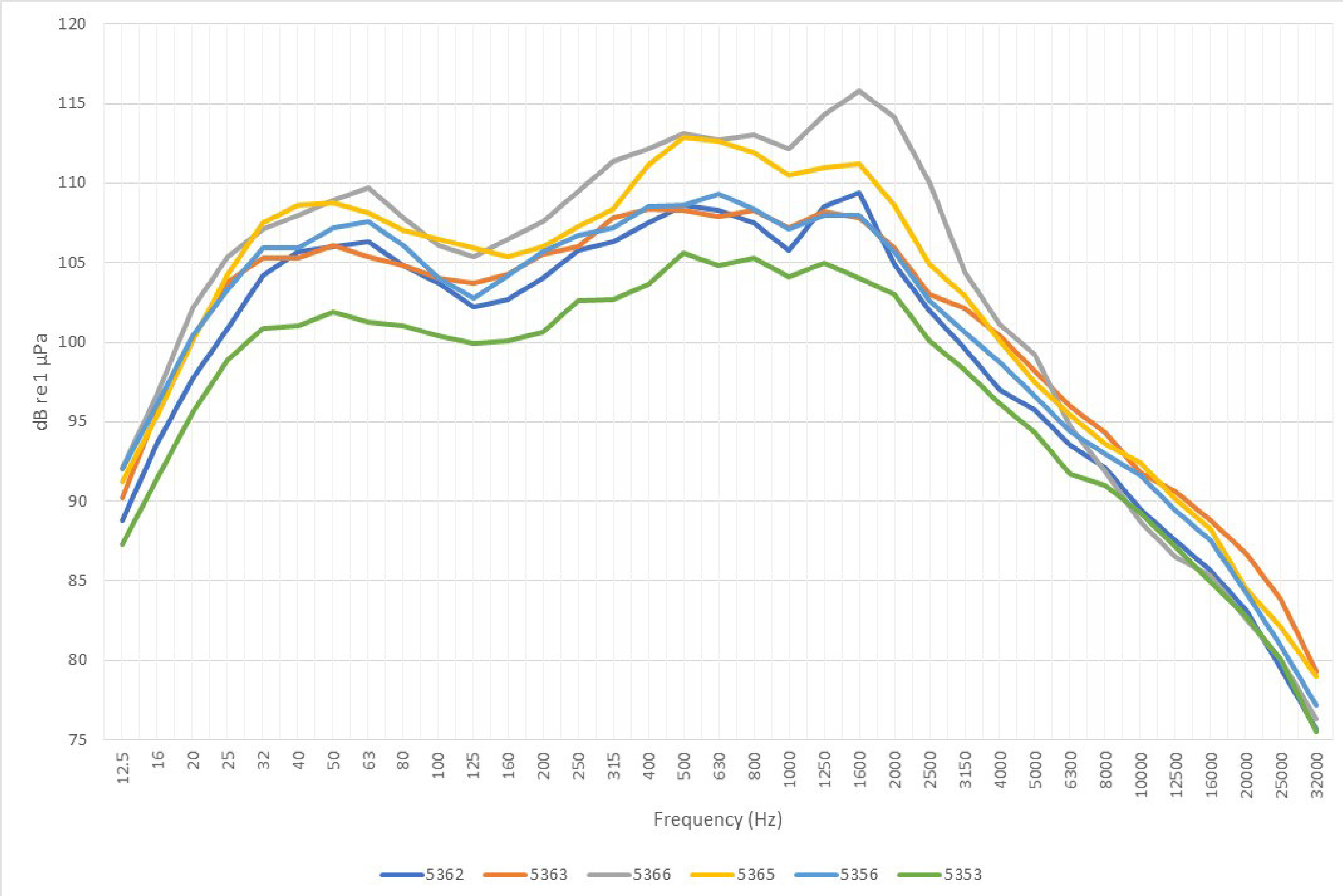

Figure B-50. SPL RMS 1/3 Octave Band Plot of S-34 Mechanical Cut from April 9, 2021, 15:07 to 16:45

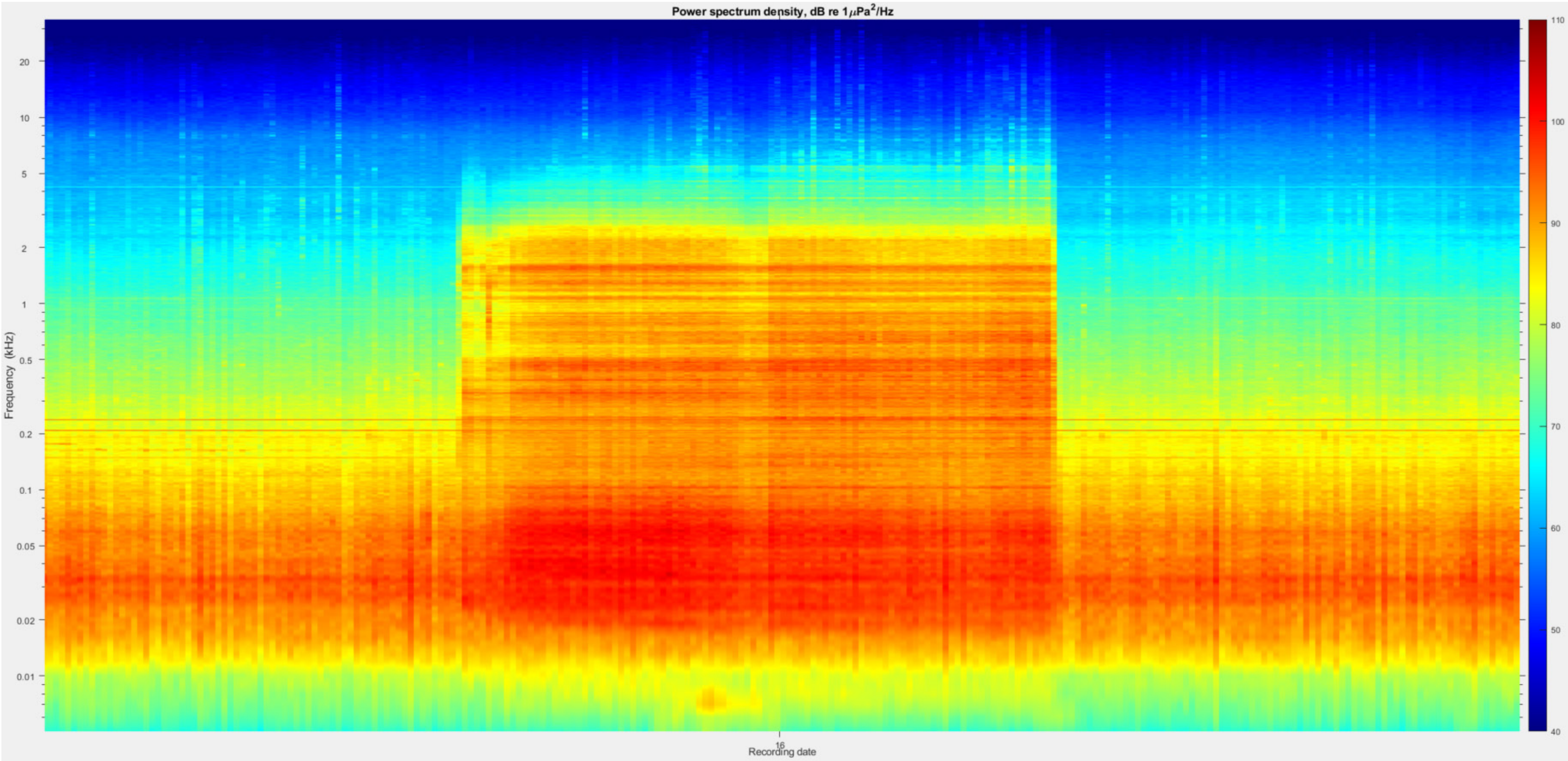

Figure B-51. PSD Spectrogram Plot of S-34 Mechanical Cut from 15:07 April 9, 2021 – 16:45 April 9, 2021

Table B-14. Wellbore Conductor B-17
(22:41 April 10, 2021 – 15:51 April 11, 2021)

Conductor	Start Time	End Time	Total Duration of Cut (minutes)	Overall Wall Thickness (inches)	Cut Depth Below Mudline (Feet)	Cutter RPM
B-17	4/10/2021 22:41	4/11/2021 1:10	149	1.919	20	60
	4/11/2021 4:40	4/11/2021 15:51	671			

Conductor	Start Time	End Time	Direction	Monitor Station Name	Distance to Conductor (m)	L_p	Max L_p	Min L_p	$L_{p,pk}$	L_E
B-17	4/10/2021 22:41	4/11/2021 1:10	North	5362	155.82	117.7	125.2	112.1	147.2	157.2
			North	5363	155.82	118.5	125.6	113.5	151.4	158.0
			East	53661	111.89	--	--	--	--	--
			South	5365	118.56	119.5	127.6	110.3	150.6	159.0
			West	5356	144.03	118.1	125.7	111.7	146.1	157.6
			South	5353	277.33	114.9	121.8	108.7	147.7	154.4
	4/11/2021 4:40	4/11/2021 15:51	North	5362	155.82	122.0	128.9	108.7	156.9	168.0
			North	5363	155.82	123.2	129.2	109.0	159.0	168.2
			East	5366	111.89	125.8	133.3	108.5	161.4	171.8
			South	5365	118.56	124.1	131.4	109.2	159.2	170.1
			West	5356	144.03	122.0	130.8	110.3	156.3	168.1
			South	5353	277.33	118.9	125.2	106.9	150.8	164.1

L_p and $L_{p,pk}$ = (dB re 1 μPa); L_E = (dB re 1 μPa^2·s)

Conductor	Start Time	End Time	Monitor Station Name	L_p				L_E			
				LF	MF	HF	PP	LF	MF	HF	PP
B-17	4/10/2021 22:41	4/11/2021 1:10	5362	115.9	97.0	93.5	108.8	155.5	136.6	133.0	148.3
			5363	116.6	99.6	96.3	110.2	156.1	139.1	135.8	149.7
			5366	--	--	--	--	--	--	--	--
			5365	117.8	97.3	94.2	109.9	157.3	136.8	133.7	149.4
			5356	116.2	97.8	94.5	109.0	155.7	137.3	134.0	148.5
			5353	113.1	95.3	92.0	106.2	152.6	134.8	131.5	145.7
	4/11/2021 4:40	4/11/2021 15:51	5362	120.8	100.4	96.1	114.1	166.8	146.5	142.2	160.2
			5363	122.2	103.1	99.0	115.9	166.9	147.9	143.8	160.7
			5366	124.7	102.1	97.1	118.1	170.8	148.2	143.1	164.2
			5365	123.4	102.0	97.8	116.6	168.6	147.2	143.0	161.8
			5356	120.7	100.2	96.3	113.6	166.7	146.2	142.3	159.6
			5353	117.7	98.3	94.3	111.3	162.9	143.4	139.4	156.5

L_p and$L_{p,pk}$ = (dB re 1 μPa); L_E = (dB re 1 μPa^2·s)
LF – low frequency; MF – mid-frequency; HF – high frequency; PP – phocid pinnipeds

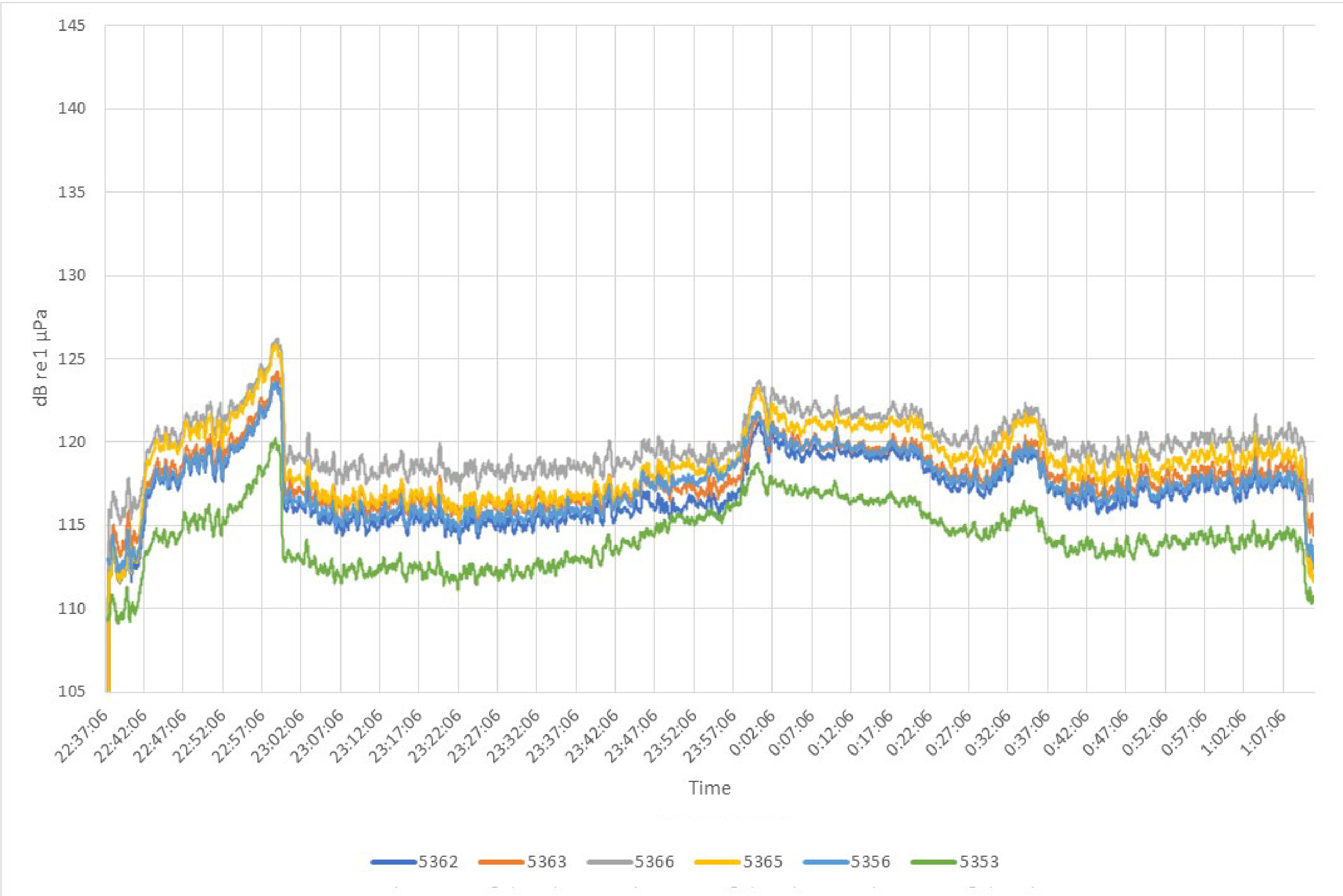

Figure B-52. Time History Plot of B-17 Mechanical Cut from April 10, 2021, 22:41 to April 11, 2021, 1:10 (20-second sample interval)

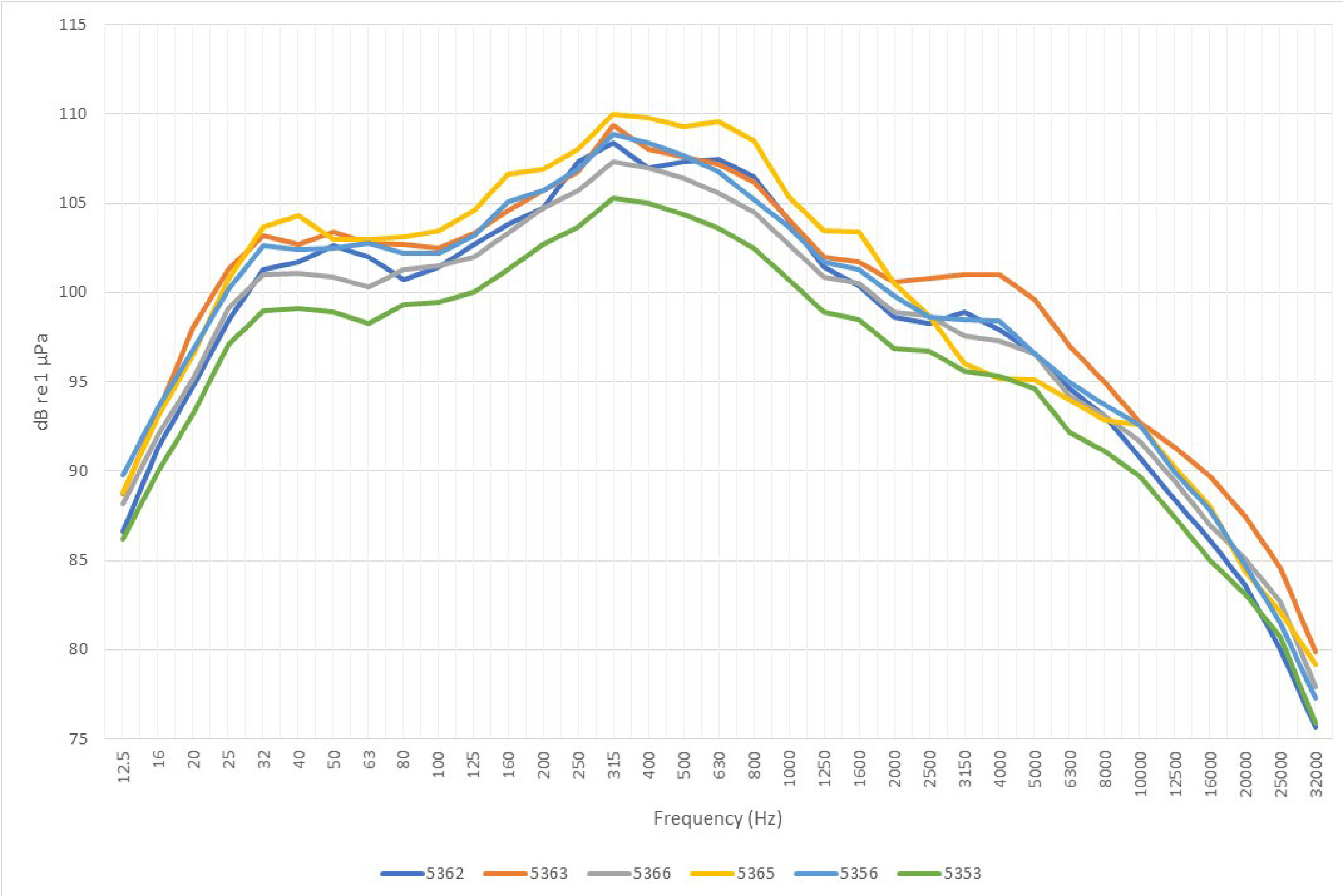

Figure B-53. SPL RMS 1/3 Octave Band Plot of B-17 Mechanical Cut from April 10, 2021, 22:41 to April 11, 2021, 1:10

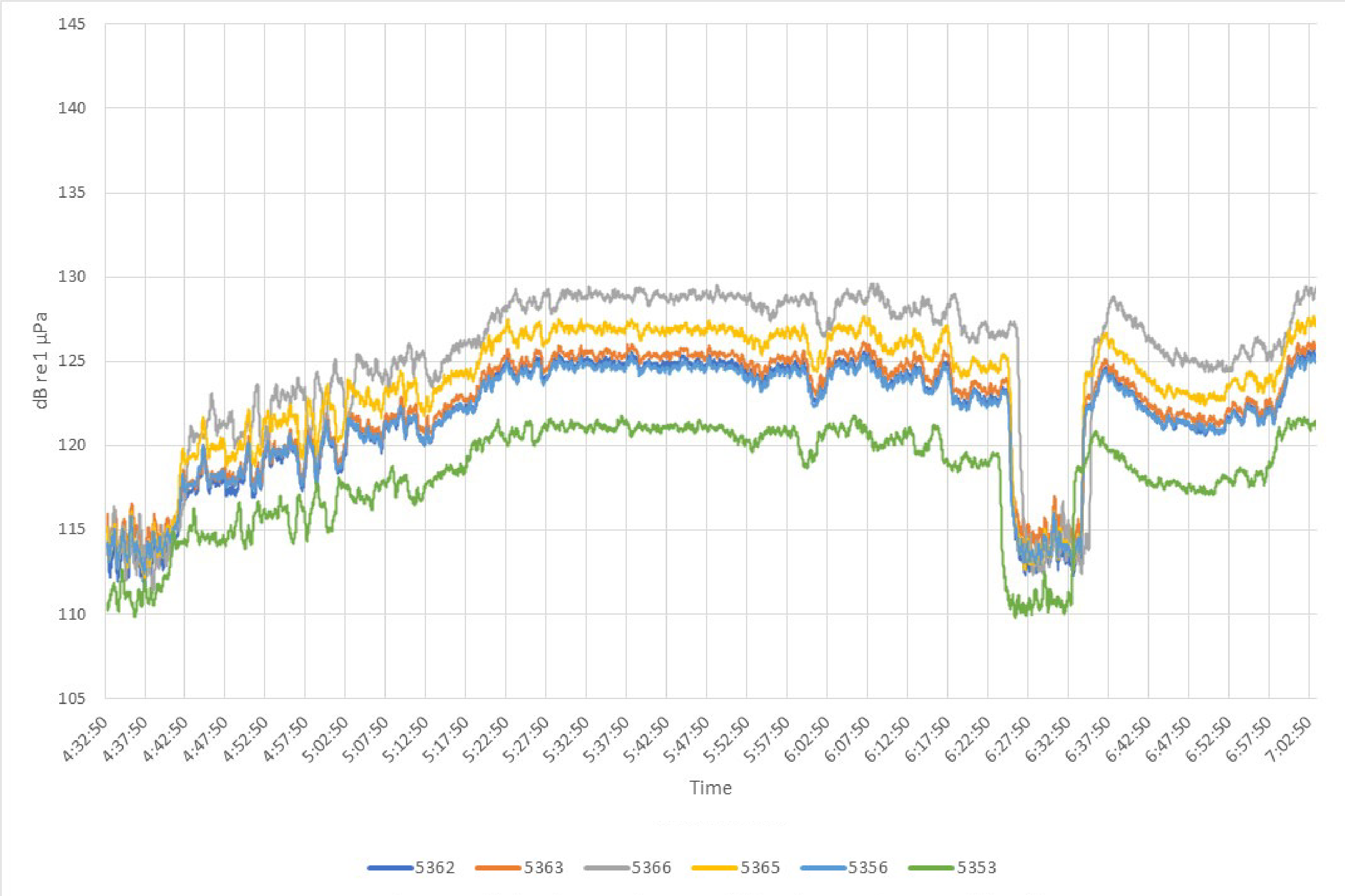

Figure B-54. Time History Plot of B-17 Mechanical Cut from B-17 Mechanical Cut from April 11, 2021, 4:40 to 15:51 (20-second sample)

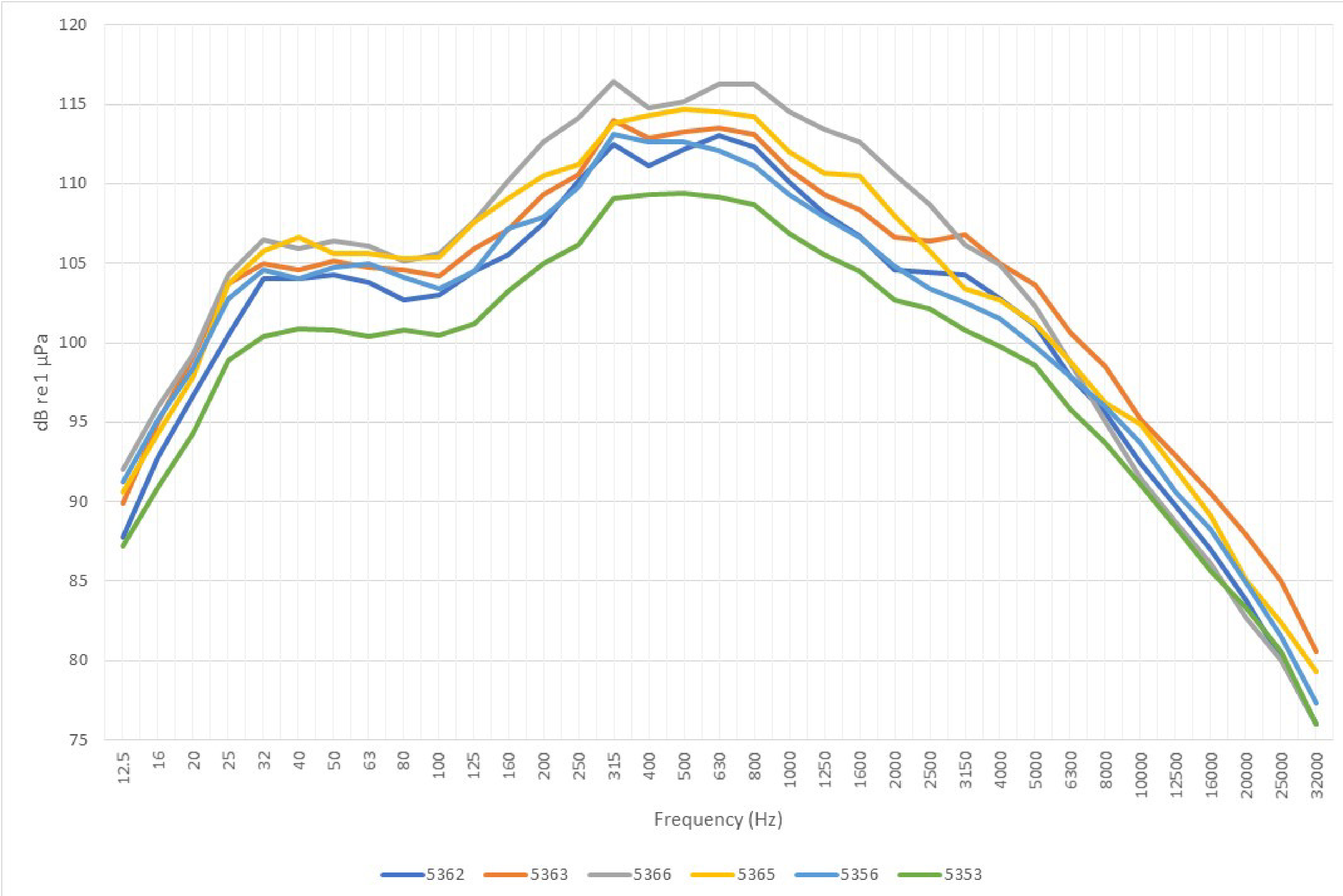

Figure B-55. SPL RMS 1/3 Octave Band Plot of B-17 Mechanical Cut from April 11, 2021, 4:40 to 15:51

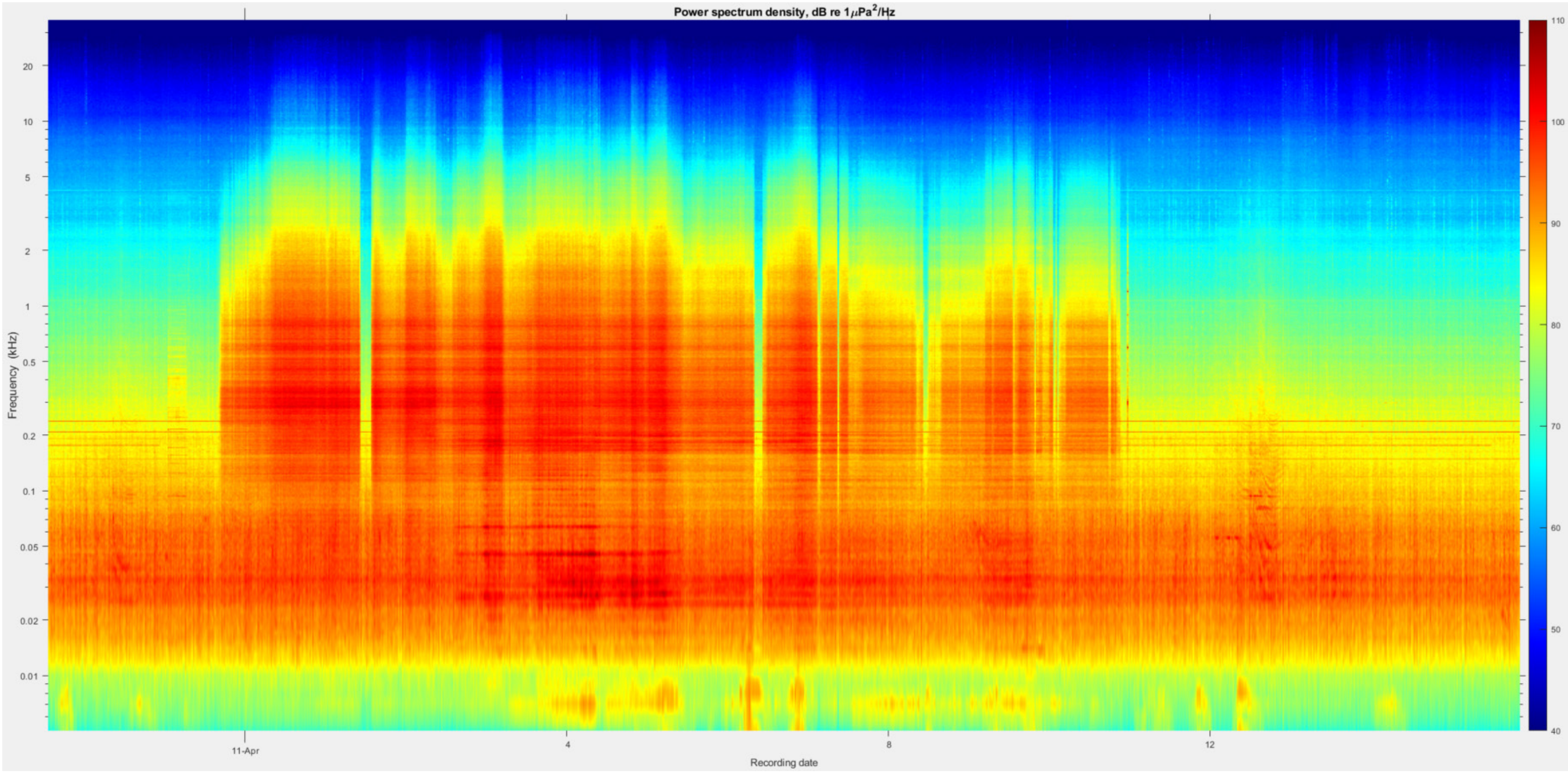

Figure B-56. PSD Spectrogram Plot of B-17 Mechanical Cut from 22:41 April 10, 2021 – 15:51 April 11, 2021

Table B-15. Empty Conductor S-41
(21:06 April 11, 2021 – 23:00 April 11, 2021)

Conductor	Start Time	End Time	Total Duration of Cut (minutes)	Overall Wall Thickness (inches)	Cut Depth Below Mudline (Feet)	Cutter RPM
S-41	4/11/2021 21:06	4/11/2021 23:00	114	0.812	20	60

Conductor	Start Time	End Time	Direction	Monitor Station Name	Distance to Conductor (m)	L_p	Max L_p	Min L_p	$L_{p,pk}$	L_E
S-41	4/11/2021 21:06	4/11/2021 23:00	North	5362	154.65	118.6	127.7	110.2	152.3	157.0
			North	5363	154.65	120.3	129.1	111.9	153.6	157.4
			East	5366	113.9	122.6	132.2	107.6	156.9	160.9
			South	5365	118.8	120.6	130.7	108.8	157.3	159.0
			West	5356	142.11	119.7	137.5	111.2	155.4	158.1
			South	5353	276.63	114.9	123.2	108.4	144.6	153.3

L_p and $L_{p.pk}$ = (dB re 1 μPa); L_E = (dB re 1 μPa²·s)

Conductor	Start Time	End Time	Monitor Station Name	L_p				L_E			
				LF	MF	HF	PP	LF	MF	HF	PP
S-41	4/11/2021 21:06	4/11/2021 23:00	5362	117.1	99.5	95.6	111.7	155.5	137.9	134.0	150.0
			5363	119.7	102.0	98.3	114.3	154.9	137.2	133.4	149.4
			5366	122.3	101.0	96.2	116.7	159.7	138.3	133.6	154.0
			5365	119.2	99.9	96.3	113.5	157.6	138.3	134.6	151.9
			5356	118.1	100.1	96.3	112.6	156.5	138.5	134.7	151.0
			5353	115.1	97.7	94.1	109.4	150.2	132.9	129.2	144.5

L_p and$L_{p.pk}$ = (dB re 1 μPa); L_E = (dB re 1 μPa²·s)
LF – low frequency; MF – mid-frequency; HF – high frequency; PP – phocid pinnipeds

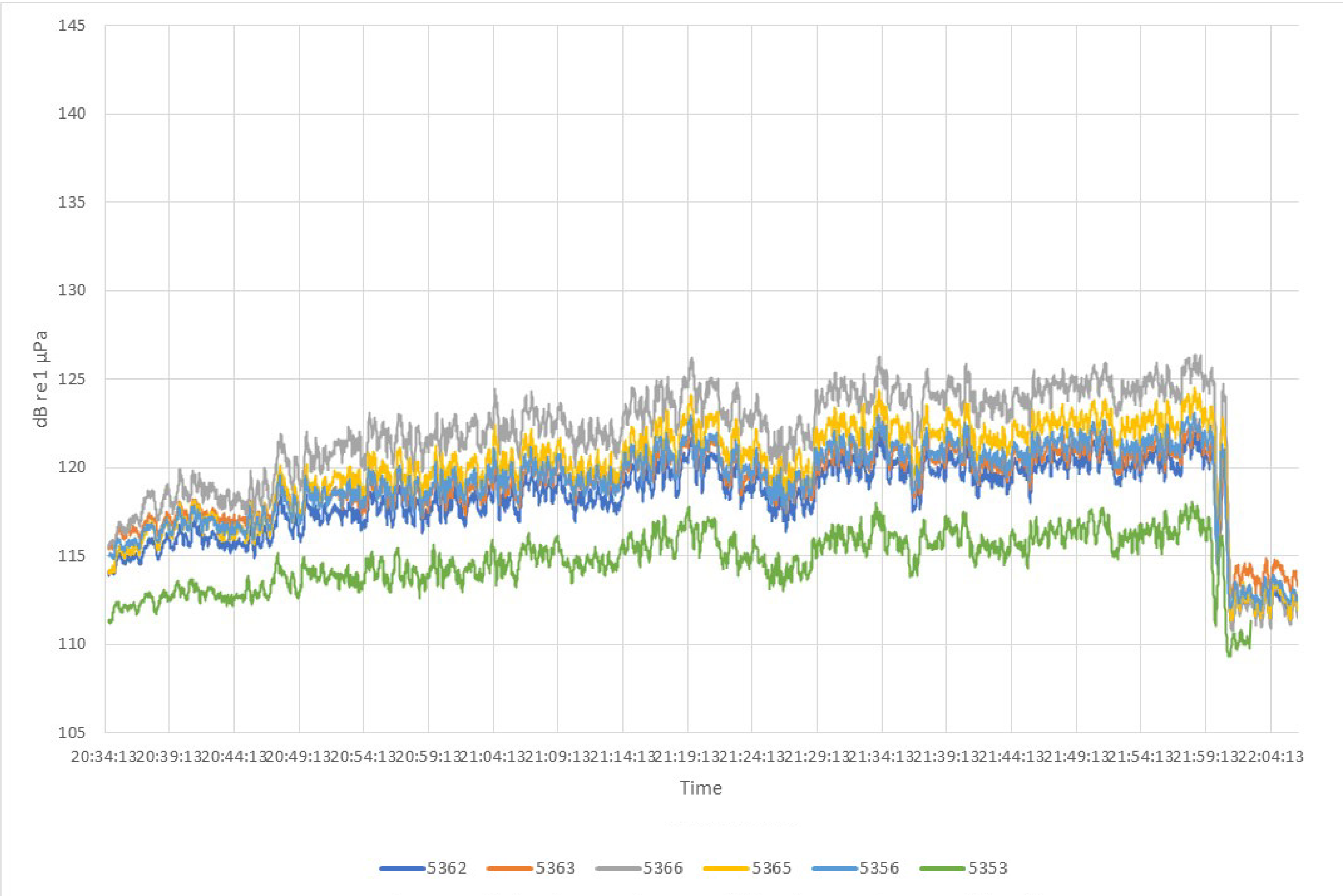

Figure B-57. Time History Plot of S-41 Mechanical Cut from April 11, 2021, 21:06 to 23:00 (20-second sample interval)

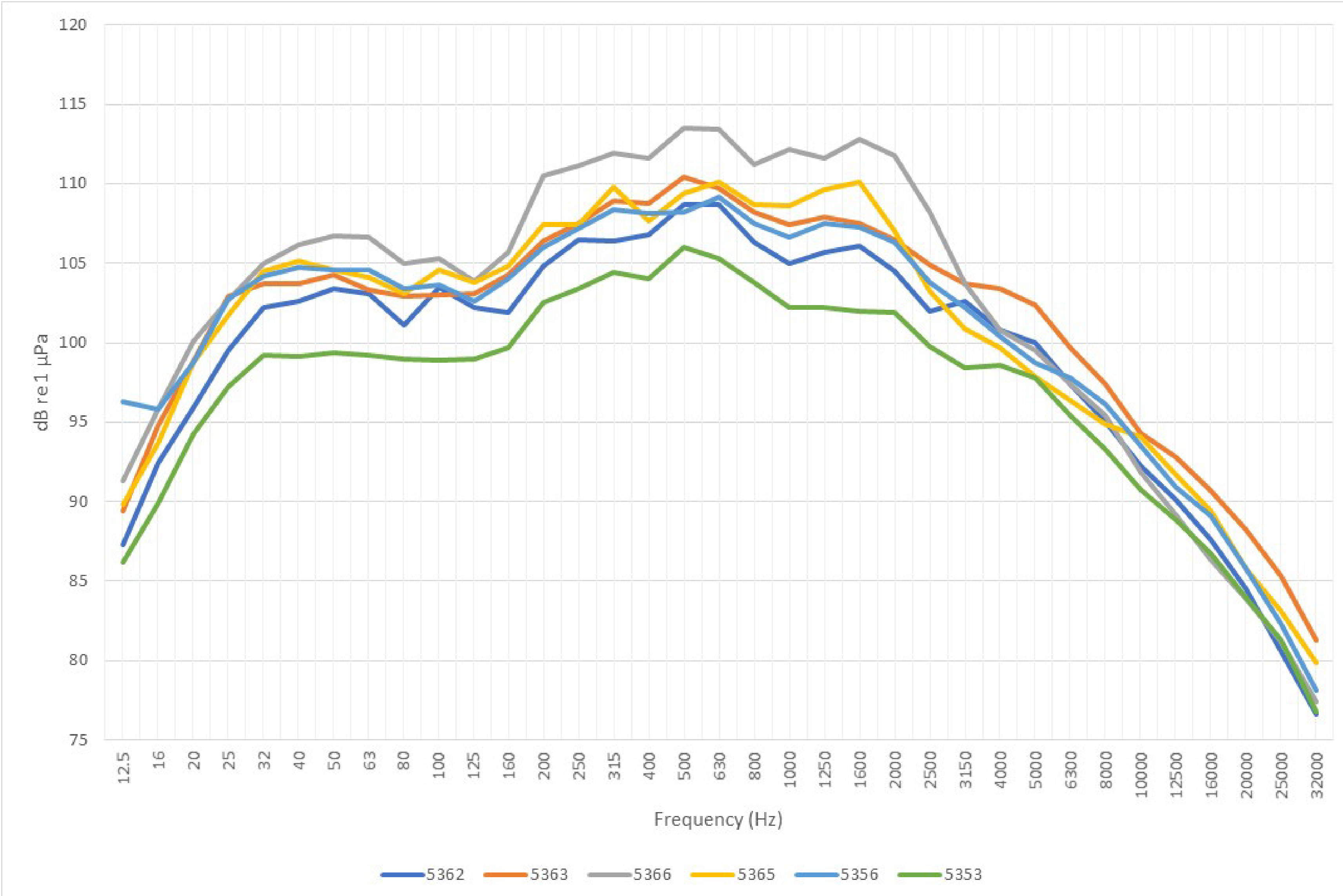

Figure B-58. SPL RMS 1/3 Octave Band Plot of S-41 Mechanical Cut from April 11, 2021, 21:06 to 23:00

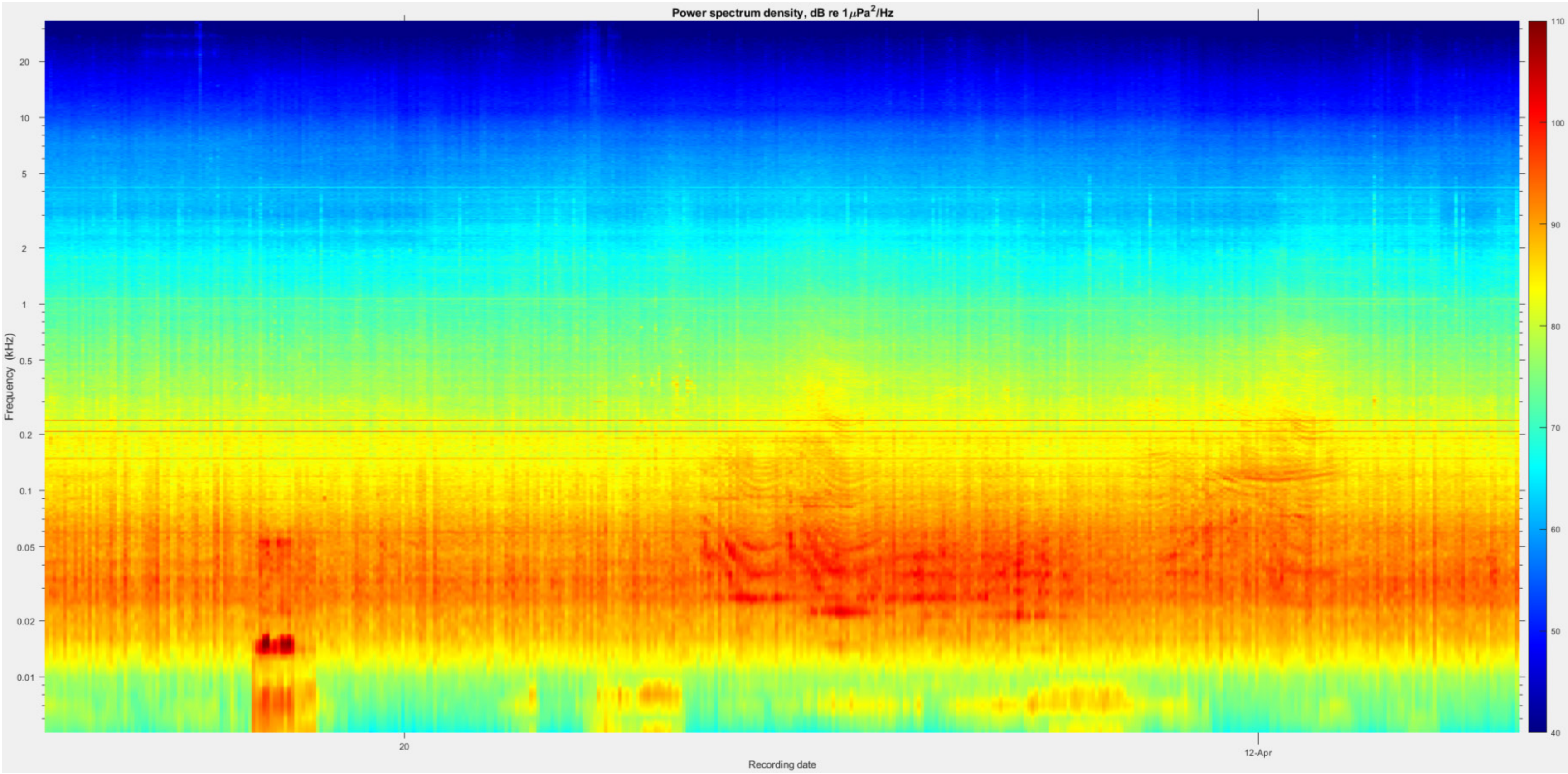

Figure B-59. PSD Spectrogram Plot of S-41 Mechanical Cut from 21:06 April 11, 2021 – 23:00 April 11, 2021

Table B-16. Empty Conductor S-28
(9:48 April 12, 2021 – 15:35 April 12, 2021)

Conductor	Start Time	End Time	Total Duration of Cut (minutes)	Overall Wall Thickness (inches)	Cut Depth Below Mudline (Feet)	Cutter RPM
S-28	4/12/2021 9:48	4/12/2021 15:35	347	0.812	20	60

Conductor	Start Time	End Time	Direction	Monitor Station Name	Distance to Conductor (m)	L_p	Max L_p	Min L_p	$L_{p,pk}$	L_E
S-28	4/12/2021 9:48	4/12/2021 15:35	North	5362	154.3	127.6	146.1	109.8	165.2	170.7
			North	5363	154.3	129.2	148.8	110.6	169.4	172.3
			East	5366	111.08	130.1	141.5	107.9	163.7	173.4
			South	5365	120.46	126.7	139.0	109.0	157.9	169.9
			West	5356	145.03	126.3	141.8	110.6	162.8	169.5
			South	5353	279.19	120.8	133.7	106.2	154.1	163.8

L_p and $L_{p,pk}$ = (dB re 1 μPa); L_E = (dB re 1 μPa²·s)

Conductor	Start Time	End Time	Monitor Station Name	L_p				L_E			
				LF	MF	HF	PP	LF	MF	HF	PP
S-28	4/12/2021 9:48	4/12/2021 15:35	5362	125.9	106.0	101.5	120.4	168.3	148.4	143.9	162.7
			5363	127.4	108.6	104.5	121.8	169.8	151.0	146.9	164.3
			5366	129.1	110.3	104.7	125.6	172.3	153.5	147.9	168.8
			5365	125.1	107.3	102.6	121.0	168.3	150.5	145.8	164.2
			5356	124.4	105.9	101.6	119.5	167.6	149.1	144.8	162.7
			5353	119.0	101.1	96.6	114.5	162.1	144.3	139.8	157.7

L_p and$L_{p,pk}$ = (dB re 1 μPa); L_E = (dB re 1 μPa²·s)
LF – low frequency; MF – mid-frequency; HF – high frequency; PP – phocid pinnipeds

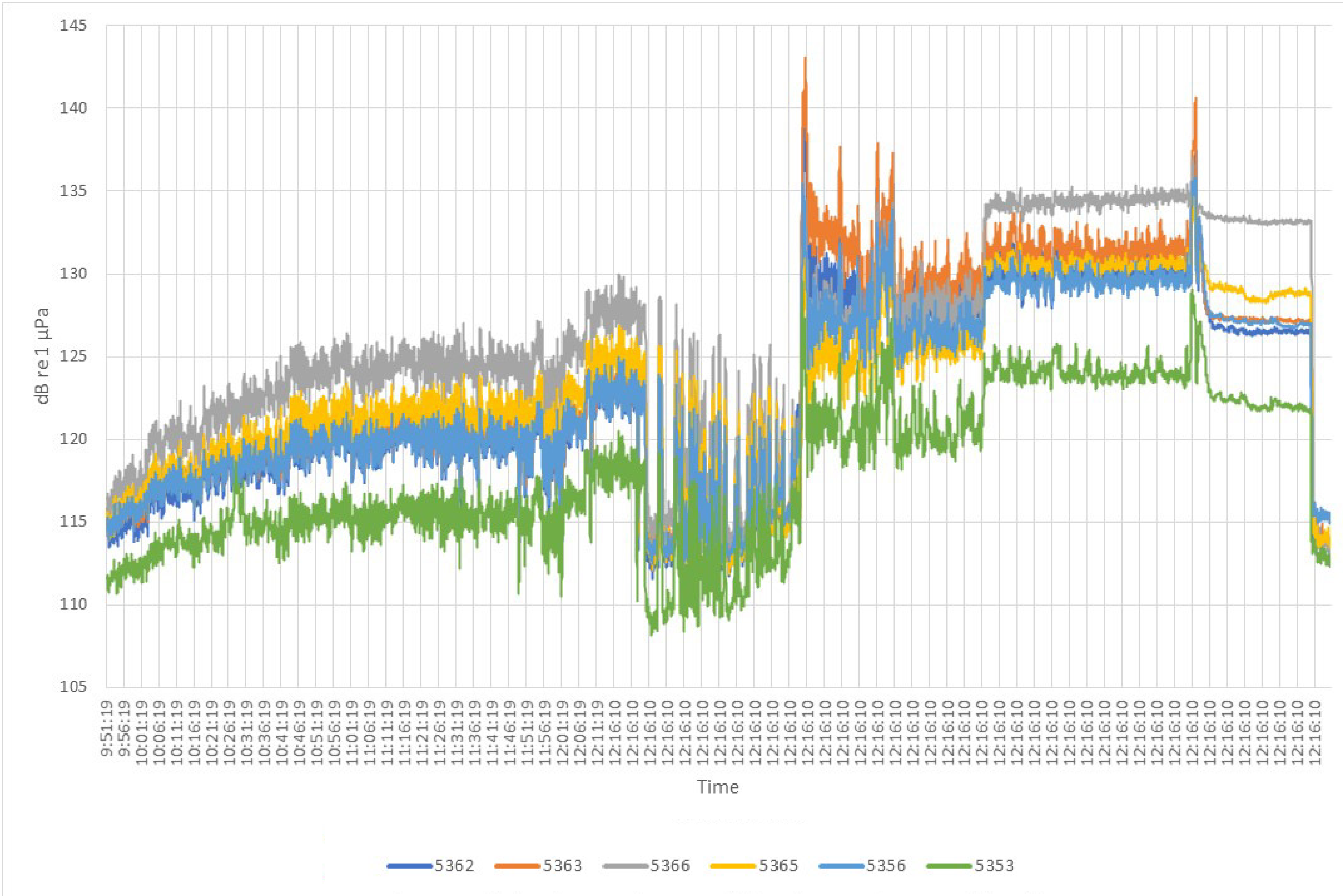

Figure B-60. Time History Plot of S-28 Mechanical Cut from April 12, 2021, 9:48 to 15:35 (20-second sample interval)

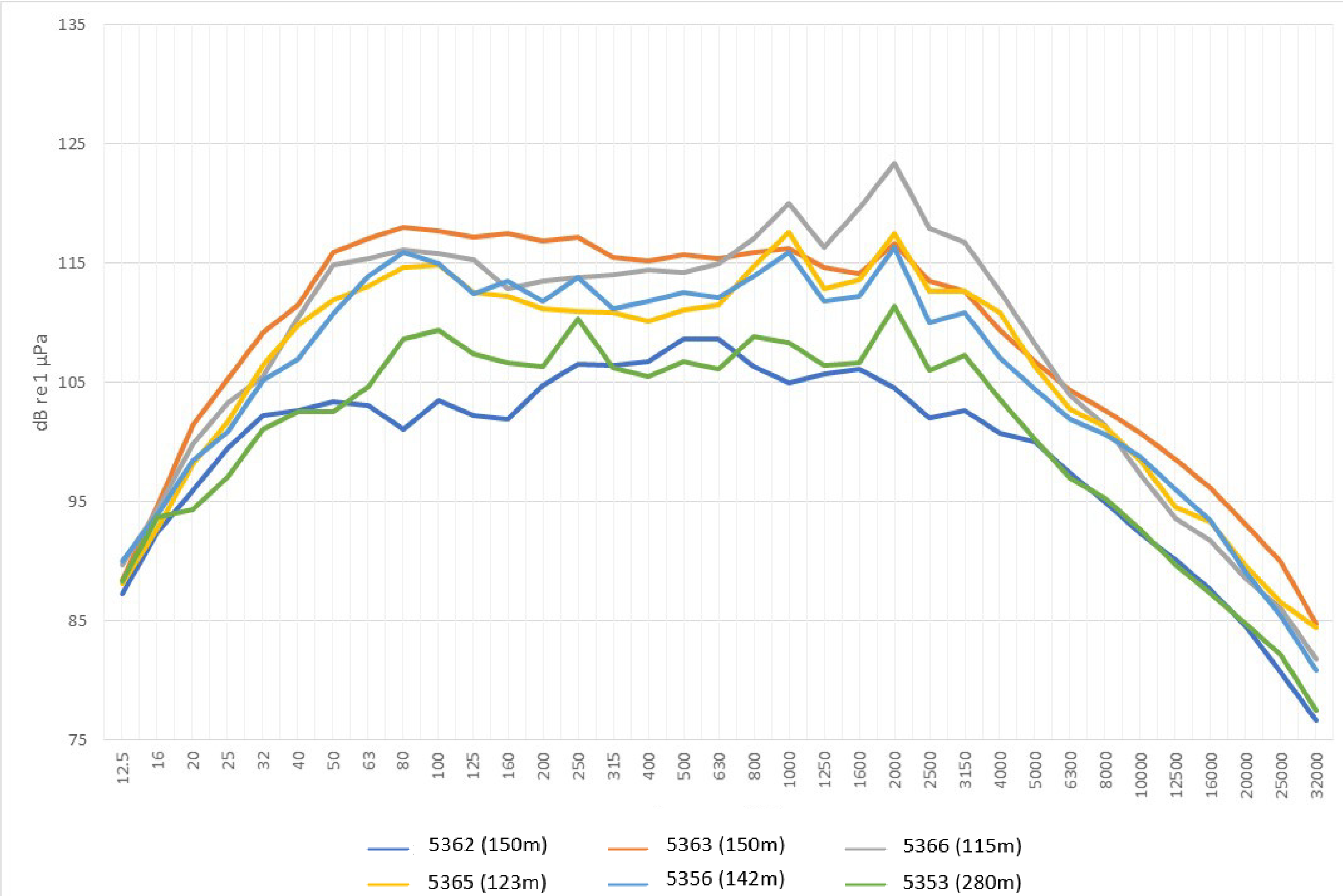

Figure B-61. SPL RMS 1/3 Octave Band Plot of S-28 Mechanical Cut from April 12, 2021, 9:48 to 15:35

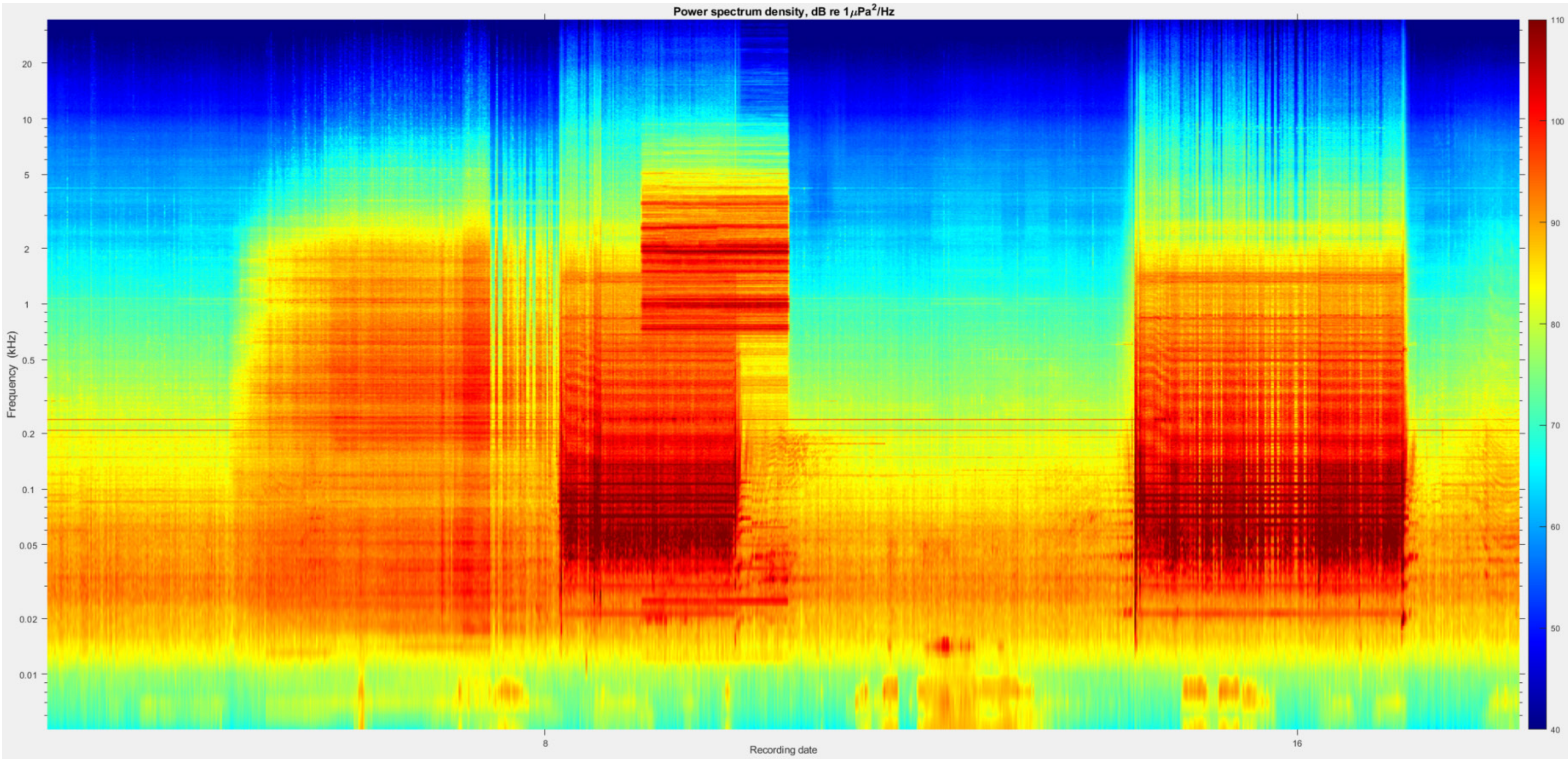

Figure B-62. PSD Spectrogram Plot of S-28 Mechanical Cut from 9:48 April 12, 2021 – 15:35 April 12, 2021

Table B-17. Empty Conductor S-12
(11:50 April 13, 2021 – 12:47 April 13, 2021)

Conductor	Start Time	End Time	Total Duration of Cut (minutes)	Overall Wall Thickness (inches)	Cut Depth Below Mudline (Feet)	Cutter RPM
S-12	4/13/2021 11:50	4/13/2021 12:47	57	0.812	20	60

Conductor	Start Time	End Time	Direction	Monitor Station Name	Distance to Conductor (m)	L_p	Max L_p	Min L_p	$L_{p,pk}$	L_E
S-12	4/13/2021 11:50	4/13/2021 12:47	North	5362	145.46	123.3	133.0	109.4	161.9	158.4
			North	5363	145.46	123.3	133.1	110.4	163.3	158.7
			East	5366	106.92	128.6	139.0	108.6	164.1	163.8
			South	5365	131.57	123.7	133.9	108.3	161.5	159.1
			West	5356	151.48	122.6	134.0	110.1	158.3	158.0
			South	5353	289.93	117.6	127.5	105.7	149.4	153.5

L_p and $L_{p,pk}$ = (dB re 1 μPa); L_E = (dB re 1 μPa²·s)

Conductor	Start Time	End Time	Monitor Station Name	L_p				L_E			
				LF	MF	HF	PP	LF	MF	HF	PP
S-12	4/13/2021 11:50	4/13/2021 12:47	5362	122.1	102.8	98.8	116.5	157.5	138.2	134.3	152.0
			5363	122.3	103.9	100.3	116.7	157.7	139.3	135.7	152.1
			5366	127.9	107.2	102.4	123.0	163.4	142.6	137.8	158.4
			5365	122.8	103.7	100.3	116.9	158.2	139.1	135.7	152.3
			5356	121.6	103.0	99.2	116.5	157.3	138.7	134.8	152.1
			5353	117.0	98.5	94.9	111.3	152.4	133.9	130.2	146.6

L_p and $L_{p,pk}$ = (dB re 1 μPa); L_E = (dB re 1 μPa²·s)
LF – low frequency; MF – mid-frequency; HF – high frequency; PP – phocid pinnipeds

Figure B-63. Time History Plot of S-12 Mechanical Cut from April 13, 2021, 11:50 to 12:47 (20-second sample interval)

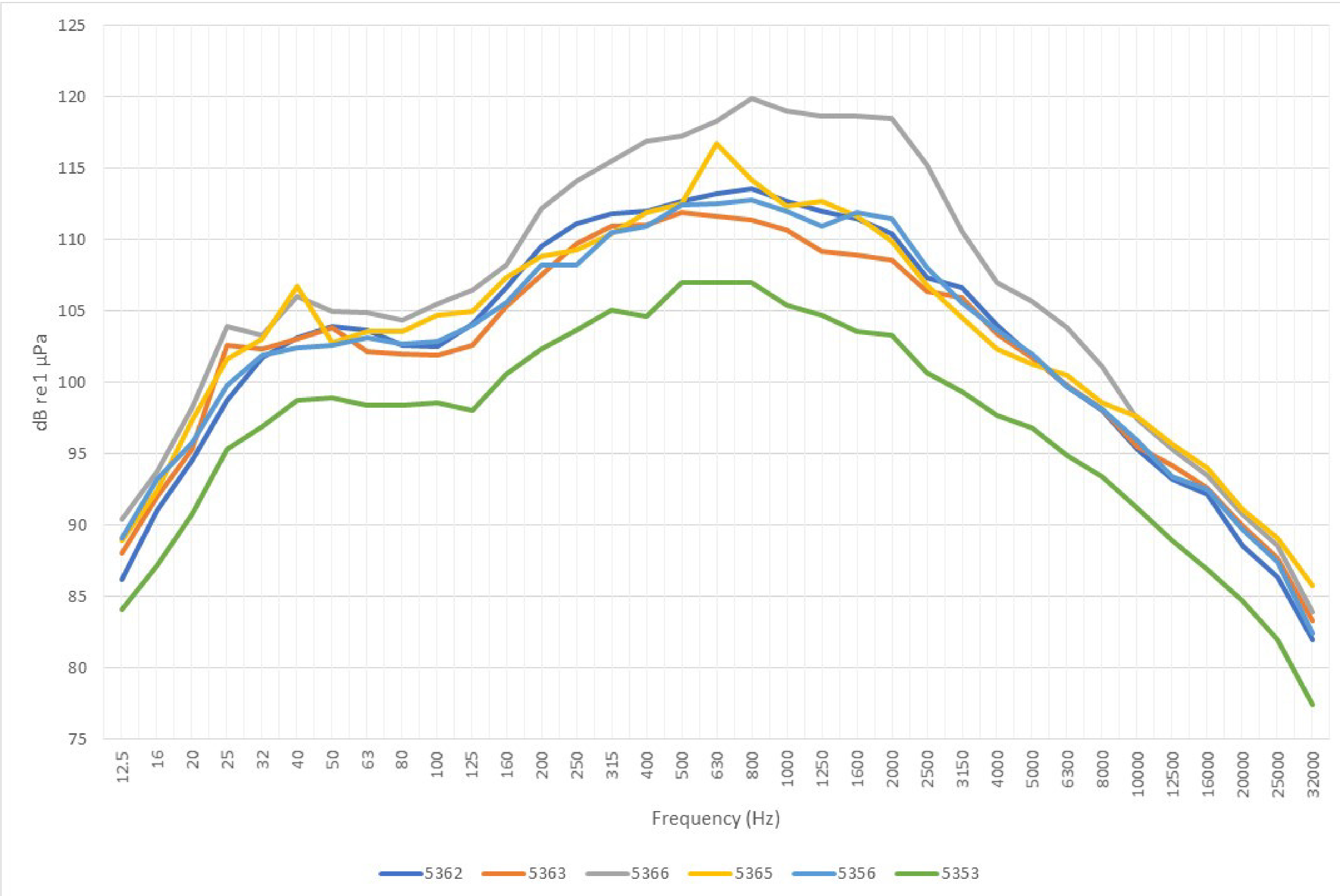

Figure B-64. SPL RMS 1/3 Octave Band Plot of S-12 Mechanical Cut from April 13, 2021, 11:50 to 12:47

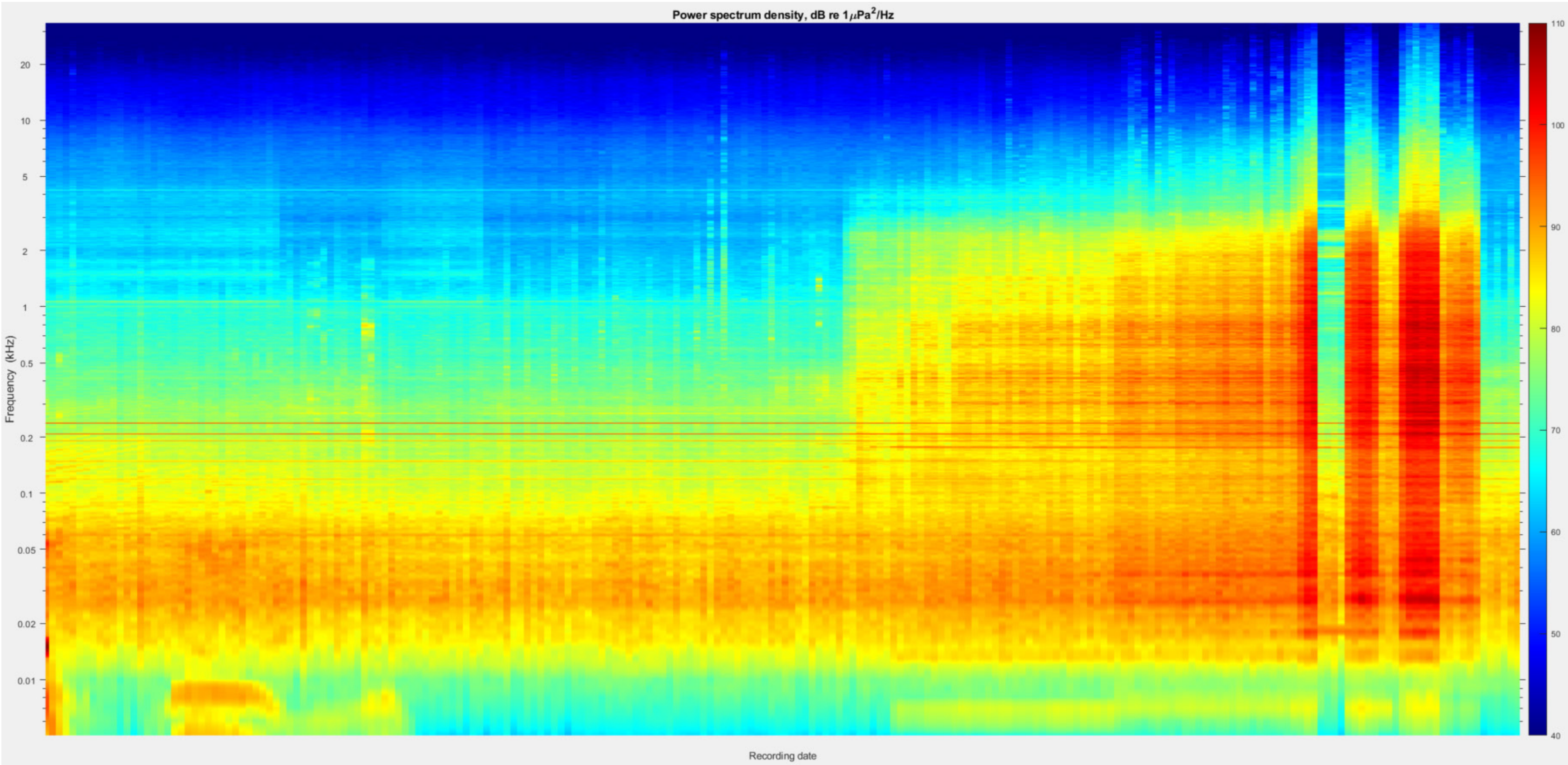

Figure B-65. PSD Spectrogram Plot of S-12 Mechanical Cut from 11:50 April 13, 2021 – 12:47 April 13, 2021

Table B-18. Empty Conductor S-23
(21:05 April 13, 2021 – 22:29 April 13, 2021)

Conductor	Start Time	End Time	Total Duration of Cut (minutes)	Overall Wall Thickness (inches)	Cut Depth Below Mudline (Feet)	Cutter RPM
S-23	4/13/2021 21:05	4/13/2021 22:29	84	0.812	20	60

Conductor	Start Time	End Time	Direction	Monitor Station Name	Distance to Conductor (m)	L_p	Max L_p	Min L_p	$L_{p,pk}$	L_E
S-23	4/13/2021 21:05	4/13/2021 22:29	North	5362	144.1	115.4	128.6	109.8	151.6	152.4
			North	5363	144.1	116.5	128.3	112.4	154.5	153.5
			East	5366	109.04	117.7	131.9	109.7	157.8	153.9
			South	5365	131.82	127.3	142.8	108.9	162.4	168.1
			West	5356	149.65	115.3	128.3	111.4	157.2	152.3
			South	5353	289.29	111.3	122.6	106.7	143.0	148.4

L_p and $L_{p,pk}$ = (dB re 1 μPa); L_E = (dB re 1 μPa²·s)

Conductor	Start Time	End Time	Monitor Station Name	L_p				L_E			
				LF	MF	HF	PP	LF	MF	HF	PP
S-23	4/13/2021 21:05	4/13/2021 22:29	5362	114.1	98.6	94.5	110.0	151.1	135.6	131.6	147.0
			5363	115.2	102.5	98.8	112.2	152.2	139.5	135.8	149.2
			5366	115.8	96.5	92.2	110.5	152.8	133.6	129.2	147.6
			5365	122.7	102.8	99.8	114.6	163.6	143.7	140.7	155.5
			5356	113.7	100.0	96.4	110.0	150.8	137.0	133.4	147.0
			5353	109.8	98.0	94.4	107.0	146.9	135.1	131.4	144.1

L_p and$L_{p,pk}$ = (dB re 1 μPa); L_E = (dB re 1 μPa²·s)
LF – low frequency; MF – mid-frequency; HF – high frequency; PP – phocid pinnipeds

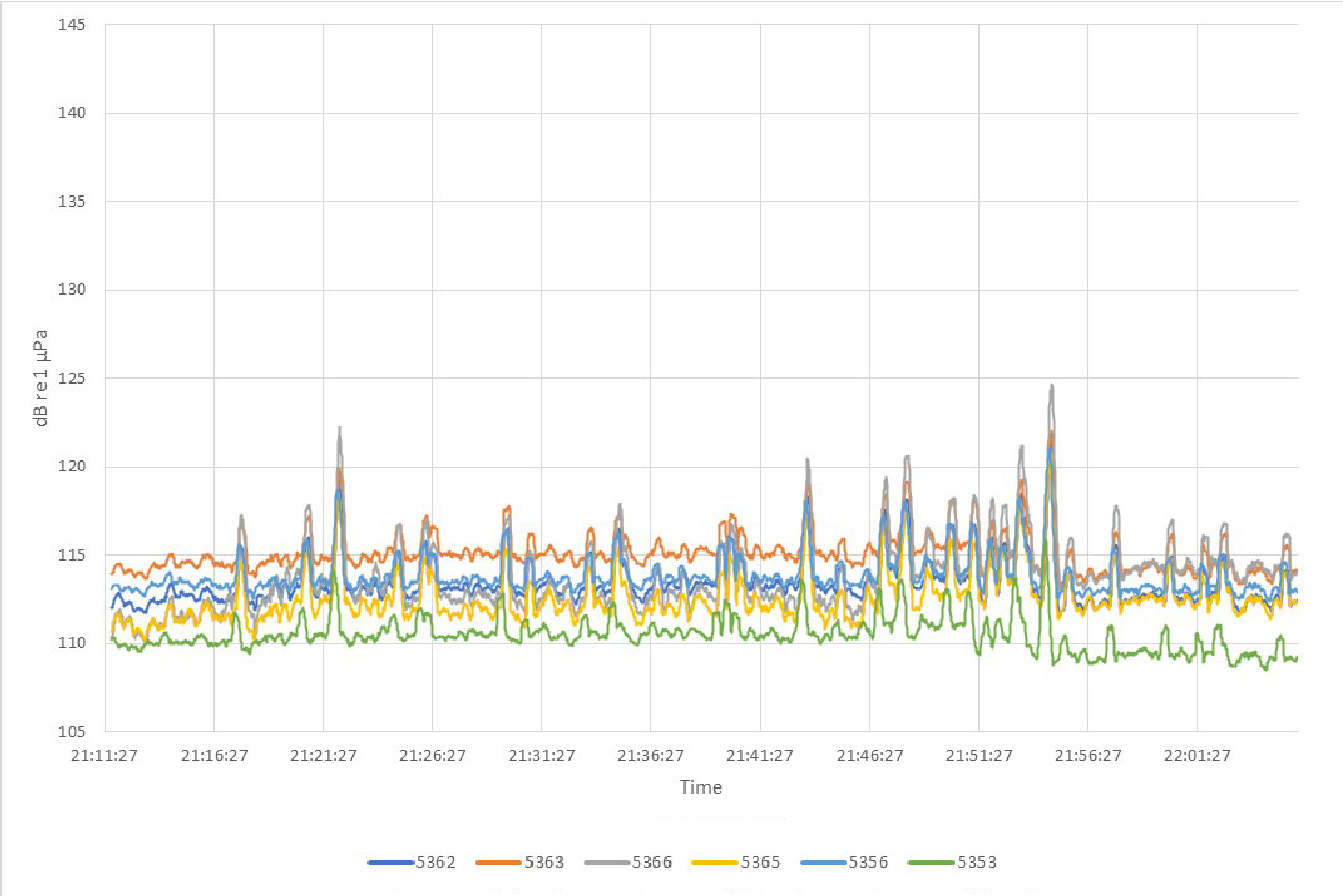

Figure B-66. Time History Plot of S-23 Mechanical Cut from April 13, 2021, 21:05 to 22:29 (20-second sample interval)

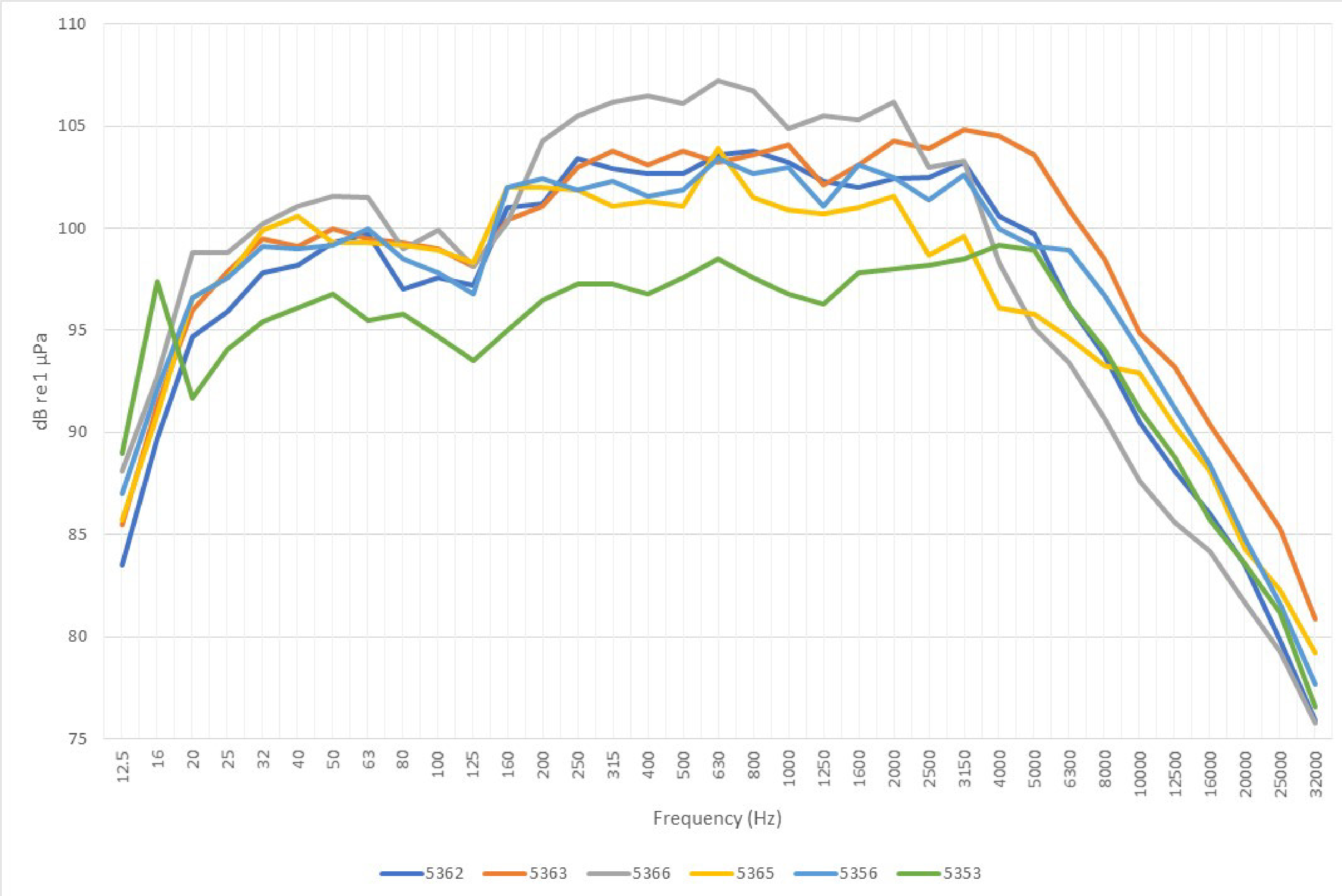

Figure B-67. SPL RMS 1/3 Octave Band Plot of S-23 Mechanical Cut from April 13, 2021, 21:05 to 22:29

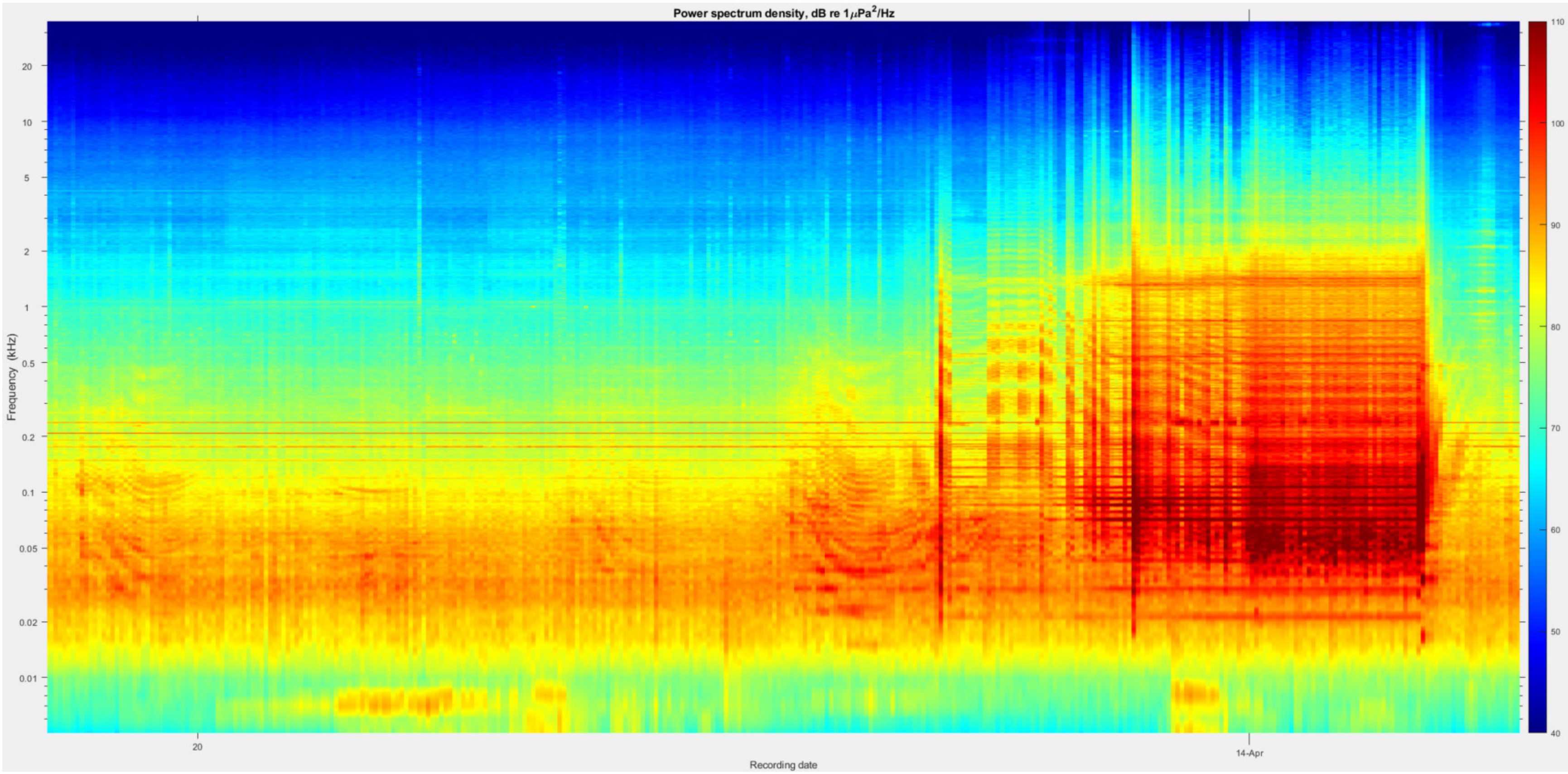

Figure B-68. PSD Spectrogram Plot of S-23 Mechanical Cut from 21:05 April 13, 2021 – 22:29 April 13, 2021

Table B-19. Empty Conductor S-21
(7:44 April 14, 2021 – 10:48 April 14, 2021)

Conductor	Start Time	End Time	Total Duration of Cut (minutes)	Overall Wall Thickness (inches)	Cut Depth Below Mudline (Feet)	Cutter RPM
S-21	4/14/2021 7:44	4/14/2021 10:48	184	0.812	20	60

Conductor	Start Time	End Time	Direction	Monitor Station Name	Distance to Conductor (m)	L_p	Max L_p	Min L_p	$L_{p,pk}$	L_E
S-21	4/14/2021 7:44	4/14/2021 10:48	North	5362	142.52	128.9	145.3	119.5	163.5	169.3
			North	5363	142.52	130.2	147.1	115.0	164.7	170.6
			East	5366	108.42	128.6	141.1	115.9	163.4	169.0
			South	5365	133.81	130.0	146.9	114.5	166.1	170.4
			West	5356	150.86	130.3	144.6	112.4	164.7	170.8
			South	5353	291.21	124.6	137.3	112.6	162.6	165.1

L_p and $L_{p.pk}$ = (dB re 1 μPa); L_E = (dB re 1 $μPa^2$·s)

Conductor	Start Time	End Time	Monitor Station Name	L_p				L_E			
				LF	MF	HF	PP	LF	MF	HF	PP
S-21	4/14/2021 7:44	4/14/2021 10:48	5362	125.2	104.7	101.1	117.2	165.7	145.1	141.5	157.6
			5363	127.1	107.9	104.5	119.5	167.5	148.4	145.0	160.0
			5366	124.8	104.7	101.5	117.0	165.2	145.1	141.9	157.4
			5365	125.9	107.2	104.1	118.6	166.3	147.6	144.5	159.1
			5356	127.2	107.3	103.9	119.8	167.6	147.8	144.3	160.2
			5353	121.7	104.0	100.8	115.1	162.2	144.5	141.3	155.5

L_p and$L_{p.pk}$ = (dB re 1 μPa); L_E = (dB re 1 $μPa^2$·s)
LF – low frequency; MF – mid-frequency; HF – high frequency; PP – phocid pinnipeds

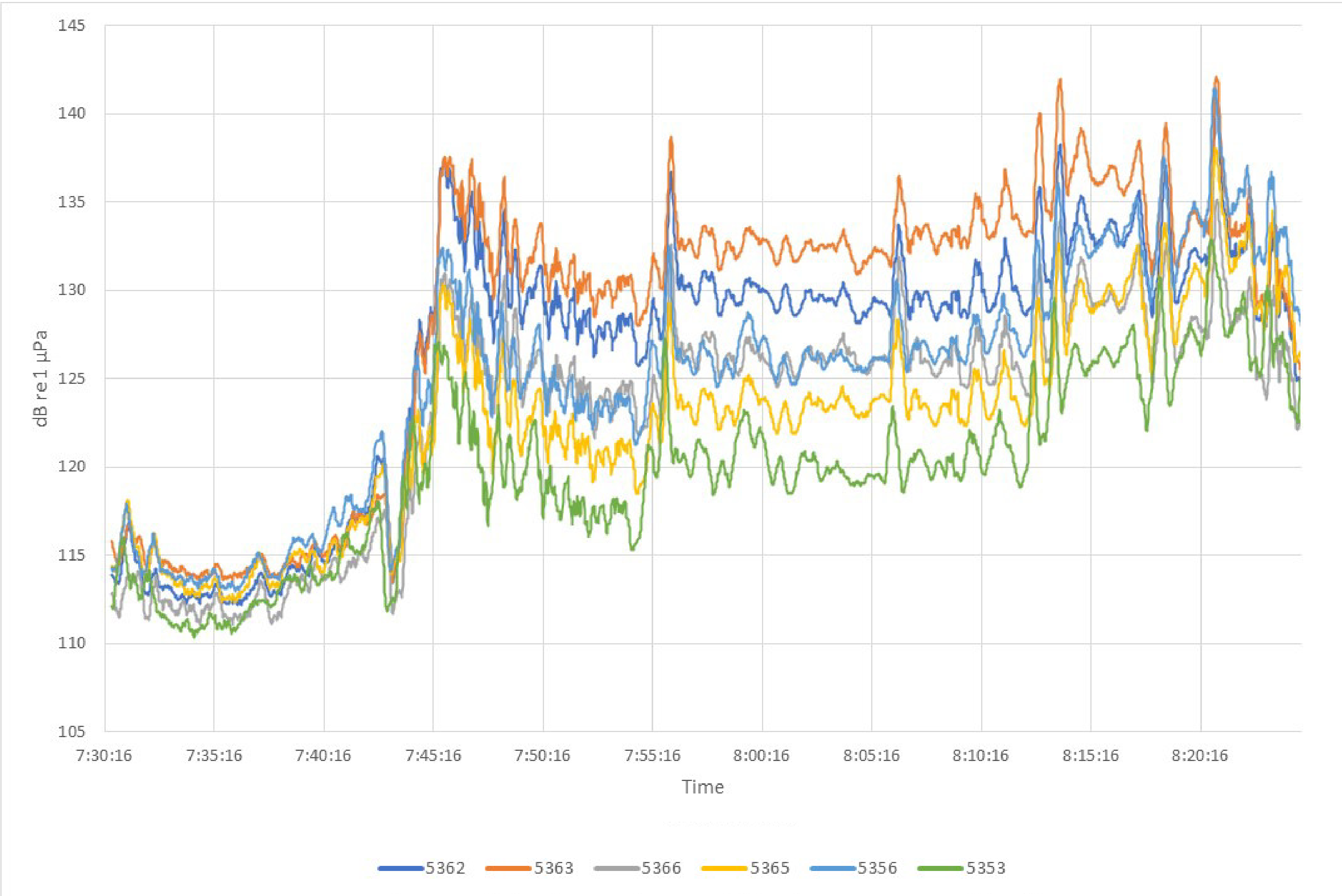

Figure B-69. Time History Plot of S-21 Mechanical Cut from April 14, 2021, 7:44 to 10:48 (20-second sample interval)

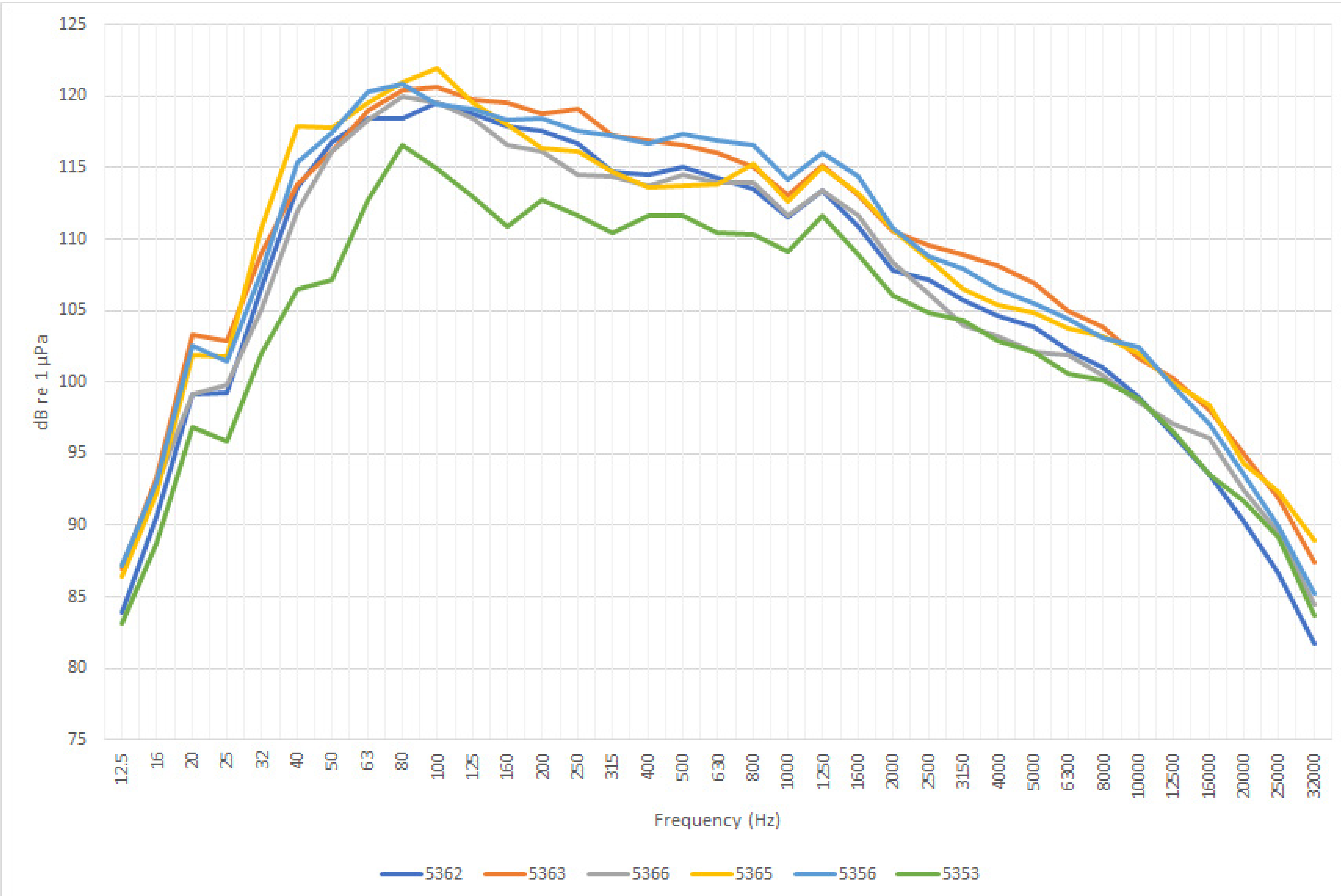

Figure B-70. SPL RMS 1/3 Octave Band Plot of S-21 Mechanical Cut from April 14, 2021, 7:44 to 10:48

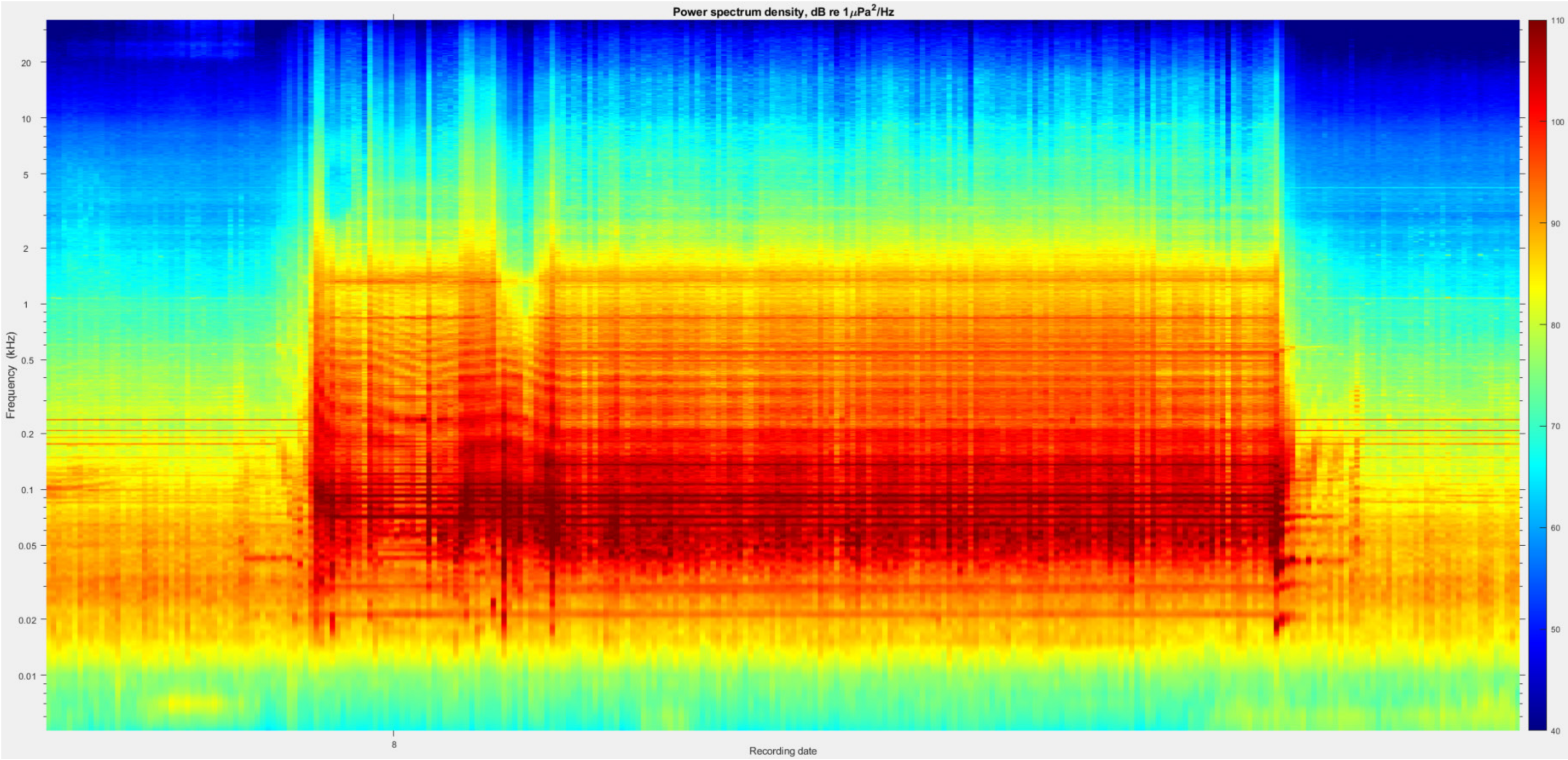

Figure B-71. PSD Spectrogram Plot of S-21 Mechanical Cut from 7:44 April 14, 2021 – 10:48 April 14, 2021

Table B-20. Conductor B-14 Noise Monitoring Results Summary
(17:06 April 14, 2021 – 10:59 April 15, 2021)

Conductor	Start Time	End Time	Total Duration of Cut (minutes)	Overall Wall Thickness (inches)	Cut Depth Below Mudline (Feet)	Cutter RPM
B-14	4/14/2021 17:06	4/14/2021 19:05	119	1.919	20	60
	4/15/2021 1:05	4/15/2021 10:59	599			

Conductor	Start Time	End Time	Direction	Monitor Name	Distance to Conductor (m)	L_p	Max L_p	Min L_p	$L_{p,pk}$	L_E
B-14	4/14/2021 17:06	4/14/2021 19:05	North	5362	143.97	125.3	132.9	112.9	156.9	163.8
			North	5363	143.97	125.1	136.0	113.4	159.4	163.7
			East	5366	106.27	129.7	137.1	117.3	161.3	168.2
			South	5365	133.52	125.1	132.9	109.5	158.9	163.6
			West	5356	152.65	124.5	133.0	110.5	157.3	163.1
			South	5353	291.82	119.6	129.0	106.9	149.9	158.2
	4/15/2021 1:05	4/15/2021 10:59	North	5362	143.97	118.7	129.5	109.5	151.5	164.2
			North	5363	143.97	118.7	127.4	112.4	149.7	164.3
			East	5366	106.27	122.6	133.3	107.1	158.0	168.2
			South	5365	133.52	118.4	127.8	109.8	148.2	163.9
			West	5356	152.65	118.2	127.4	110.7	153.2	163.7
			South	5353	291.82	114.3	121.7	107.6	144.3	159.8

L_p and $L_{p,pk}$ = (dB re 1 μPa); L_E = (dB re 1 $μPa^2 \cdot s$)

Conductor	Start Time	End Time	Monitor Station Name	L_p				L_E			
				LF	MF	HF	PP	LF	MF	HF	PP
B-14	4/14/2021 17:06	4/14/2021 19:05	5362	124.5	100.8	96.2	117.3	163.1	139.4	134.8	155.9
			5363	124.3	103.2	99.2	117.2	162.9	141.7	137.8	155.7
			5366	129.0	102.6	96.8	121.7	167.6	141.2	135.4	160.3
			5365	124.2	100.1	96.0	116.8	162.8	138.7	134.6	155.4
			5356	123.8	101.0	96.8	116.7	162.4	139.5	135.3	155.3
			5353	118.7	98.3	94.5	111.5	157.3	136.9	133.1	150.0
	4/15/2021 1:05	4/15/2021 10:59	5362	117.4	98.2	94.5	110.4	162.9	143.8	140.0	155.9
			5363	117.2	101.2	97.8	106.5	162.8	146.8	143.3	157.0
			5366	121.4	95.4	91.0	113.0	167.0	140.9	136.6	158.5
			5365	116.6	97.3	94.3	108.8	162.2	142.8	139.8	154.3
			5356	116.6	98.7	95.2	110.0	162.2	144.2	140.7	155.6
			5353	112.3	96.6	93.3	106.3	157.9	142.2	138.8	151.8

L_p and $L_{p,pk}$ = (dB re 1 μPa); L_E = (dB re 1 μPa²·s)
LF – low frequency; MF – mid-frequency; HF – high frequency; PP – phocid pinnipeds

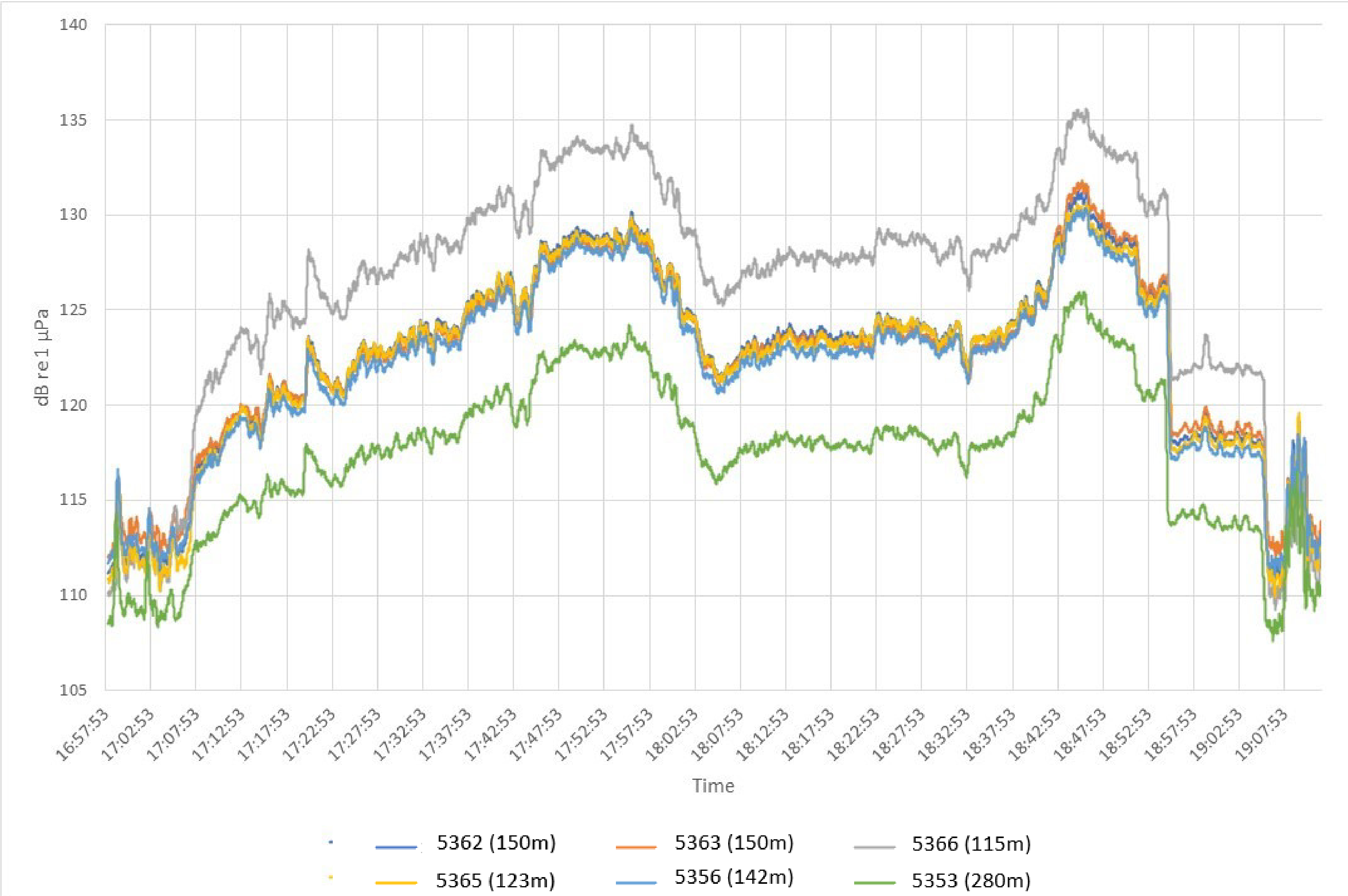

Figure B-72. Time History Plot of B-14 Mechanical Cut from April 14, 2021, 17:06 to 19:05 (20-second sample interval)

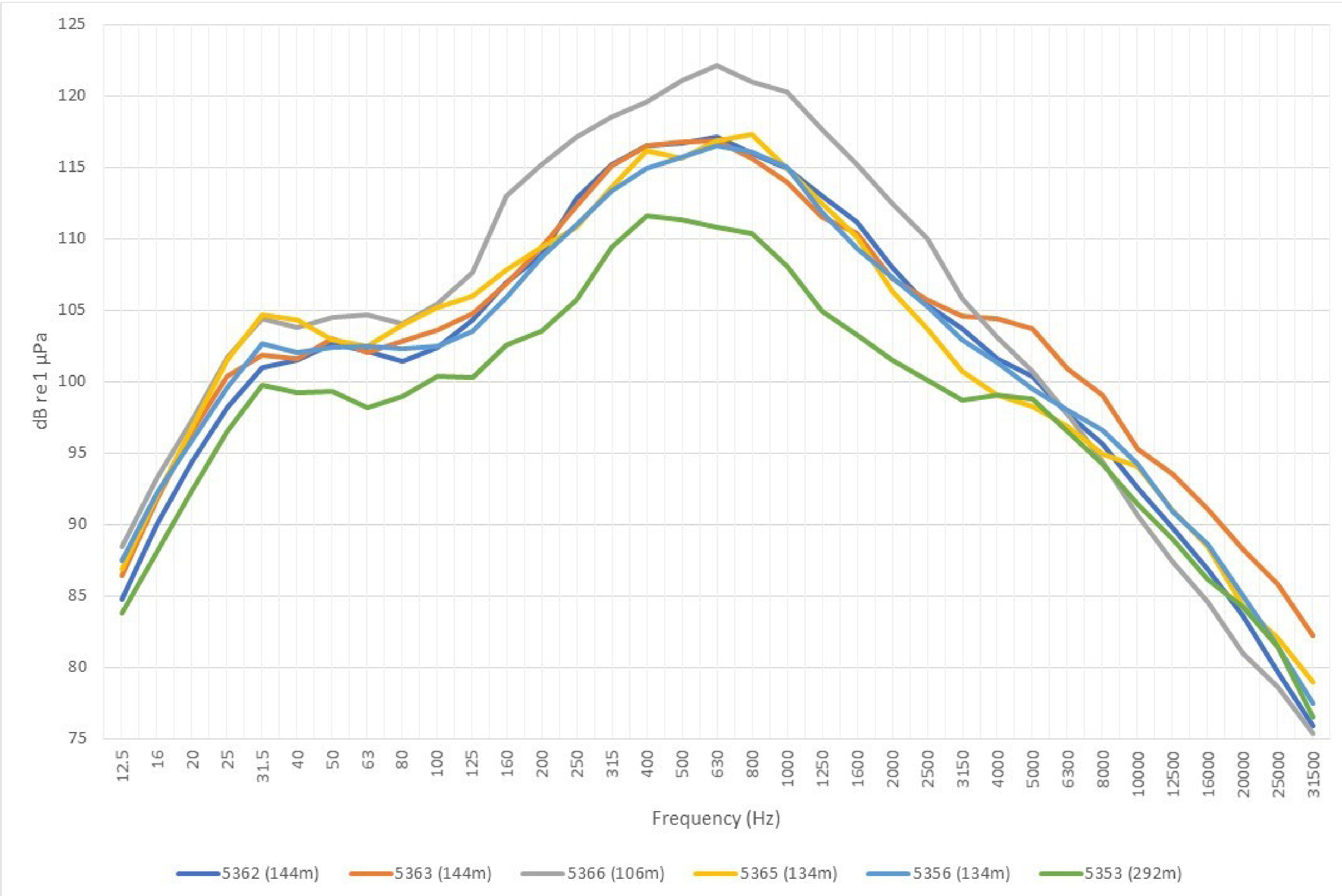

Figure B-73. SPL RMS 1/3 Octave Band Plot of B-14 Mechanical Cut from April 14, 2021, 17:06 to 19:05

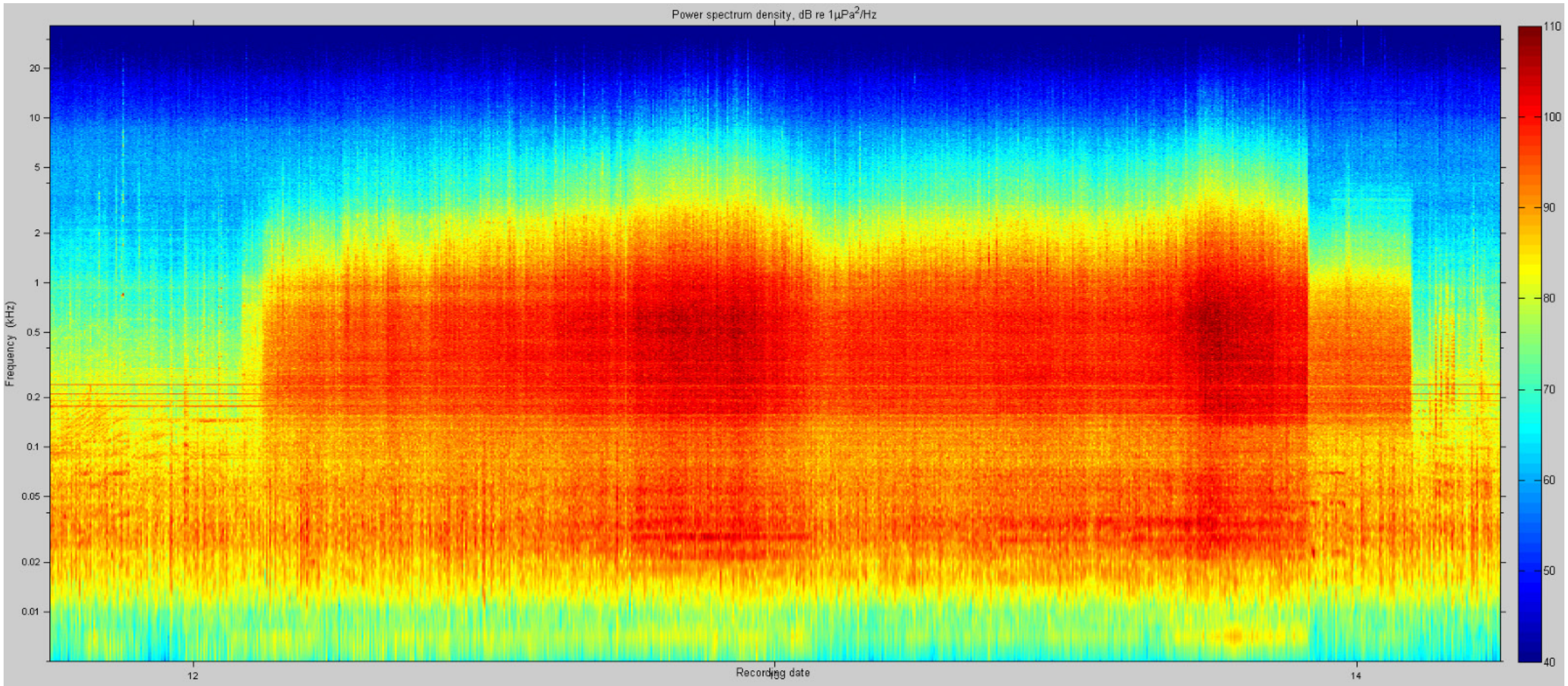

Figure B-74. PSD Spectrogram Plot of B-14 Mechanical Cut from April 14, 2021, 17:06 to 19:05 (SoundTrap 5366)

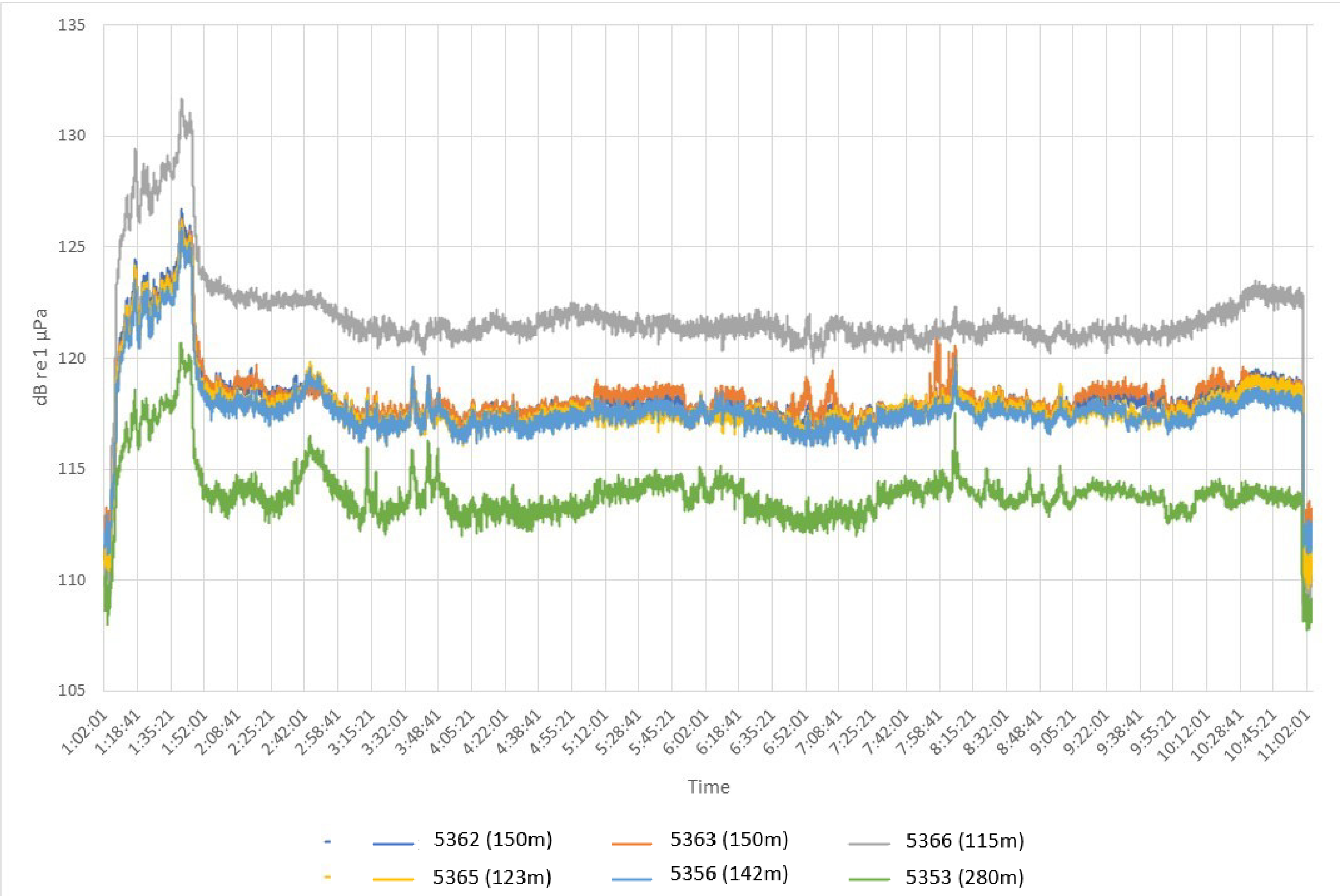

Figure B-75. Time History Plot of B-14 Mechanical Cut from April 15, 2021, 1:05 to 10:59 (20-second sample interval)

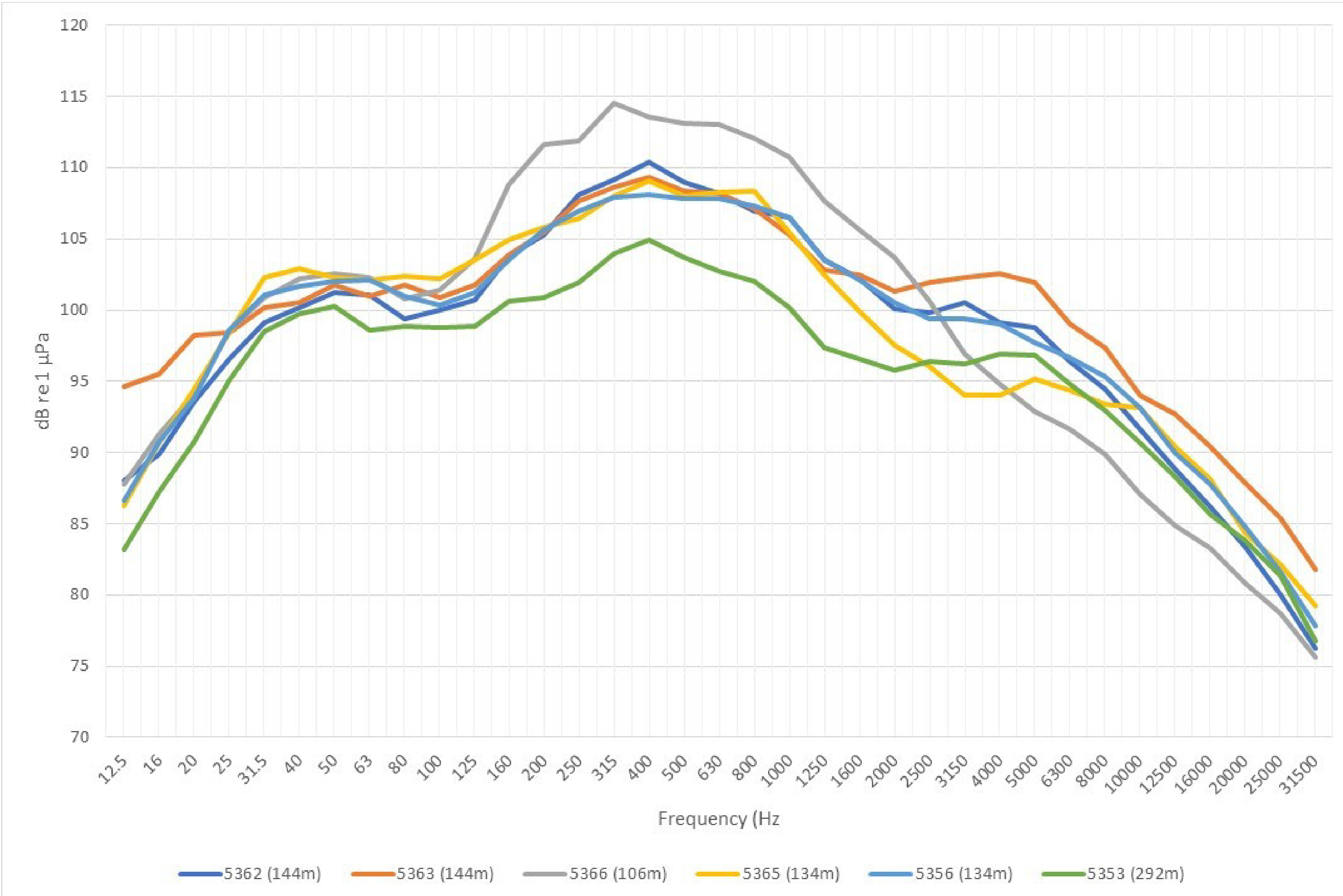

Figure B-76. SPL RMS 1/3 Octave Band Plot of B-14 Mechanical Cut from April 15, 2021 1:05 to 10:59

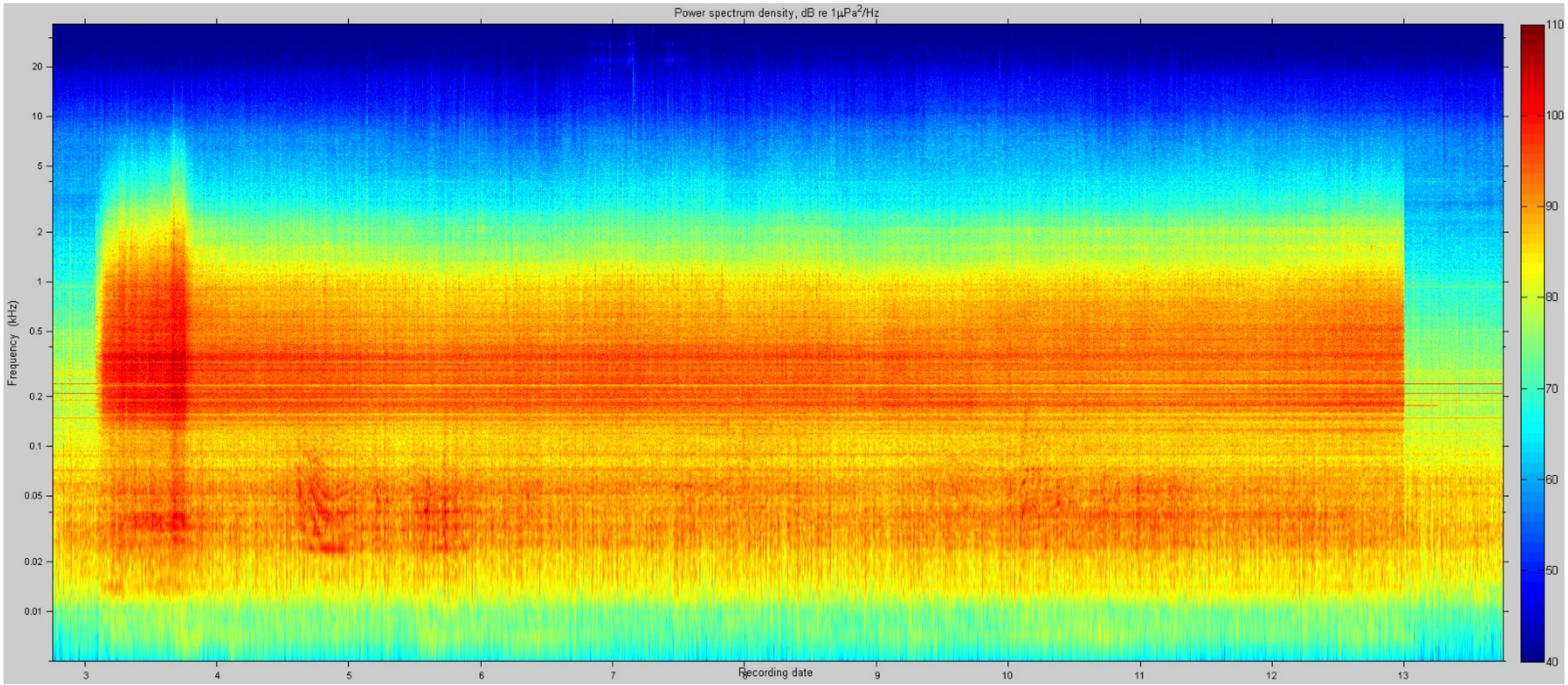

Figure B-77. PSD Spectrogram Plot of B-14 Mechanical Cut from April 15, 2021, 1:05 to 10:59 (SoundTrap 5366)

Table B-21. Empty Conductor S-9
(18:23 April 15, 2021 – 20:01 April 15, 2021)

Conductor	Start Time	End Time	Total Duration of Cut (minutes)	Overall Wall Thickness (inches)	Cut Depth Below Mudline (Feet)	Cutter RPM
S-9	4/15/2021 18:23	4/15/2021 20:01	98	0.812	20	60

Conductor	Start Time	End Time	Direction	Monitor Station Name	Distance to Conductor (m)	L_p	Max L_p	Min L_p	$L_{p,pk}$	L_E
S-9	4/15/2021 18:23	4/15/2021 20:01	North	5362	145.87	131.7	145.3	116.5	165.8	169.4
			North	5363	145.87	133.7	149.0	119.7	171.6	171.2
			East	5366	103.26	131.5	142.5	123.7	165.9	168.9
			South	5365	133.35	128.3	139.2	116.3	158.5	166.0
			West	5356	155.25	129.5	140.6	118.1	165.5	167.2
			South	5353	292.83	122.7	133.9	114.4	155.0	160.4

L_p and $L_{p,pk}$ = (dB re 1 μPa); L_E = (dB re 1 μPa^2·s)

Conductor	Start Time	End Time	Monitor Station Name	L_p				L_E			
				LF	MF	HF	PP	LF	MF	HF	PP
S-9	4/15/2021 18:23	4/15/2021 20:01	5362	128.3	107.8	104.1	120.4	166.0	145.5	141.9	158.1
			5363	130.3	111.1	107.7	122.8	168.0	148.8	145.4	160.5
			5366	127.7	106.6	103.0	120.1	165.4	144.3	140.7	157.8
			5365	124.0	103.9	101.0	115.5	161.7	141.6	138.7	153.2
			5356	126.1	106.9	103.6	118.3	163.8	144.6	141.4	156.1
			5353	119.4	100.6	97.6	111.4	157.1	138.3	135.3	149.1

L_p and $L_{p,pk}$ = (dB re 1 μPa); L_E = (dB re 1 μPa^2·s)
LF – low frequency; MF – mid-frequency; HF – high frequency; PP – phocid pinnipeds

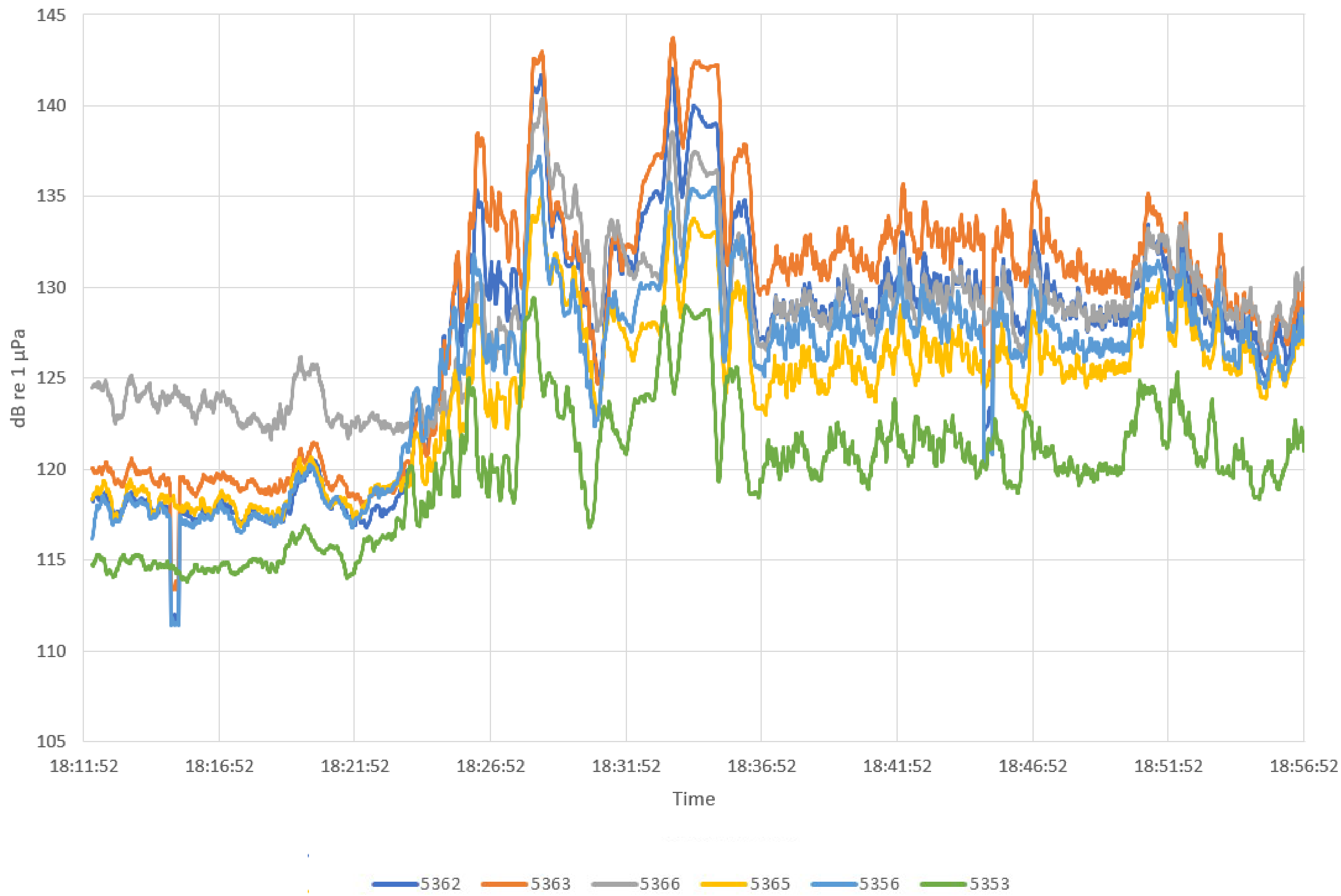

Figure B-78. Time History Plot of S-9 Mechanical Cut from April 15, 2021,18:23 to 20:01 (20-second sample interval)

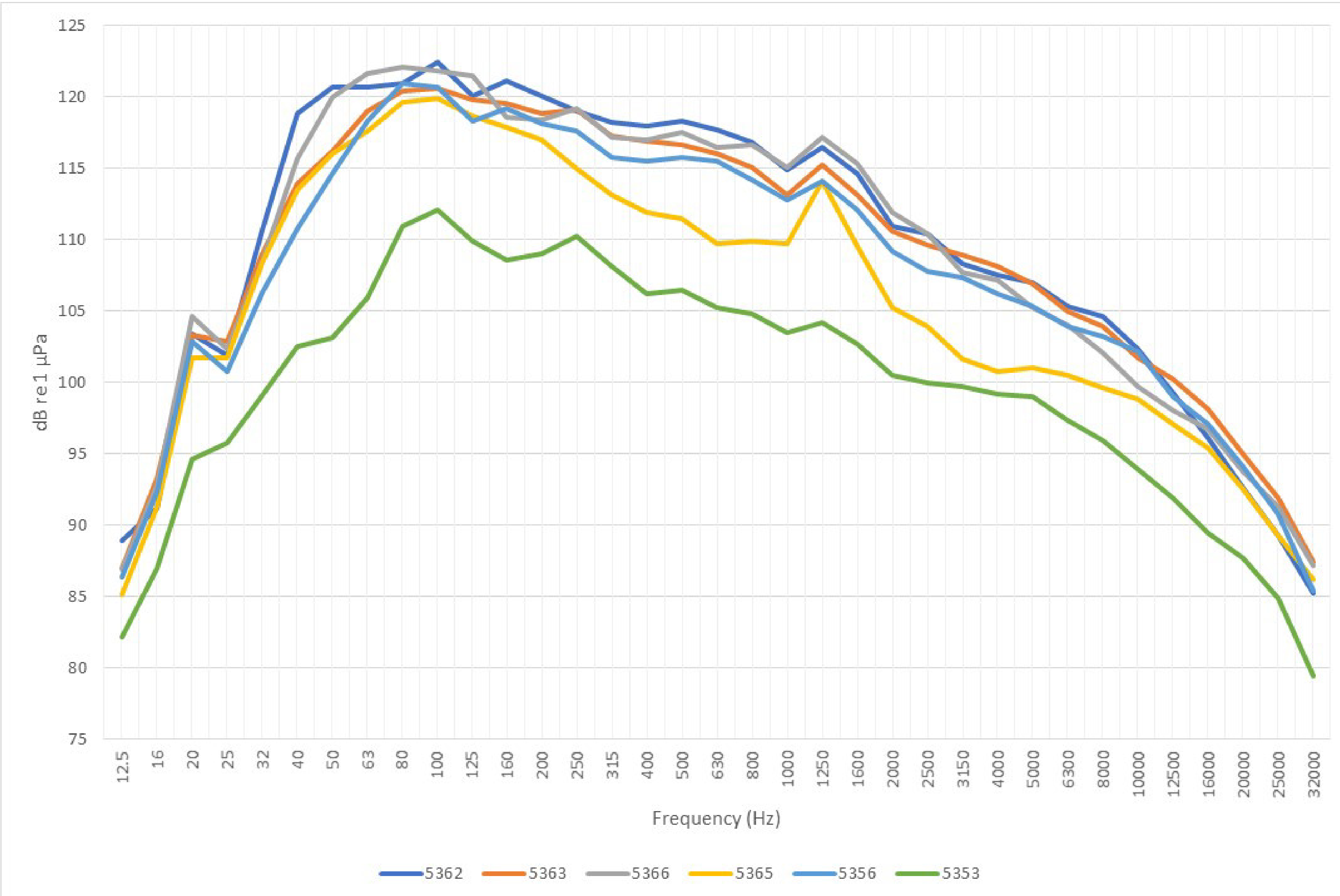

Figure B-79. SPL RMS 1/3 Octave Band Plot of S-9 Mechanical Cut from April 15, 2021, 18:23 to 20:01

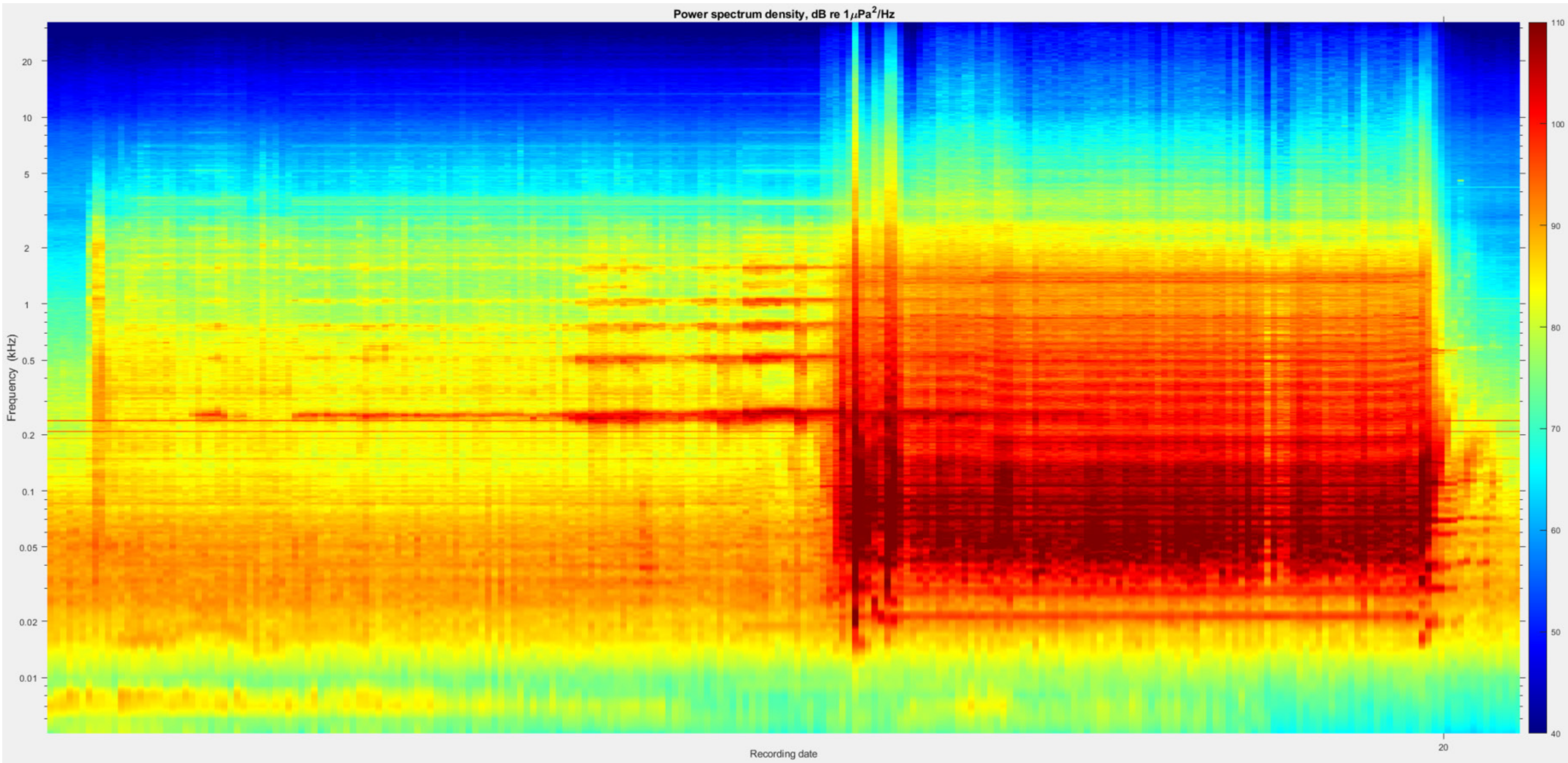

Figure B-80. PSD Spectrogram Plot of S-9 Mechanical Cut from 18:23 April 15, 2021 – 20:01 April 15, 2021

Table B-22. Wellbore Conductor B-08
(8:33 April 16, 2021 – 18:32 April 16, 2021)

Conductor	Start Time	End Time	Total Duration of Cut (minutes)	Overall Wall Thickness (inches)	Cut Depth Below Mudline (Feet)	Cutter RPM
B-08	4/16/2021 8:33	4/16/2021 10:21	108	1.919	20	60
	4/16/2021 13:07	4/16/2021 18:32	325			

Conductor	Start Time	End Time	Direction	Monitor Station Name	Distance to Conductor (m)	L_p	Max L_p	Min L_p	$L_{p,pk}$	L_E
B-08	4/16/2021 8:33	4/16/2021 10:21	North	5362	140.59	123.9	129.8	115.3	158.7	162.0
			North	5363	140.59	124.2	130.3	115.8	154.0	162.4
			East	5366	111.45	124.9	130.4	114.5	158.0	163.0
			South	5365	134.21	122.1	127.9	113.2	152.7	160.3
			West	5356	148.34	122.8	128.5	113.5	155.8	161.0
			South	5353	290.33	118.7	123.8	111.1	149.1	156.9
	4/16/2021 13:07	4/16/2021 18:32	North	5362	140.59	124.2	133.2	111.3	159.5	167.1
			North	5363	140.59	124.4	132.1	113.0	157.1	167.3
			East	5366	111.45	125.0	132.9	107.7	161.7	167.9
			South	5365	134.21	122.4	129.7	109.2	155.6	165.3
			West	5356	148.34	123.1	130.9	111.9	154.5	166.0
			South	5353	290.33	119.0	126.0	109.4	151.2	161.9

L_p and $L_{p,pk}$ = (dB re 1 μPa); L_E = (dB re 1 μPa^2·s)

Conductor	Start Time	End Time	Monitor Station Name	L_p				L_E			
				LF	MF	HF	PP	LF	MF	HF	PP
B-08	4/16/2021 8:33	4/16/2021 10:21	5362	122.8	100.2	95.9	115.6	160.9	138.3	134.0	153.7
			5363	123.1	102.5	98.6	116.0	161.2	140.7	136.8	154.2
			5366	123.6	96.7	91.8	115.4	161.7	134.8	129.9	153.5
			5365	120.5	98.1	94.7	112.3	158.7	136.3	132.8	150.4
			5356	121.6	100.3	96.4	114.2	159.8	138.4	134.5	152.4
			5353	117.5	98.0	94.3	110.5	155.6	136.1	132.4	148.6
	4/16/2021 13:07	4/16/2021 18:32	5362	123.5	100.3	95.8	116.2	166.0	142.8	138.4	158.7
			5363	123.3	102.2	98.3	116.1	166.2	145.1	141.2	159.0
			5366	123.7	96.9	91.9	115.6	166.6	139.8	134.8	158.5
			5365	120.8	98.1	94.5	112.6	163.7	141.0	137.4	155.5
			5356	121.9	99.9	95.8	114.5	164.8	142.8	138.7	157.4
			5353	117.7	97.5	93.7	110.6	160.6	140.4	136.6	153.5

L_p and $L_{p,pk}$ = (dB re 1 µPa); L_E = (dB re 1 µPa^2·s)
LF – low frequency; MF – mid-frequency; HF – high frequency; PP – phocid pinnipeds

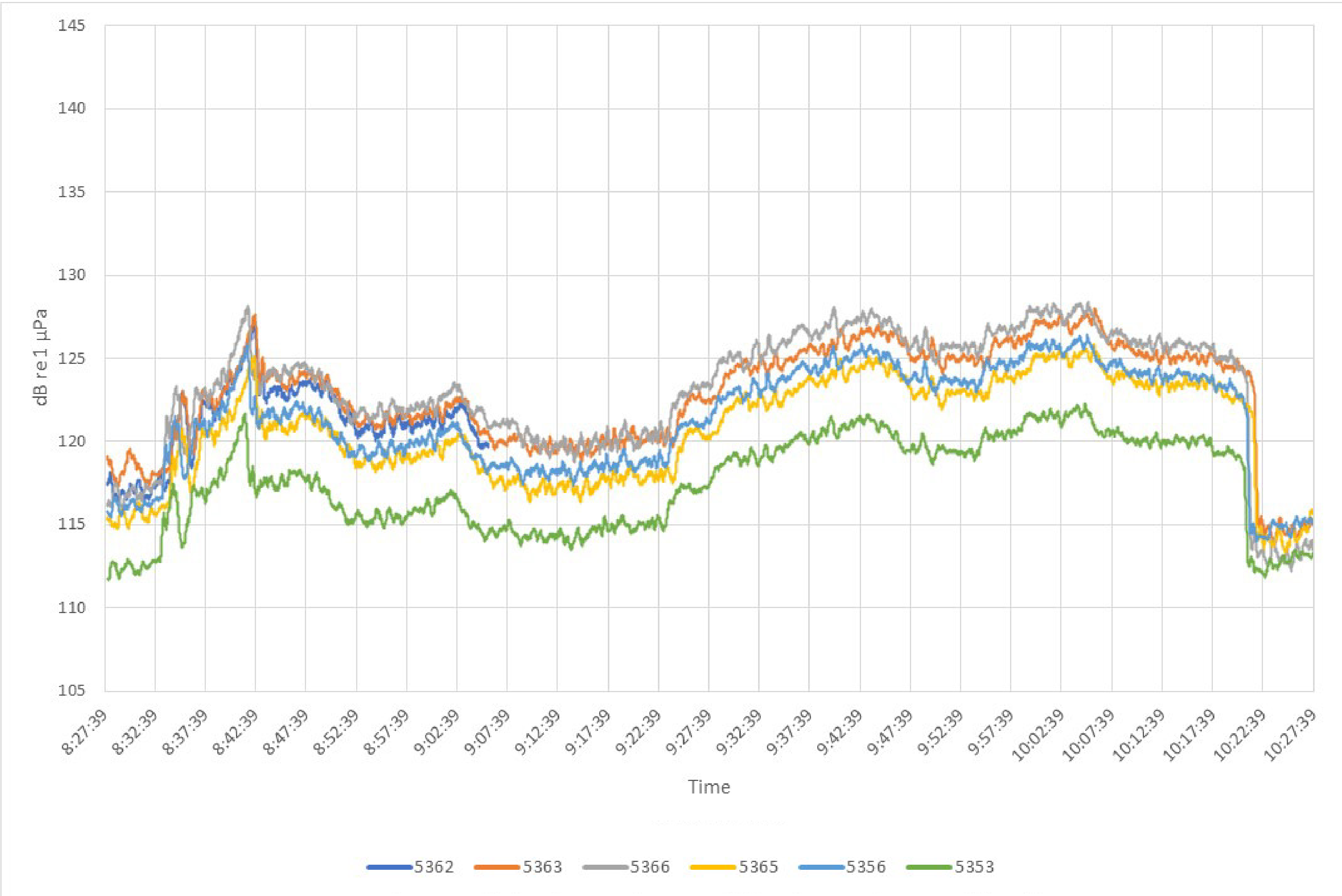

Figure B-81. Time History Plot of B-8 Mechanical Cut from April 16, 2021, 8:33 to 10:21 (20-second sample interval)

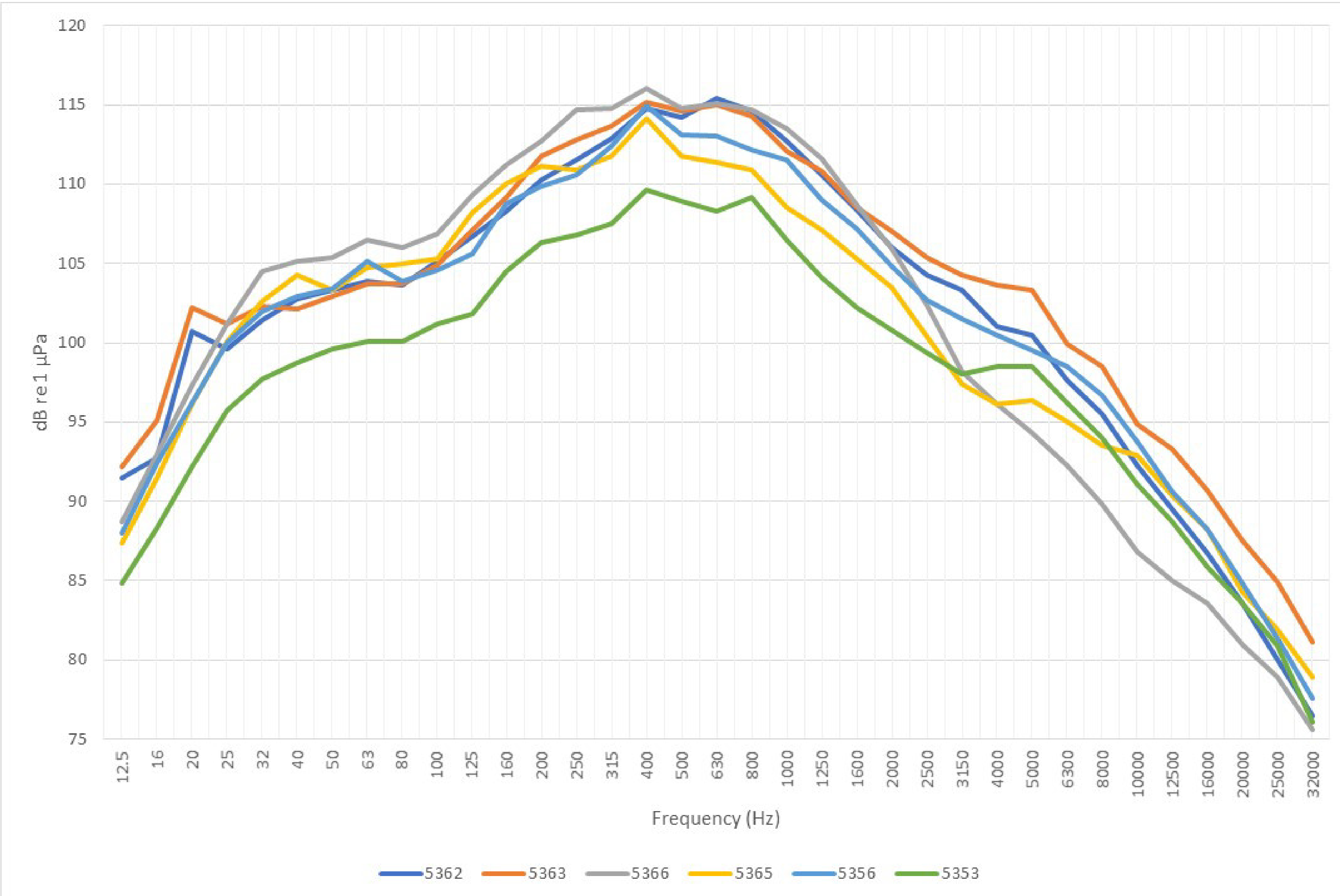

Figure B-82. SPL RMS 1/3 Octave Band Plot of B-8 Mechanical Cut from April 16, 2021, 8:33 to 10:21

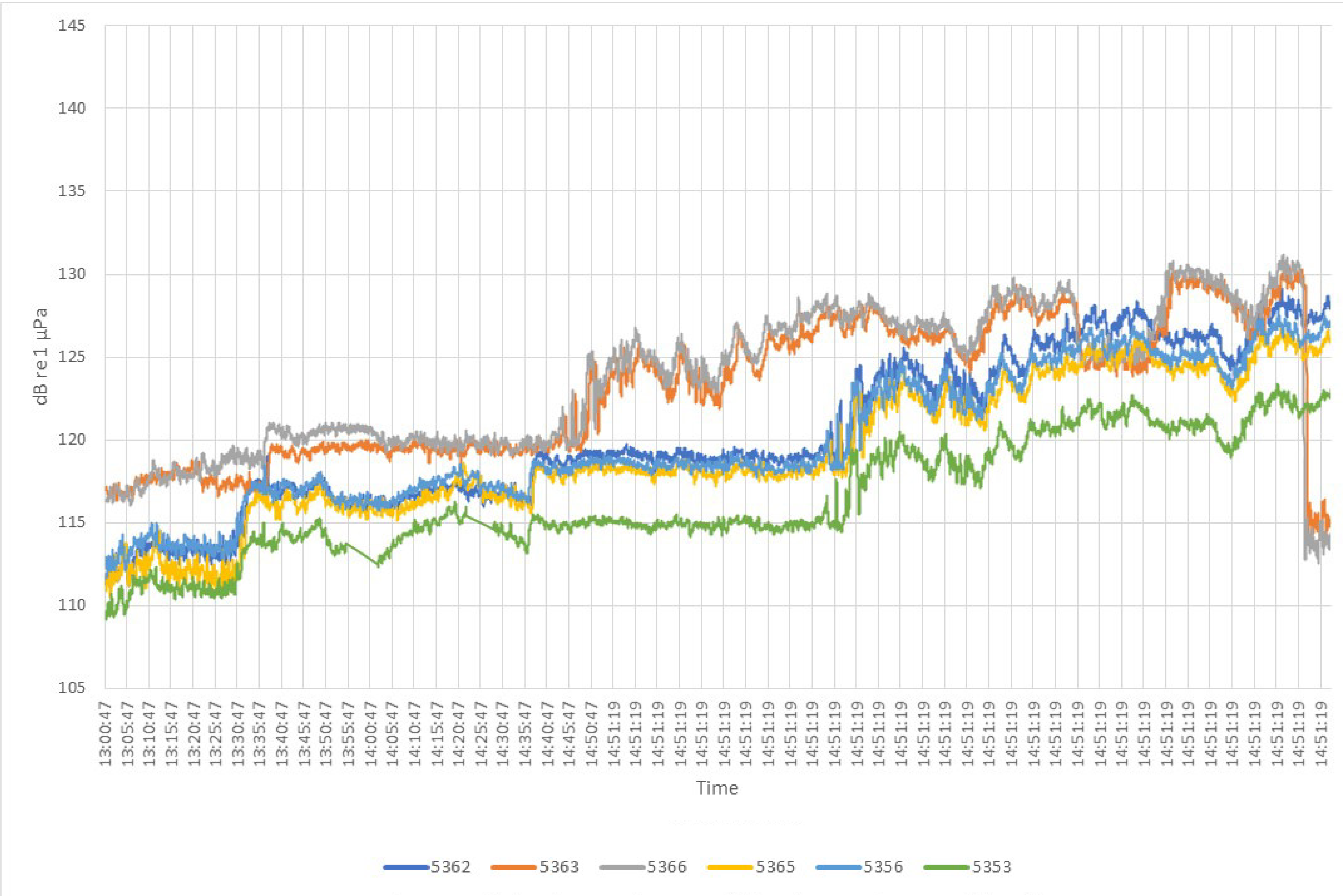

Figure B-83. Time History Plot of B-8 Mechanical Cut from April 16, 2021, 13:07 to 18:32 (20-second sample interval)

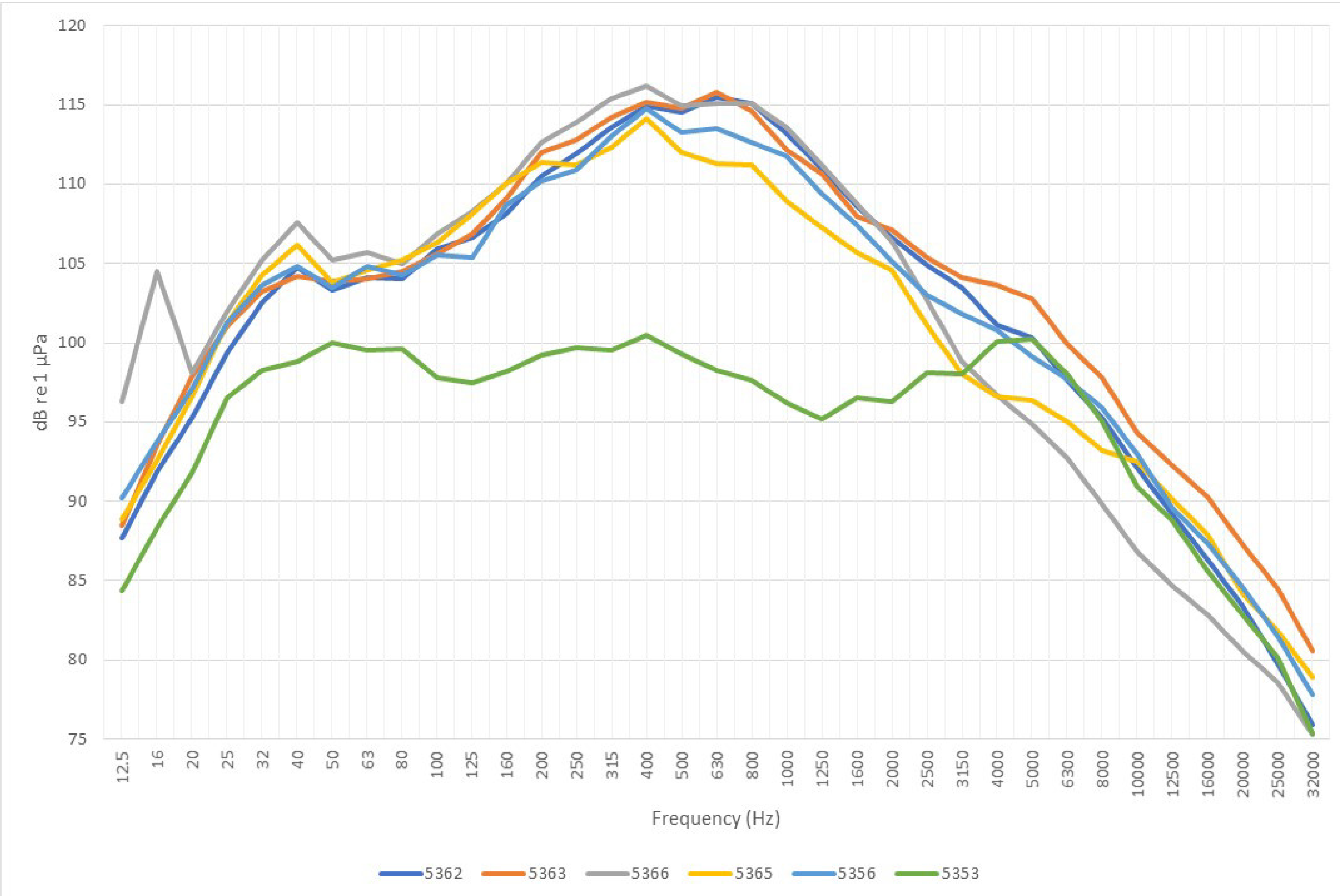

Figure B-84. SPL RMS 1/3 Octave Band Plot of B-8 Mechanical Cut from April 16, 2021, 13:07 to 18:32

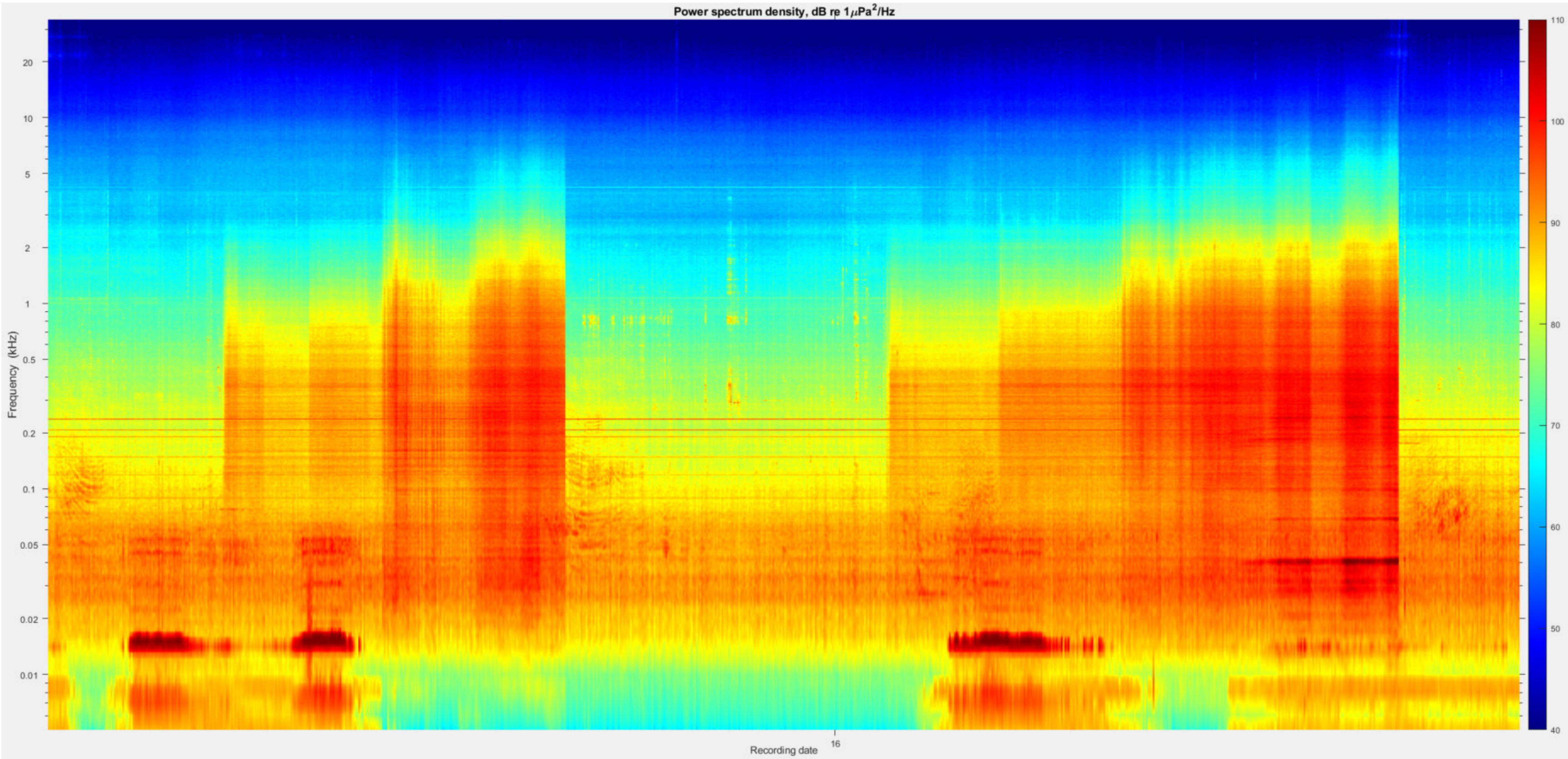

Figure B-85. PSD Spectrogram Plot of B-08 Mechanical Cut from 8:33 April 16, 2021 – 18:32 April 16, 2021

Table B-23. Wellbore Conductor B-13
(1:54 April 17, 2021 – 3:56 April 18, 2021)

Conductor	Start Time	End Time	Total Duration of Cut (minutes)	Overall Wall Thickness (inches)	Cut Depth Below Mudline (Feet)	Cutter RPM
B-13	4/17/2021 1:54	4/17/2021 3:41	107	2.354	20	60
	4/17/2021 7:02	4/17/2021 15:48	526			
	4/17/2021 17:09	4/18/2021 3:56	647			

Conductor	Start Time	End Time	Direction	Monitor Station Name	Distance to Conductor (m)	L_p	Max L_p	Min L_p	$L_{p,pk}$	L_E
B-13	4/17/2021 1:54	4/17/2021 3:41	North	5362	139.12	126.6	144.6	112.1	162.4	164.7
			North	5363	139.12	127.7	147.1	113.1	168.5	165.6
			East	5366	110.9	127.8	143.9	112.2	163.9	165.8
			South	5365	136.11	125.1	141.4	112.4	165.2	163.2
			West	5356	149.57	125.0	139.9	112.6	162.4	163.1
			South	5353	292.2	120.2	132.2	109.9	160.3	158.3
	4/17/2021 7:02	4/17/2021 15:48	North	5362	139.12	120.6	127.5	116.7	150.8	165.5
			North	5363	139.12	120.9	129.8	116.1	150.2	165.9
			East	5366	110.9	121.8	128.6	113.1	157.0	166.8
			South	5365	136.11	119.2	126.7	111.9	148.6	164.2
			West	5356	149.57	119.9	126.0	113.8	148.2	164.9
			South	5353	292.2	116.4	130.8	112.2	144.4	161.4
	4/17/2021 17:09	4/18/2021 3:56	North	5362	139.12	126.1	145.6	110.2	163.1	172.0
			North	5363	139.12	127.2	147.9	111.8	167.7	173.1
			East	5366	110.9	127.0	143.8	109.5	162.5	172.8
			South	5365	136.11	123.8	139.9	109.6	157.8	169.6
			West	5356	149.57	127.4	141.2	115.0	162.1	167.4
			South	5353	292.2	119.5	132.8	108.1	153.9	165.4

L_p and $L_{p,pk}$ = (dB re 1 μPa); L_E = (dB re 1 μPa^2·s)

Conductor	Start Time	End Time	Monitor Station Name	L_p				L_E			
				LF	MF	HF	PP	LF	MF	HF	PP
B-13	4/17/2021 1:54	4/17/2021 3:41	5362	122.8	104.5	101.9	115.4	160.8	142.5	140.0	153.4
			5363	123.9	107.2	104.7	116.9	161.9	145.2	142.8	155.0
			5366	100.7	124.3	127.8	116.7	138.8	162.3	165.8	154.7
			5365	121.1	103.9	102.1	113.1	159.1	142.0	140.1	151.1
			5356	121.4	104.2	102.0	113.8	159.5	142.3	140.1	151.9
			5353	117.4	101.1	99.1	110.0	155.5	139.1	137.2	148.0
	4/17/2021 7:02	4/17/2021 15:48	5362	119.0	98.3	94.3	111.5	164.0	143.3	139.3	156.5
			5363	119.2	100.5	96.9	112.3	164.2	145.5	141.9	157.3
			5366	120.3	95.6	91.2	112.2	165.3	140.7	136.2	157.2
			5365	117.2	97.1	94.0	108.6	162.2	142.1	139.0	153.6
			5356	118.1	98.5	94.9	110.7	163.1	143.5	139.9	155.7
			5353	114.1	96.2	92.7	107.1	159.1	141.2	137.7	152.1
	4/17/2021 17:09	4/18/2021 3:56	5362	124.0	102.7	98.6	116.8	169.9	148.6	144.5	162.7
			5363	124.8	104.8	101.2	117.7	170.6	150.7	147.1	163.5
			5366	125.4	101.6	96.9	117.9	171.2	147.4	142.7	163.7
			5365	121.3	100.1	96.8	113.1	167.1	146.0	142.7	159.0
			5356	122.6	102.2	98.5	115.3	168.5	148.0	144.4	161.1
			5353	117.6	98.6	95.2	110.4	163.5	144.5	141.1	156.3

L_p and $L_{p,pk}$ = (dB re 1 μPa); L_E = (dB re 1 μPa²·s)
LF – low frequency; MF – mid-frequency; HF – high frequency; PP – phocid pinnipeds

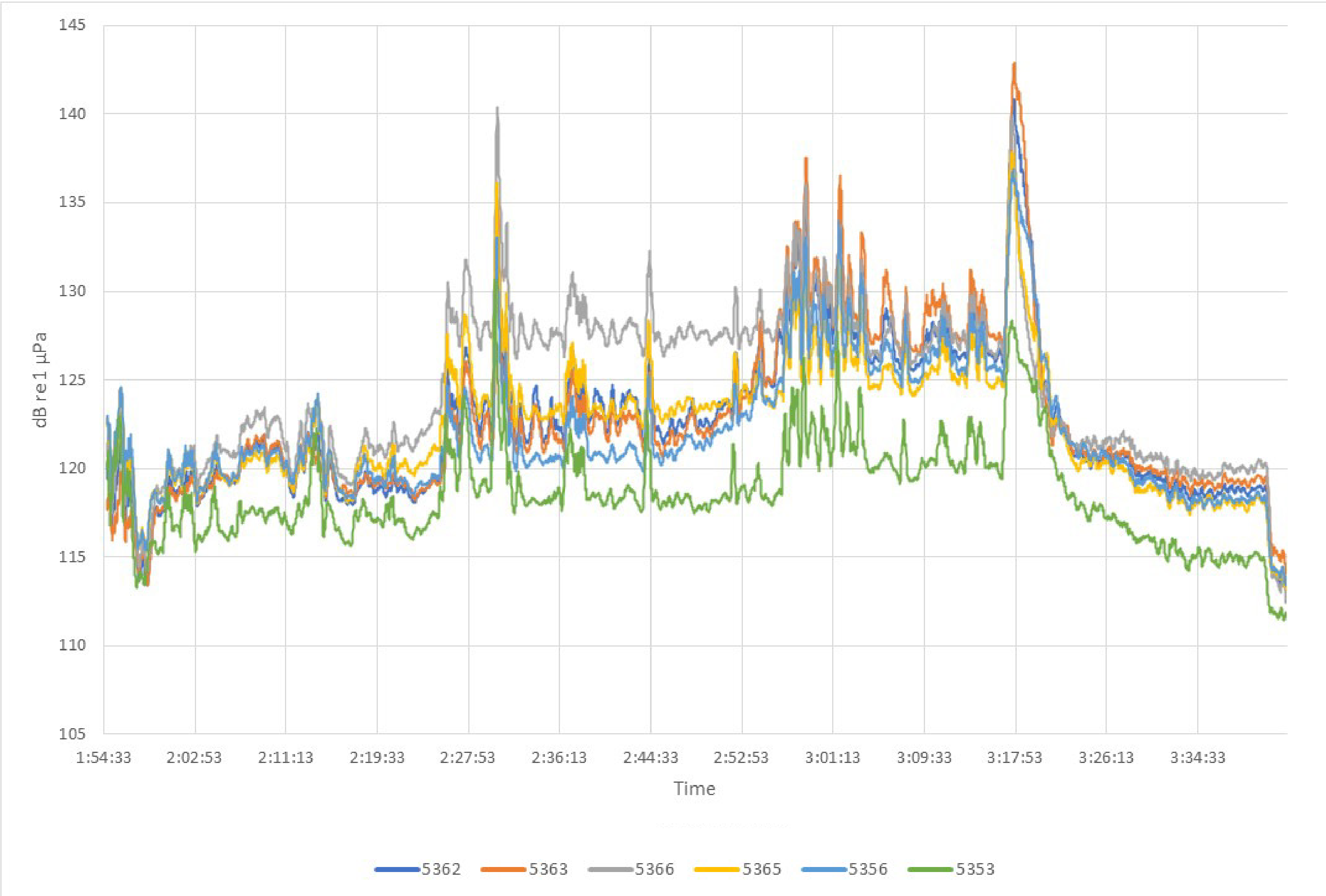

Figure B-86. Time History Plot of B-13 Mechanical Cut from April 17, 2021, 1:54 to 3:41 (20-second sample interval)

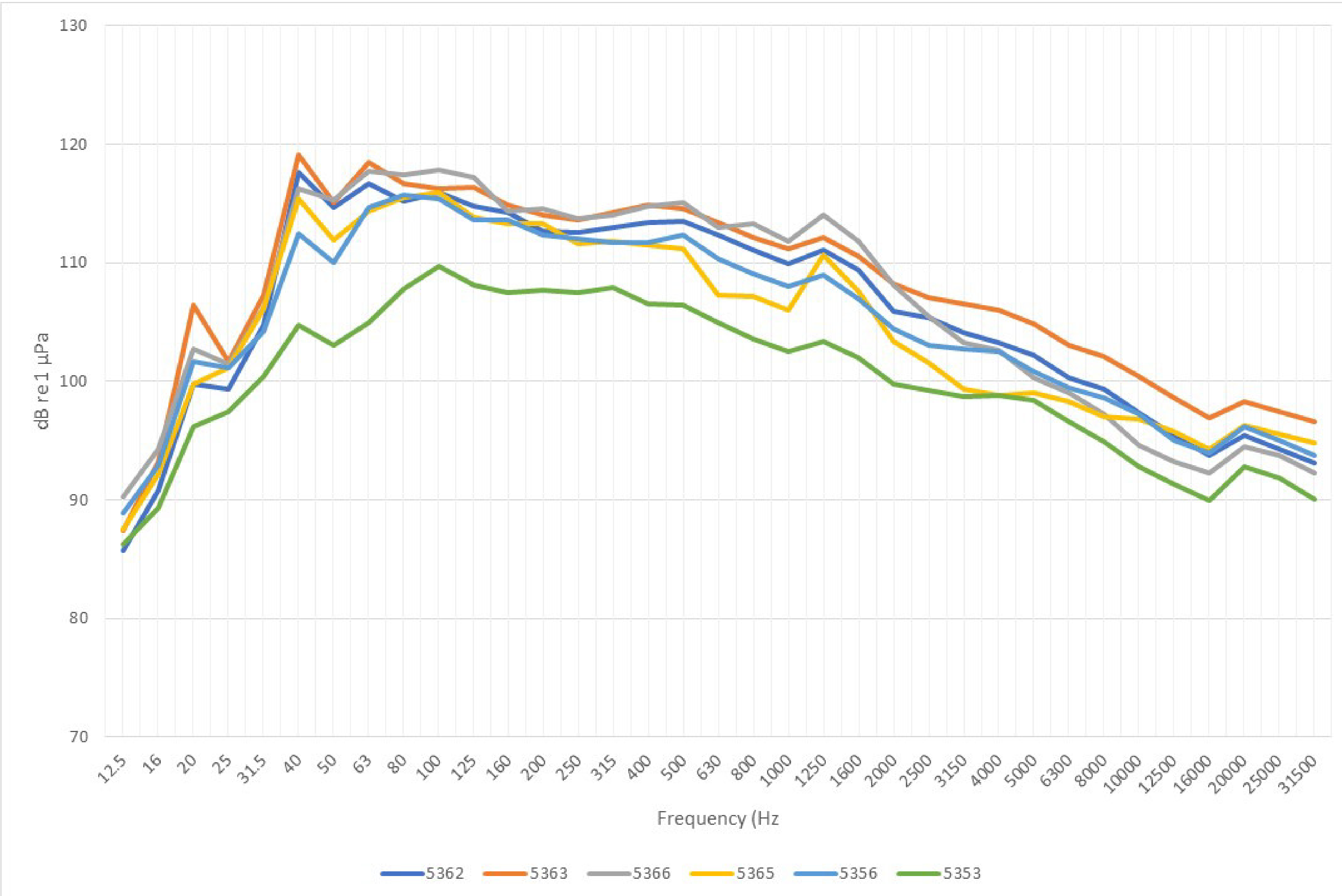

Figure B-87. SPL RMS 1/3 Octave Band Plot of B-13 Mechanical Cut from April 17, 2021, 1:54 to 3:41

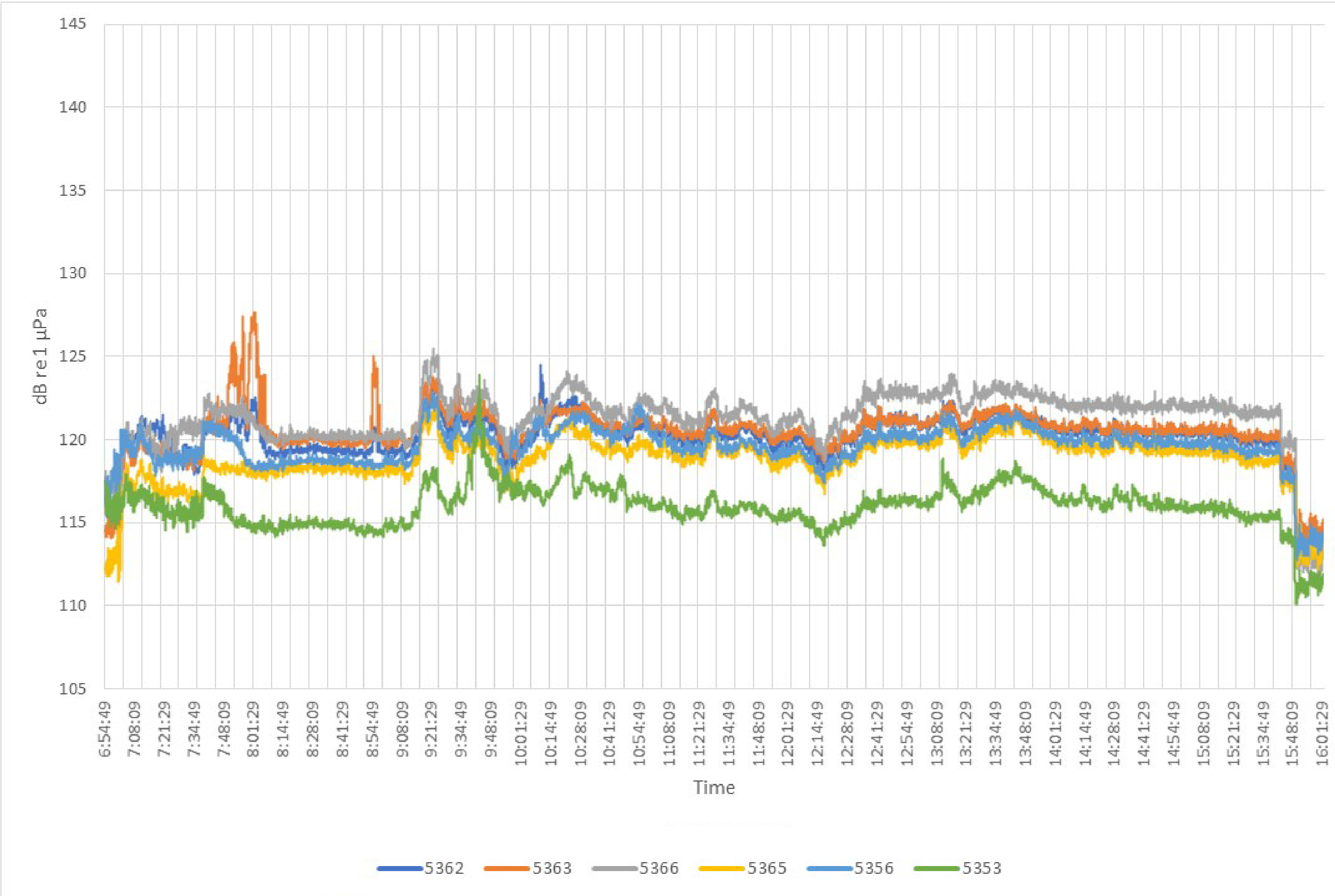

Figure B-88. Time History Plot of B-13 Mechanical Cut from April 17, 2021, 7:02 to 15:48 (20-second sample interval)

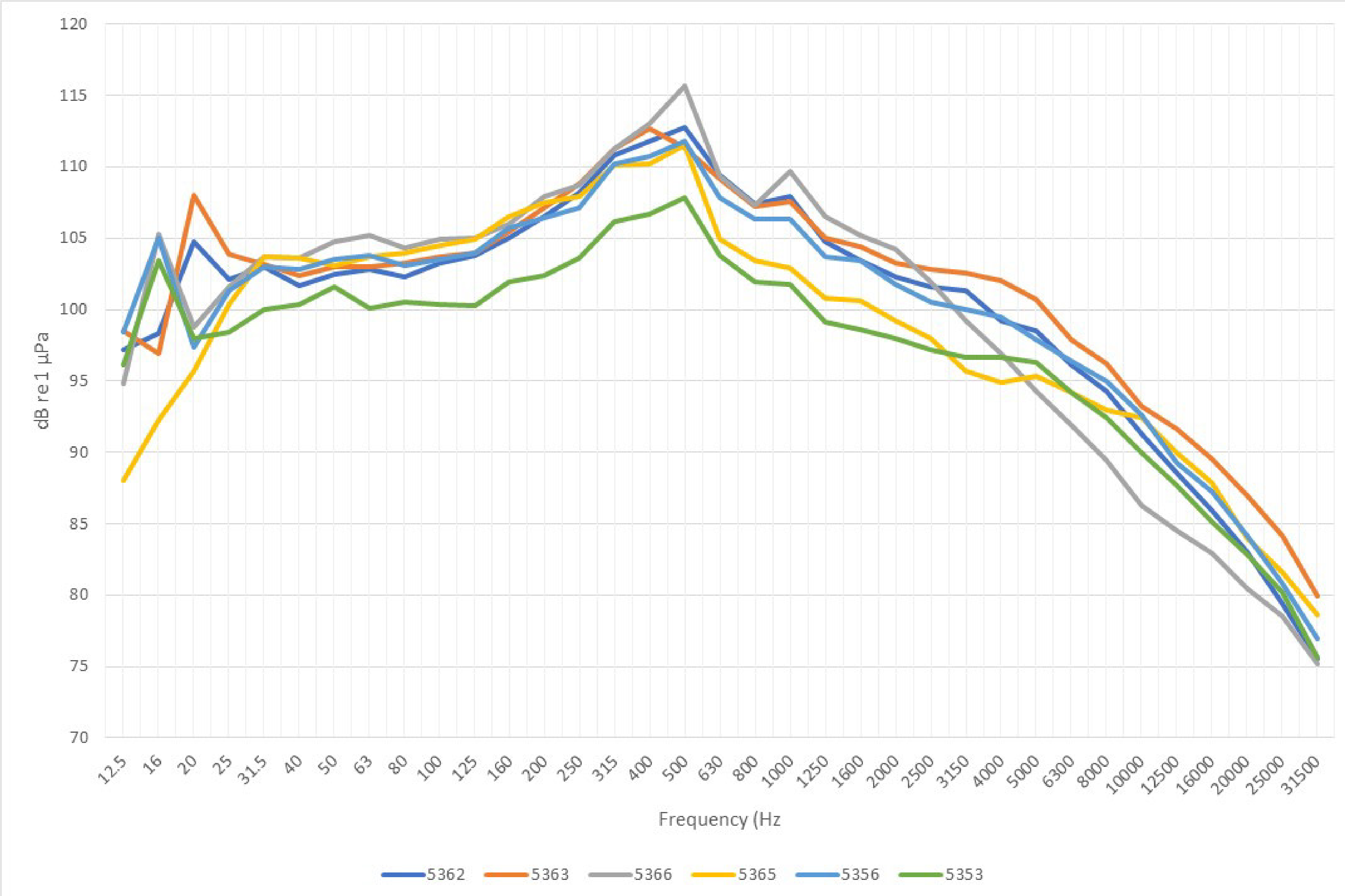

Figure B-89. SPL RMS 1/3 Octave Band Plot of B-13 Mechanical Cut from April 17, 2021, 7:02 to 15:48

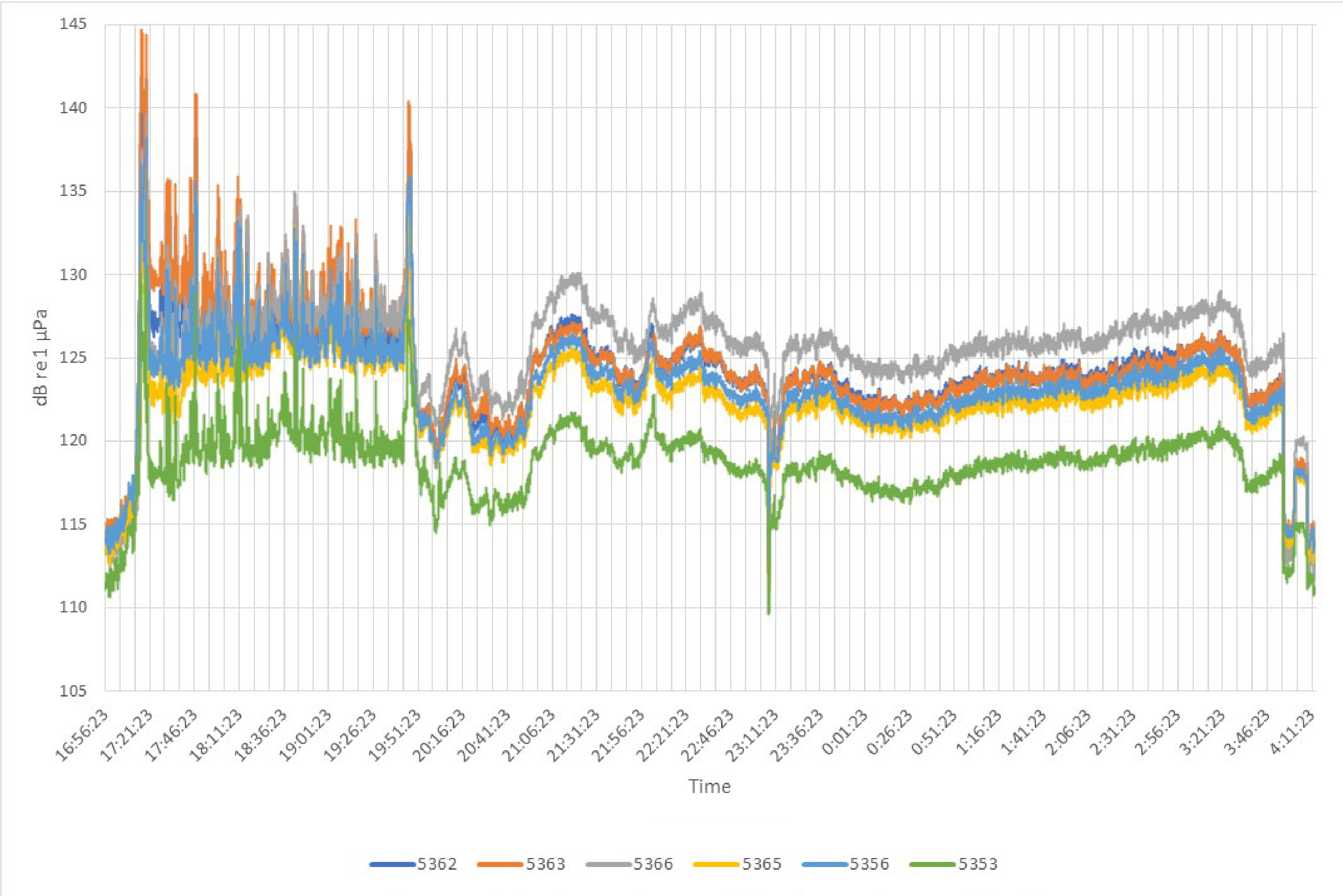

Figure B-90. Time History Plot of B-13 Mechanical Cut from April 17, 2021, 17:09 to April 18, 2021, 3:56 (20-second sample interval)

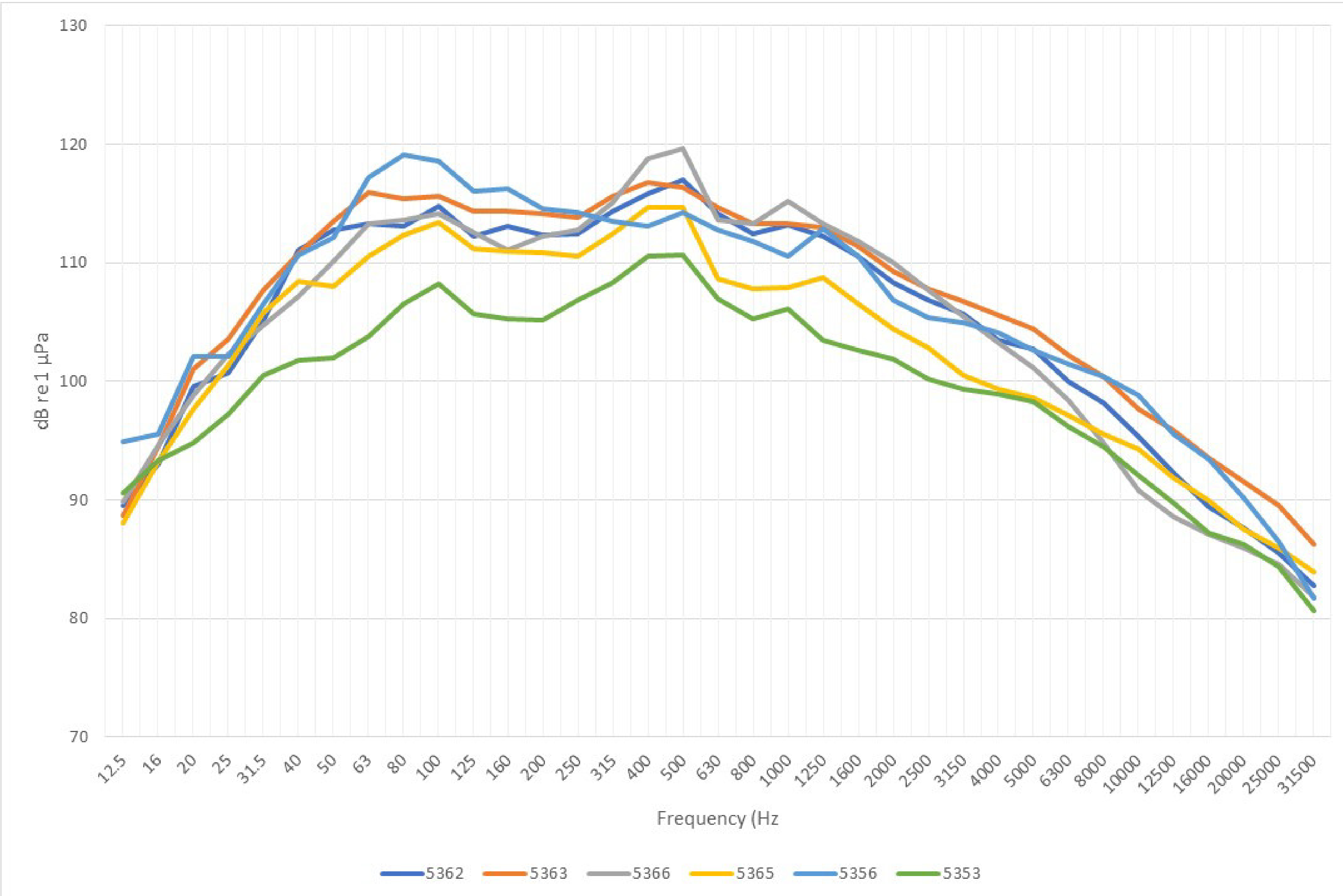

Figure B-91. SPL RMS 1/3 Octave Band Plot of B-13 Mechanical Cut from April 17, 2021, 17:09 to April 18, 2021, 3:56

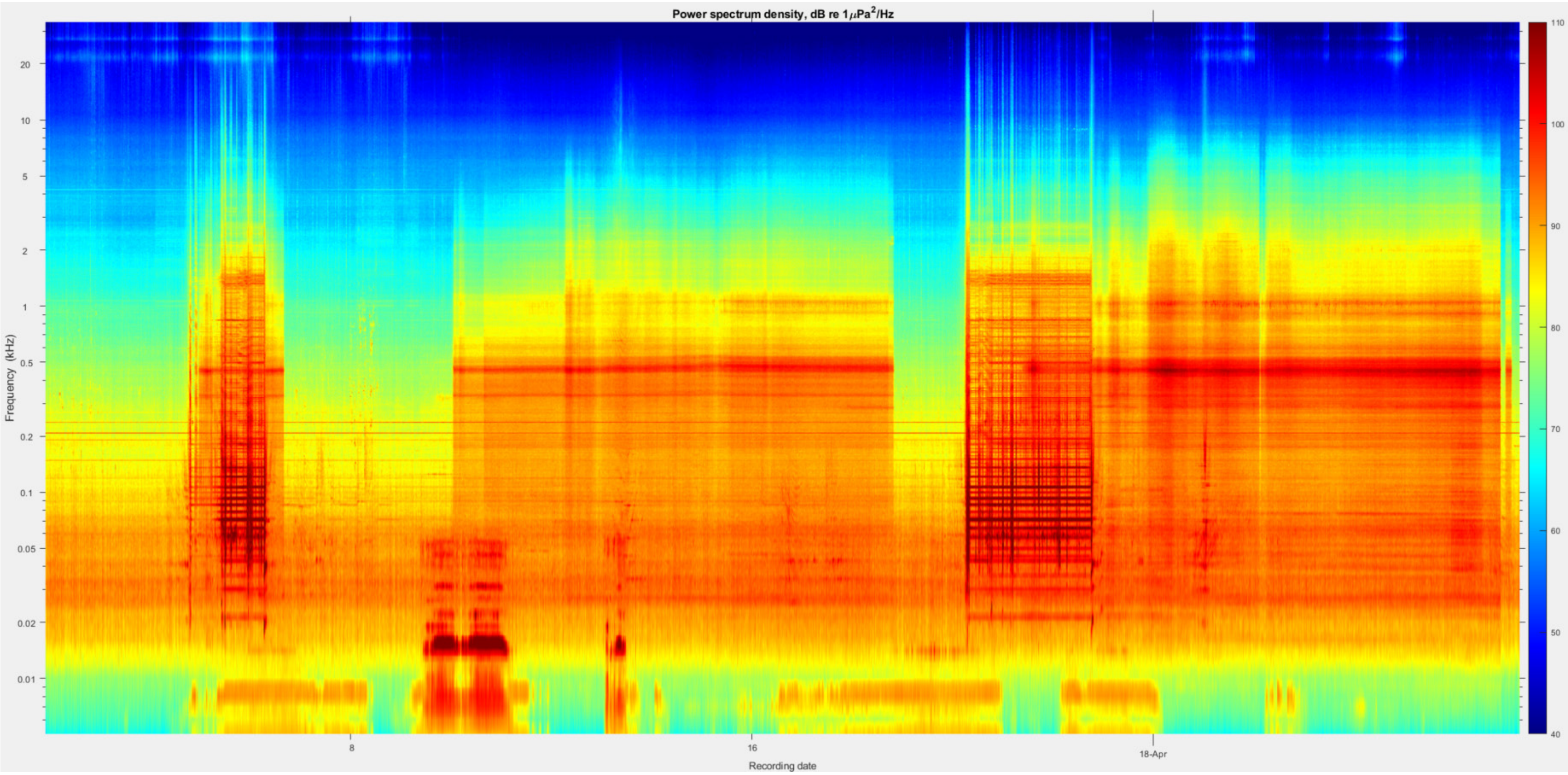

Figure B-92. PSD Spectrogram Plot of B-13 Mechanical Cut from 1:54 April 17, 2021 – 3:56 April 18, 2021

Table B-24. Wellbore Conductor B-10
(12:47 April 18, 2021 – 1:52 April 19, 2021)

Conductor	Start Time	End Time	Total Duration of Cut (minutes)	Overall Wall Thickness (inches)	Cut Depth Below Mudline (Feet)	Cutter RPM
B-10	4/18/2021 12:47	4/18/2021 14:30	103	1.919	20	60
	4/18/2021 15:58	4/18/2021 17:17	79			
	4/18/2021 21:06	4/18/2021 23:02	116			
	4/18/2021 23:22	4/19/2021 1:52	150			

Conductor	Start Time	End Time	Direction	Monitor Station Name	Distance to Conductor (m)	L_p	Max L_p	Min L_p	$L_{p,pk}$	L_E
B-10	4/18/2021 12:47	4/18/2021 14:30	North	5362	141.03	118.6	130.5	112.9	154.4	156.4
			North	5363	141.03	118.9	129.9	110.5	150.0	156.8
			East	5366	107.83	119.9	132.6	110.9	154.0	157.8
			South	5365	135.74	117.1	127.5	110.0	145.2	155.0
			West	5356	152.13	117.8	128.4	112.7	147.0	155.7
			South	5353	293.12	114.4	123.4	107.9	144.3	152.3
	4/18/2021 15:58	4/18/2021 17:17	North	5362	141.03	122.2	130.5	111.4	158.2	159.0
			North	5363	141.03	122.1	128.4	112.2	153.1	158.9
			East	5366	107.83	124.6	132.1	110.9	159.7	161.4
			South	5365	135.74	120.0	128.1	110.7	155.7	156.8
			West	5356	152.13	120.7	127.9	111.5	156.6	157.5
			South	5353	293.12	116.3	122.4	108.9	148.7	153.1
	4/18/2021 21:06	4/18/2021 23:02	North	5362	141.03	120.4	130.3	111.6	156.2	157.7
			North	5363	141.03	120.6	129.9	112.6	153.3	158.9
			East	5366	107.83	122.3	133.1	108.5	158.5	160.8
			South	5365	135.74	118.3	127.0	109.8	148.9	156.7
			West	5356	152.13	118.7	127.3	111.7	153.2	157.1
			South	5353	293.12	114.6	122.5	109.0	145.3	153.0
	4/18/2021 23:22	4/19/2021 1:52	North	5362	141.03	124.1	131.0	110.4	162.5	163.7
			North	5363	141.03	124.3	130.7	114.0	159.0	163.9
			East	5366	107.83	126.8	133.4	109.1	163.0	166.3
			South	5365	135.74	122.1	128.4	110.0	150.8	161.7
			West	5356	152.13	122.7	129.8	112.0	158.1	162.2
			South	5353	293.12	117.9	124.2	108.6	150.3	157.4

L_p and $L_{p,pk}$ = (dB re 1 μPa); L_E = (dB re 1 μPa^2·s)

Conductor	Start Time	End Time	Monitor Station Name	L_p				L_E			
				LF	MF	HF	PP	LF	MF	HF	PP
B-10	4/18/2021 12:47	4/18/2021 14:30	5362	117.3	97.6	93.6	110.2	155.2	135.5	131.5	148.1
			5363	117.5	102.0	98.3	111.9	155.4	139.9	136.2	149.8
			5366	118.6	93.8	90.1	110.1	156.5	131.7	128.0	148.0
			5365	114.7	96.3	93.3	106.6	152.7	134.2	131.2	144.5
			5356	116.0	99.1	95.5	109.5	153.9	137.0	133.4	147.4
			5353	112.3	97.5	93.9	106.9	149.9	135.2	131.5	144.5
	4/18/2021 15:58	4/18/2021 17:17	5362	121.2	98.0	94.1	113.5	158.0	134.8	130.9	150.3
			5363	121.0	101.0	97.4	113.9	157.8	137.8	134.2	150.7
			5366	123.6	97.8	93.0	116.1	160.4	134.6	129.8	152.9
			5365	118.4	97.5	94.3	110.5	155.2	134.3	131.1	147.3
			5356	119.4	98.3	94.6	112.2	156.2	135.1	131.4	149.0
			5353	114.7	96.1	92.7	107.8	151.5	132.9	129.5	144.6
	4/18/2021 21:06	4/18/2021 23:02	5362	119.2	99.5	96.1	112.2	157.7	138.0	134.6	150.7
			5363	119.3	102.5	99.2	113.2	157.7	140.8	137.6	151.6
			5366	121.5	97.4	93.5	114.3	159.8	135.7	131.8	152.6
			5365	116.5	98.3	95.6	109.1	155.0	136.7	134.0	147.5
			5356	117.4	99.1	95.9	110.9	155.8	137.4	134.3	149.2
			5353	113.1	97.8	94.6	107.5	151.5	136.2	133.1	145.9
	4/18/2021 23:22	4/19/2021 1:52	5362	123.2	100.3	96.1	115.7	162.7	139.8	135.7	155.2
			5363	123.3	102.4	98.7	116.0	162.8	142.0	138.2	155.5
			5366	125.8	100.4	95.3	118.3	165.3	139.9	134.9	157.8
			5365	120.6	98.7	95.5	112.5	160.2	138.2	135.0	152.1
			5356	121.5	99.9	96.2	114.1	161.0	139.4	135.7	153.6
			5353	116.6	97.5	94.0	109.7	156.1	137.0	133.5	149.2

L_p and $L_{p,pk}$ = (dB re 1 µPa); L_E = (dB re 1 µPa^2·s)
LF – low frequency; MF – mid-frequency; HF – high frequency; PP – phocid pinnipeds

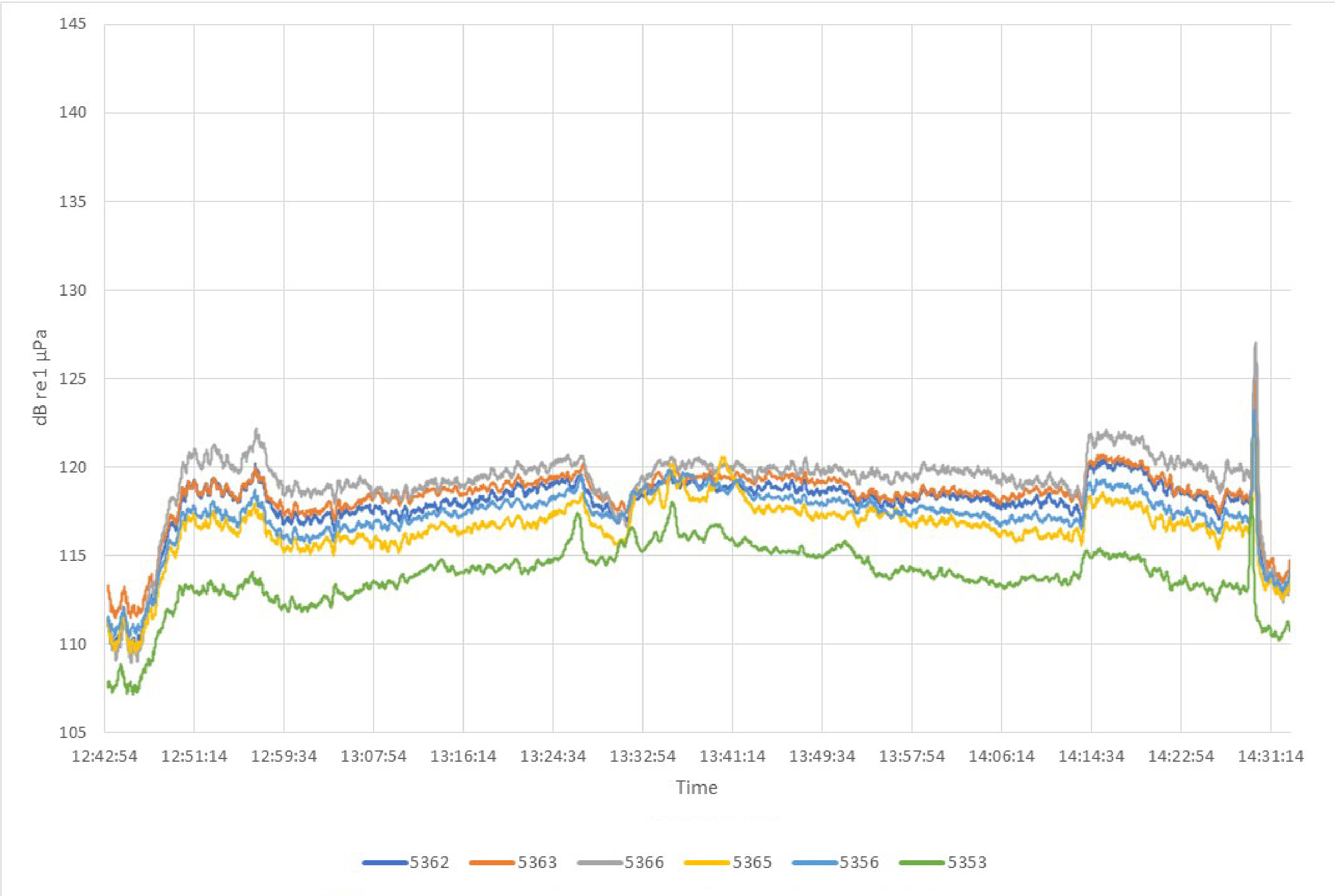

Figure B-93. Time History Plot of B-10 Mechanical Cut from April 18, 2021, 12:47 to 14:30 (20-second sample interval)

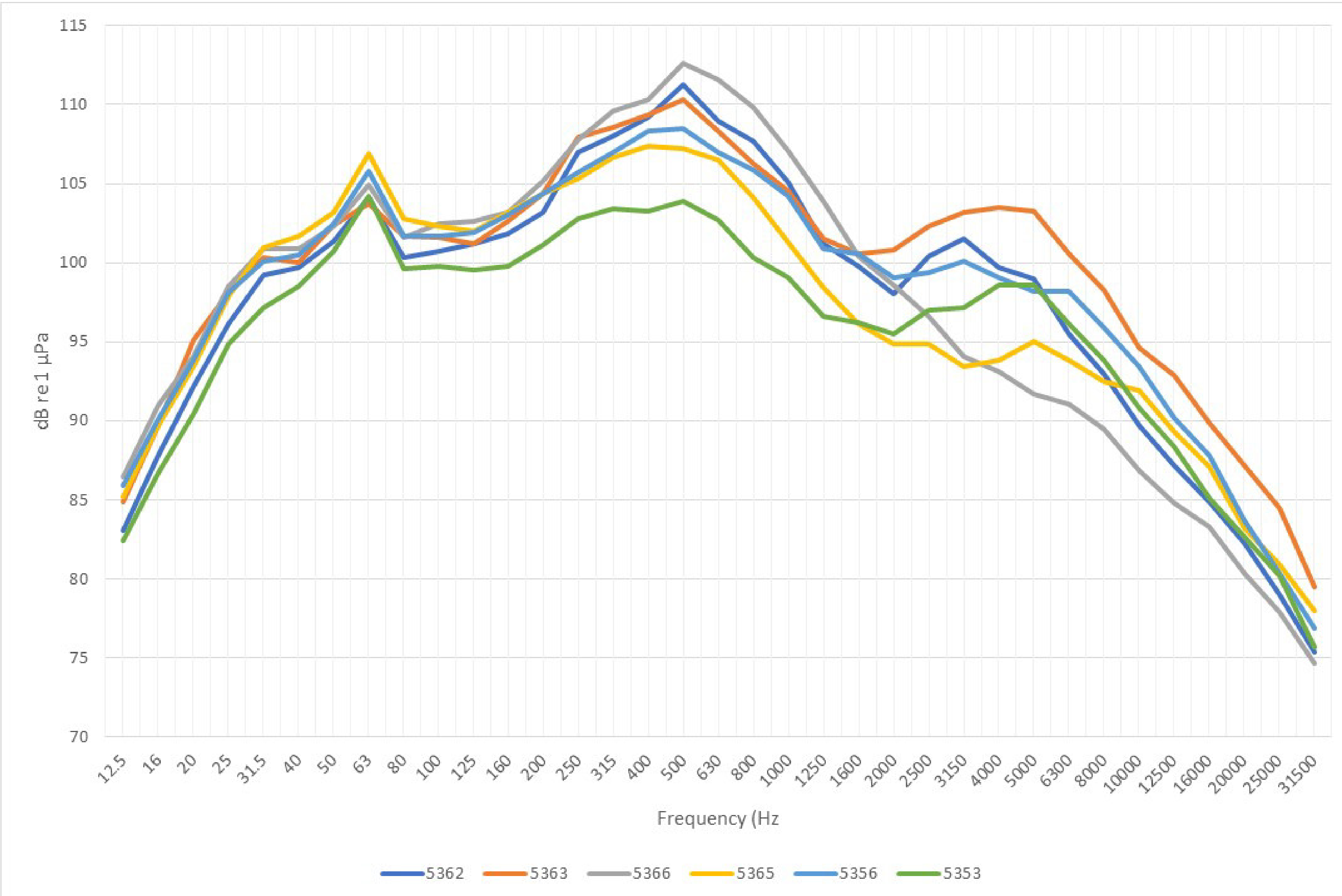

Figure B-94. SPL RMS 1/3 Octave Band Plot of B-10 Mechanical Cut from April 18, 2021, 12:47 to 14:30

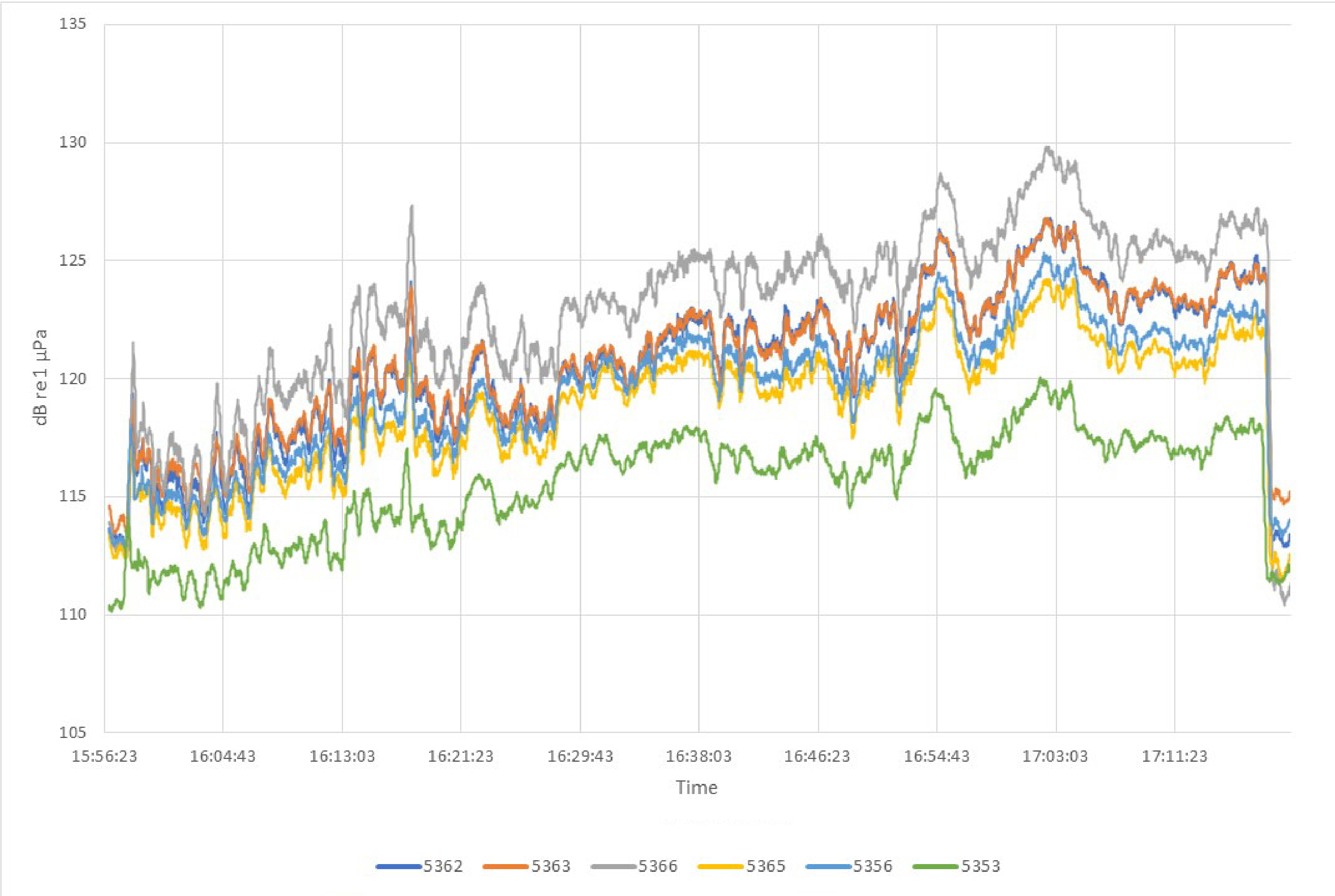

Figure B-95. Time History Plot of B-10 Mechanical Cut from April 18, 2021, 15:58 to 17:17 (20-second sample interval)

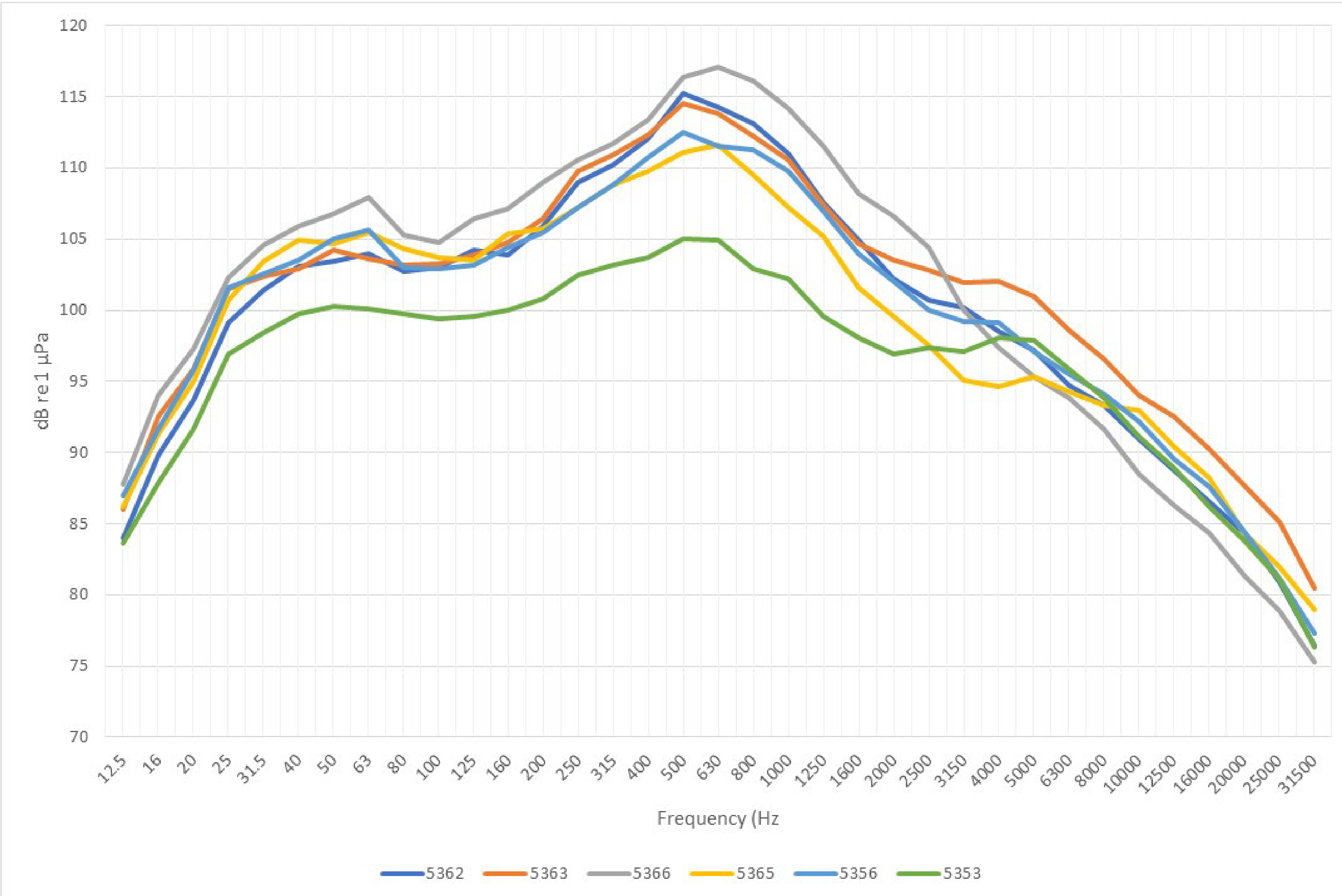

Figure B-96. SPL RMS 1/3 Octave Band Plot of B-10 Mechanical Cut from April 18, 2021, 15:58 to 17:17

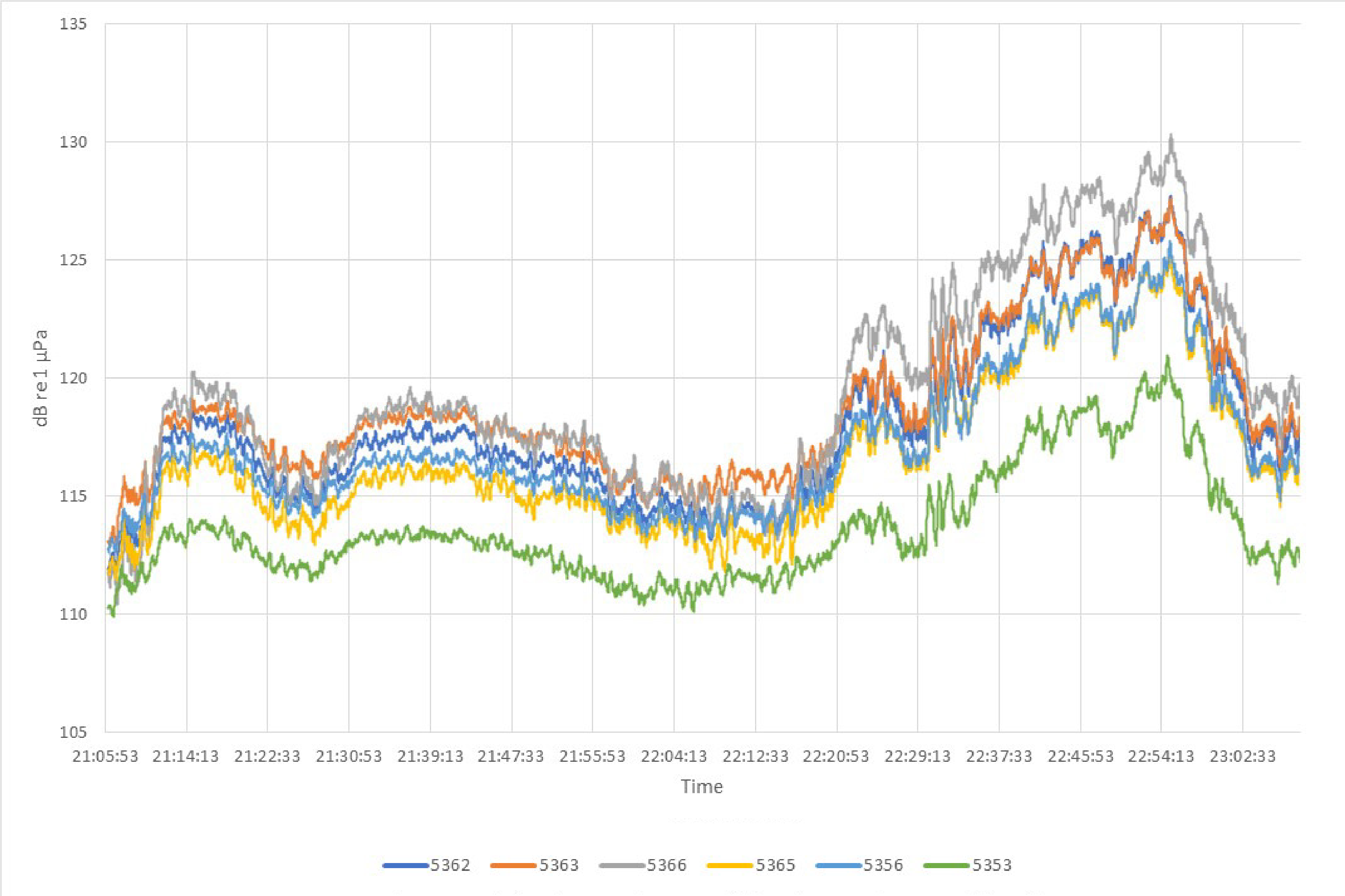

Figure B-97. Time History Plot of B-10 Mechanical Cut from April 18, 2021, 21:06 to 23: 02 (20-second sample interval)

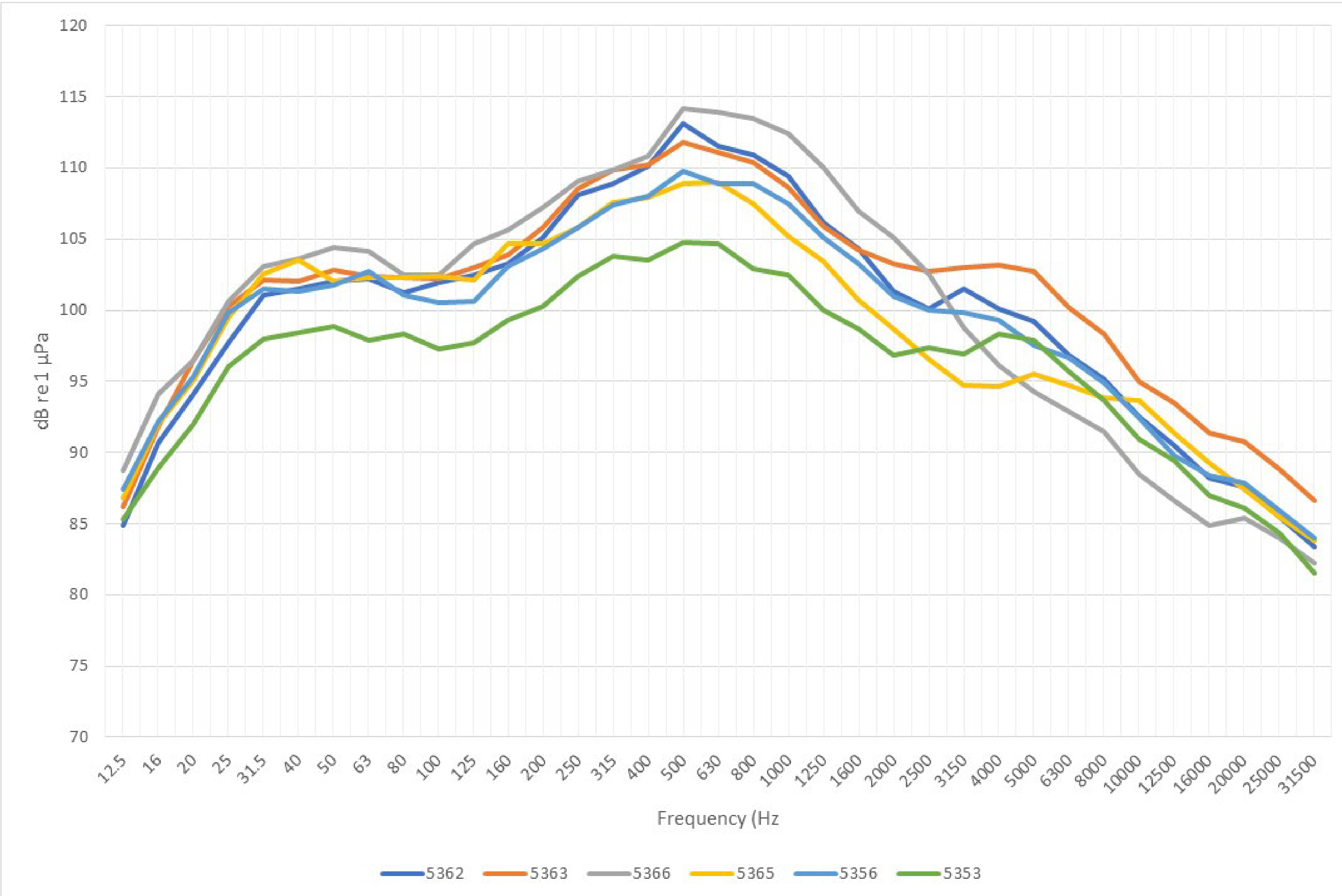

Figure B-98. SPL RMS 1/3 Octave Band Plot of B-10 Mechanical Cut from April 18, 2021, 21:06 to 23:02

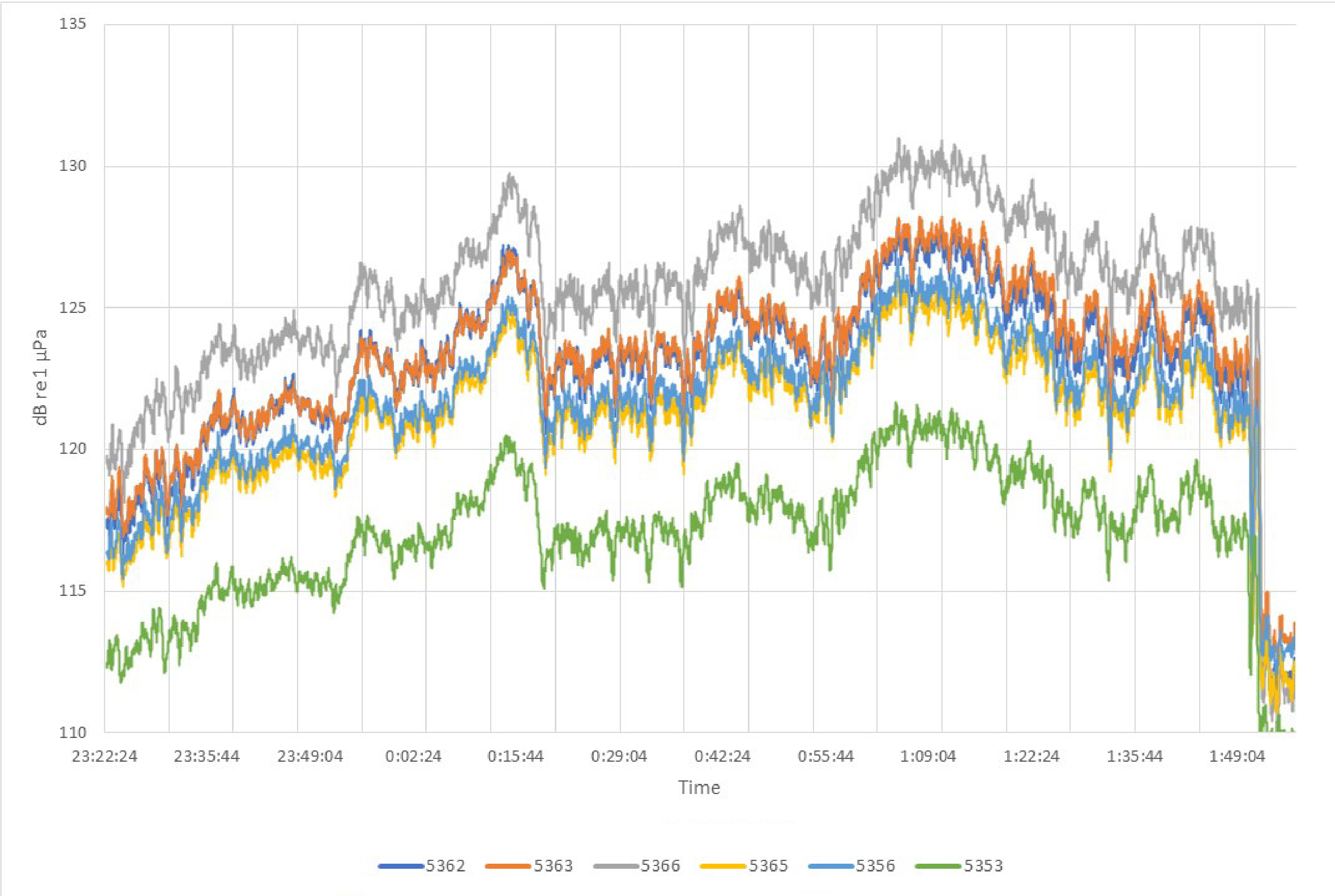

Figure B-99. Time History Plot of B-10 Mechanical Cut from April 18, 2021, 23:22 to April 19, 2021, 1:52 (20-second sample interval)

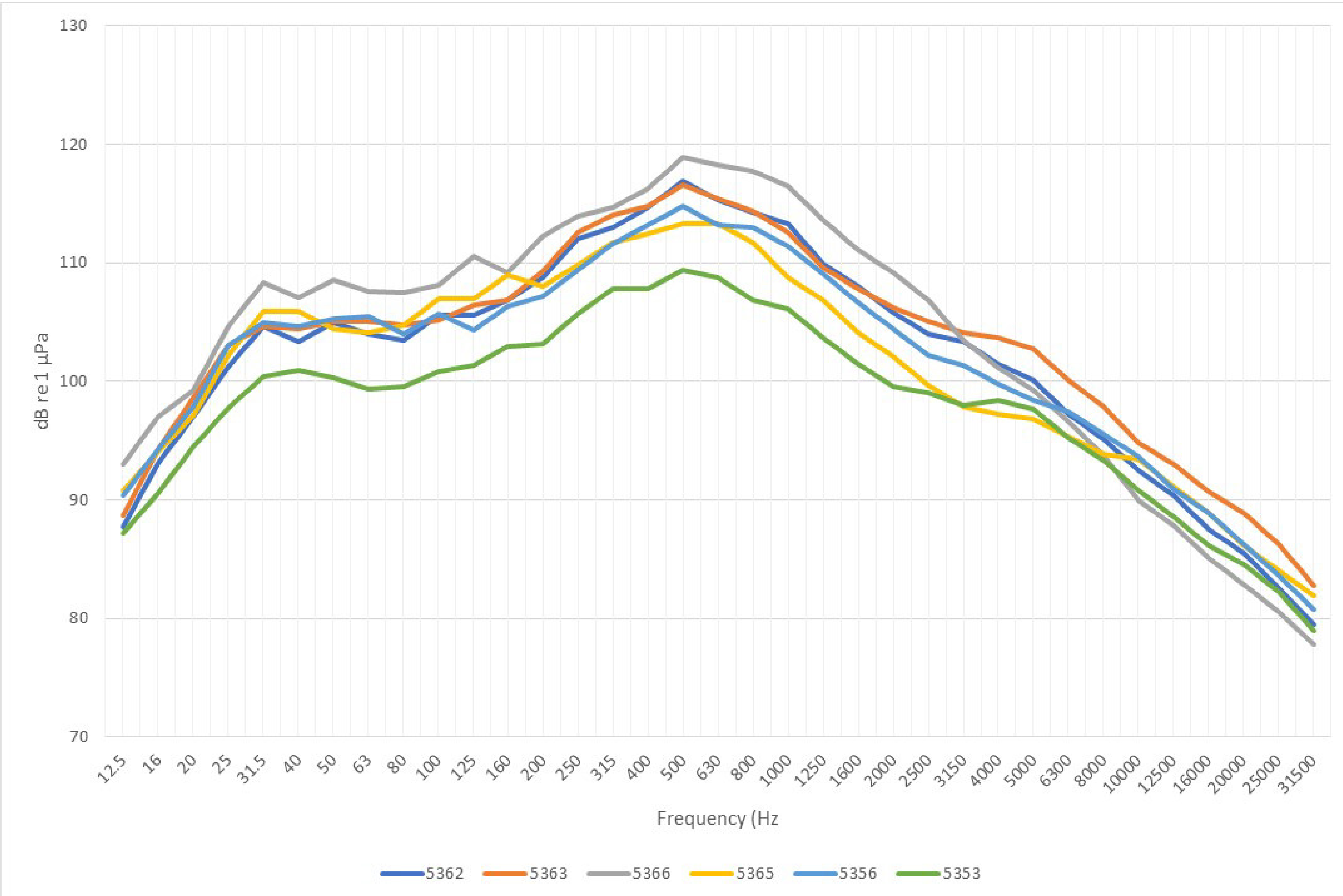

Figure B-100. SPL RMS 1/3 Octave Band Plot of B-10 Mechanical Cut from April 18, 2021, 23:22 to April 19, 2021, 1:52

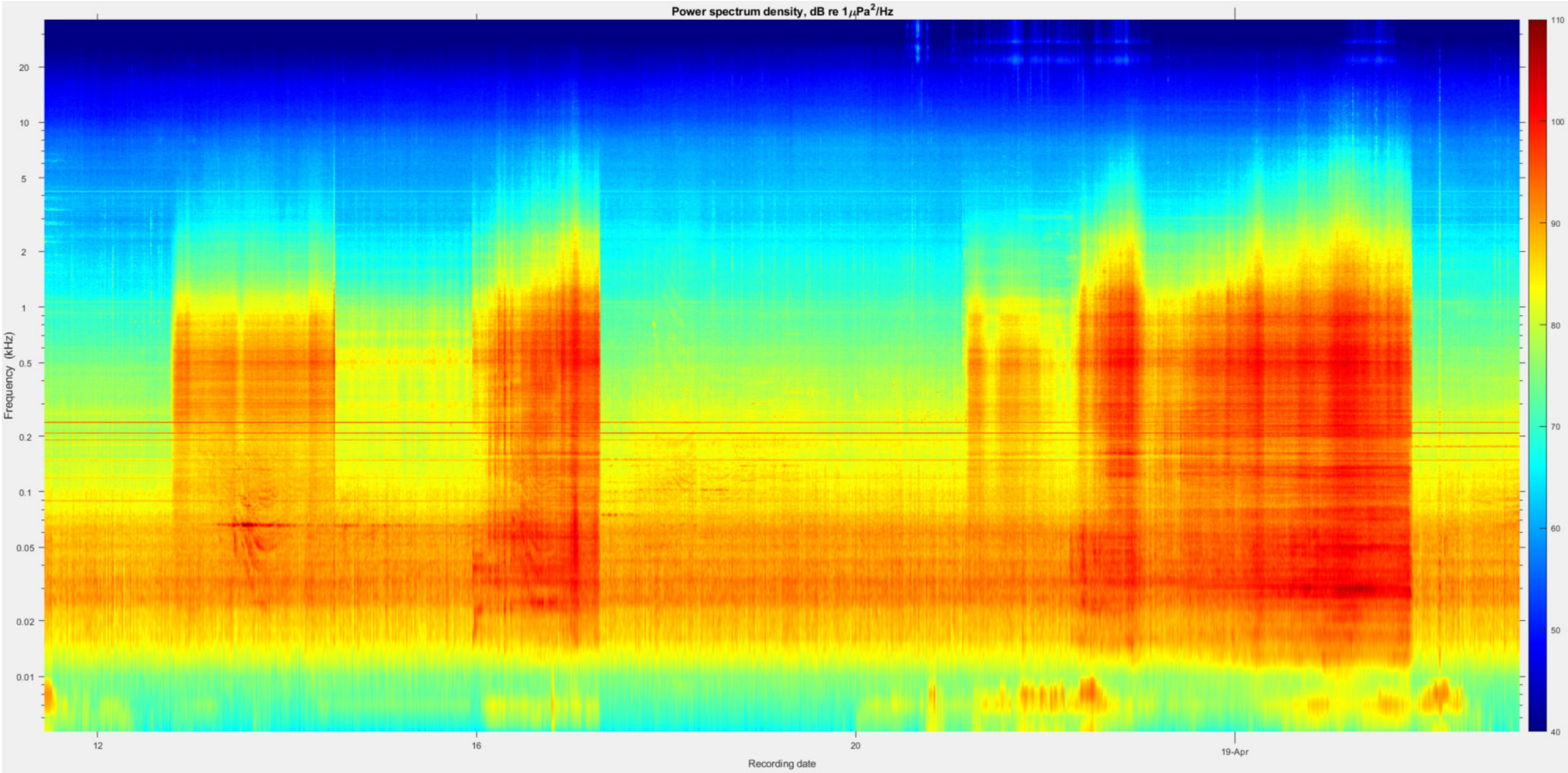

Figure B-101. PSD Spectrogram Plot of B-10 Mechanical Cut from 12:47 April 18, 2021 – 1:52 April 19, 2021

Table B-25. Empty Conductor S-7
(7:41 April 19, 2021 – 10:20 April 19, 2021)

Conductor	Start Time	End Time	Total Duration of Cut (minutes)	Overall Wall Thickness (inches)	Cut Depth Below Mudline (Feet)	Cutter RPM
S-7	4/19/2021 7:41	4/19/2021 10:20	159	0.812	20	60

Conductor	Start Time	End Time	Direction	Monitor Station Name	Distance to Conductor (m)	L_p	Max L_p	Min L_p	$L_{p,pk}$	L_E
S-7	4/19/2021 7:41	4/19/2021 10:20	North	5362	144.47	129.1	145.9	112.1	174.0	168.8
			North	5363	144.47	130.5	146.8	112.9	173.7	170.2
			East	5366	102.61	129.0	141.9	111.3	163.6	168.8
			South	5365	135.26	127.8	141.5	112.1	164.1	167.6
			West	5356	156.46	130.4	146.0	114.4	163.2	170.1
			South	5353	294.72	124.0	137.4	111.4	159.3	163.9

L_p and $L_{p.pk}$ = (dB re 1 μPa); L_E = (dB re 1 μPa²·s)

Conductor	Start Time	End Time	Monitor Station Name	L_p				L_E			
				LF	MF	HF	PP	LF	MF	HF	PP
S-7	4/19/2021 7:41	4/19/2021 10:20	5362	126.0	108.0	104.5	119.6	165.8	147.8	144.3	159.4
			5363	127.4	109.7	106.4	120.8	167.2	149.5	146.2	160.6
			5366	127.1	106.1	101.7	121.6	166.9	145.9	141.5	161.4
			5365	124.6	106.0	102.9	117.6	164.4	145.8	142.7	157.4
			5356	127.0	106.1	102.2	119.6	166.8	145.9	142.0	159.4
			5353	121.3	102.7	99.2	114.4	161.1	142.5	139.0	154.2

L_p and $L_{p.pk}$ = (dB re 1 μPa); L_E = (dB re 1 μPa²·s)
LF – low frequency; MF – mid-frequency; HF – high frequency; PP – phocid pinnipeds

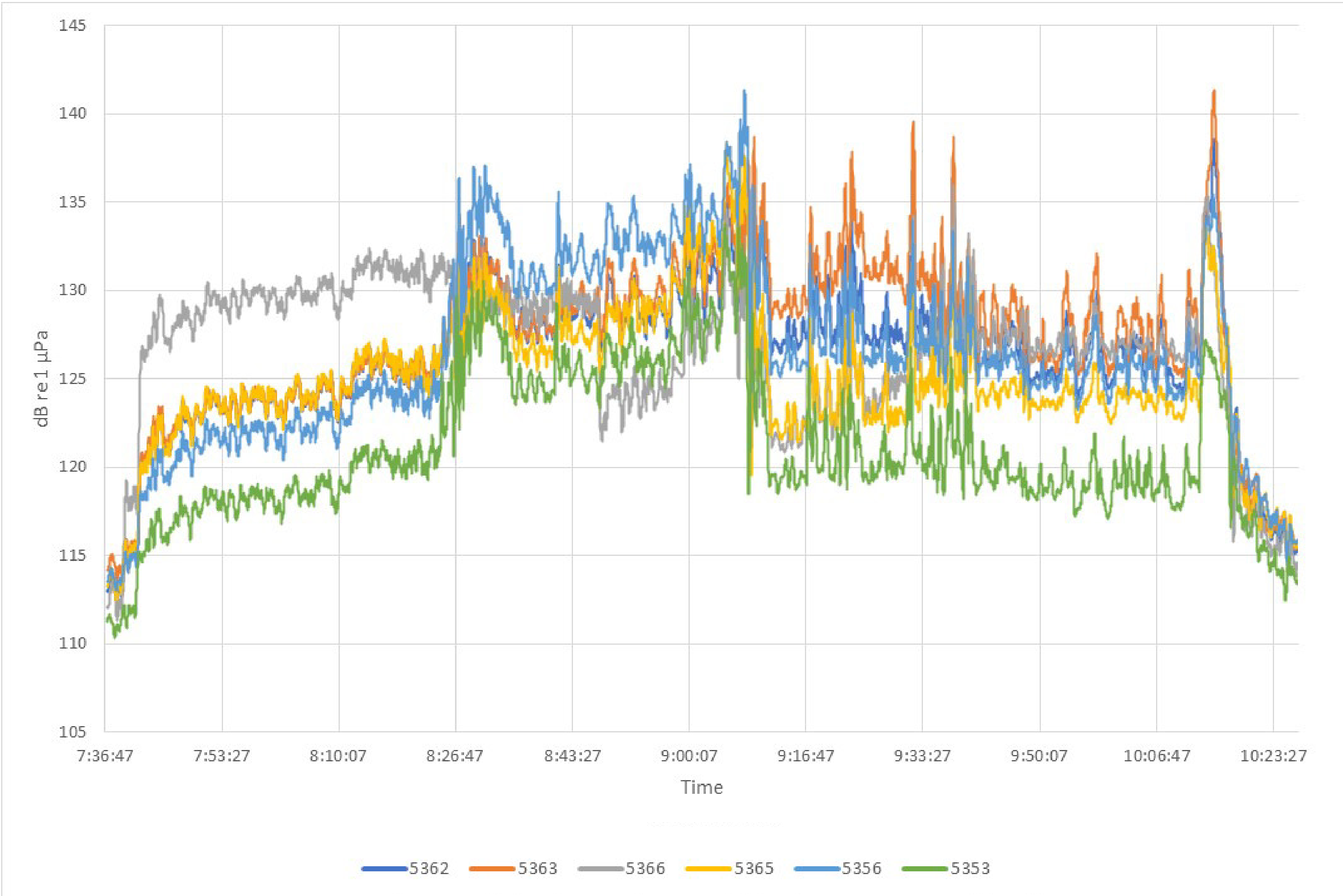

Figure B-102. Time History Plot of S-7 Mechanical Cut from April 19, 2021, 7:41 to 10:20 (20-second sample interval)

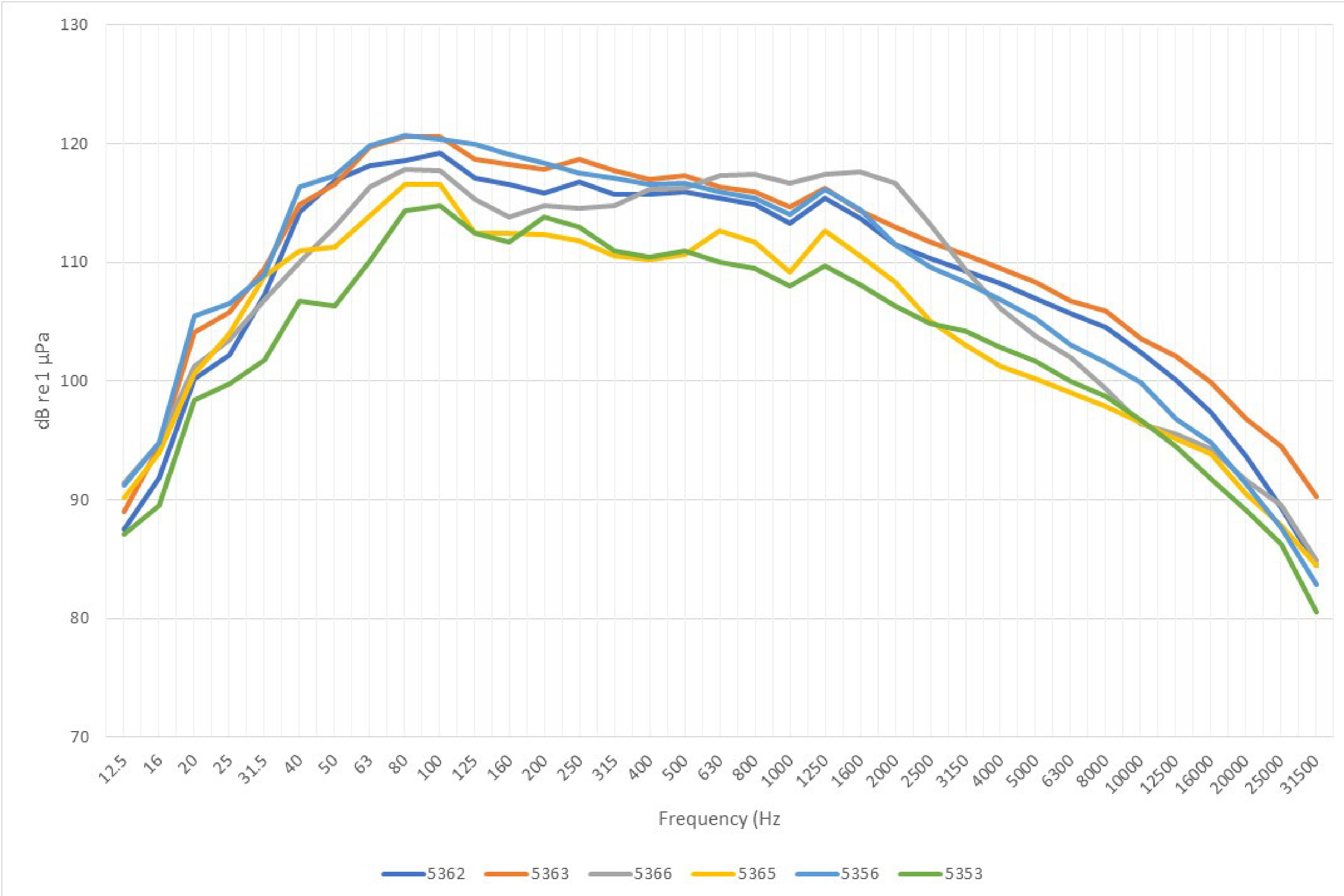

Figure B-103. SPL RMS 1/3 Octave Band Plot of S-7 Mechanical Cut from April 19, 2021, 7:41 to 10:20

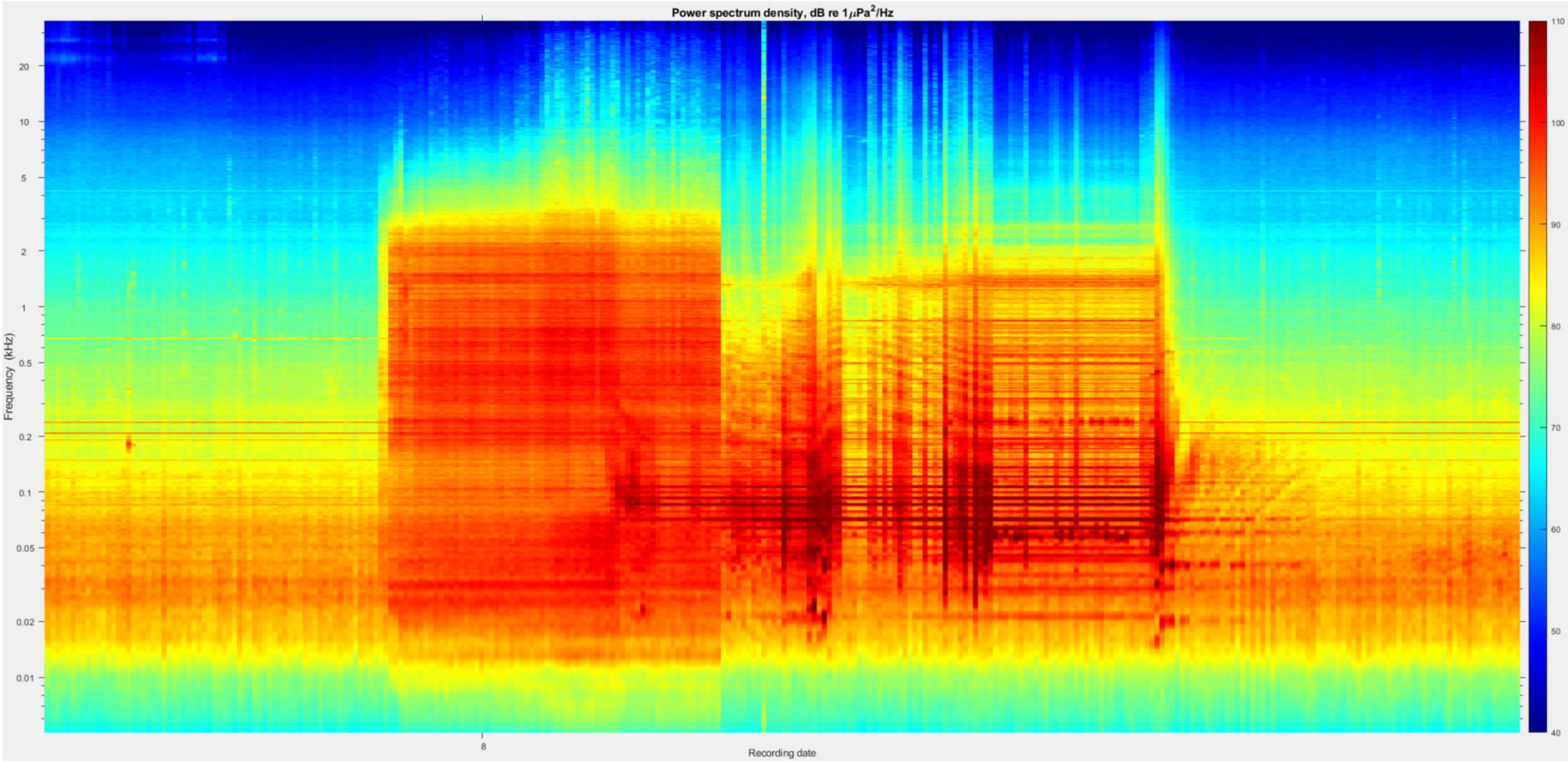

Figure B-104. PSD Spectrogram Plot of S-7 Mechanical Cut from 7:41 April 19, 2021 – 10:20 April 19, 2021

Table B-26. Empty Conductor S-6
(15:47 April 19, 2021 – 23:37 April 19, 2021)

Conductor	Start Time	End Time	Total Duration of Cut (minutes)	Overall Wall Thickness (inches)	Cut Depth Below Mudline (Feet)	Cutter RPM
S-6	4/19/2021 15:47	4/19/2021 23:37	470	0.812	20	60

Conductor	Start Time	End Time	Direction	Monitor Station Name	Distance to Conductor (m)	L_p	Max L_p	Min L_p	$L_{p,pk}$	L_E
S-6	4/19/2021 15:47	4/19/2021 21:37	North	5362	140.94	129.1	145.9	112.1	174.0	168.8
			North	5363	140.94	131.1	149.7	116.7	165.8	172.9
			East	5366	105.12	128.6	141.0	114.6	170.9	176.6
			South	5365	137.48	125.3	138.2	112.1	160.2	169.9
			West	5356	155.09	126.1	140.5	115.8	167.9	170.6
			South	5353	295.64	119.8	133.1	113.5	162.8	164.3

L_p and $L_{p.pk}$ = (dB re 1 μPa); L_E = (dB re 1 μPa²·s)

Conductor	Start Time	End Time	Monitor Station Name	L_p				L_E			
				LF	MF	HF	PP	LF	MF	HF	PP
S-6	4/19/2021 15:47	4/19/2021 21:37	5362	125.9	104.7	100.8	118.9	174.0	152.8	148.9	167.0
			5363	127.5	108.6	105.2	121.0	170.7	151.8	148.4	164.2
			5366	126.3	105.6	101.4	120.5	174.4	153.7	149.5	168.6
			5365	122.5	103.0	99.8	115.7	166.4	146.9	143.7	159.6
			5356	123.3	104.6	101.1	117.1	167.9	149.2	145.7	161.7
			5353	117.5	99.7	96.3	111.3	161.4	143.6	140.2	155.2

L_p and $L_{p.pk}$ = (dB re 1 μPa); L_E = (dB re 1 μPa²·s)
LF – low frequency; MF – mid-frequency; HF – high frequency; PP – phocid pinnipeds

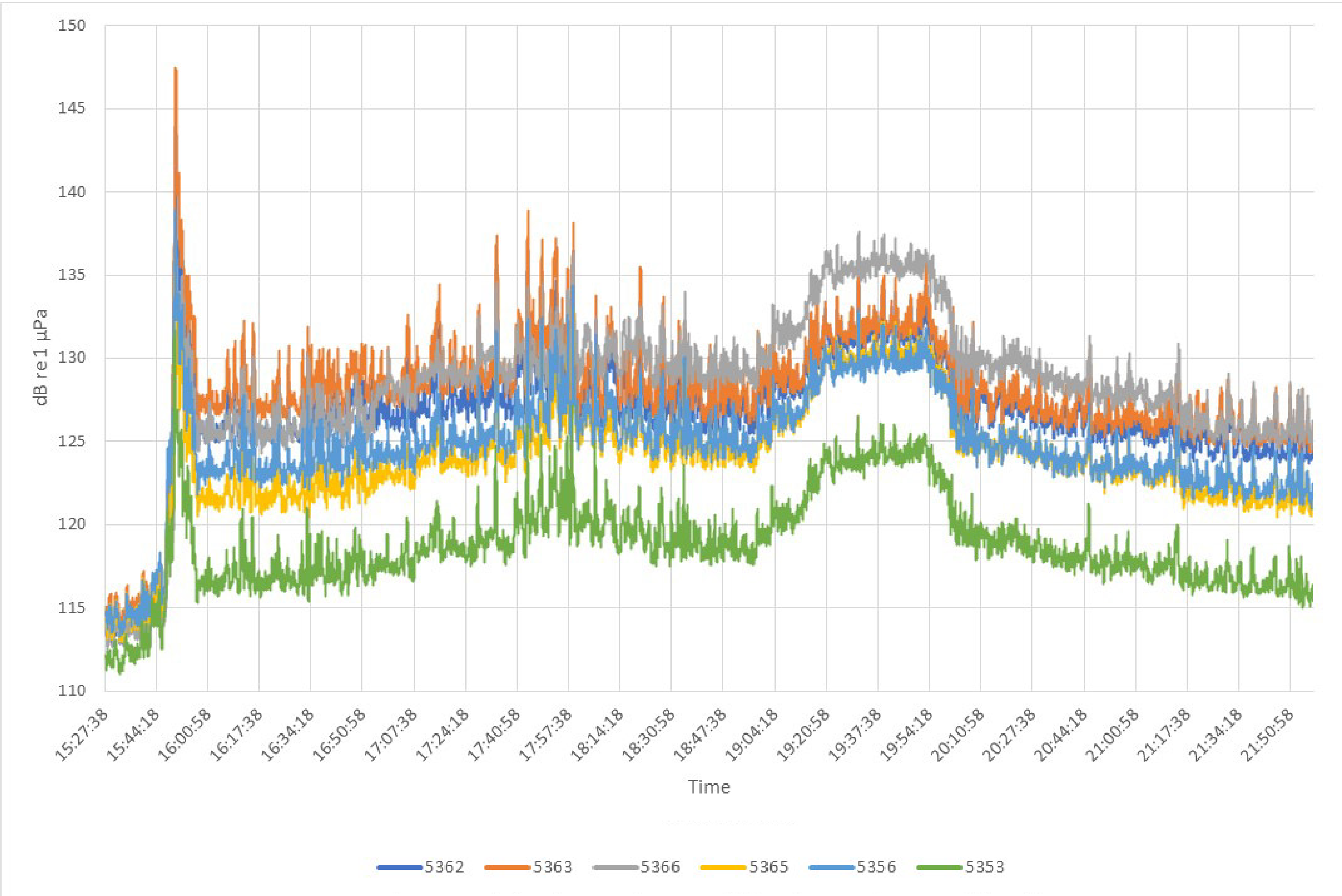

Figure B-105. Time History Plot of S-6 Mechanical Cut from April 19, 2021, 15:47 to 23:37 (20-second sample interval)

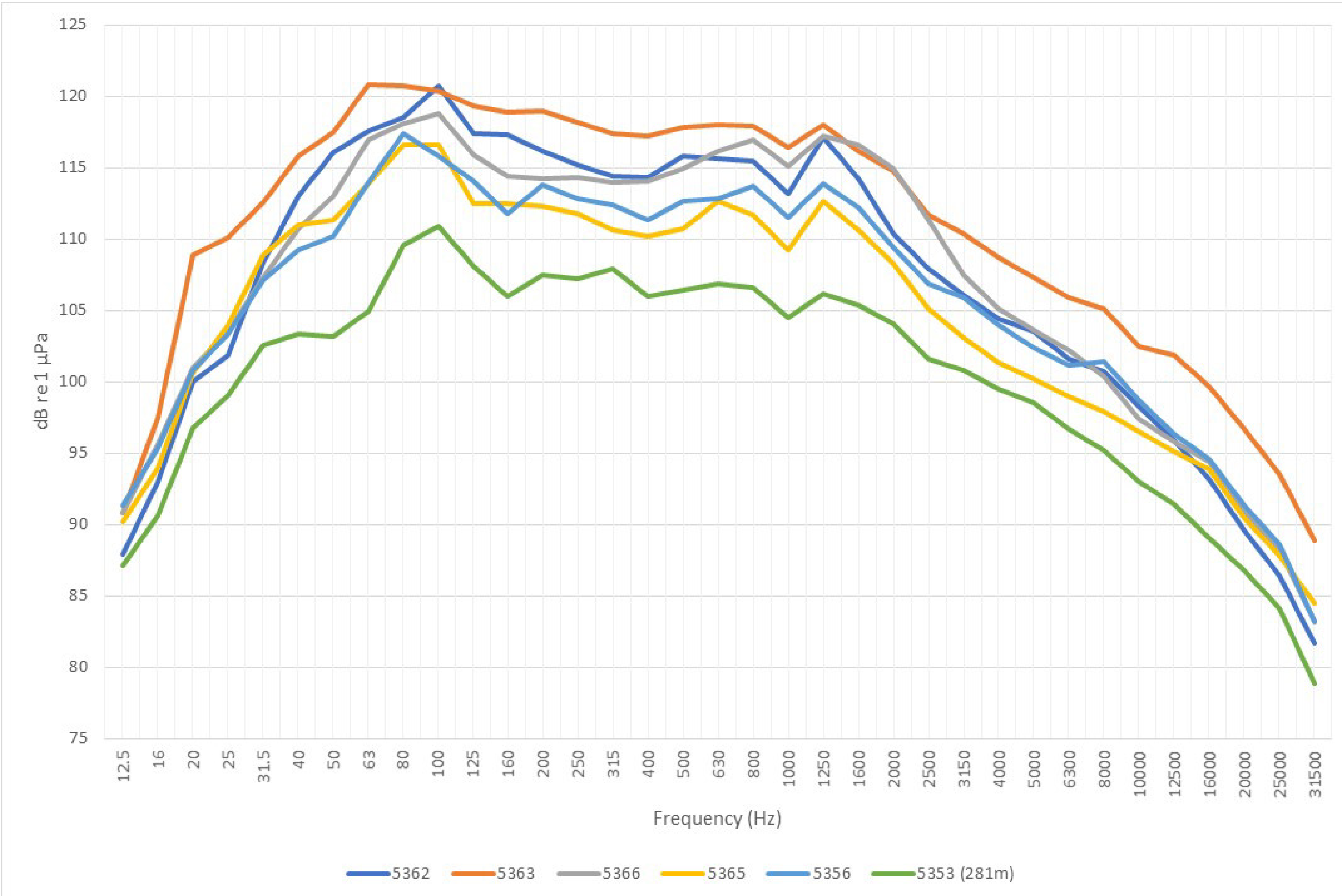

Figure B-106. SPL RMS 1/3 Octave Band Plot of S-6 Mechanical Cut from April 19, 2021, 15:47 to 23:37

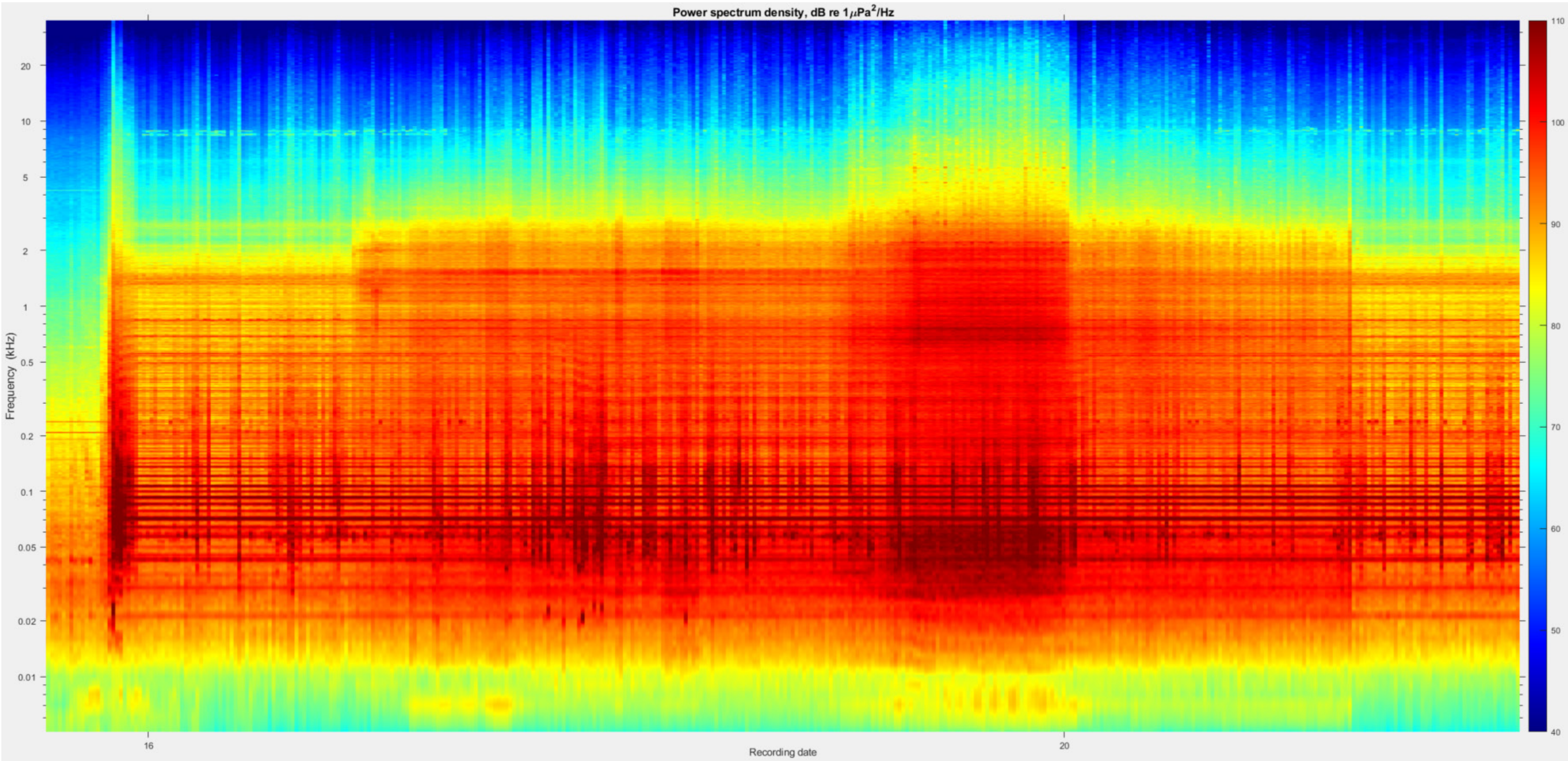

Figure B-107. PSD Spectrogram Plot of S-6 Mechanical Cut from April 19, 2021, 15:47 to 23:37

Table B-27. Conductor S-4 Noise Monitoring Results Summary

Conductor	Start Time	End Time	Total Duration of Cut (minutes)	Overall Wall Thickness (inches)	Cut Depth Below Mudline (Feet)	Cutter RPM
S-4	4/20/2021 11:30	4/20/2021 12:55	85	0.812	20	60

Conductor	Start Time	End Time	Direction	Monitor Name	Distance to Conductor (m)	L_p	Max L_p	Min L_p	$L_{p,pk}$	L_E
S-4	4/20/2021 11:30	4/20/2021 12:55	North	5362	139.45	130.1	138.2	122.3	165.3	167.2
			North	5363	139.45	130.2	137.9	120.5	164.3	167.3
			East	5366	104.59	133.0	141.6	115.9	174.5	170.1
			South	5365	139.43	127.8	134.2	117.5	157.3	165.0
			West	5356	156.36	127.7	135.9	118.7	162.4	164.9
			South	5353	297.56	123.2	131.8	115.6	156.3	160.4

L_p and $L_{p,pk}$ = (dB re 1 μPa); L_E = (dB re 1 μPa²·s)

Conductor	Start Time	End Time	Monitor Station Name	L_p				L_E			
				LF	MF	HF	PP	LF	MF	HF	PP
S-4	4/20/2021 11:30	4/20/2021 12:55	5362	128.6	110.9	107.5	123.4	165.7	148.0	144.6	160.5
			5363	128.5	112.3	109.6	123.3	165.6	149.5	146.8	160.5
			5366	132.2	113.1	108.9	127.8	169.3	150.2	146.1	164.9
			5365	126.0	106.7	103.4	120.0	163.2	143.9	140.5	157.1
			5356	126.0	107.7	104.2	120.3	163.2	144.8	141.4	157.5
			5353	121.3	102.1	98.7	115.2	158.4	139.2	135.7	152.3

L_p and $L_{p,pk}$ = (dB re 1 μPa); L_E = (dB re 1 μPa²·s)
LF – low frequency; MF – mid-frequency; HF – high frequency; PP – phocid pinnipeds

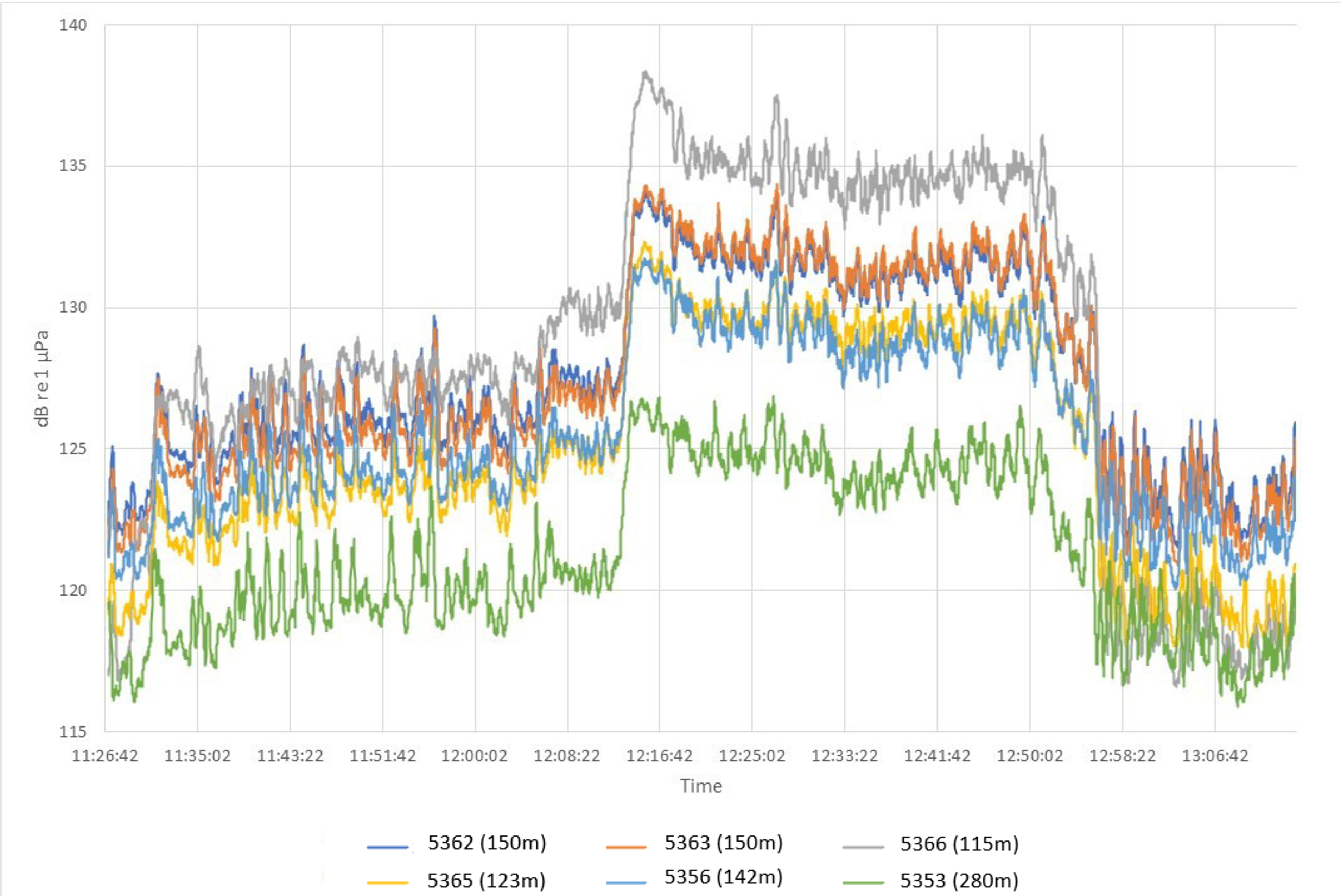

Figure B-108. Time History Plot of S-4 Mechanical Cut from April 20, 2021, 11:30 to 12:55 (20-second sample interval)

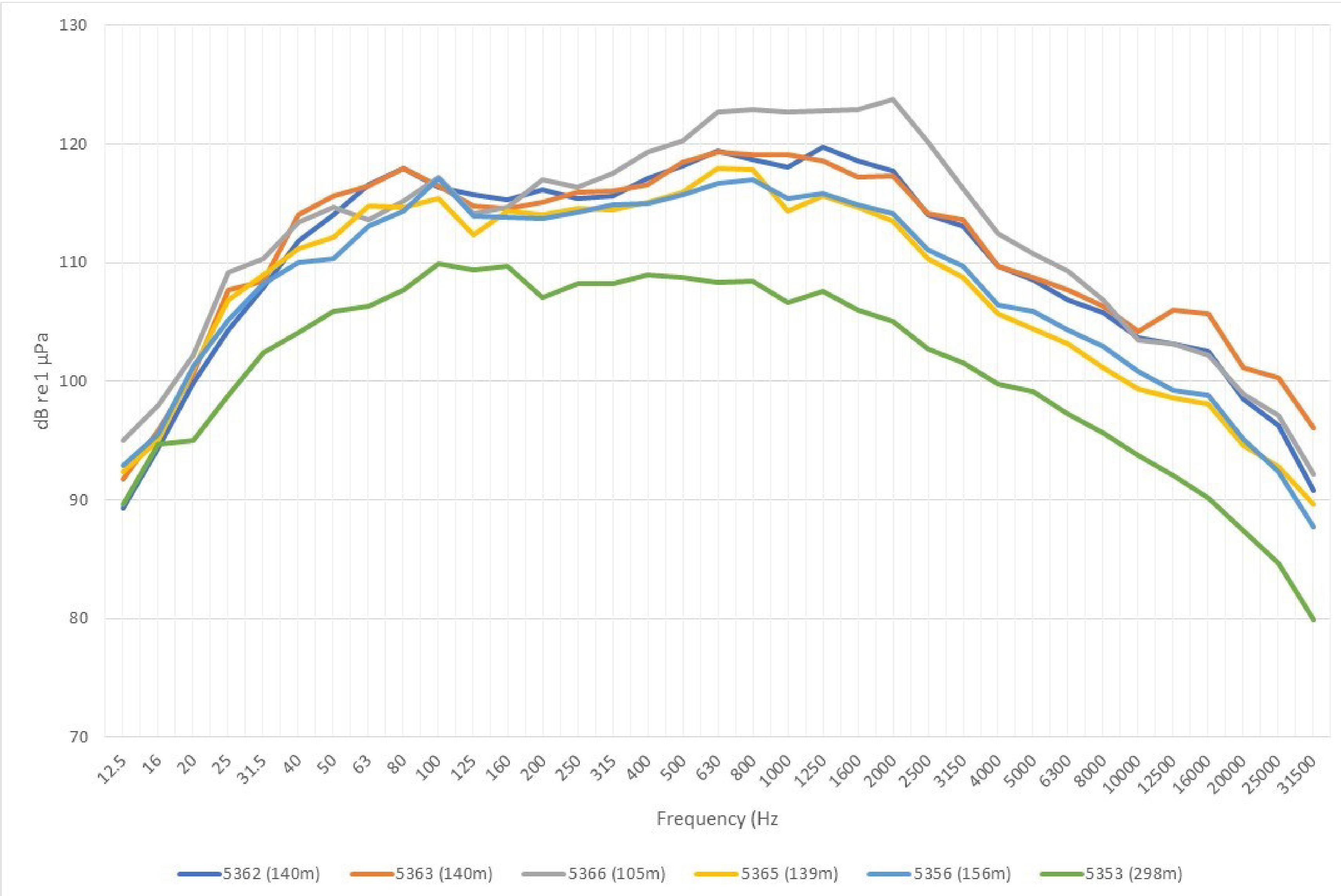

Figure B-109. SPL RMS 1/3 Octave Band Plot of S-4 Mechanical Cut from April 20, 2021, 11:30 to 12:55

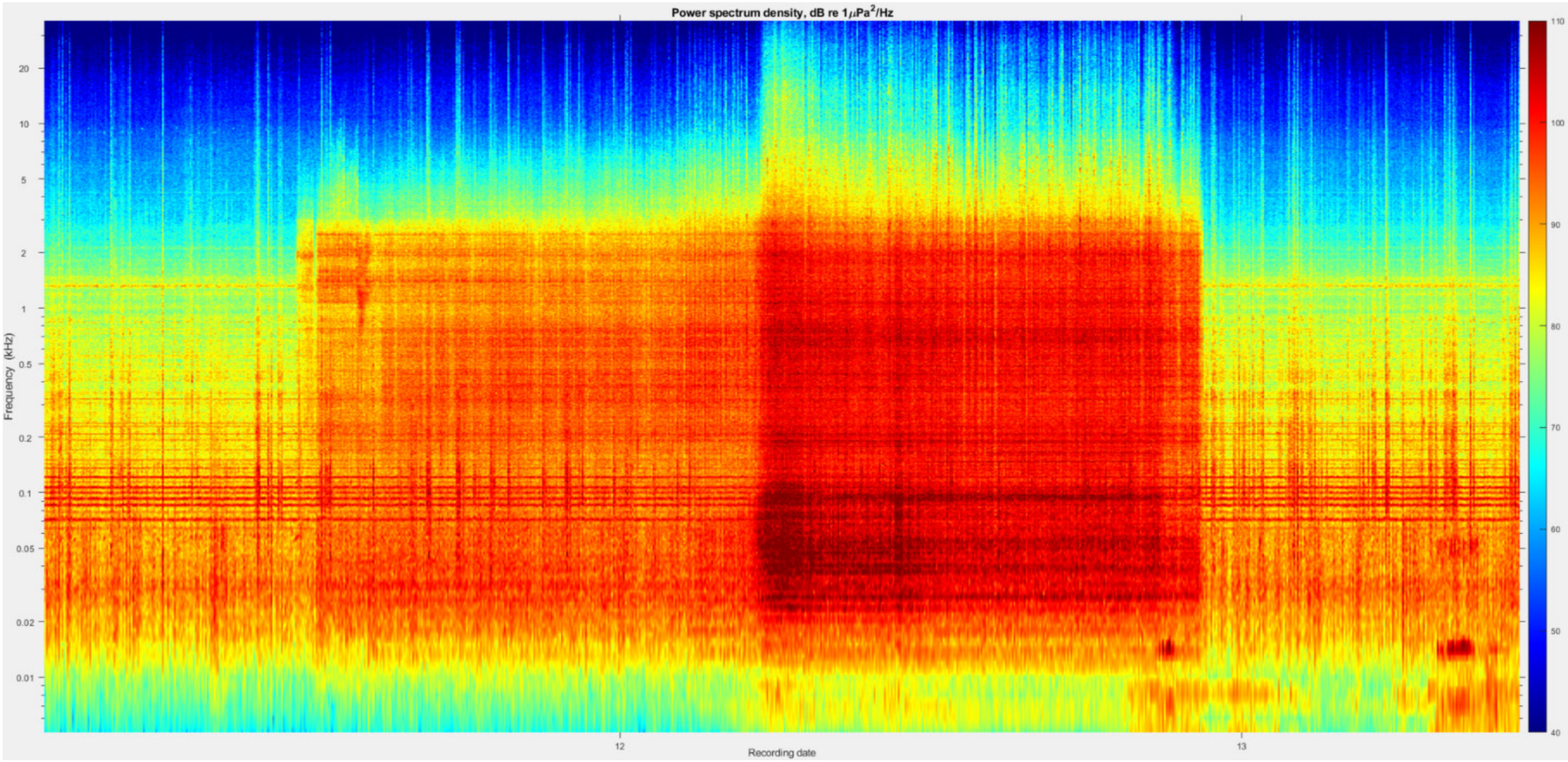

Figure B-110. PSD spectrogram plot of S-4 mechanical cut from April 20, 2021, 11:30 to 12:55 (SoundTrap 5366)

Table B-28. Conductor B-16 Noise Monitoring Results Summary (Secondary Operational Events)

Conductor	Start Time	End Time	Direction	Monitor Station Name	Distance to Conductor (m)	SPL RMS	Max SPL RMS	Min SPL RMS	Peak	SEL
B-16	4/4/2021 9:06	4/4/2021 10:21	North	5362	149.69	112.9	117.9	109.2	139.3	149.5
			North	5363	149.69	114.5	121.0	110.2	148.4	151.1
			East	5366	115.23	112.6	119.1	108.1	146.2	147.8
			South	5365	123.11	112.2	118.5	108.4	145.0	148.7
			West	5356	141.64	113.2	117.9	109.4	141.6	149.8
			South	5353	279.47	110.5	125.9	104.9	149.9	147.1
	4/5/2021 9:06	4/5/2021 10:21	North	5362	149.69	116.0	126.1	110.4	147.2	152.1
			North	5363	149.69	115.2	125.9	110.2	146.0	151.7
			East	5366	115.23	111.1	121.9	106.8	152.4	148.0
			South	5365	123.11	112.9	125.0	108.2	146.1	149.4
			West	5356	141.64	114.4	125.5	109.9	143.5	151.0
			South	5353	279.47	111.9	125.6	105.5	145.1	147.9

L_p and $L_{p,pk}$ = (dB re 1 μPa); L_E = (dB re 1 μPa^2·s)

Figure B-111. Time History Plot of B-16 Secondary Operational Event from April 4, 2021, 9:06 to 10:21 (20-second sample interval)

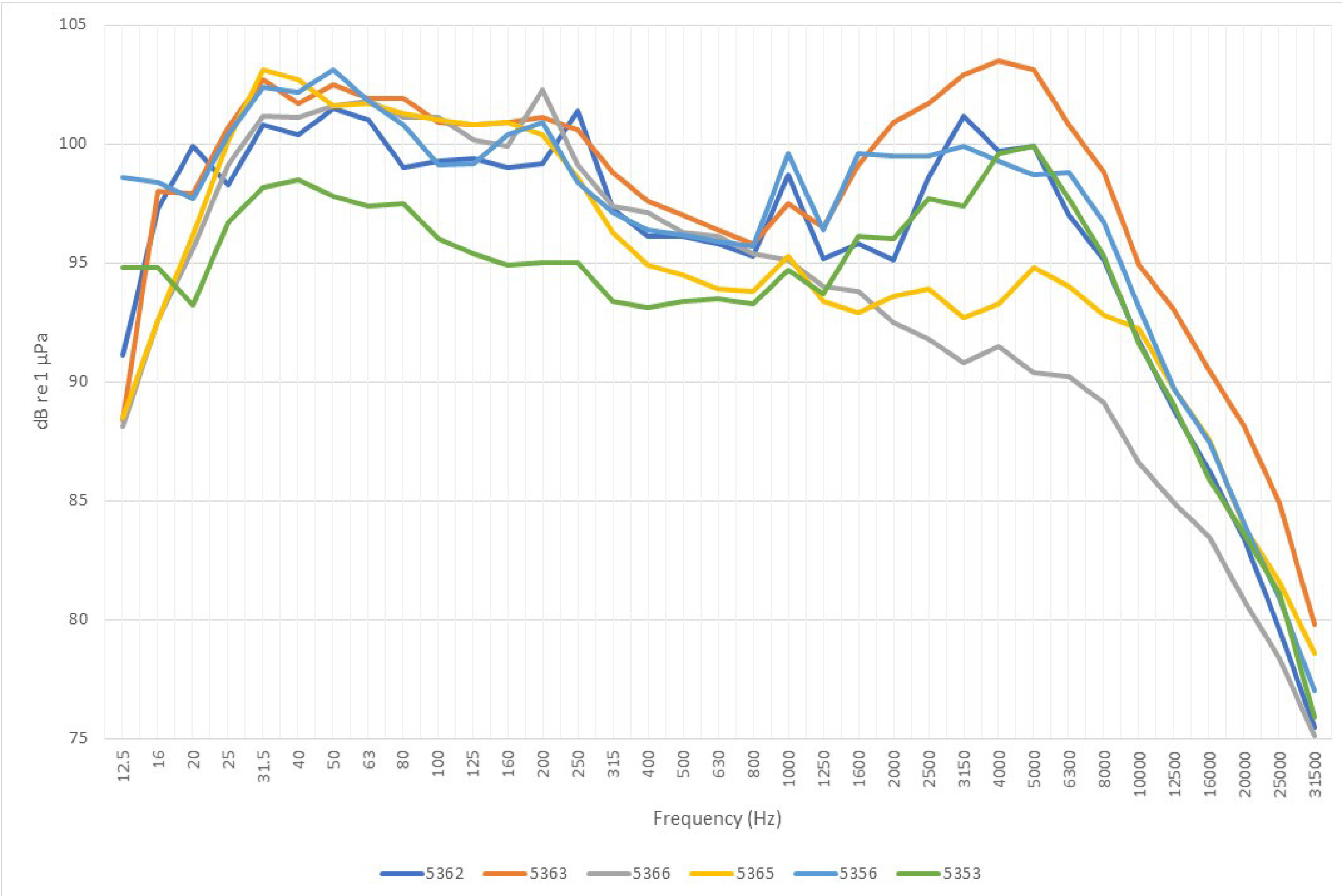

Figure B-112. SPL RMS 1/3 Octave Band Plot of B-16 Secondary Operational Event from April 4, 2021 9:06 to 10:21

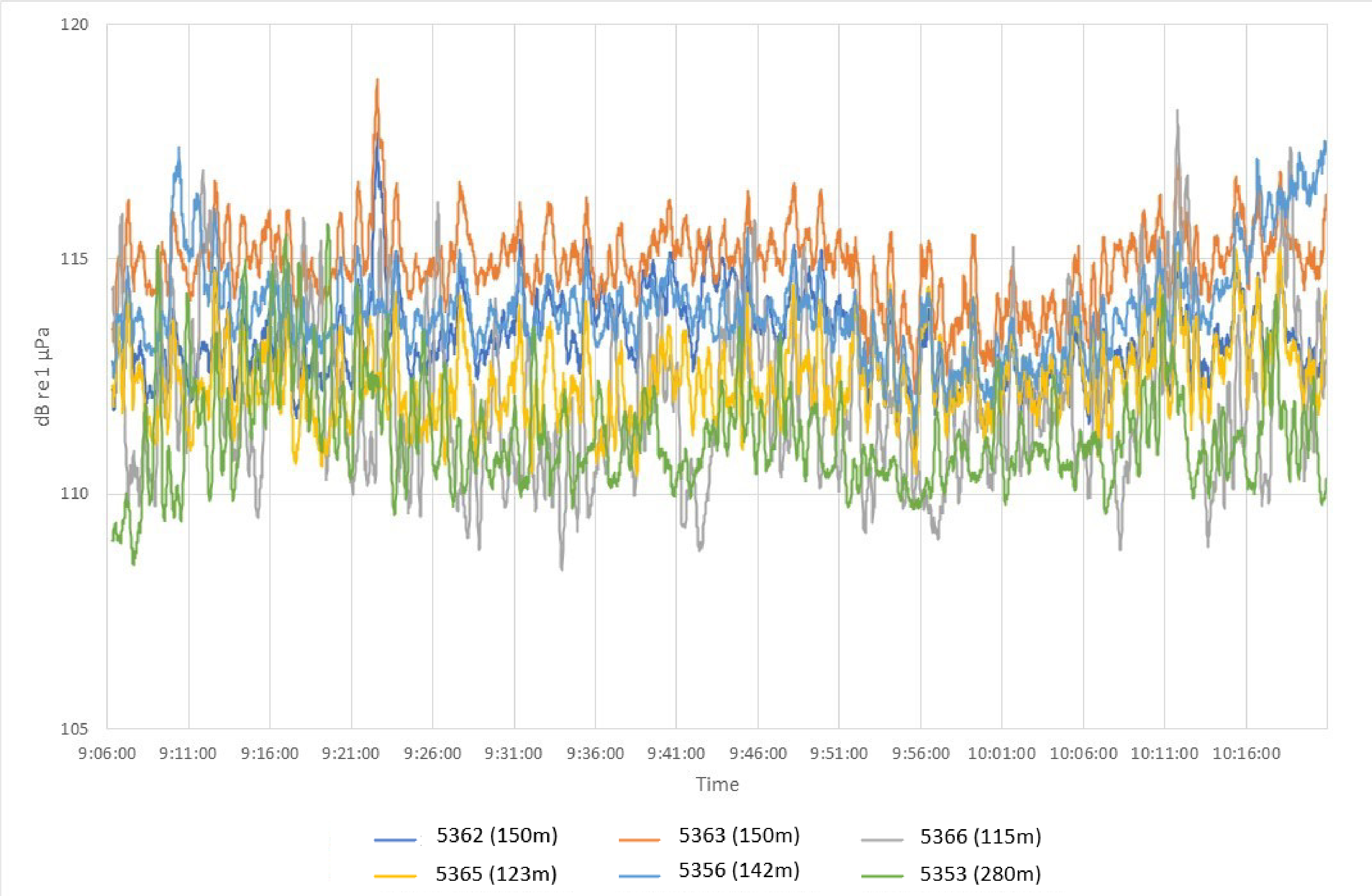

Figure B-113. Time History Plot of B-16 Secondary Operational Event from April 5, 2021, 9:06 to 10:21 (20-second sample interval)

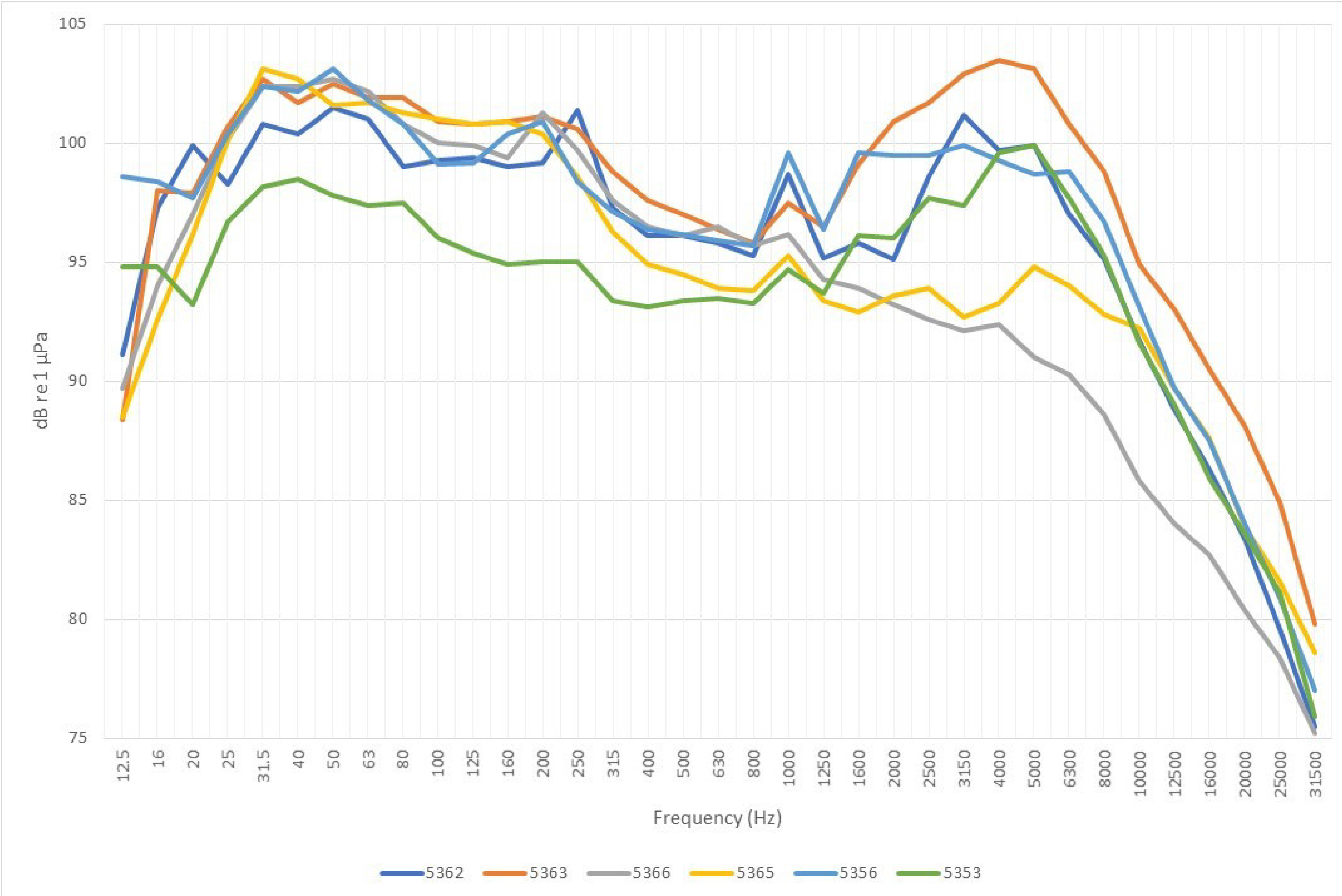

Figure B-114. SPL RMS 1/3 Octave Band Plot of B-16 Secondary Operational Event from April 5, 2021, 9:06 to 10:21

Table B-29. Conductor B-14 Noise Monitoring Results Summary (Secondary Operational Events)

Conductor	Start Time	End Time	Direction	Monitor Station Name	Distance to Conductor (m)	L_p	Max L_p	Min L_p	$L_{p,pk}$	L_E
B-14	4/15/2021 13:06	4/15/2021 14:20	North	5362	143.97	111.5	115.7	108.7	138.4	148
			North	5363	143.97	113.7	118.8	109.4	141	150.2
			East	5366	106.27	110.2	116.4	107.1	146	147.1
			South	5365	133.52	111.0	116.7	108.7	139	147.4
			West	5356	152.65	113.0	122	109.3	140	155.2
			South	5353	291.82	110.2	119.6	105.9	137.9	146.7
	4/15/2021 21:06	4/15/2021 22:21	North	5362	143.97	115.4	122.7	109.9	144.2	153.9
			North	5363	143.97	116.4	124.2	111	147.7	154.8
			East	5366	106.27	119.2	130.4	109.2	156.4	157.6
			South	5365	133.52	115.5	124.1	109.6	143.3	153.9
			West	5356	152.65	115.3	122.1	110.7	143	153.7
			South	5353	291.82	112.4	119.5	107.7	139.5	150.8

L_p and $L_{p.pk}$ = (dB re 1 μPa); L_E = (dB re 1 μPa^2·s)

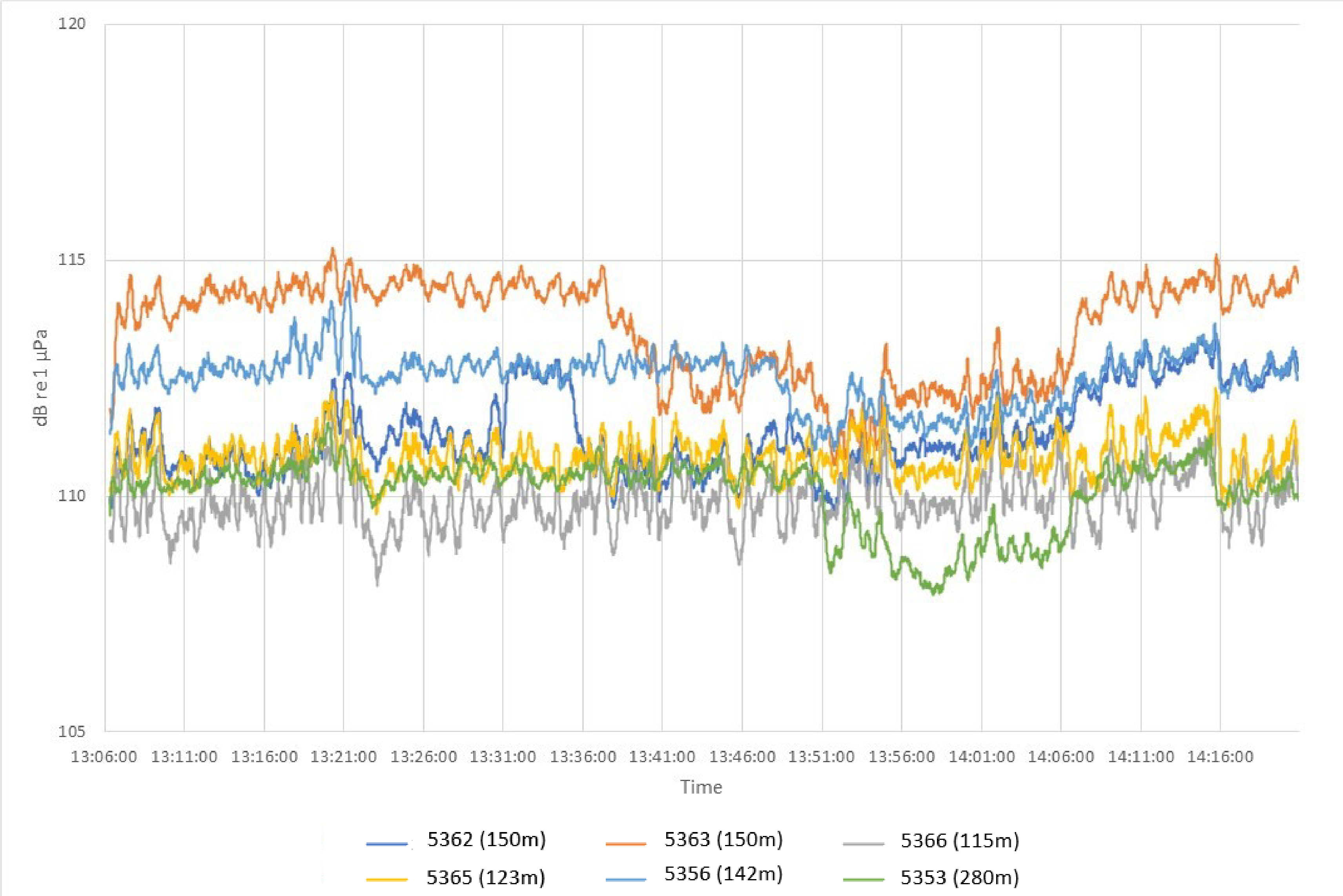

Figure B-115. Time History Plot of B-14 Secondary Operational Event from April 15, 2021, 13:06 to 14:20 (20-second sample interval)

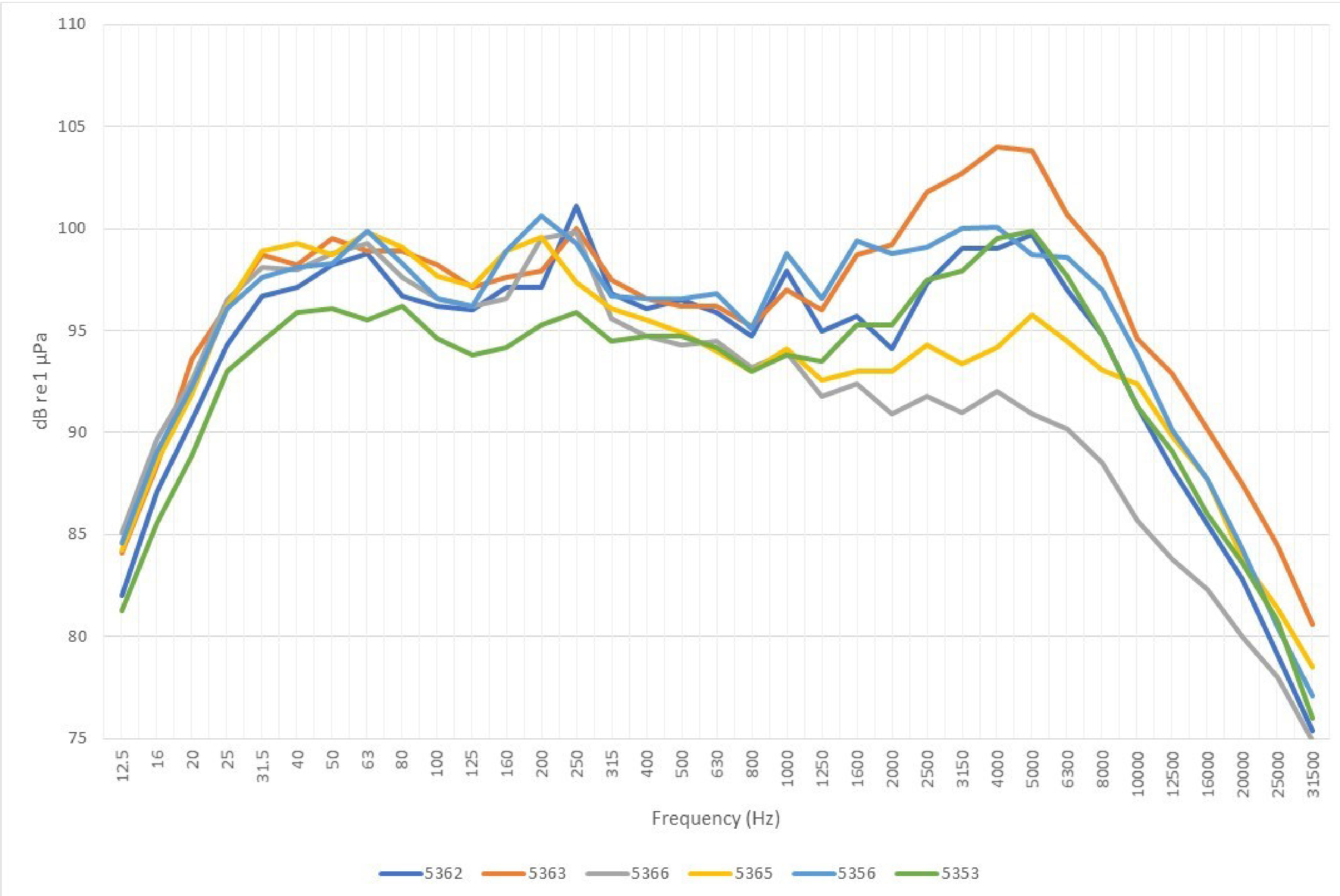

Figure B-116. SPL RMS 1/3 Octave Band Plot of B-14 Secondary Operational Event from April 15, 2021, 13:06 to 14:20

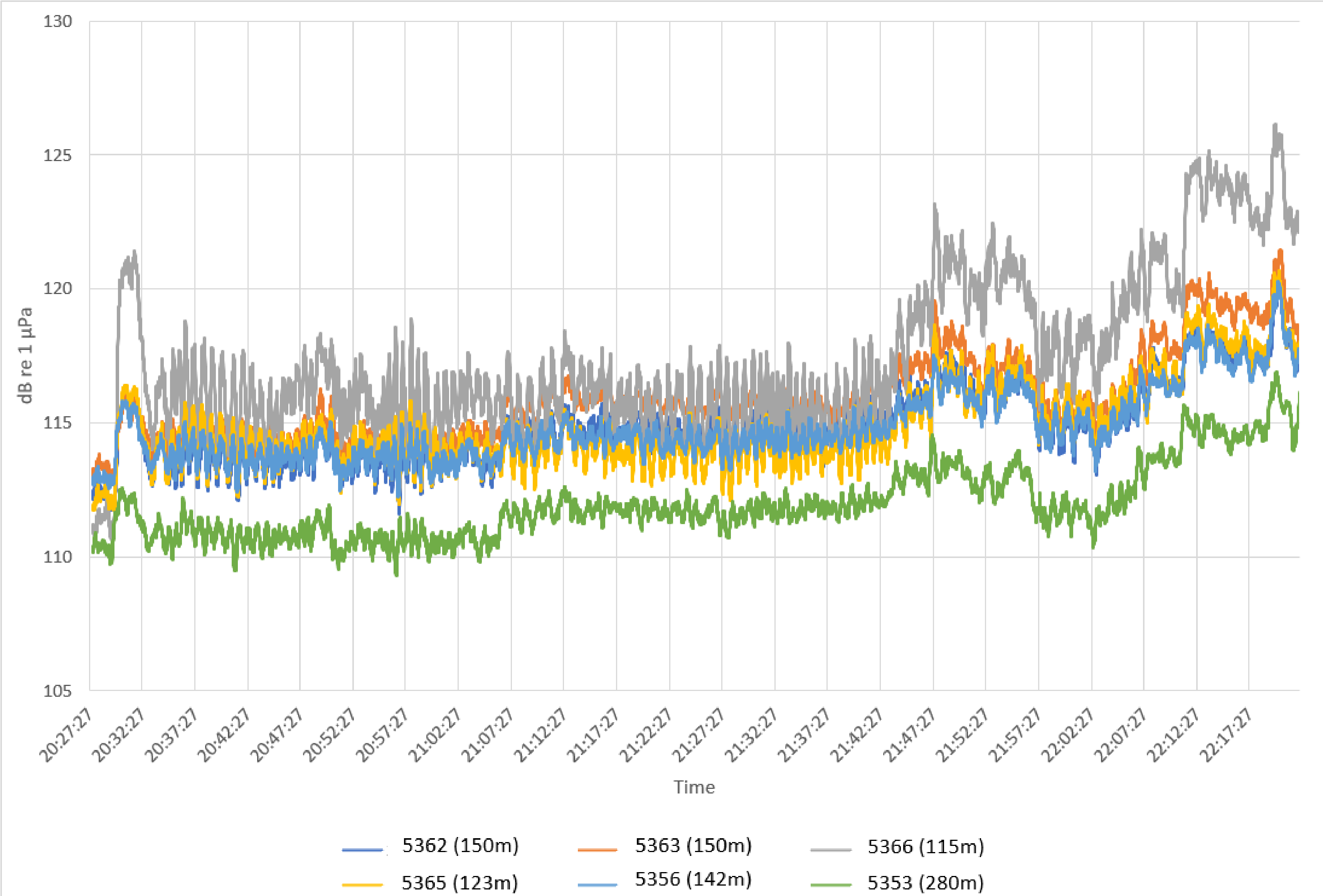

Figure B-117. Time History Plot of B-14 Secondary Operational Event from April 15, 2021, 21:06 to 22:21 (20-second sample interval)

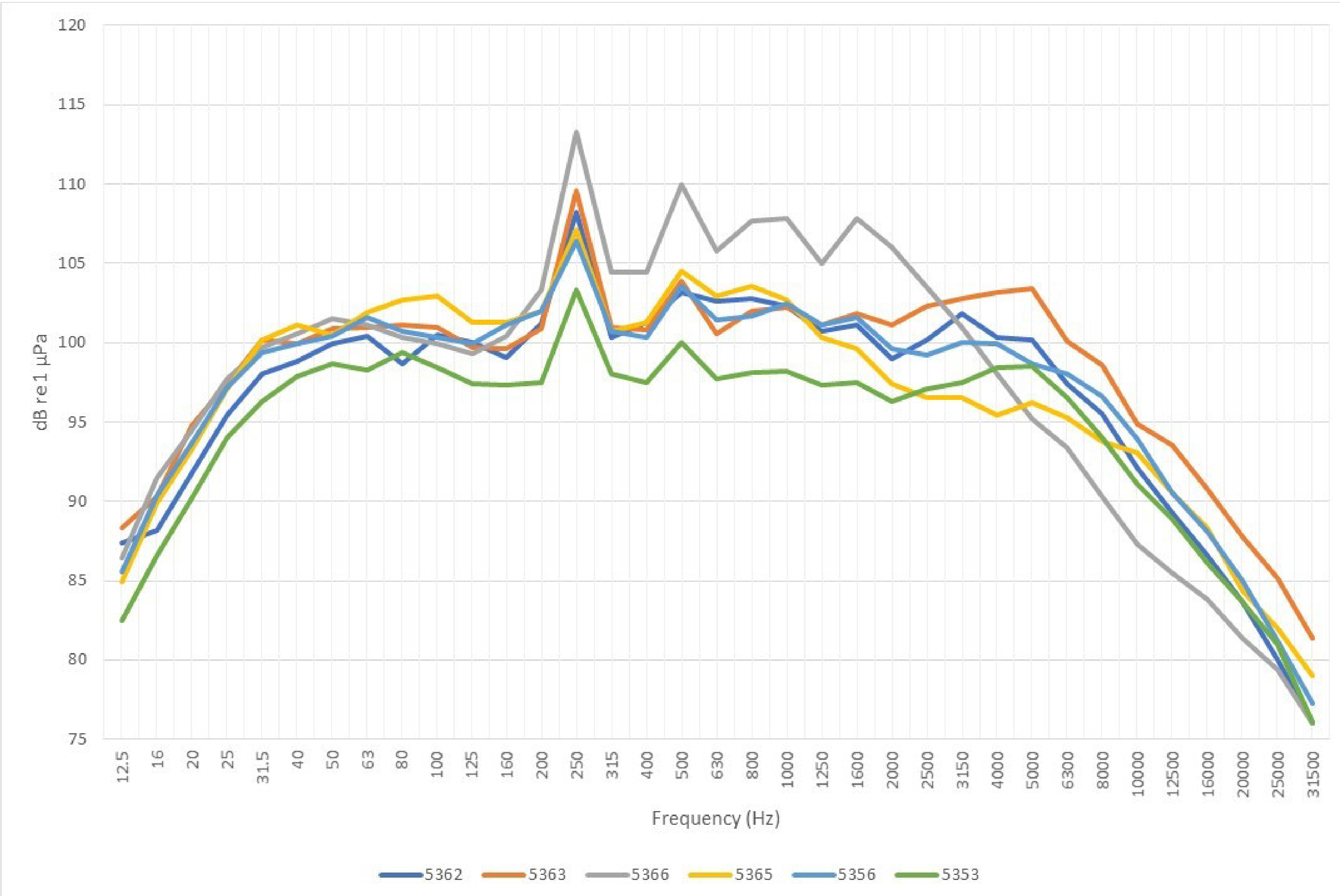

Figure B-118. SPL RMS 1/3 Octave Band Plot of B-14 Secondary Operational Event from April 15, 2021, 21:06 to 22:2

Appendix C: Acoustic Analysis: Study Report A, Determination of Periods of Vocally Active Marine Mammals and Evaluation of Acoustic Indices

Contents

List of Figures

List of Tables

List of Abbreviations and Acronyms

ACI	Acoustic Complexity Index
AMP	Amplitude
BOEM	Bureau of Ocean Energy Management
BI	Bioacoustic Index
BSEE	Bureau of Safety and Environmental Enforcement
dB	decibel
dB 1μPa^{2}s	decibel re 1 micropascal squared
FFT	Fast Fourier Transform
Freeport	Freeport-McMoRan Oil & Gas LLC.
Hz	hertz
kHz	kilohertz
km	kilometers
LTSA	Long-term Spectral Average
m	meters
Mdn	median
MMO	Marine Mammal Observer
NDSI	Normalized Difference Soundscape Index
NOAA	National Oceanic and Atmospheric Administration
nmi	nautical miles
OSA	Ocean Science Analytics

PAM	Passive Acoustic Monitoring
PSD	power spectral density
PSO	Protected Species Observers
PTS	Permanent Threshold Shift
PSD	Power Spectral Density
PST	Pacific Standard Time
QA/QC	Quality Assurance/Quality Control
SEL_{cum}	Cumulative sound exposure
TTS	Temporary Threshold Shift
Tetra Tech	Tetra Tech, Inc.
Study	Characteristics and Contributions of Noise Generated by Mechanical Cutting During Conductor-removal Operations Study
μPa	micropascal
V	Volts
.wav	Raw audio

C.1 Study Summary and Introduction

The Bureau of Ocean Energy Management (BOEM) has identified 23 oil platforms planned for decommissioning within federal waters offshore of southern California. Freeport-McMoRan Oil & Gas LLC (Freeport) submitted Applications for Permits to Modify (30 Code of Federal Regulations Part 250.1704) to remove well conductors and casings on three Point Arguello Unit Platforms (Hidalgo, Harvest, and Hermosa). The Bureau of Safety and Environmental Enforcement (BSEE) and BOEM contracted Tetra Tech, Inc. (Tetra Tech) to characterize noise generated by conductor cutting during conductor removal operations for the Characteristics and Contributions of Noise Generated by Mechanical Cutting During Conductor-removal Operations Study (Study).

A series of passive acoustic recorders were deployed by Tetra Tech to monitor the noise contribution generated by conductor cutting during the process of oil rig decommissioning operations. Specifically, passive acoustic data was collected in proximity to the Hermosa Point Arguello Unit Platform. Ocean Science Analytics (OSA) was responsible for analyzing data from one of the recorders to determine the occurrence of vocalizing marine mammals and evaluate their contribution to the recording site soundscape. The broadband hydrophone data was annotated in a series of three processing runs to streamline the review for all potential marine mammal species. In addition to documenting marine mammal calls and cutting noise acoustic events, we evaluated the utility of three acoustic indices for their potential in rapidly identifying periods of marine mammal sounds and cutting noise.

This analysis is intended to provide information regarding the biological contributions to power spectral density (PSD) and other soundscape metrics. Accounting for the biological contribution to the soundscape provides a more accurate assessment of underwater ambient noise levels and the noise levels produced by conductor cutting processes. Additionally, evaluation of the additional acoustic indices allows for insight into their utilization as a more cost-effective method for use in the future for quickly identifying periods of vocalizing marine mammals, as the practice of using semi-automated annotation is time consuming and expensive. In addition to this report describing details of marine mammal calls recorded during the BOEM Conductor Cutting field effort, Appendix C Attachment C-1 contains an inventory of supplemental analytical products and files. Appendix C Attachment C-2 provides details on the cutting events themselves.

C.1.1 Methods

C.1.1.1 Analysis Methods: Acoustic Events

The following methods were used to detect and annotate marine mammal acoustic events and periods of noise associated with conductor operations occurring during the passive acoustic monitoring (PAM) field component period of the Study.

A. Data Collection

The dataset consisted of continuous broadband passive acoustic data collected at a sampling rate of 72 kilohertz (kHz) for a period of three weeks from 03/31/2021 – 04/22/2021 (~550 hours). One recorder from a series of recorders in close proximity to one another and the platform was analyzed for the occurrence of marine mammal species. This recorder was placed in close proximity to the cutting operation at a depth of approximately 200 meters (m). Additional information regarding the equipment and deployment can be found in the main body of the report. Additional files associated with this analysis are inventoried in Appendix C Attachment C-1 of this report.

B. Marine Mammal Calls

The acoustic dataset was processed using PAMGuard (version 2.01.05; Gillespie et al. 2009) during a two-stage process. PAMGuard is a widely used, open access software program that includes automated and semi-automated modules for the detection and localization of marine mammals. Stage 1 of data processing included using PAMGuard's standard mode and involved automated detection of calls from several marine mammal species using a combination of the click and whistle and moan detectors. Stage 2 involved using PAMGuard's ViewerMode for the post-automation annotation of the automated detections. During annotation, several modules are used to expedite the review of automated detections and parse out true detections from noise (e.g., the click detector, the long-term spectral average; LTSA). Calls attributable to marine mammals that occur within close proximity to each other are then grouped into "acoustic events" according to species or species group (e.g., Delphinid species, fin whale). Additional details of these stages of processing are described below.

To increase efficiency of the Stage 2 annotation process, three analysis iterations were completed to allow the analyst to focus on classifying calls from a subset of possible species/species groups. Separate processing for marine mammal groups allowed for better resolution in detection for all possible vocalizing animals. Figure C-1 below shows a schematic the workflow of acoustic data processing, and indicates which species were the focus of each processing run. The frequency range for each "run" was selected to review for the following acoustic events:

1. **Mid Frequency Run (2 - 36 kHz)**: all odontocetes including sperm whales (*Physeter macrocephalus*) and delphinid species that have overlapping call characteristics. These include e.g., northern right whale dolphin (*Lissodelphis borealis*), Risso's dolphins (*Grampus griseus*), energy from humpback whale (*Megaptera novaeangliae*) calls above 2 kHz, and sources of anthropogenic noise such as conductor cutting and ships.
2. **Low Frequency Run (200 Hertz [Hz] – 2 kHz)**: humpback whales, minke whales (*Balaenoptera acutorostrata*), sei whales (*Balaenoptera borealis*), and fish sounds.
3. **Very Low Frequency Run (10 - 200 Hz)**: fin whales (*Balaenoptera physalus*) and blue whales (*Balaenoptera musculus*).

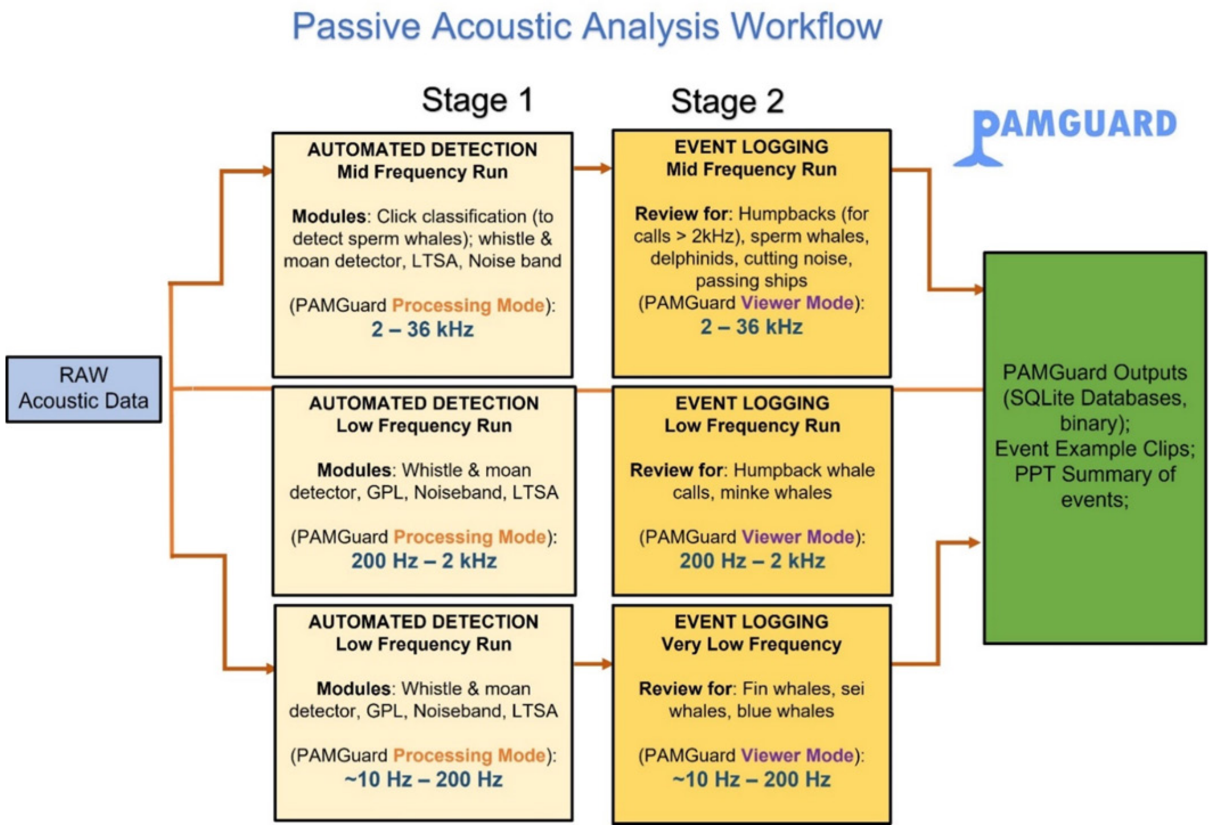

Figure C-1. Workflow diagram for passive acoustic data analysis involving PAMGuard
The raw data collected go through three iterations of processing involving two stages. Each iteration targets a unique set of species based on known call characteristics. "Stage 1" is an automated process, and "Stage 2" involves review of detections and assignment into "acoustic events" that include information on species/species group based on analyst evaluation.

PAMGuard is an ideal software tool for efficient review of large datasets due to the functionality available for automated and semi-automated processing and the ability to customize detection for a wide range of marine mammals (Macaulay et al. 2017; Malinka et al. 2018; Miller et al. 2016). The following PAMGuard tools were used for each stage:

- **Stage 1**: PAMGuard Automated Processing Mode
  Raw audio (.wav) files were organized and processed by week and included sets of custom parameterized detectors for detection of whistles, tonal calls, burst pulses, and echolocation clicks. The inbuilt "Whistle and Moan Detector" was used for all three configuration files, as it is versatile for the detection of all tonal and burst pulsed calls. The native "Click Detector" and parameterized click type classifiers for sperm whales and delphinids was employed in the mid-frequency run. For the low frequency runs, an additional "Generalized Power Law Detector" was utilized to capture calls that may have been missed by the "Whistle and Moan Detector." For all runs, data was collected using the SQLite database and binary storage modules. The SQLite database stores information on the timing and general information for automated and logged detections, while the binary storage (a PAMGuard-specific element) compresses information regarding spectral features and clips. An LTSA module was added to all configuration files to assist with rapid identification of noise and marine mammal vocal activity periods.

- **Stage 2:** PAMGuard Viewer Mode Review and Annotation
  The binary and database files are used in the manual annotation process through PAMGuard Viewer Mode. An experienced data analyst used the 'Detection Group Localiser' to mark the start and end of each acoustic event (defined by a minimum elapsed time between the end of a series of continuous calls and beginning of another, e.g., 30 minutes). The analyst is an essential role to the process in order to differentiate between true positives and false positives (e.g., noise misclassified as calls). This process also resulted in the extraction of high quality, representative calls from each marine mammal acoustic event. Data were summarized in a spreadsheet as well as in a PowerPoint document that provides examples and call density graphs from each event.

The temporal distribution of marine mammal acoustic events was summarized, and data associated with call frequency and parameters were extracted from PAMGuard using PAMpal, an R package developed by Taiki Sakai to extract information from PAMGuard database and binary files (v0.13.0; Sakai 2020).

C. Sound Source Location

The location of vocalizing marine mammals is indeterminable through analysis of a single acoustic recorder as it does not allow for triangulation. Therefore, it was not possible to determine the exact position of vocalizing marine species relative to the platform. However, we can provide general information about the detection distances of the most frequently detected species, which are humpback whales and delphinid species.

> **Humpback whale**: Due to the variable source levels and frequency ranges of humpback whale calls, detection distances are significantly impacted by regional bathymetric characteristics and ambient noise levels. A general detection distance of 10 – 20 kilometers (km) (5.4 – 10.8 nautical miles; nmi) is adopted by most current models, with detection distances of up to 30 km (16.2 nmi) observed in conditions that favor extended sound propagation (Clark and Clapham 2004; Helble et al. 2013).
>
> **Delphinid species:** Delphinids produce a variety of calls including whistles, echolocation clicks, and burst pulses. In a study of detection distances from towed hydrophone arrays in the Pacific Ocean, Rankin et al. (2008) described mean detection distances for delphinids between 1 - 5.5 km (0.5 – 3 nmi). That study reported detection distances varied depending on species and vocalization type and reported that whistles propagate further than echolocation clicks.

D. Anthropogenic Sounds

During the process of detection and annotation of marine mammal acoustic events, anthropogenic noise was also documented. Sources of anthropogenic noise include passing ships, echosounders, platform noise, noise associated with adjacent moorings, and conductor cutting noise. For the purposes of this effort, we only documented conductor cutting, easily distinguishable echosounder pings, and ships that were in close proximity to the recorder. Cutting noise is visible as a block of increased energy that floods more of the lower frequencies (~100 Hz – 8 kHz). Echosounders (from passing ship equipment) are brief pulses detected by the whistle and moan detector, and ship outputs have a distinct shape when approaching and leaving the area where recorders are deployed. Periods of conductor cutting that were clearly visible in the spectrogram were marked by documenting the start and end time. Conductor cutting noise was compared to the provided operations cutting sheet time stamps that documented known periods of cutting and any discrepancies or additional cutting noise above what was reported was noted.

E. Threshold Categories

In 2018, NOAA provided revised guidelines for evaluating the underwater thresholds for the onset of marine mammal permanent threshold shift (PTS) and temporary threshold shift (TTS) now organized by marine mammal hearing group (NOAA Fisheries 2018; Table C-1). PTS results in permanent changes in hearing sensitivity versus TTS which involves acute changes in hearing sensitivity that can recover over time. PTS due to noise exposure has been known to lead to injury and death of marine mammals. The revised 2018 thresholds are used to determine noise levels at which behavioral responses of marine mammals can be observed, in addition to the physical harm to auditory anatomy.

The "low-frequency" cetacean hearing group includes baleen whales such as fin, humpback, sei, and blue whales with a generalized hearing range of 7 Hz to 35 kHz. The "mid-frequency" cetacean hearing group includes odontocetes such as delphinids, sperm whales, and beaked whales with a generalized hearing range of 150 Hz – 160 kHz. The "high-frequency" cetaceans were not a group of concern during this Study based on a pre-defined list of priority species (i.e., they were not expected in the Study acoustic footprint). Conductor cutting falls is considered non-impulsive anthropogenic noise and is evaluated based on the cumulative sound exposure level over a period of 24 hours. Table 1 represents the PTS and TTS received levels associated with each hearing group as given in the NOAA-NMFS technical guidelines (NOAA Fisheries 2018). We incorporated this information in the summary of marine mammal acoustic events for reference.

Table C-1. NOAA-NMFS technical guidelines on decibel (dB) thresholds
These are used to assess anthropogenic noise effects on marine mammals. The new guidance organizes impacts by PTS and TTS by species functional hearing group. Impulsive and non-impulsive sounds for PTS are identified.

Hearing Group	Weighted **TTS onset threshold** (SEL_{cum}*)	**PTS Onset Threshold Impulsive** (Cumulative sound exposure level per 24 hours; $1\mu Pa^2 s$.)	**PTS Onset Threshold Non-Impulsive** (Cumulative sound exposure level per 24 hours; $1\mu Pa^2 s$.)
Low-Frequency Cetaceans	179 dB	183 dB	199 dB
High-Frequency Cetaceans	178 dB	185 dB	198 dB

* SELcum = the cumulative energy from multiple noise events, measured in dB 1μPa

For each marine mammal acoustic event, we included the appropriate PTS or TTS threshold limit in the "AcousticEvents_AllRuns.xlsx" summary file (location of file available from **Appendix C Attachment C-1** of this report).

F. Call Frequency Parameters in Response to Noise

One initial objective of this Study involved evaluating marine mammal behavioral responses to noise, which originally involved collecting data before and after the conductor cutting operations. A change in the deployment schedule resulted a reduction in this data collection to only include the period with conductor cutting. Due to the periodic nature of the conductor cutting periods, we explored the possibility of evaluating marine mammal vocalizations immediately preceding, during, and immediately following cutting events. PAMGuard calculates the received level call amplitude of marine mammals, which is not ideal for assessing vocal behavioral response, and is influenced by animal movement and masked by overlapping anthropogenic noise. However, changes in frequency parameters to compensate for increasing background noise has been documented (Papale et al. 2015).

The frequency parameters of tonal calls as used by Papale et al. include measurements of the minimum, maximum, beginning, and end frequencies. These values are independent of amplitude and can be easily observed if a high signal to noise ratio of calls exists. We first identified conductor cutting noise periods that overlapped with the annotated marine mammal acoustic events. We then reviewed each appropriate period to determine if signal to noise ratio and the occurrence of calls within an acoustic event were sufficient for the analysis. Identified calls could then be measured manually to obtain better resolution in the frequency parameters than were determined in autodetection. These data would then be compared to values of third octave band sound pressure levels (SPLs) to evaluate changes in the spectral characteristics. Finally, we determined that the humpback whale dataset was best for this analysis due to the large number of acoustic events in the dataset.

C.1.1.2 Analysis Methods: Acoustic Indices

A. Background

Soundscape ecology, or the study of acoustic relationships between organisms and their environment, is increasingly used as a tool for evaluating biodiversity and for monitoring environments (Merchant et al. 2015; Pijanowski et al. 2011; Risch and Parks 2017; Sueur et al. 2014). Pijanowski et al. (2011) described the theory of soundscape ecology and the ability to compute indices for use in both quantifying biodiversity and assessing the pervasiveness of anthropogenic noise. His description included characterization of sounds produced by biological organisms (biophony), geological activity (geophony), and anthropogenic sources of sound (anthrophony). This emerging field of environmental monitoring was initially established within terrestrial environments, but in recent years has been evaluated for the applicability of assessing marine environments (Bertucci et al. 2016; Bohnenstiehl et al. 2018; Erbe et al. 2015; Haver et al. 2018; Parks et al. 2014). Lindseth and Lobel (2018) described metrics best suited for underwater environments and noted the standard use of Power Spectral Density (PSD) to measure overall spectral energy of an environment, but also proposed use of additional methods for evaluating the spectral energy attributable to biological sources.

The PSD index is discussed in the main body of this report. This Appendix addresses three of the more recently developed indices: the Acoustic Complexity Index (ACI), the Bioacoustic Index (BI), and the Normalized Difference Soundscape Index (NDSI). A description of how those indices is evaluated is also provided.

ACI

Recent marine-based studies have repeatedly reported that ACI, which is a direct quantification of the intensity of sounds likely to be attributable to biological sound sources, is a promising biodiversity metric (Bolgan et al. 2018; Davies et al. 2020; Pieretti et al. 2017). For example, Pieretti et al. (2017) found there to be noise associated with higher PSD levels and lower ACI levels and documented higher values in ACI at night corresponding to increased fish vocal activity. These novel studies indicate a link to changes in the biological assemblages within their respective study areas but offer caution when interpreting results and suggest ACI is specific to the particular environment. When these metrics are validated through comparison to periods of documented vocal activity, better interpretation of the metrics is possible (Haver et al. 2018). As a means of an indirect measure, the ACI may represent a quantitatively efficient and biologically meaningful indicator of the biodiversity of marine mammals found within an ecosystem.

BI and NDSI

In addition to ACI, the BI and NDSI measurements are long-standing metrics used in terrestrial acoustic monitoring but are less prevalent in marine-based studies. The BI was originally developed by Boelman et al. (2007) to determine avian abundance and corresponds well with measures of avian diversity. Another worthy candidate of underwater evaluation is the NDSI, which provides an estimate of anthropogenic disturbance by finding the ratio of an anthrophony frequency band to a biophony frequency band (Boelman et al. 2007; Kasten et al. 2012). The NDSI index relies on the consistent nature of anthropogenic noise in separate frequency bands from biophony.

Collectively, these three indices provide a unique set of measurements to evaluate in this application. Review of passive acoustic data for periods of vocalizing marine mammals is a time intensive process. While automated detection can streamline the process, most methods still require a human operator to validate at least some detections. Additionally, machine learning methods of processing are often only useful for specific calls or species, which limits their use when a Study requires that all marine mammals be documented. Sound ecology metrics (i.e., PSD, ACI, BI, and NDSI) can be quickly quantified from a large dataset using various analytical software. Depending on performance with a specific dataset and environment, use of these metrics can be a viable means of determining periods of biological activity, thus providing an efficient means of quickly reviewing the data. For these reasons, our analyses included incorporation of these indices.

B. Description of Acoustic Indices Calculation Methods

The ACI is an algorithm developed by Farina (2019) to provide a fast and direct quantification of biological sounds based on intensity. It calculates the differences in amplitude in adjacent time samples in each frequency bin, then adds together the difference, thus representing a measure of complexity of the acoustic environment. The concept behind this metric is that biological sounds are more variable with respect to intensity than anthropogenic sounds, and several studies have demonstrated ACI use for evaluating species diversity (Davies et al. 2020; Pieretti et al. 2017).

The BI is a straightforward measurement which calculates the area under the mean frequency spectrum minus the value of the lowest bin (Boelman et al. 2017). This index considers the entirety of the raw audio file and does not partition the measurement into smaller duration segments.

The NDSI operates on the assumption that anthropogenic noise is found in a band below that of the biophony and calculates the ratio of those separate bands (biophony – anthrophony) – (biophony + anthrophony). A limitation to this calculation is that underwater biological sounds can frequently occupy the same acoustic space as anthropogenic noise sources. However, with persistent anthrophony as is known to occur during this Study, it is possible to define the frequency band of noise and differentiate it from calls outside of that band (specifically any call that falls above 8 kHz).

C. Acoustic Indices Study Specific Calculation Methods

Calculations of ACI, BI, and NDSI were made for five-minute duration files for the entirety of the available data. Once the analysis was completed, those variables were merged with output of the PAMGuard acoustic event review. Acoustic event-based information on the species identification, the frequency of calls (number of calls per audio file, per species), and select additional parameters were extracted. Select parameters calculated from the “contours” (which are the detections made by the whistle and moan detector) included the mean call amplitude, the mean minimum and maximum frequencies of the call, and information on the start time of the first call for each five-minute period. We elected to only use contour information, as the echolocation clicks detected during this process were mostly overlapping with noise and thus were less meaningful for measurements. We only evaluated two species: humpback whales and delphinids, as they were most frequently encountered in the data.

Acoustic Indices measurements and statistical analysis were done using R 4.0.5 (R Core Team 2021). Measurements of ACI, BI, and NDSI were calculated from five-minute duration raw audio .wav files using the ‘sound ecology’ package (v1.3.3; Villanueva-Rivera and Pijanowski 2018). This information was merged with measurements of call frequency and select parameters from marine mammal acoustic events extracted using the package 'PAMpal' (v0.13.0; Sakai 2020). All statistical analysis was performed using the native stats package in R (v3.6.2).

Statistical tests were performed to determine the relationship between the marine mammal acoustic events, cutting noise, and the three acoustic indices. We performed a Kruskal Wallis test to look for statistical differences across humpback whales, delphinids, and periods without calling animals. However, a statistically significant result only evaluates the probability of obtaining the sample outcome by chance and does not indicate how big the difference is. We calculated effect size to provide information on the relevance of the significance, in order to provide a practical interpretation of p-values. An eta squared effect size was calculated for all Kruskal Wallis tests to determine the magnitude of any statistically significant differences. We performed a Mann-Whitney U Test to look for significant differences in the acoustic indices associated with periods with and without cutting. We used the Cohen's D effect size to determine the magnitude of this difference for Mann-Whitney U tests. Finally, we looked for correlations between the acoustic indices and the extracted call parameters using a Spearman's Correlation.

D. Acoustic Deliverables

All outputs of the review are accessible via the deliverable hard drive. An inventory of analytical products is available and folder/file descriptions is available in Appendix C Attachment C-1.

C.1.2 Analysis Methods: Data Management

Configuration files were developed and tested with the data prior to processing. All PAMGuard derived acoustic events were reviewed by a second experienced analyst to provide quality assurance in event determination and to confirm species or species group identification. During the process of acoustic analysis, several steps were taken to properly organize and run the data in addition to the methods mentioned in PAMGuard processing above. They include:

1. Settings for the SoundTrap recorder calibration were used to enter the hydrophone sensitivity for the data as in the figure below. The recommended peak-to-peak voltage range of 2 Volts (V) for SoundTrap recorders was also included in the settings.
2. The recorder was set to Central Standard Time when deployed. In order to adjust for this +2-hour offset, the file times were adjusted in PAMGuard when loading audio files. This was done to ensure that the data corresponded accurately to periods of cutting noise. All acoustic event times are in local time (Pacific Standard Time; PST).
3. Noise often overlapped with marine mammal calls. By filtering noise occurring in the frequency bands below representative calls, we were able to increase the auditory clarity in some calls. Example clips for delphinids were filtered when possible to reduce noise if it improved audio for representative files. All humpback whale calls overlapped noise so filtering representative calls was not possible. This was only done for the example clips and filtering of raw audio was not performed when processing data. Any filtering used in PAMGuard processing was specific to detection and did not influence the raw audio input.
4. We define an acoustic "event" as a species (or species specific) vocalizing marine mammal where the period of vocalization can be defined. The end of the vocal period is determined when the elapsed time between the last call of an event and the start of another spans a period of 30 minutes for delphinids and 60 minutes for baleen whales and sperm whales. Noise events are visually determined as described below.
5. Delphinids are difficult species to classify (particularly when the full bandwidth of their calls is not available), so we grouped all tonal whistles, burst pulses, and echolocation clicks with energy starting ~20 kHz as "Delphinid species"

6. We did not assign an acoustic event to a detection if the calls exhibited the following:
    a. Insufficient number of calls (<5).
    b. Low quality as determined by experienced acousticians; and
    c. If calls amplitude exhibited too low of a signal to noise ratio given the recorded soundscape.
7. Detections and data outputs underwent Quality Assurance/Quality Control (QA/QC) to mitigate unintentional sources of error.

C.2 Results

C.2.1 Marine Mammal Acoustic Detection Event Summary

Marine mammals were acoustically detected throughout the three-week monitoring deployment. A summary of the acoustic events by species or species group is described in **Table C-2**. Within these data, humpback whales occurred most frequently in over half of the total deployment duration, followed by delphinid species. Sperm whales were only encountered intermittently during three events, and the intermittent nature of clicks suggest they were distant animals. The infrequency with which sperm whale clicks were detected and recorded is expected due to the shallow depth of the recorders. The 'Unidentified Low frequency Sounds' listed in TableC-2 could not be identified as a specific species or species group. Abundant noise in the low frequencies primarily contributed to this, but also because the sounds could be attributable to one of several species. The single unidentified odontocete event was labeled as such because we could not confirm it was attributable to a delphinid.

Table C-2. Summary of acoustic events by species
This table includes cumulative event duration across all events for each species or species group.

Species/Species Groups	Number of Events	Cumulative Event Duration (Hour: Minute)
Delphinid Species	40	76:05
Humpback Whale	40	295:14
Sperm Whale	3	2:38
Unidentified Low Frequency Sounds	5	9:52
Unidentified Odontocete	1	1:05

Humpback whales and delphinid species were encountered often during the monitoring period. These calls were discernable despite the noisy shallow environment of the recorder mooring. Humpback whale calls only occurred in lower frequencies (between 200 Hz and 2 kHz) and were audibly discernible. **Figure C-2** provides an example of typical calls encountered.

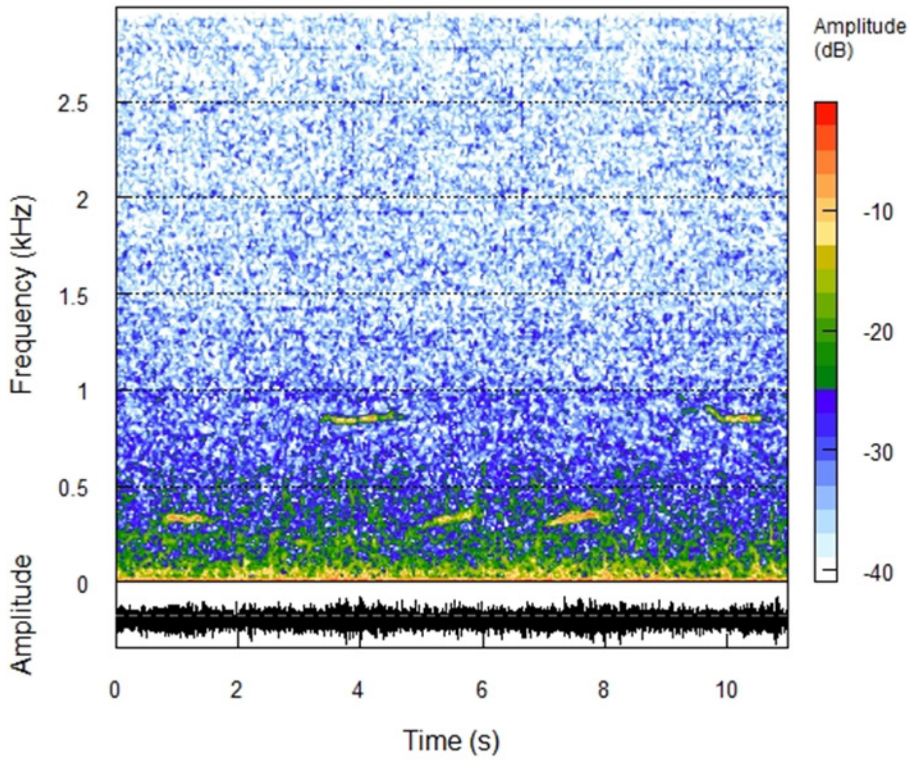

Figure C-2. Waveform and spectrogram of tonal calls from a humpback whale
Original sampling rate of 72 kHz down sampled to 6 kHz for spectrogram image; 512 Fast Fourier Transform (FFT) size, 75% overlap; Hamming window function.

Delphinids encountered during this monitoring period often produced echolocation clicks and burst pulsed calls. The burst pulse calls were easily detected above the upper range of the anthropogenic noise. An example of the commonly encountered burst pulsed calls is provided in **Figure C-3**.

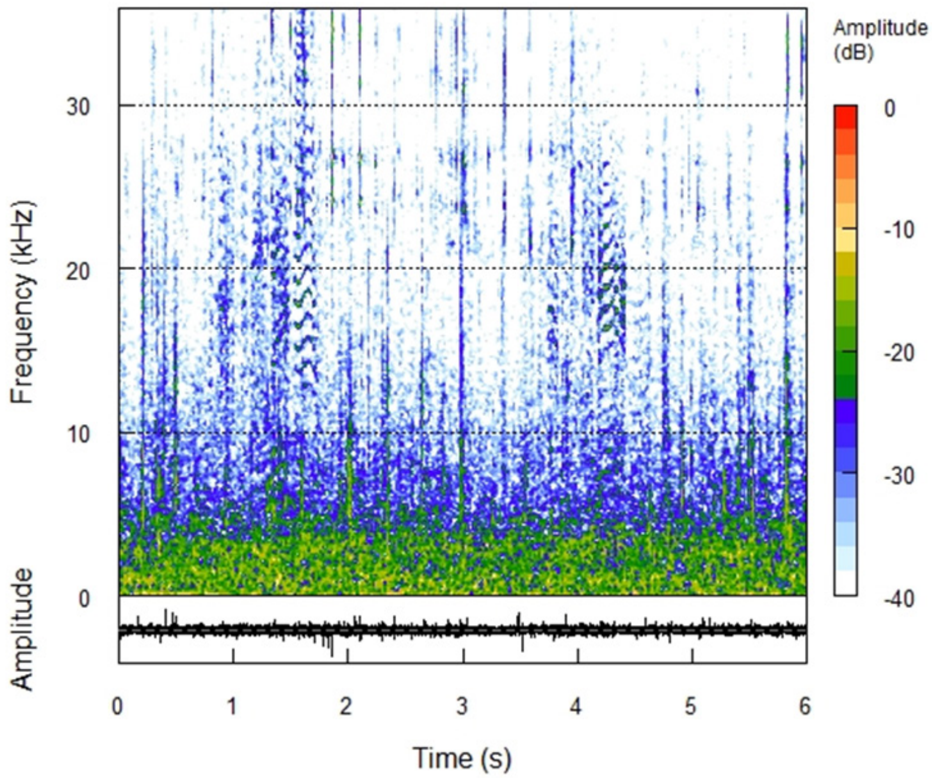

Figure C-3. Waveform and spectrogram of tonal calls from a delphinid species event (no species identification possible)
Represented here are burst pulsed calls frequently encountered. Sampling rate of 72 kHz; 512 FFT size, 75% overlap; Hamming window function.

Marine mammal acoustic events were distributed throughout the three-week period. The temporal distribution of marine mammal acoustic events often overlapped that of anthropogenic noise, which includes the category used to describe cutting noise. Occurrence of marine mammal acoustic events per day and periods of cutting noise (denoted as “Anthropogenic Noise”) during the field deployment are indicated in **Figure C-4**.

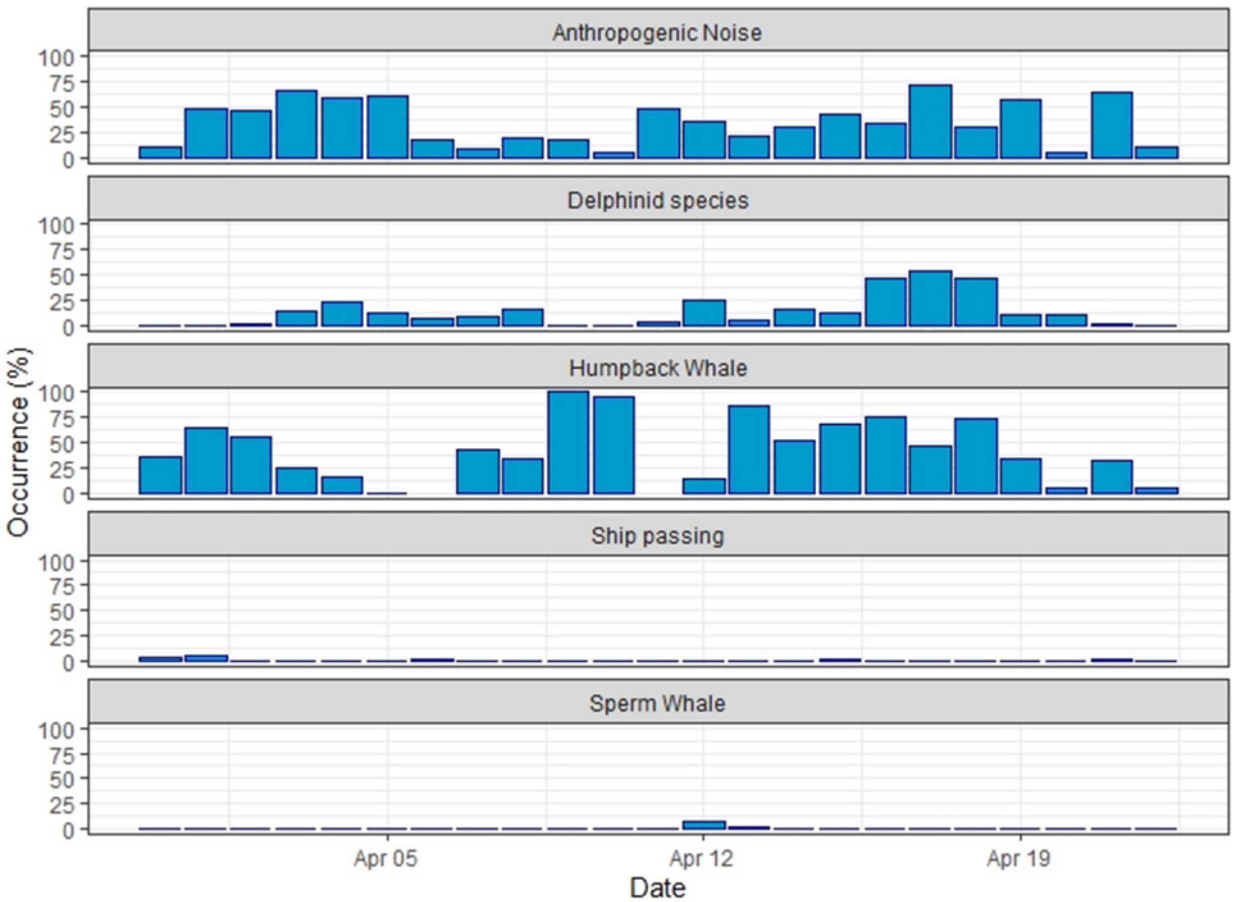

Figure C-4. Percent occurrence per day for all acoustic events by species or sound type
Data are derived from start and end time of event, and do not include details of call density. This period includes the entire deployment from 03/31/2021 – 04/22/2021. Anthropogenic noise refers to conductor cutting periods.

Supplemental Files:

- The "**AcousticEvents_AllRuns.xlsx**" provides an excel summary of all acoustic events detected during our review, including sources of anthropogenic noise.
- The "**BOEM_TT_Acoustic_Events_2021.ppt**" provides a power point summary of the duration, density of calls, and an example audio clip for all marine mammal acoustic events.
- "**Cutting_Times_Comparison.xlsx**: Comparison of PAMGuard logged noise events to cutting periods.

Additional files related to marine mammal acoustic events including PAMGuard binary files and databases can be found in **Appendix C-1**.

C.2.2 Anthropogenic Noise Events

During the process of this review, we documented the component of anthropogenic noise contributed by conductor cutting periods which were easily identified through review of the LTSA or Spectrogram modules. We also noted other sources of anthropogenic noise. In general, sources of anthropogenic noise (i.e., cutting periods) dominated the 0-~12 kHz bandwidth of data, due to close proximity of the shallow recorder (>200 m) to the platform. The persistent sources of noise (e.g., cutting periods, ship traffic to and from the platform, etc.) periodically masked the marine mammal signals of interest, which reduced the ability to detect calls with a lower signal to noise ratio. However, PAMGuard's detectors perform well in noisy environments and detection of marine mammal calls of sufficient amplitude that overlap with the various sources of anthropogenic noise was still possible and only calls audible above the anthropogenic noise level were selected for events. Table C-3 provides a summary of the duration of anthropogenic noise events encountered during this analysis and compares them to species acoustic events.

Table C-3. Summary of anthropogenic noise source detections by number of events and duration

Type of Noise	Number of Events	Cumulative Event Duration (Hour: Minute)
Anthropogenic Noise (cutting & presumed cutting noise)	79	223:00
Echosounder	5	00:40
Ship passing	12	4:43

Cutting noise occurred throughout the monitoring period and was able to be visibly detected using the LTSA module in PAMGuard. Start and end times of these cutting events were easily discernible and were compared to the list of cutting events in **Appendix C Attachment C-2,** provided by Freeport. Out of a total of 79 cutting events identified in the PAMGuard review process, 45 matched the periods of time where cutting operations were documented by Freeport. There were 34 periods of conductor cutting that did not align with the documented conductor cutting sheet. **Figure C-5** is an example of an LTSA from a noise event that matches a documented cutting event, whereas **Figure C-6** represents an acoustic event that does not match a documented cutting period. The operations cutting sheet used in this comparison is labeled "Hermosa Mechanical Cutting Times."

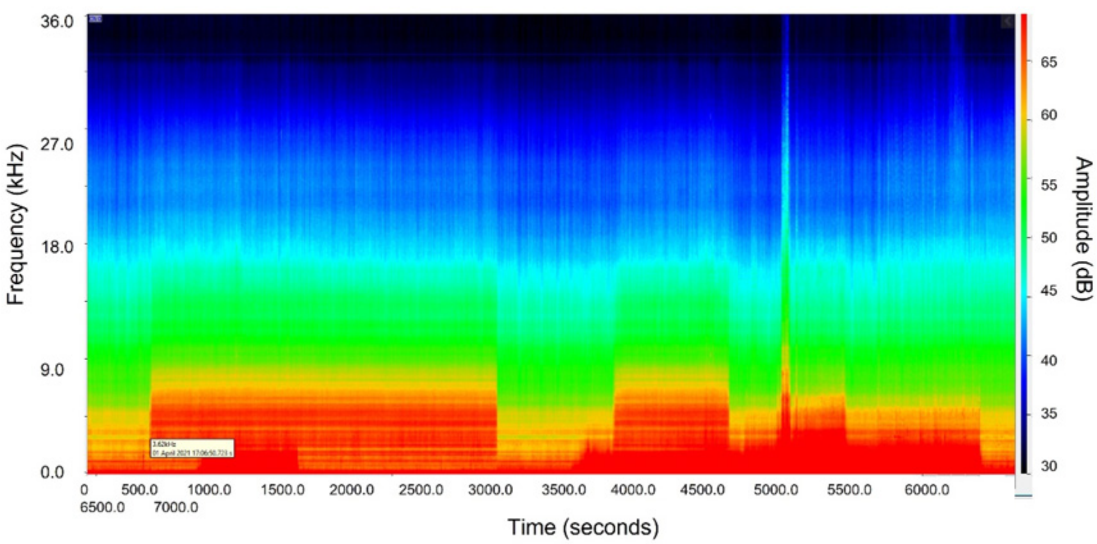

Figure C-5. Example of a cutting event as represented in a LTSA figure
This is acoustic event (UID22, from Week 1 MF) which corresponds to the B-1 identifier on the operations cutting sheet.

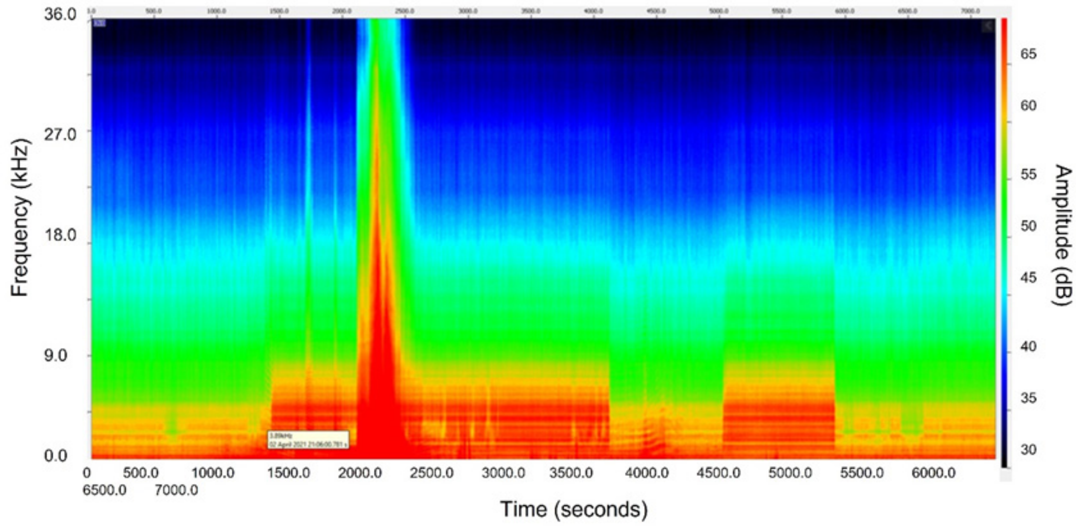

Figure C-6. Example of a 90-minute presumed cutting event
This image is from the LTSA module that was not found to match an entry on the operations cutting sheet (UID 32 from Week 1 MF).

C.2.3 Call Frequency Parameters in Response to Noise

As mentioned in Methods, our first step to assessing the call frequency parameter response to noise analysis was to determine which of the two prevalent species, delphinids or humpback whales, were more appropriate to evaluate. Due to the numerous humpback whale acoustic events in the dataset, we selected this species for the analysis. We identified five conductor cutting instances that overlapped temporally with humpback whale acoustic events. A second layer of reviewing the data involved determining if there was a sufficient sample size of humpback whale calls that fell within the period immediately preceding, during, and immediately following each conductor cutting instance. Finally, we evaluated the signal to noise ratio of the humpback whale calls to the conductor cutting noise, as a final determinate of suitability for this analysis. Due to a combination of an insufficient number of calls in all before/during/after time blocks associated with three of the five overlapping cutting events, in addition to the low signal to noise ratio of humpback whales for one cutting event, we did not have the necessary sample size to conduct this analysis. Similarly, this was also the case for the delphinid acoustic events which had an even smaller overlap of detectable calls with cutting events.

C.2.4 Acoustic Indices

The results of the acoustic indices analysis are organized into three categories that compare the measurements to marine mammal calls and cutting periods. We only evaluated the data corresponding the delphinid species and humpback whales, as these had a sufficient sample size to evaluate indices. In the field, each .wav files was 30 minutes in duration, and prior to this analysis the files were parsed into shorter, 5-minute files. The ACI, BI, and NDSI calculations were successfully calculated for all of the 5-minute .wav files spanning the period of 4/1/2021 – 4/20/2021. The smaller file size allowed for faster calculation of these values, and the processing was completed after approximately 16 hours of automated processing.

C.2.4.1 Indices and Marine Mammal Sounds

The distribution of acoustic indices values calculated during periods with and without marine mammal vocalizations are indicated in Figure C-7. All indices were non-parametric, so we performed a Kruskal Wallis Test to look for differences between the values calculated for periods with delphinids, periods with humpback whales, and periods without vocalizing marine mammals. We found statistically significant differences for ACI ($H(2) = 82.29$, $p < 0.001$), BI ($H(2) = 32.41$, $p<0.001$), and NDSI ($H(2) = 96.06$, $p<0.001$), however, the effect size for this difference is trivial for ACI ($\eta 2 = 0.015$), BI ($\eta 2 = 0.006$), and NDSI ($\eta 2 = 0.018$). Post hoc comparisons using a Dunn's test for ACI values showed significant differences both between delphinids and no vocalizations ($p < 0.001$), and humpback whales and no vocalizations ($p < 0.001$), and there was no significant difference between values with delphinids and humpback whales ($p = 0.475$). Post hoc comparisons for the BI values reflected the same differences as ACI. For the NDSI variable, the post hoc comparisons indicate a significant difference between values with delphinids versus humpbacks ($p < 0.001$) and humpback whales and no vocalizations ($p < 0.001$) but no difference between periods with delphinids and no vocalizations ($p = 0.207$).

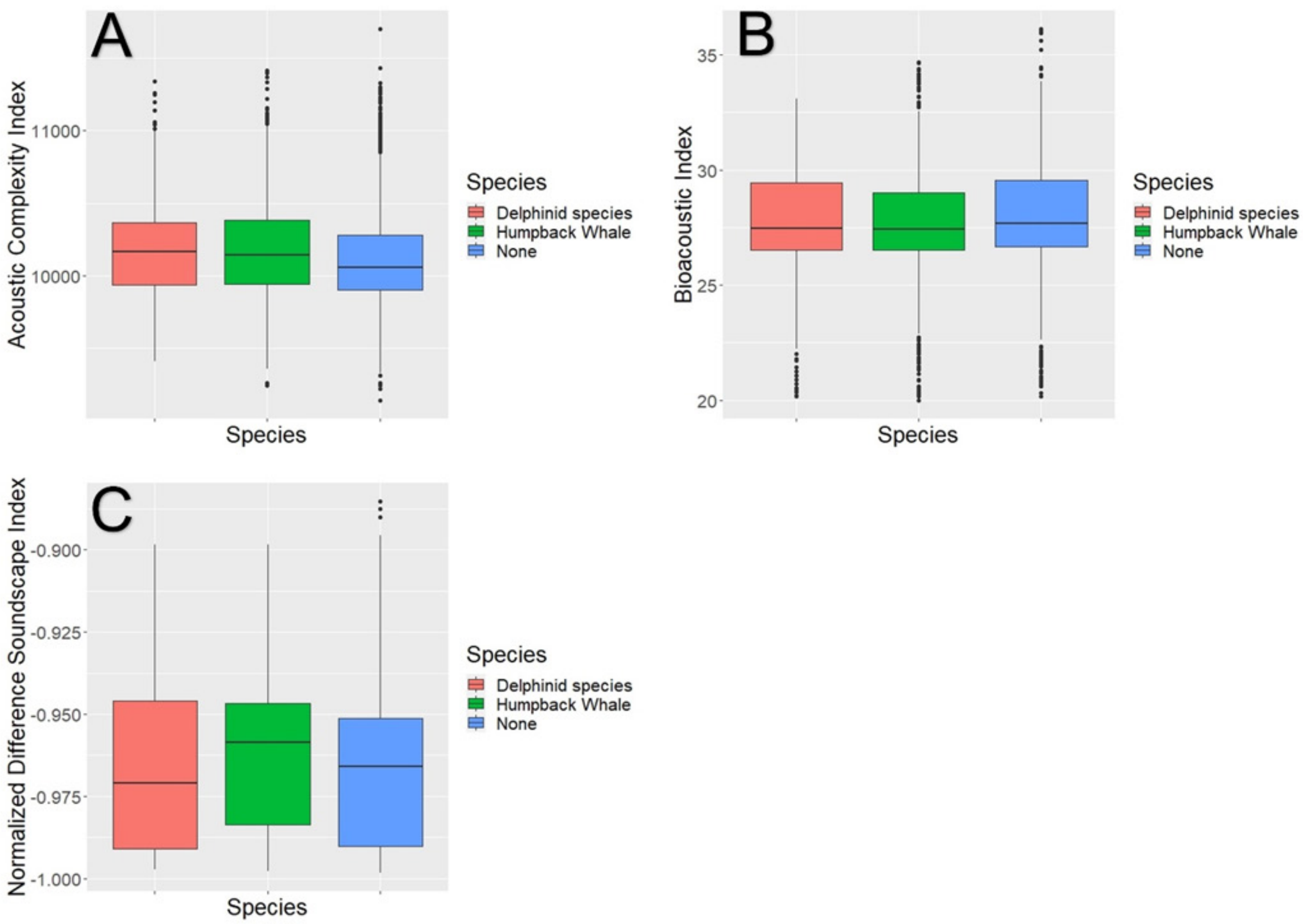

Figure C-7. Comparison of indices by species (humpback whale and delphinid species) and when no species were calling

ACI (A) and BI (B) show a similar distribution of data, particularly as compared to NDSI (C). Statistically significant differences between all groups were found, but effect size values indicated these differences were minute.

C.2.4.2 Indices and Conductor Cutting

The distribution of acoustic indices values measured during periods with and without cutting are indicated in Figure C-8. We ran a Mann-Whitney U Test to look for statistically significant differences in these values.

There was a statistically significant difference in the ACI values for periods with cutting (Mdn = 10,059, $\sigma = 314$) and without cutting (Mdn = 10,132, $\sigma = 339$; U = 4.35e+6, $p < 0.001$), although the effect size indicated this was only a small difference (rB = 0.124).

Similarly BI had a statistically significant difference in the values for periods with cutting (Mdn = 27.707, $\sigma = 2.063$) and without cutting (Mdn = 27.461, $\sigma = 2.144$; U = 3.55e+6, $p < 0.001$), and also reported a small effect size (rB = -0.083).

The analysis for NDSI indicated an even smaller difference in effect size (rB = 0.042) between the values for periods with cutting (Mdn = -0.963, $\sigma = 0.021$) and without cutting (Mdn = -0.962, $\sigma = 0.022$; U = 4.03e+6, $p = 0.007$).

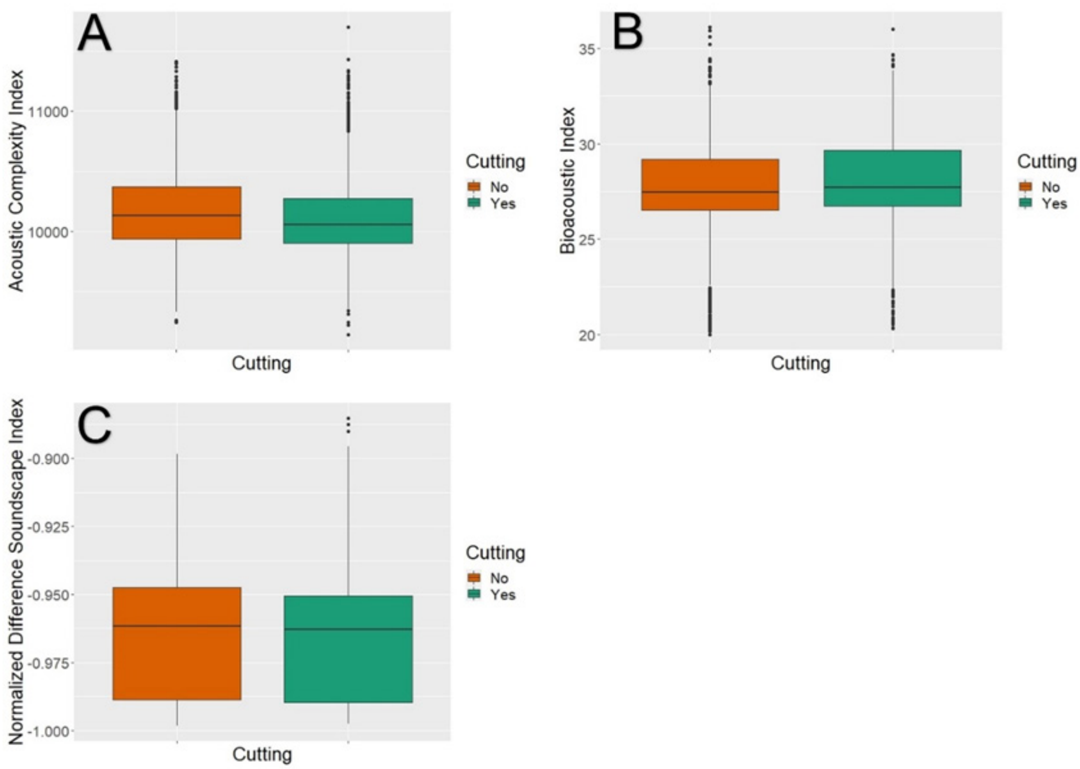

Figure C-8. Comparison of with and without cutting occurring
ACI (A) and BI (B) show a similar distribution of data, particularly as compared to NDSI (C). Statistical differences were observed for all datasets (all p-values < 0.05) but effect size indicated these were relatively trivial differences.

C.2.4.3 Correlation of Indices to Call Parameters

We compared the three indices to several call parameters including call count (number of calls in each .wav file, mean amplitude (AMP), and mean minimum frequency and mean maximum frequency of the detected calls from humpback whales and from delphinid species. The matrix of values in **Figure C-9** indicates the Pearson's correlation values (r) that represent the correlation between the variables in each column and row. The only relationships demonstrating medium to strong correlations occur among indices and between the call parameters as indicated by the darker colors and larger values. For instance, in the cell corresponding to "MeanMinFreq" and "MeanMaxFreq" we see a dark purple color and positive 0.974, indicating a strong correlation between these two variables.

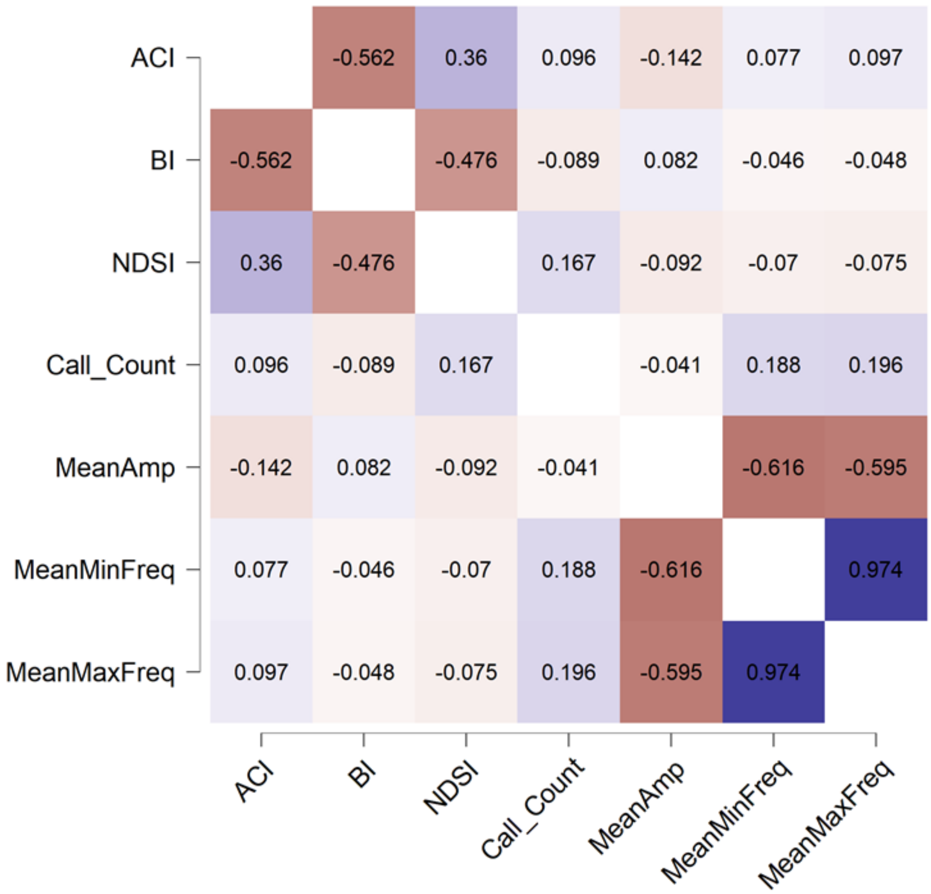

Figure C-9. Pearson correlation values between all indices and several call parameters
Results do not indicate any strong relationships between the selected parameters and indices. Labels for call parameters indicate the mean amplitude of calls in the five-minute period (MeanAmp) and the mean minimum frequency of calls (MeanMinFreq) and mean maximum frequency of the calls (MeanMaxFreq).

C.3 Discussion

PAM is a proven analytical tool for studying marine mammals. As part of such monitoring efforts, we suggest that the contribution of sound by marine mammals to the overall soundscape can have implications for reported sound exposure levels. Specifically, we observed a significant contribution of sounds from delphinid species and humpback whales during the entirety of the monitoring period. The calls from both humpback whales and delphinids overlap with the generalized hearing range of both low- and mid-frequency hearing groups, which artificially increases the sound exposure level observed in the power spectral density analysis. The vocalizations of these animals were of a high enough amplitude that they were detected during periods of conductor cutting (as shown in section A of the results), suggesting their source levels are contributing to the overall spectral observations.

Although the distance to vocalizing marine mammal groups was not possible to determine given the nature of the Study scope and monitoring plan, the intensity of calls attributable to humpback whales potentially indicates a proximity of callers under 10 km (5.4 nmi) from operations. Depending on environmental conditions and platform height, marine mammals, especially large whales, or large groups of delphinids, can be sighted typically between 6-8 nmi and would likely be able to be seen from the cutting platform in good sea state and clear sky conditions. Similarly, the burst pulse calls from delphinids place them in a proximity to the platform (under ~5 km, 3 nmi) that would make these animals accessible to visual observations. The passive acoustic results suggest this is a region is occupied by regularly occurring protected marine mammal species as was noted during the month of this field effort. These acoustic-based observations are useful for understanding the spring (April) distribution of these species within the region.

The results of the acoustic indices analysis provided insight into the dynamics of sound in this environment but did not show a useful relationship to marine mammal vocalizations. While statistical tests indicated significant differences between most of the comparisons of the soundscape metrics and periods with vocalizing marine mammals or without (Figure C-7), the magnitude of these differences was quite trivial as shown by the effect size.

A similar scenario emerged for the soundscape metrics in relation to periods with and without conductor cutting noise (Figure C-8). While it is tempting to pursue use of these metrics for identifying periods with marine mammal or with cutting noise, the overall low effect size and clear overlap in the distributions suggests they are not suited in this very noisy environment. Additionally, the correlations matrix demonstrated that there were moderate to strong positive and negative relationships between the indices themselves and between the few call variables used but demonstrated low to no relationships between indices and call parameters. We believe the ambient and anthropogenic noise sources are too overwhelming to reflect the biological content in the data. However, we do believe that evaluating these metrics at a further distance from the platform would be helpful. If recorders were placed at a sufficient distance from the platform (~1 km) so the noise does not overwhelm the recordings, then a more accurate assessment of their utility is possible.

This analysis provided a perspective on the capabilities of PAM as a monitoring tool. The consistent vocal activity of marine mammals within the region was unexpected due to the low number of reported visual observations. Visual observations are not always possible due to inclement weather, glare, and effort during concurrent platform operations. The effective use of PAM to enhance what is visually observed was demonstrated in this study. Evaluating marine mammal vocal behavior and assessing the quality of the surrounding acoustic habitat is important to incorporate in PAM monitoring protocols Suggestions regarding future passive acoustic monitoring methods are presented in Future Recommendations.

C.4 Future Recommendations

C.4.1 Passive Acoustic Monitoring (PAM)

Acoustic monitoring was proven successful in revealing the presence of marine mammal species that were not sighted visually during conductor cutting. We recommend continuing to incorporate acoustic monitoring into future cutting studies for this reason. This recommendation is based on the findings herein, in which the information on marine mammal occurrence during conductor cutting would have been otherwise unobserved. However, we recommend additional PAM focus. Future efforts could include use of time synchronized recorders to allow for marine mammal localization, and/or, the addition of deeper water recorders to increase the capacity to pick up other species e.g., sperm whales or beaked whales.

It is well known and accepted that PAM provides additional meaningful data for use in marine mammal monitoring which in turn, provides a more substantive basis for NEPA impact evaluations. Given that it may not be practicable to have Protected Species Observers (PSOs) on the platform or on vessels in the Study Area and with the knowledge that the cutting personnel are not trained observers and also are not on effort i.e., are busy with their cutting tasks, PAM provides a supplemental way to monitor for marine mammals if they are calling. Combining visual and acoustic monitoring is a well-accepted practice for marine mammal monitoring. We recommend at minimum, future conductor cutting place an enhanced focus on marine mammal monitoring via the use of hydrophones at close and further distances from cutting than was done in this pilot study.

Further information concerning the environment's sound propagation qualities and call source levels is needed to either confirm the presence of humpbacks in close (<10km) proximity to cutting operations. Thus, in future studies, we recommend propagation modeling be done in order to estimate values of source levels. Alternatively, as mentioned above, we recommend employing methods to assist with localization of marine mammals in the Study area as that would illuminate more detail on their presence and location, and potentially to see if they are avoiding the area. We suggest Agencies consider use of an acoustic array of hydrophones designed to determine location to a vocalizing marine mammal. One possibility is the SonarPoint system developed by Desert Star Systems, which are a portable set of hydrophones that have localization capabilities.

Additionally, the following logistical elements are strongly recommended for future marine mammal monitoring efforts:

- Set recordings to local time to ensure accurate matching of marine mammal events to construction activities.
- Work with the contractor performing the cutting to ensure provision of detailed cutting data, times, durations, and intervals.
- Consider monitoring a wider bandwidth to accommodate the upper end of the mid-frequency hearing group. This group includes beaked whales that could potentially be influenced by anthropogenic noise produced during these activities. Specifically, within the Southern California region, Baird's beaked whale (Berardius bairdii) which have a multi-peak structure to their echolocation clicks at frequencies of ~9, 16, 25 and 40 kHz (Baumann-Pickering et al. 2013). The lower end of these clicks falls within the noise contributed by conductor cutting. Due their echolocation clicks containing energy above the upper end of the bandwidth recorded during this Study (36 kHz), we require a greater bandwidth to correctly classify acoustic events as Baird's.
- Suggest using trained PSOs and Marine Mammal Observers (MMOs) versus contractor crew members who likely have divided duties and less or no training for marine mammal observation protocols or species identification.

C.4.2 Additional Monitoring Considerations

Although the attempts to employ an analysis of changes in call frequency parameters in response to noise, and to find utility in acoustic indices were unsuccessful, a modification to the survey plan could results in a more meaningful outcome. First, by increasing the deployment duration to include additional time before and more time after the conductor cutting operations, the call parameter response to noise analysis could be viable. Secondly, while the acoustic indices did not demonstrate a strong relationship to biophony or anthrophony in this study, the close proximity to the platform likely made accurate measurements difficult. Stationing a recorder or recorders far from the platform e.g., 1-1.5 nautical miles away but still within the study area, could provide insight into the utility of these acoustic indices for efficient monitoring of marine mammals. As their calls are detected within this distance, this would provide a buffer from overwhelming platform noise. We recommend additional testing of these concepts to gain insight into their applicability.

C.5 Glossary

Acoustic Complexity Index: A measure of the degree of complexity within a .wav file. The calculation sums the absolute difference between two adjacent values of intensity in a single frequency bin.

Acoustic Diversity Index: mathematical calculation of the heterogeneity of the sound produced in an environment using temporal or spectral analysis. Typically, indices are utilized as a means of measuring local biodiversity within a region.

Anthrophony: human derived sounds that contribute to the soundscape of an ecosystem.

Bioacoustic Index: A measure of abundance originally designed for bird vocalizations that calculates the area under the mean frequency spectrum.

Biophony: sounds contributed to the soundscape of an ecosystem from living organisms.

dB 1μPa2s: the decibel expressed in relation to standard unit of acoustic pressure

Geophony: sounds contributed to the soundscape by geophysical activity of the Earth such as earthquakes, rain, etc.

Kruskal Wallis test: A non-parametric test (equivalent to parametric one-way ANOVA test) that compares the medians of two or more independent groups.

Mann-Whitney U Test: a non-parametric means of determining if there is a statistical difference between the medians of two independent sample groups.

Normalized Difference Soundscape Index: A measure of the amount of anthropogenic disturbance on a soundscape by calculating the differences between anthrophony and biophony acoustic components.

Soundscape: contributions of sound to a regional environment that are either biological, geophysical, or anthropogenic in nature and vary over space and time.

Spearman's Correlation: A non-parametric rank-ordered test which provides a statistical measure of the strength of the relationships between two variables, with a value between -1 and 1, where 0.0 shows no linear relationship.

C.6 References

Baumann-Pickering S, Yack TM, Barlow J, Wiggins SM, Hildebrand JA. 2013. Baird's beaked whale echolocation signals. The Journal of the Acoustical Society of America, 133(6), 4321-4331.

Bertucci F, Parmentier E, Lecellier G, Hawkins AD, Lecchini D. 2016. Acoustic indices provide information on the status of coral reefs: an example from Moorea Island in the South Pacific. Scientific Reports, *6*, 33326.

Boelman NT, Asner GP, Hart PJ, Martin RE. 2007. Multi-trophic invasion resistance in Hawaii: bioacoustics, field surveys, and airborne remote sensing. Ecological Applications, *17*(8), 2137-2144.

Bohnenstiehl DR, Lyon RP, Caretti ON, Ricci SW, Eggleston DB. 2018. Investigating the utility of ecoacoustic metrics in marine soundscapes. J. Ecoacoustics, *2*, R1156L.

Bolgan M, Amorim MCP, Fonseca PJ, Di Iorio L, Parmentier E. 2018. Acoustic Complexity of vocal fish communities: a field and controlled validation. Scientific reports, *8*(1), 1-11.

Clark CW, Clapham PJ. 2004. Acoustic monitoring on a humpback whale (Megaptera novaeangliae) feeding ground shows continual singing into late spring. Proceedings of the Royal Society B: Biological Sciences, 271(1543).

Davies BF, Attrill MJ, Holmes L, Rees A, Witt MJ, Sheehan EV. 2020. Acoustic Complexity Index to assess benthic biodiversity of a partially protected area in the southwest of the UK. Ecological Indicators, 1*11*, 106019.

Erbe C, Verma A, McCauley R, Gavrilov A, Parnum I. 2015. The marine soundscape of the Perth Canyon. Progress in Oceanography, 13*7*, 38-51.

Farina A. 2019. Ecoacoustics: A quantitative approach to investigate the ecological role of environmental sounds. Mathematics, 7(1), 21.

Gillespie D, Mellinger DK, Gordon J, McLaren D, Redmond P, McHugh R, Trinder P, Deng XY, Thode A. 2009. PAMGUARD: Semiautomated, open source software for real-time acoustic detection and localization of cetaceans. The Journal of the Acoustical Society of America, *125*(4), 2547-2547.

Haver SM, Gedamke J, Hatch LT, Dziak RP, Van Parijs S, McKenna MF, Barlow J, Berchok C, DiDonato E, Hanson B, Haxel J. 2018. Monitoring long-term soundscape trends in US waters: The NOAA/NPS ocean noise reference station network. Marine Policy, *90*, 6-13.

Helble TA, D'Spain GL, Hildebrand JA, Campbell GS, Campbell RL, Heaney KD. 2013. Site specific probability of passive acoustic detection of humpback whale calls from single fixed hydrophones. The Journal of the Acoustical Society of America, *134*(3), 2556-2570.

Kasten EP, Gage SH, Fox J, Joo W. 2012. The remote environmental assessment laboratory's acoustic library: An archive for studying soundscape ecology. Ecological Informatics, *12*, 50-67.

Lindseth AV, Lobel PS. (2018). Underwater soundscape monitoring and fish bioacoustics: a review. Fishes, *3*(3), 36.

Macaulay J, Gordon J, Gillespie D, Malinka C, Northridge S. 2017. Passive acoustic methods for fine-scale tracking of harbour porpoises in tidal rapids. The Journal of the Acoustical Society of America, *141*(2), 1120-1132.

Malinka CE, Gillespie DM, Macaulay JD, Joy R, Sparling CE. 2018. First in situ passive acoustic monitoring for marine mammals during operation of a tidal turbine in Ramsey Sound, Wales. Marine Ecology Progress Series, *590*, 247-266.

Merchant ND, Fristrup KM, Johnson MP, Tyack PL, Witt MJ, Blondel P, Parks SE. 2015. Measuring acoustic habitats. Methods in Ecology and Evolution, *6*(3), 257-265.

Miller BS, Calderan S, Gillespie D, Weatherup G, Leaper R, Collins K, Double MC. 2016. Software for real-time localization of baleen whale calls using directional sonobuoys: A case study on Antarctic blue whales. The Journal of the Acoustical Society of America, *139*(3), EL83-EL89.

NOAA Fisheries. 2018. 2018 Revisions to: Technical Guidance for Assessing the Effects of Anthropogenic Sound on Marine Mammal Hearing (Version 2.0): Underwater Thresholds for Onset of Permanent and Temporary Threshold Shifts. U.S. Dept. of Commer., NOAA. NOAA Technical Memorandum NMFS-OPR-59, 167 p.

Papale E, Gamba M, Perez-Gil M, Martin VM, Giacoma C. 2015. Dolphins adjust species-specific frequency parameters to compensate for increasing background noise. PLoS One, 1*0*(4), e0121711.

Parks SE, Miksis-Olds JL, Denes SL. 2014. Assessing marine ecosystem acoustic diversity across ocean basins. Ecological Informatics, *21*, 81-88.

Pieretti N, Martire ML, Farina A, Danovaro R. 2017. Marine soundscape as an additional biodiversity monitoring tool: A case study from the Adriatic Sea (Mediterranean Sea). Ecological Indicators, *83*, 13-20.

Pijanowski BC, Villanueva-Rivera LJ, Dumyahn SL, Farina A, Krause BL, Napoletano BM, Gage SH, Pieretti N. 2011. Soundscape ecology: the science of sound in the landscape. BioScience, *61*(3), 203-216.

R Core Team. 2021. R: A language and environment for statistical computing. R Foundation for Statistical Computing, Vienna, Austria. URL https://www.R-Study.org/

Rankin S, Oswald JN, Barlow J. 2008. Acoustic behavior of dolphins in the Pacific Ocean: Implications for using passive acoustic methods for population studies. Canadian Acoustics, 3*6*(1), 88-92.

Risch D, Parks SE. 2017. Biodiversity assessment and environmental monitoring in freshwater and marine biomes using ecoacoustics. Ecoacoustics. The Ecological Role of Sounds, edited by Farina A. and Gage SH Oxford, UK: Wiley, 145-68.

Sakai T. 2020. " PAMpal: Load and process passive acoustic data," R package version 0.9.14, http://CRAN.R-Study.org/package=PAMpal

Sueur J, Farina A, Gasc A, Pieretti N, Pavoine S. 2014. Acoustic indices for biodiversity assessment and landscape investigation. Acta Acustica united with Acustica, 100(4), 772-781.

Villanueva-Rivera LJ, Pijanowski BC. 2018. soundecology: Soundscape Ecology. R package version 1.3.3. https://CRAN.R-Study.org/package=soundecology

Attachment C-1: List of Deliverables

Deliverables are organized by the following folder structure. These may be the hard drive provided to BOEM:

I. **Acoustic_Event_Summaries**:

a. "**BOEM_Tt_Acoustic_Events_2021.ppt**": PowerPoint summary of all acoustic events including call density plots and example spectrogram and audio clip. Includes all marine mammal acoustic events and ship passing events.

b. "**AcousticEvents_AllRuns.xlsx**": Spreadsheet summary of all acoustic events, across all runs, along with details of the noise threshold levels associated with the species or species group. Table columns correspond to the following:
   - **Week and Run columns**: correspond to the organization of data for processing; "MF" refers to Mid-Frequency processing (2-36 kHz), "LF-2kHz" refers to 200 Hz – 2 kHz processing and "LF-200Hz" refers to the 10 – 200 Hz processing.
   - **ID**: unique identifier for each acoustic event in the dataset (regardless of run)
   - **UID**: PAMGuard reference ID that links back to processed files
   - **StartTime & StartTime_Milliseconds**: Start time in PST for an event; in PG this was derived by subtracting two hours from the filename time (as .wav files do not have a header file with time). In PG they are natively referred to as "UTC" and "UTCMilliseconds"
   - **EndTime**: Time of last contour or click select as part of an event.
   - **EventDuration**: Total elapsed time for the event
   - **EventDuration_decimal**: Elapsed time converted to decimal time for ease of additional calculations
   - **DataCount**: Number of contours/sounds included in an event. For "Ship" or "Anthropogenic Noise" this was only corresponding to a "click" at the start and end of the events, and the full number of detections was not selected as we only used this to derive start and end time. Noise events often misclassified as clicks, so they offer a way to annotate these events.
   - **Analyst**: Initials of analyst who processed data
   - **Species_ID**: label assigned by analyst
   - **Sound_Type**: For the MF runs, this was the type of calls or sounds that were detected in the data, even if not possible to parse out and select for annotation/logging. The abbreviations include EC=Echolocation Click, BP=Burst Pulse, WH=Whistle
   - **Comments**: This is where comments related to the even as well as if an Anthropogenic Noise event was a match to cutting or not, is described
   - **During_Cutting_Event & During_Noise_Event**: Used to help in indicate if marine mammal events overlapped either a cutting event or other form of noise
   - **TTSThreshold_DB**: Corresponds to the TTS Onset value described in the table able and is specific to the hearing group
   - **PTSThresh_Imp_DB**: Corresponds to the Impulsive sound PTS value described in the table able and is specific to the hearing group
   - **PTSThresh_NonImp_DB**: Corresponds to the Non-Impulsive sound PTS value described in the table able and is specific to the hearing group

c. "**Cutting_Times_Comparison.xlsx**: Comparison of PAMGuard logged noise events to cutting periods. This information is also available in Appendix II. The columns include the following:
   - **Stat Date**: Date of the cutting event
   - **Received ID**: ID found on the provided sheet of logged cutting events
   - Start and End Cutting Event: times indicated on the sheet of documented periods of logging
   - **Acoustic match?**: Indicates if the acoustic event is a match to the logged cutting event

- **Event Start and Event End time**: represents times used to define cutting period in PAMGuard.
- **Acoustic Run**: indicates what run each event was found
- **UID**: corresponds to the PAMGuard identifier for that run.

d. "**NOISE_LTSAs**": folder containing screenshots of the noise events that were associated with cutting periods ("With Cutting Overlap") and those that were not ("Without Cutting Overlap").

II. **Acoustic_Indices:**

a. "WK2_All_Indices.csv": csv output from acoustic index analysis of week 2 data in R. Raw output of the index values for potential use with other soundscape metrics. These include values of Acoustic Complexity Index (ACI), the Bioacoustics Index (BI) and the Normalized Difference Soundscape Index (NDSI). Calculations are made for every file (one measurement every 30 minutes).

III. **PAMGuard_Processed_Files:**

a. "01_QAQC" Folder: Link to folder containing the example clips from all marine mammal events.
b. "Binary_and_sqlite: folder containing the PAMGuard Sqlite databases and binary storage folders for all processing runs.
c. "NBM_CSVs.zip": zipped folder of all exports from the sqlite databases relating to third octave noiseband measurements calculated during processing.

IV. **OSA_BOEM_TT_Acoustic_Analysis_Report_Final**: this report

Attachment C-2: Noise Cutting Comparison

Below is the summary of PAMGuard determined noise cutting events in comparison to periods documented during operations. For a list of column descriptions, refer to Attachment C-1, section I-c.

Start Date	Received ID	Start Cutting Event	End Cutting Event	Acoustic match?	EventStart time	EventEnd time	Acoustic Run	UID
31-Mar				N	17:06	18:22	MF - WK1	16
31-Mar				N	19:54	20:39	MF - WK1	3
31-Mar				N	21:05	22:23	MF - WK1	17
1-Apr				N	1:05	2:20	MF - WK1	18
1-Apr				N	5:06	10:21	MF - WK1	20
1-Apr				N	11:14	12:42	MF - WK1	6
1-Apr				N	13:05	14:22	MF - WK1	21
1-Apr	B-1	17:00	19:00	Y	17:06	18:54	MF - WK1	22
2-Apr	B-1	0:00	4:10	Y	1:05	4:07	MF - WK1	27
2-Apr				N	6:06	6:21	MF - WK1	28
2-Apr				N	9:07	11:09	MF - WK1	29
2-Apr				N	13:06	14:21	MF - WK1	30
2-Apr	B-9	17:30	19:00	Y	17:06	19:18	MF - WK1	31
2-Apr				N	21:05	22:21	MF - WK1	32
2-Apr	B-9	23:30	04:30	Y	23:26	6:37	MF - WK1	33
3-Apr				N	9:07	10:21	MF - WK1	34
3-Apr				N	13:05	14:21	MF - WK1	35
3-Apr	B-9	15:30	17:30	Y	15:35	22:21	MF - WK1	36
4-Apr				N	1:06	6:43	MF - WK1	37
4-Apr				N	9:06	10:21	MF - WK1	38
4-Apr	B-16	15:00	16:30	Y	13:06	16:37	MF - WK1	39
4-Apr	B-16	21:00	8:00	Y	17:06	8:03	MF - WK1	40
5-Apr				N	9:06	10:21	MF - WK1	42
5-Apr	B-16	12:00	23:30	Y	11:57	23:27	MF - WK1	43
5-Apr	B-16	12:00	23:30	Y	22:19	0:17	MF - WK2	37
6-Apr	B-3	8:00	9:30	Y	7:58	9:38	MF - WK2	1
6-Apr	B-3	14:00	20:30	Y	12:52	15:18	MF - WK2	2
7-Apr	S-25	10:00	11:00	Y	9:51	10:53	MF - WK2	7
7-Apr	S-29	19:00	19:30	Y	18:23	19:16	MF - WK2	8
8-Apr	S- 33	4:00	6:00	Y	4:04	5:46	MF - WK2	11
8-Apr	S-46	13:00	15:30	Y	12:46	15:45	MF - WK2	12
9-Apr	S-47	0:00	1:30	Y	0:20	1:40	MF - WK2	13
9-Apr	S- 36	7:00	8:00	Y	7:08	8:00	MF - WK2	14
9-Apr	S-34	15:00	16:30	Y	15:06	16:45	MF - WK2	15
10-Apr	B-17	22:30	1:00	Y	22:41	1:10	MF-WK2	38
11-Apr	B-17	4:30	16:00	Y	4:41	13:30	MF - WK2	16
11-Apr	S-41	22:00	23:30	Y	21:30	23:00	MF - WK2	18
12-Apr	S-28	9:45	15:45	Y	9:50	15:35	MF - WK2	21
12-Apr				N	19:15	22:12	MF - WK2	22
13-Apr				N	1:40	3:42	MF - WK2	26

Start Date	Received ID	Start Cutting Event	End Cutting Event	Acoustic match?	EventStart time	EventEnd time	Acoustic Run	UID
13-Apr	S-12	11:30	13:00	Y	11:09	12:47	MF - WK2	27
13-Apr	S-23	19:00	22:30	N	21:05	22:29	MF-WK2	39
14-Apr				N	3:46	6:00	MF - WK2	32
14-Apr	S-21	9:00	10:00	Y	7:34	10:48	MF - WK2	34
14-Apr	B-14	17:00	22:00	Y	17:06	18:54	MF - WK2	36
15-Apr	B-14	1:00	11:00	Y	1:05	1:50	MF - WK3	3
15-Apr	B-14	1:00	11:00	Y	5:05	6:20	MF - WK3	5
15-Apr	B-14	1:00	11:00	Y	9:04	10:59	MF - WK3	6
15-Apr				N	13:06	14:20	MF - WK3	68
15-Apr	S-9	16:30	19:00	Y	16:30	20:15	MF - WK3	69
15-Apr				N	21:06	22:21	MF - WK3	10
16-Apr				N	1:03	2:21	MF - WK3	14
16-Apr				N	5:06	6:20	MF - WK3	17
16-Apr	B-08	7:00	10:30	Y	8:31	10:20	MF - WK3	19
16-Apr	B-08	13:30	18:30	Y	13:06	13:50	MF - WK3	20
16-Apr	B-08	13:30	18:30	Y	14:04	14:20	MF - WK3	22
16-Apr	B-08	13:30	18:30	Y	15:45	18:32	MF - WK3	23
17-Apr	B-13	2:00	3:30	Y	1:04	3:31	MF - WK3	26
17-Apr				N	5:04	6:23	MF - WK3	27
17-Apr	B-13	7:00	16:00	Y	9:28	10:24	MF - WK3	28
17-Apr	B-13	7:00	16:00	Y	13:08	14:21	MF - WK3	29
17-Apr	B-13	18:30	4:00	Y	17:09	3:56	MF - WK3	30
18-Apr				N	5:08	7:09	MF - WK3	33
18-Apr				N	9:06	10:20	MF - WK3	34
18-Apr	B-10	13:00	17:30	Y	13:06	14:21	MF - WK3	35
18-Apr	B-10	13:00	17:30	Y	17:07	18:21	MF - WK3	36
18-Apr	B-10	21:00	2:00	Y	21:06	23:02	MF - WK3	38
19-Apr	B-10	21:00	2:00	Y	0:20	2:22	MF - WK3	39
19-Apr				N	5:04	6:15	MF - WK3	42
19-Apr	S-7	8:00	9:00	Y	7:41	10:24	MF - WK3	44
19-Apr	S-6	17:00	21:30	Y	15:40	23:03	MF - WK3	45
20-Apr				N	1:06	2:20	MF - WK3	50
20-Apr				N	5:05	6:21	MF - WK3	51
20-Apr	S-4	11:30	13:00	Y	9:05	10:21	MF - WK3	52
21-Apr				N	13:06	14:22	MF - WK3	56
21-Apr				N	17:28	20:08	MF - WK3	57
21-Apr				N	21:05	22:21	MF - WK3	58
22-Apr				N	1:06	2:21	MF - WK3	60
22-Apr				N	5:06	6:21	MF - WK3	62

Appendix D: Marine Mammal Acoustic Analysis: Study Report B, Development of a Deep Neural Network for Humpback Whales and Delphinids

Contents

List of Tables

List of Abbreviations and Acronyms

BOEM	Bureau of Ocean Energy Management
BSEE	Bureau of Safety and Environmental Enforcement
CNN	Convolutional neural network
Faster-RCNN	Regional convolutional neural network
FFT	Fast Fourier Transform
GUI	graphical user interface
kHz	kilohertz
km	kilometers
MATLAB	Proprietary multi-paradigm programming language and numeric computing environment developed by MathWorks.
MERIDIAN	(Marine Environmental Research Infrastructure for Data Integration and Application Network)
OSA	Ocean Science Analytics

Study	Characteristics and Contributions of Noise Generated by Mechanical Cutting During Conductor-removal Operations Study
Resnet	Residual neural network
SNR	signal to noise ratio
Tetra Tech	Tetra Tech, Inc.

D.1 Study Summary and Introduction

Passive acoustic data was collected during the monitoring stage of the BOEM/BSEE Contract No. 14M0120C0011, “Characteristics and Contributions of Noise Generated by Abrasive Cutting during Conductor Removal Operations.” A series of independent acoustic recorders were deployed to monitor the noise contribution generated by conductor cutting during the process of oil rig decommissioning operations. Ocean Science Analytics (OSA) documented the vocal occurrence of marine mammals using a semi-automated process involving a suite of detectors in PAMGuard (version 2.01.05; Gillespie et al. 2009) and subsequent annotation of true acoustic events from noise by an experienced analyst. Although this approach reduces time required to annotate a large acoustic dataset to a certain extent, processing of large acoustic datasets for long-term monitoring is still a laborious task that requires an experienced analyst to decipher marine mammal signals from noise.

Deep learning methods of detection and classification are increasing in utility within the underwater acoustic community (Allen et al. 2021; Shui et al. 2020; Vickers et al. 2021). A variety of signal processing, pattern recognition and machine learning techniques have improved detection and classification of marine mammal sounds through automation, but vary with respect to performance level (Usman et al. 2020). Deep learning models are a form of machine learning that applies different filter banks at different scales and determines features used to discriminate signals during a learning stage (Bianco et al. 2019). The models are thus not reliant on meeting criteria for a series of target values, but rather independently determine important features using one of several neural networks. Two forms of common networks used in imagery recognition and classification are convolutional neural networks (CNN) and residual neural networks (Resnet). Several studies report high percentages of precision and recall, and improved performance when testing involved multiple datasets collected in variable acoustic conditions (Kirsebom et al. 2020; Shiu et al. 2020). In addition to improved detection, deep neural networks offer capabilities in classifying marine mammal vocalizations, allowing for their use with multi-species analyses (Thomas et al. 2019).

During a 2019 workshop hosted by MERIDIAN (Marine Environmental Research Infrastructure for Data Integration and Application Network) and Ocean Networks Canada, developments in deep learning models were shared among the underwater acoustic communities (Frazao et al. 2020). As a result of this workshop, the well-documented software package Ketos was released providing users the capability of creating a deep neural network. The program highlights the use of a ResNet network, which has increased processing performance over CNNs. In a recent upgrade to PAMGuard (version 2.02.01), a deep learning module was incorporated that allows a user to import a neural network created in Ketos through integration of deep neural networks, advanced detection and classification algorithm within the reliable, multi-faceted framework of PAMGuard.

Additionally in 2019, Dr. Kevin Coffey of the University of Washington developed a MATLAB-based open access deep learning program called DeepSqueak (Coffey et al. 2019). The program was originally designed to detect and classify ultrasonic vocalizations from rats using a regional convolutional neural network (Faster-RCNN). Dr. Coffey focused on optimization of the network by reducing noise and incorporated a user-friendly graphical user interface (GUI) to allow any use to easily process and analyze acoustic signals of interest.

PROBLEM: Large acoustic datasets in noisy environments can be time consuming and laborious to review. Extensive anthropogenic noise can also confound the confirmation of calls from marine mammal species, requiring expert analysts to the review the acoustic data.

TASK OBJECTIVE: The objective of this effort is to develop a deep neural network that successfully detects marine mammal sounds of interest and reduces detection of noise within a large passive acoustic dataset. Detection using a deep neural network is beneficial for allowing a novice analyst to review detections for which the detector is able to accurately identify calls. These networks also reduce the amount of noise detected within the dataset as compared to other methods of machine learning, such as energy detectors that simply look for energy in a specific frequency band. This further streamlines the review process for analyst with varying experience. Our intent was to provide a scalable deep neural network that can be used easily for future analyses via one of the two tools described above.

D.1.1 Methods

D.1.1.1 Data Preparation

We selected several audio files across multiple detections throughout the deployment. We reviewed the to determine files with varying levels of call intensity for both humpback whales and delphinid species. We selected approximately 60 percent of the data subset to be used in the training and validation, and 40 percent to be used for testing. We tested both the data from the original recorder (5353) and an adjacent recorder (5356), in order to determine how well the network performed on detecting the same calls with different ambient noise.

For all data used in training and validation, we used the software program Raven to annotate calls of interest and store those annotations in a selection table. Both Ketos and DeepSqueak require a selection table to build a network. We generated selection tables for both the burst pulse signals from delphinids and the low frequency moans from humpback whales. Selection tables were then formatted as per each software program.

D.1.1.2 Ketos/PAMGuard Network Development

Ketos is a Python-based program that incorporates the use of the TensorFlow machine learning platform. We selected the Resnet model for development of the networks, which was guided by the extensive instruction and training modules provided by MERIDIAN and worked with developers to work through difference in processing our data. Once the network was developed, we tested its use in PAMGuard using a parameterized configuration file that included the deep neural network model.

D.1.1.3 DeepSqueak Network Development

DeepSqueak is a MATLAB-based, open access program that has been tested for use with moderate to high frequency tonal calls. We used a version modified specifically for use with underwater acoustic data and was originally parameterized to classify delphinid signals. This version had not previously been tested with either of the call types in the BOEM dataset, so we developed a neural network model using the annotated selection tables. We then trained the model iteratively within DeepSqueak through processing of detections within the framework and accepting true calls, rejecting noise, and further annotating any missed calls. This iterative process resulted in further training of the network to continually improve performance. Finally, we tested a small dataset with the final network in order to determine its performance for calls on two recorders. We calculated precision, recall and an f-score for the testing datasets. Precision is the ratio between the true positives and all of the positives and indicates how good the model is at detecting.

$$\text{Precision} = \frac{\text{True positives}}{\text{True positives + False positives}} = \frac{\text{Calls correctly detected}}{\text{Calls correctly detected + noise incorrectly detected as calls}}$$

Recall relates to the sensitivity of the model and indicates how correct it is at identifying true positives.

$$\text{Recall} = \frac{\text{True positives}}{\text{True positives + False negatives}} = \frac{\text{Calls correctly detected}}{\text{Calls correctly detected + calls not detected as calls}}$$

An f-score combines the precision and recall of a classifier into a single metric to compare different models.

$$\text{F1 score} = 2 * \frac{\text{Precision * recall}}{\text{Precision + recall}}$$

We use this instead of a simple average because it punishes extreme values. A classifier with a precision of 1 and recall of 0 has a simple average of 0.5 but an F1 score of “0”. If we want to create a classification model with the optimal balance of recall and precision, we try and maximize the F1 score.

Collectively, these values provide a means of evaluating detector performance. It should be noted that while we did wish to provide a functional network for this effort, we did not exhaustively train the model to perfect it. This is largely because of the scope of this effort as well as the need to incorporate more variability in calls from additional datasets that would be analyzed using this detector.

D.1.2 Results

D.1.2.1 Ketos/PAMGuard Network

After working through the network training process within Ketos, we developed a humpback whale network that performed well with our validation dataset. The next step involved importing the network for evaluation of the test data in PAMGuard. Due to unresolved issues relating to the network configuration, we were unable to import the network and refocused our efforts on the second option. Although the completion of a network via this method did not occur, we are continuing the development and coordinating with PAMGuard developers to finalize the process of importing outside of this effort and expect the process will be resolved in the coming months.

D.1.2.2 DeepSqueak Network

We developed two networks within DeepSqueak for detection of humpback whales (SOCAL_Humpback_CNN_v2.mat) and delphinids (SOCAL_Delphinid_Network.mat). These networks were trained with a dataset of approximately 1500 and 2,200 calls each, respectively. The call types used to train the networks consisted of the predominant call types that were found during the initial stage of this Study. Humpback whale calls from the BOEM deployment tend to be lower frequency (>1,000 Hz), tonal non-harmonic calls of short duration. The delphinid species encountered predominantly produced burst pulses and echolocation clicks. We selected the burst pulses as the signal for training the delphinid network. It should be noted that while we originally intended to develop a multi-species network that encompassed both species, we determined that the large difference in frequencies for each call type would have resulted in spectrogram samples that were not representative of the humpback whale calls. Multi-species networks are possible when the calls occur within a similar bandwidth.

The training process started by importing Raven selection tables and underwent iterative training through review of detection files withing DeepSqueak. These steps are described in the following section on instructions. We encountered several programmatic issues that needed to be resolved to enable low frequency call detection within DeepSqueak. A number of errors were resolved during this process with several refinements and improvements under development. Performance metric results for the humpback whale network are reported in Table D-1, and for the delphinid burst pulse network are reported in Table D-2. The calls included in the training for humpback whales were low frequency (200 Hz – 1,000 Hz), short and often tonal and non-harmonic. Approximately 1,600 calls were used in training this network. The calls included in training for the delphinid species network were burst pulses that contained variable structure and duration in the 5 kHz – 36 kHz bandwidth. Approximately 2,000 burst pulse calls were used in the training of this network. Echolocation clicks were often present in training files but were not included in the training process. During the course of training the networks, the performance metrics improved over time through review of training files in DeepSqueak. We trained the networks with files that included variable levels of noise, and both low intensity and moderate to high intensity calls. Results were obtained through testing of two, 30-minute files containing several hundred calls for each species. The same audio file (or as close as possible) was selected for two recorders, 5353 and 5356 to evaluate the performance of the networks on recorders that should detect the same number of calls but had varying ambient noise.

Table D-1. Performance measurements for the humpback whale neural network
This includes the number and percentage of true positives, false positives and false negatives, and calculations of precision, recall and an F1-score- The recorder identification is indicated and audio files from the same time period were selected for testing of each recorder.

Audio File	5353.21040309150	5353.21040702450	5356.21040309150	5356.21040702450
Call Type	Low Freq tonals (200 Hz - 1,000 Hz)	Low Freq tonals (200 Hz - 1,000 Hz)	Low Freq tonals (200 Hz - 1,000 Hz)	Low Freq tonals (200 Hz - 1,000 Hz)
Recorder	5353	5353	5356	5356
Run Date	2022-01-16 4_04 PM	2022-01-16 4_17 PM	2022-01-16 4_49 PM	2022-01-16 4_50 PM
Training/Testing	Testing	Testing	Testing	Testing
# of True Positives	30	131	28	79
True Positive %	5.16	55.04	3.47	16.06
# of False Negatives	11	61	10	49
False Negative %	1.89	25.63	1.24	9.96
# of False Positives	540	46	770	364
False Positive %	92.94	19.33	95.3	73.98
Precision	0.05	0.74	0.04	0.18
Recall	0.73	0.68	0.74	0.62
F1-Score	0.1	0.71	0.07	0.28

Table D-2. Performance measurements for the delphinid burst pulse neural network
This includes the number and percentage of true positives, false positives and false negatives, and calculations of precision, recall and an F1-score. The recorder identification is indicated and audio files from the same time period were selected for testing of each recorder.

Audio File	5353.2104050545	5353.2104182353	5356.2104050545	5356.2104182351
Call Type	Delphinid Burst Pulses	Delphinid Burst Pulses	Delphinid Burst Pulses	Delphinid Burst Pulses
Recorder	5353	5353	5656	5656
Run Date	2022-01-19 8_29 PM	2022-01-19 8_29 PM	2022-01-20 2_12 PM	2022-01-20 2_13 PM
Training/Testing	Testing	Testing	Testing	Testing
# of True Positives	502	136	479	151
True Positive %	63.22	44.44	65.71	45.90
# of False Negatives	104	42	115	30
False Negative %	13.10	13.73	15.78	9.12
# of False Positives	188	128	135	148
False Positive %	23.68	41.83	18.52	44.98
Precision	0.73	0.52	0.78	0.51
Recall	0.83	0.76	0.81	0.83
F1-Score	0.77	0.62	0.79	0.63

We observed two difference trends in the performance metrics for each network. In Table D-1, the humpback whale network included varying levels of precision for test files within and between recorders (0.04 – 0.74), and similar values of recall across all test files (0.62 – 0.74). This translates to a highly variable number of false detections and a moderate – high number of calls being correctly detected. The difference in within recorder precision is likely due to varying intensities of noise, as the second test file for the first recorder (5353) performed quite well. The difference in precision between recorders is visible in the second test files (5353.21040702450 & 5356.21040702450) which included values of 0.74 and 0.18 respectively. This difference is likely attributable to different ambient and instrument noise between the two recorders, as the network was only trained with noise from the 5353 recorder. Varying signal to noise ratio of humpback whale calls within the data contributed to the slightly different recall variables. However, these values were comparable between the two recorder datasets, indicating the ability of the network to correctly identify calls it is trained with despite unique noise. The predominantly low precision for humpback whales is not unexpected due to the limited time available for improving the network, and also due to these calls overlapping frequency bands dominated by noise. However, with increased training, the recall metrics were increasingly similar to some other studies using deep neural networks (Rasmussen and Širović 2021).

The delphinid network performed better than the humpback whale network, largely due to the reduced noise above 10 kHz where most of the burst pulses were detected (Table D-2). Values of precision were much greater than the humpback whale network indicating fewer false detections (0.51 – 0.78) and recall performed consistently well indicating a greater percentage of calls being detected (0.76 – 0.83). The results in Table D-2 indicate that there is very little difference in the performance of this network on a secondary recorder, which is subject to different instrument and mooring related noise. For example, the first test recording for delphinids (5353.2104050545) reported very similar measures of precision and recall (0.73 and 0.83 respectively) as compared to the test recording for the second recorder (precision of 0.78 and recall of 0.81). Echolocation clicks were sometimes identified as detections that were labeled as "false", but ambient noise was often disregarded by the network. Variability in the burst pulse structure, duration and frequency did not inhibit the detection of these calls.

The network files and example test files are provided on the hard drive of deliverables.

D.1.2.3 Instructions for Using DeepSqueak D.1.2.3

These instructions first take you through how to use an existing network, then how to refine that network. You can download the version used in this analysis from Gabi Alongi's branch on Github. Download the folder of code and save to your computer (be sure to unzip folder).

A recorded demonstration of this process can be found via this DeepSqueak Instructions link.

Prior to Beginning

Ensure that you have the appropriate version of MATLAB installed – you will need version 2020b, nothing prior as it will not have the correct upgrades for incorporating the Deep Neural Networks. You will also need the following toolboxes:

Product
MATLAB
Computer Vision Toolbox
Curve Fitting Toolbox
Deep Learning Toolbox
Image Processing Toolbox
Parallel Computing Toolbox
Signal Processing Toolbox
Statistics and Machine Learning Toolbox

There are several types of .mat files created in DeepSqueak:

- **Network Training Table**: .mat file used to create the network.
- **Network file**: the .mat file that is generated to contain information on the network.
- **Detections files**: DeepSqueak formatted .mat file of boxed calls that can be viewed and adjusted

Detection Using a Network & Network Refinement

1. Prior to starting MATLAB, create a folder for you Audio files, your Network, and your Detections Output that you can navigate to.
2. Save the network you wish to use in the network folder (e.g. SOCAL_Humpback_CNN.mat)
3. Once MATLAB is open, Set the Path to where you have downloaded DeepSqueak.
4. Then type "DeepSqueak" in the command window and the GUI will open.
5. Go to File → Select Audio Folder and select the folder with .wav .wav files.

6. Go to File → Select Network Folder and chose folder with network.
7. Go to File → Select Detection Folder and select a folder for your detection mat files output.
8. In the bottom under "Detect, Load & Record", select "Multi Detect".

1. 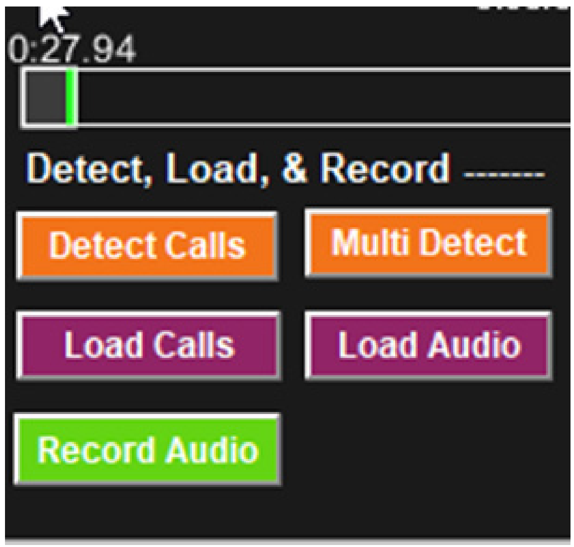

9. You will be prompted to select .wav files – select all you wish and hit ok (these will be used to further train the network, so you should be using a validation dataset, not the test dataset).

10. Then you will be prompted to select the network. Select SOCAL_Humpback_CNN.mat or whatever one you are working with.

11. You will then need to select several values. Total Analysis Length can be kept at 0 for full duration; Freq Cut Off in kHz should be upper end of bandwidth (4 kHz for this dataset); Freq Cut Off Low (kHz) should be set at 0.01 (**NOTE:** it cannot be "0").; Don't recall what score threshold is; Append Date to Filename is a Yes if you want to keep track of versions.

2. 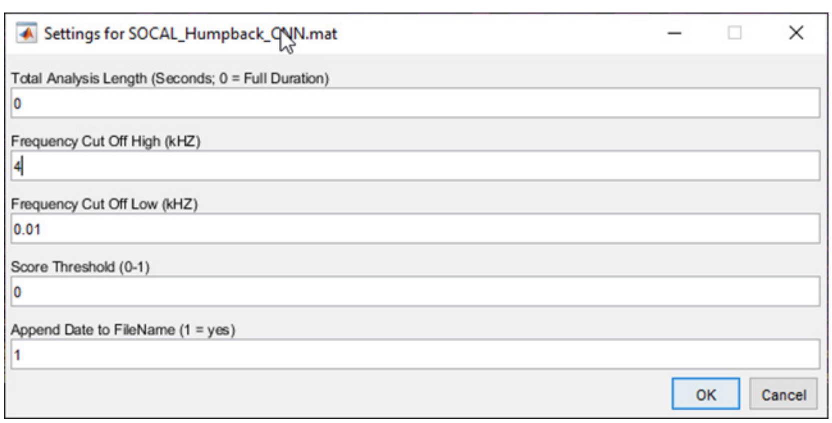

12. Once you hit "Ok" it will start running the detections for each .wav file.

13. When complete under the section where you selected "Multi Detect" you will select "Load Audio" and "Load Calls", but first, make sure you have the corresponding audio file and detected files in the bottom left panel (file names from .wav file should match):

3. 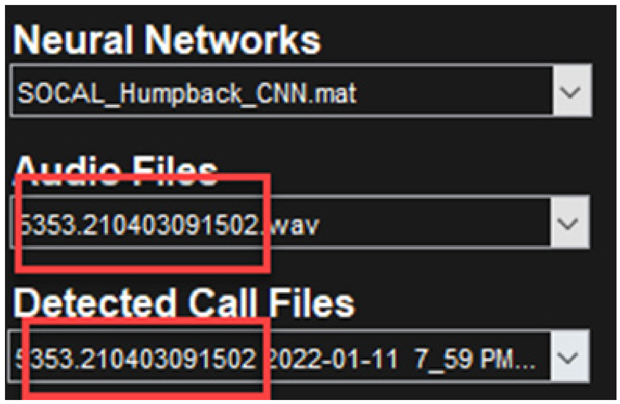

14. When you hit Load Audio & Load Calls, you will get the following window, with letters corresponding to these features:

    A. Detection review window.
    B. Larger portion of the data with detection density in the panel below. You can click anywhere on this lower spectrogram and navigate to it, if you need to box a call that was missed, etc.
    C. You can adjust your spectrogram parameters as well as the duration in each spectrogram window in this section.
    D. Here is where you perform detection (by selecting Multi Detect or Detect Calls) and Load the Audio and Calls that were detected.
    E. Accepting or rejected a boxed call, as well as drawing an unboxed call occurs here.
    F. Scrolling from one boxed call to the next (inner arrows) and scrolling to through file and to next .wav file (pink arrows) occurs here.

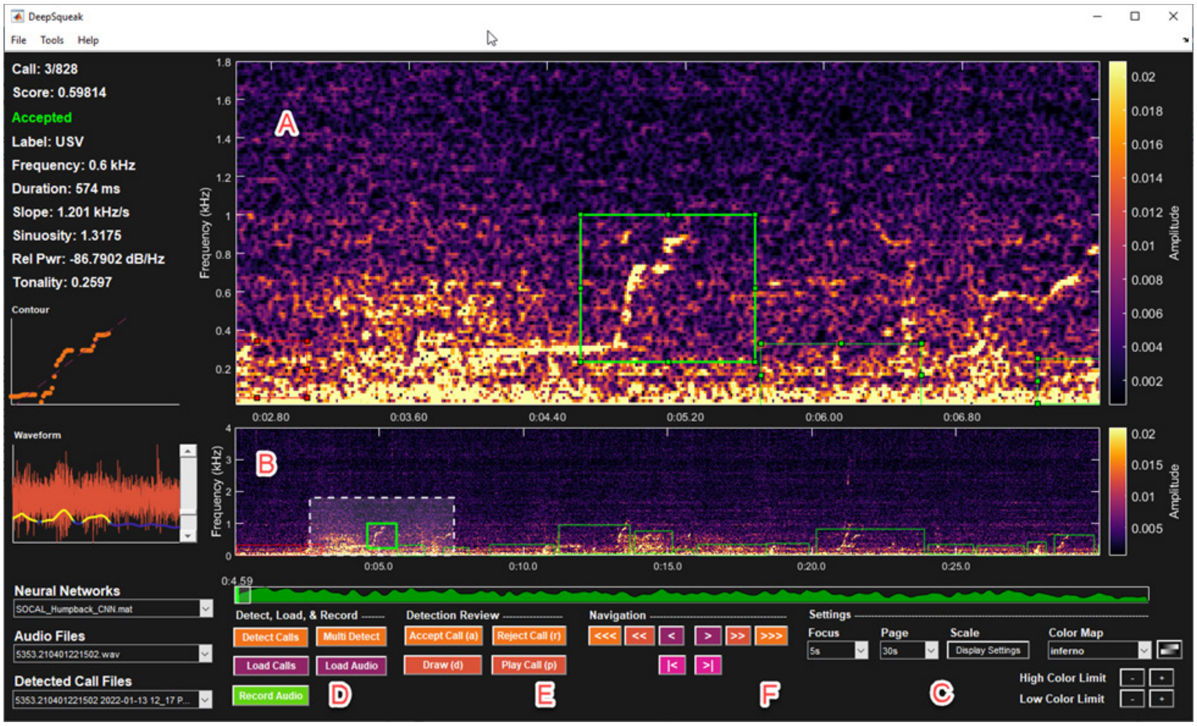

15. You can review the detections by using the buttons below:

A. Move to next detection in the file
B. Move to previous or next .wav file
   a. If you would like to use the network as is, you can simply review detections and go through and reject any noise, keep any true positives. There are buttons for accepting and rejecting in the bottom panel and letters "a" and "r" for accepting and rejecting. You can also draw a box around a call if it is missed.
   b. This step can also be used to further refining the network so you would need to save changes to the detection .mat file and then run through the next steps

If you are refining the network to include more diversity of sounds, data from a new recorder, etc., here are the steps you would take after finishing the step above:

16. Go to Tools → Create Detection Network Training Images and select the detections.mat file (e.g., 5353.210401224502-01-10 8_29 PM.mat, which corresponds to the .wav file name that was run and the date/time of the run).

17. You will then be prompted with the window below for the spectrogram settings used to train the network. Here's the details related to these settings:

    a. **Window Length** (s): this is your FFT setting but calculated in seconds. You should determine a good FFT for your data that's not too computationally intensive (bigger = more computation). Then to calculate, you divide your FFT by the sampling rate of the files. Good place to start is with an FFT of 512 or 1024. In an example, if I select an FFT of 512 and have a sampling rate of 8,000 Hz in my data, then I would divide 512/8,000 = 0.064 which is the value I put in as my window length. DeepSqueak automatically calculates a value for a 512 FFT based on your audio file sample size.

    b. **Overlap**: percentage overlap for spectrogram signal processing – good to stick with the default of 50% as increasing reduced the number of images created.

    c. **NFFT** (s) should be the same as FFT.
    d. **Duration** has a default of 0.5 – as of 1/13 error not resolved regarding the creation of images, but an increase to 1 second increases number of images. Working to resolve this issue so all that are boxed create images.
    e. **Augmentation** duplicates the dataset to increase the amount of files available for training the network by shifting the box slightly; it is useful with smaller datasets as indicated in this article[1] . Recommend selecting 2 as it reduces the amount of false positives in the detection process.

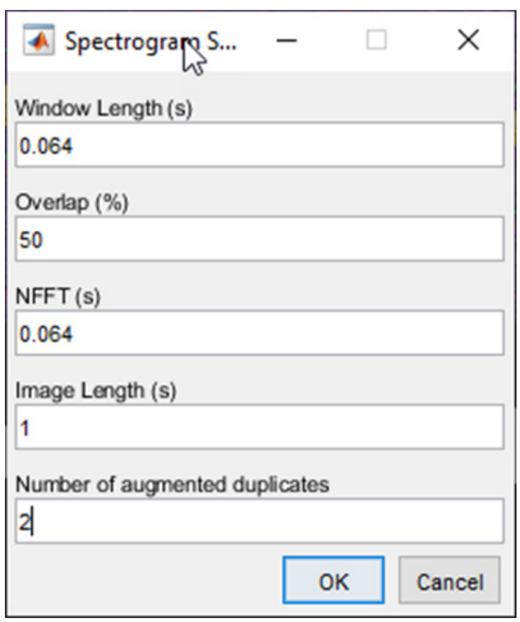

Soon as you hit "Ok" it will run. The image creation process will result in images that are placed in the "Training" folder of the DeepSqueak programs folder.

---

[1] Data Augmentation | How to use Deep Learning when you have Limited Data (nanonets.com)

18. Then you will train the network by going to Tools → Network Training → Train Detection Network. You will be prompted to select the .mat file that was created for images. You will then be asked if you would like to train a new or existing network. If you are adding to an existing network, then select it.

19. Next the program jumps right into the training with the window below, let it run, then save the resulting network (if building on one, overwrite it, keeping a backup):

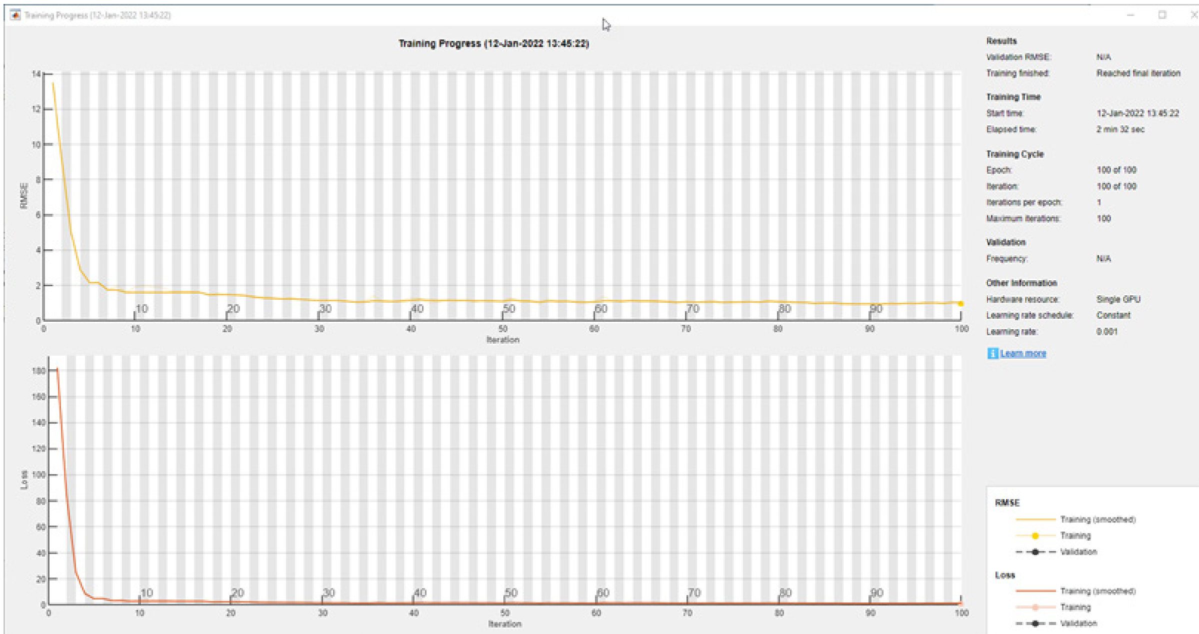

Starting a New Network with Raven Selection Table

If you are wanting to train a new detection network, you would do something similar to above, but would first start with a dataset that has been annotated using Raven. In Raven you would need to include several columns that DeepSqueak requires. They include:

- Selection
- View
- Channel
- Begin Time (s)
- End Time (s)
- Low Freq (Hz)
- Hight Freq (Hz)
- Delta Time (s)
- Delta Freq (Hz)
- Avg Power Density (dB FS)
- Annotation (essentially a label of 1 for true positive – explore more multiple species with this at a different time).

These are the steps to get started with a network using a Raven selection table:

1. Go to File → Import → Import from Raven

2. You will be prompted to navigate to the selection table and then the audio file. NOTE: a bug fix we are working on at the time of these notes (1/13/2021) includes being able to load multiple selection tables and .wav files instead or a single selection table with multiple .wav files (currently one selection table per .wav file). Stay tuned to fixes for this!

3. DeepSqueak will then create a .mat file and an image folder from the detections that are indicated in that .mat file.

4. You would then proceed with training the network as mentioned above.

D.2 Discussion and Future Recommendations

This effort resulted in the successful creation of two deep neural networks that can be used for the detection of humpback whale calls and burst pulses similar to those found in this study area. The final selection of DeepSqueak as the tool for use in future analysis provides a user-friendly interface for acousticians of varying experience to successfully detect calls in noisy environments. The scalability of the models allows for increased training with the introduction of new call types for each species or for use in a significantly different environment.

We observed several trends in the detectability of the networks. The performance metrics clearly state the need to reduce false positives attributable to noise. We found that although noise initially resulted in a larger number of detections, false detections from noise decreased with increased training. Another challenging element to this effort was the occurrence of calls with a low signal to noise ratio (SNR). Calls with a lower SNR (which were perceived as “very faint” by an acoustician) were less likely to be detected than those with a more discernable contour. Despite this, lower intensity calls could be detected, just not as frequently as calls with a higher signal to noise ratio. We therefore incorporated calls of varying intensity in the network development process. Through our testing of the separate datasets, the performance of the deep neural network is robust in when subject to varying instrument and mooring noise as indicated by similar performance metrics but does require additional training when used with a new recorder. If additional call types are encountered in future recordings, additional network training will be required.

We suggest several recommendations after this effort. The resulting networks developed for this Study can successfully detect calls similar to those found within the dataset. The objective of this effort was not to perfect these networks, so additional training is advised. We recommend collecting additional data in the area to improve the detection of additional call types that these animals produce. Additionally, incorporating noise samples from the dataset being analyzed should reduce the number of detections attributable to noise. During the development of these models, we were simultaneously working through programmatic changes to DeepSqueak to improve performance. We are continuing refinement of the program after the end of this Study and anticipate these improvements will result in improved network performance. We recommend additional network training after software improvements are complete.

D.3 Glossary

Convolutional Neural Network: a convolutional neural network (CNN, or ConvNet) is a type of artificial neural network commonly used to process and classify imagery. Using a series of layers, the network is designed for reduced processing time and takes and unsupervised approach to pattern recognition.

DeepSqueak: a MATLAB-based software program designed to detect and classify signals using a convolutional neural network enveloped in user friendly graphical user interface.

Machine Learning: a branch of artificial intelligence and computer science that incorporates the use of computer algorithms for synthesizing and analyzing data.

Neural Network: computer architecture that interconnects processors in a format modeled after neurons in the human brain.

Recall: the ratio of the correct predications and the total number of correct items in a dataset, indicating how good the item is at picking up the model is at picking the correct items.

Resnet Architecture: a residual neural network (Resnet) is an artificial neural network that is an enhanced type of convolutional neural network that differs in that it can skip layers within the model for increased image classification performance.

Precision: the ratio of the correct predictions and the total predictions, indicating how good the model is at predicting/detecting the signal of interest.

D.4 References

Allen AN, Harvey M, Harrell L, Jansen A, Merkens KP, Wall CC, Cattiau J, Oleson EM. 2021. A convolutional neural network for automated detection of humpback whale song in a diverse, long-term passive acoustic dataset. Frontiers in Marine Science, 8, 165.

Bianco MJ, Gerstoft P, Traer J, Ozanich E, Roch MA, Gannot S, Deledalle CA. 2019. Machine learning in acoustics: Theory and applications. The Journal of the Acoustical Society of America, 146(5), 3590-3628.

Coffey KR, Marx RG, Neumaier JF. 2019. DeepSqueak: a deep learning-based system for detection and analysis of ultrasonic vocalizations. Neuropsychopharmacology, 44(5), 859-868.

Frazao F, Padovese B, Kirsebom OS. 2020. Workshop Report: Detection and Classification in Marine Bioacoustics with Deep Learning. arXiv preprint arXiv:2002.08249.

Kirsebom OS, Frazao F, Simard Y, Roy N, Matwin S, Giard S. 2020. Performance of a deep neural network at detecting North Atlantic right whale upcalls. The Journal of the Acoustical Society of America, 147(4), 2636-2646.

Gillespie D, Mellinger DK, Gordon J, McLaren D, Redmond P, McHugh R, Trinder PW, Deng XY, Thode A. 2009. PAMGUARD: Semiautomated, open source software for real-time acoustic detection and localization of cetaceans. The Journal of the Acoustical Society of America, 125(4), 2547-2547.

Rasmussen JH, Širović A. 2021. Automatic detection and classification of baleen whale social calls using convolutional neural networks. The Journal of the Acoustical Society of America, 149(5), 3635-3644.

Shiu Y, Palmer KJ, Roch MA, Fleishman E, Liu X, Nosal EM, Helble T, Cholewiak D, Gillespie D, Klinck H. 2020. Deep neural networks for automated detection of marine mammal species. Scientific reports, 10(1), 1-12.

Thomas M, Martin B, Kowarski K, Gaudet B, Matwin S. 2019. Marine mammal species classification using convolutional neural networks and a novel acoustic representation. arXiv preprint arXiv:1907.13188.

Usman AM, Ogundile OO, Versfeld DJ. 2020. Review of automatic detection and classification techniques for cetacean vocalization. IEEE Access, 8, 105181-105206.

Vickers W, Milner B, Risch D, Lee R. 2021. Robust North Atlantic right whale detection using deep learning models for denoising. The Journal of the Acoustical Society of America, 149(6), 3797-3812.

Appendix E: Noise Study Photo Log

Contents

List of Photos

E.1 Noise Study Photo Log

As described in Volume 1 of this report, a field program occurred at Platform Hermosa between March 28 and April 24, 2021. This time span is inclusive of field mobilization and demobilization periods. The data collection timeframe was April 1 to April 21, 2001. As part of the field program acoustic (i.e., SoundTraps), particle motion (NoiseSpotter) monitoring equipment were deployed as well as a thermistor chain, which collected water column temperature data. The following photolog presents photos that were taken prior to the field program, during deployment, retrieval, and after the field program to provide some visuals pertaining to the equipment used for the field program and the procedures that were undertaken during the field program.

Photo 1. 3/26/2021 Hydrophone moorings loaded onto truck for delivery from Bothell, WA to Santa Barbara, CA

Photo 2. 3/29/2021 Mooring equipment loaded onto the Shearwater vessel (loading of the railroad wheel shown)

Photo 3. 3/30/2021 Hydrophone mooring prepared for deployment on the vessel (railroad wheel and rope canister shown)

Photo 4. 3/30/2021 Direction Photo Taken: Facing West - Hydrophone mooring prepared for deployment on the vessel (SoundTrap enclosure and buoys shown)

Photo 5. 3/30/2021 Railroad wheels, rope canister, and buoys organized on the vessel for deployment

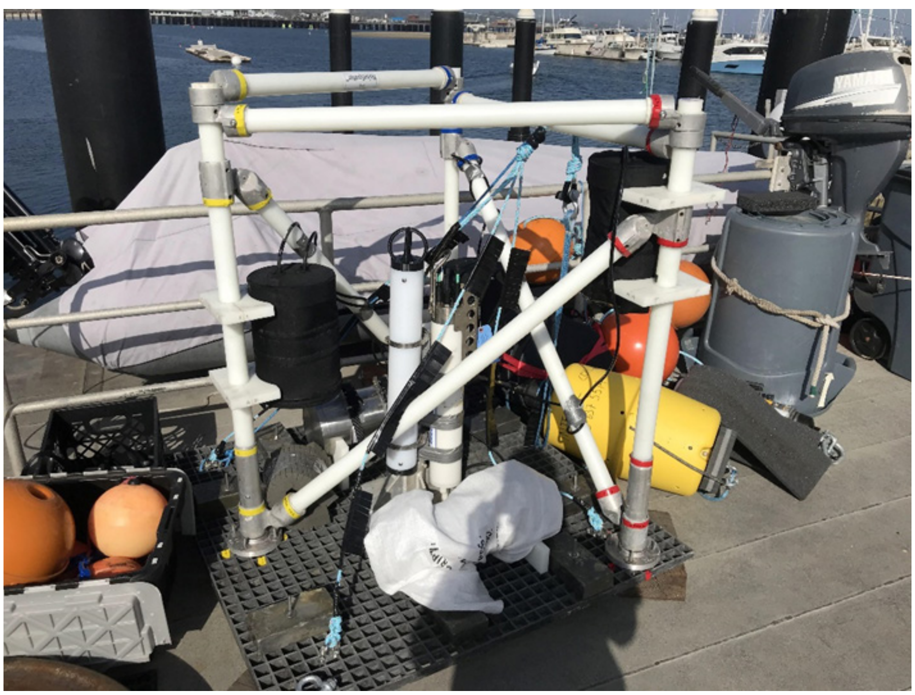

Photo 6. 3/30/2021 NoiseSpotter prepared; SoundTrap attached to the NoiseSpotter

Photo 7. 3/31/2021 Arrived at the Platform Hermosa

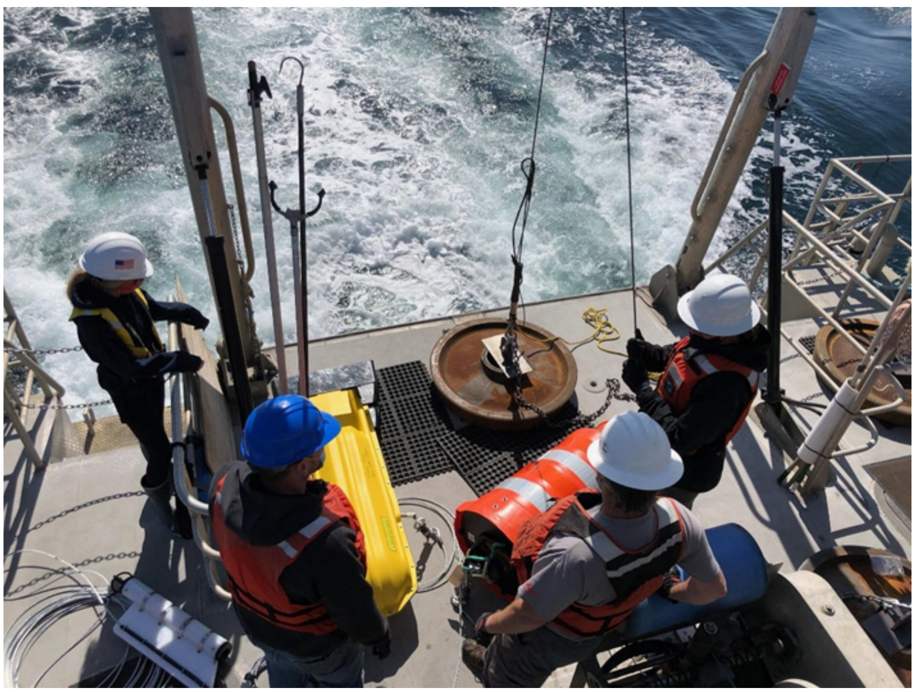

Photo 8. 3/31/2021 Preparing to deploy hydrophone moorings

Photo 9. 3/31/2021 Deploying hydrophone mooring with a SoundTrap at mid-water column and a SoundTrap at the bottom

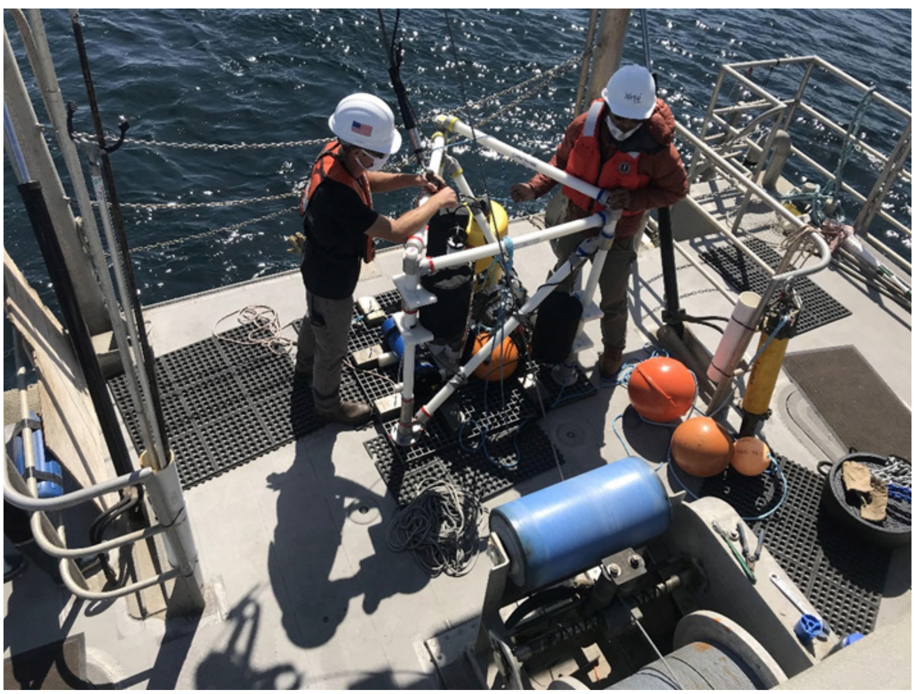

Photo 10. 3/31/2021 Preparing to deploy the NoiseSpotter

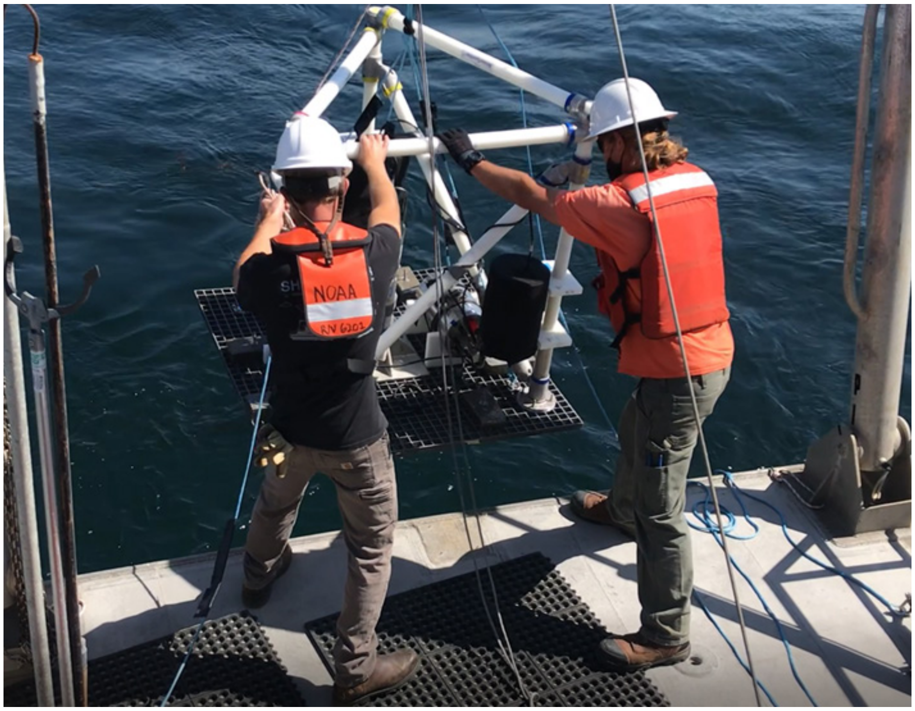

Photo 11. 3/31/2021 Deployment of the NoiseSpotter

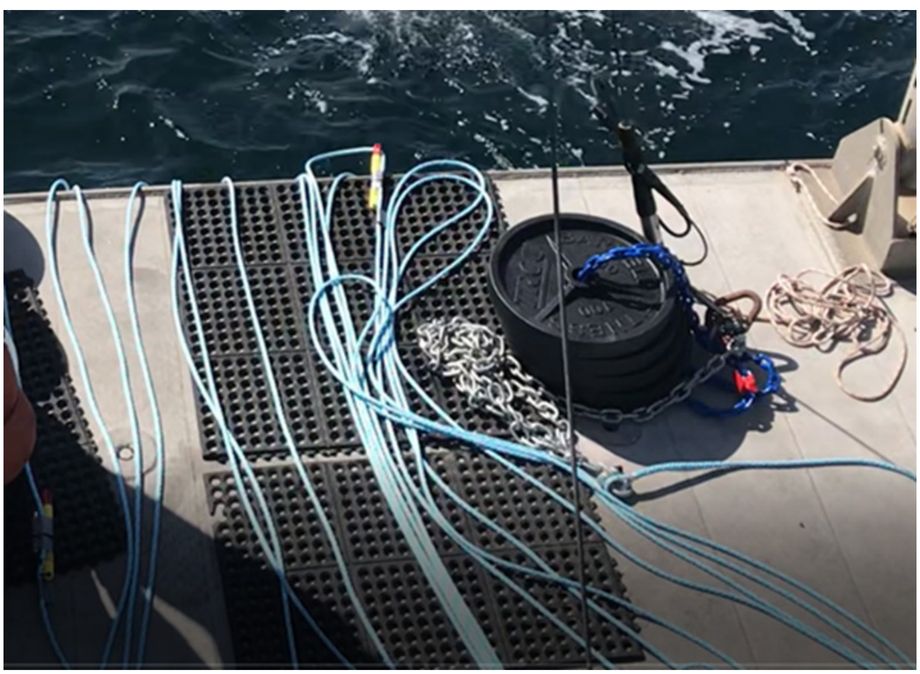

Photo 12. 3/31/2021 Thermistor Chain laid out prior to deployment

Photo 13. 3/31/2021 Deployment of the Thermistor Chain

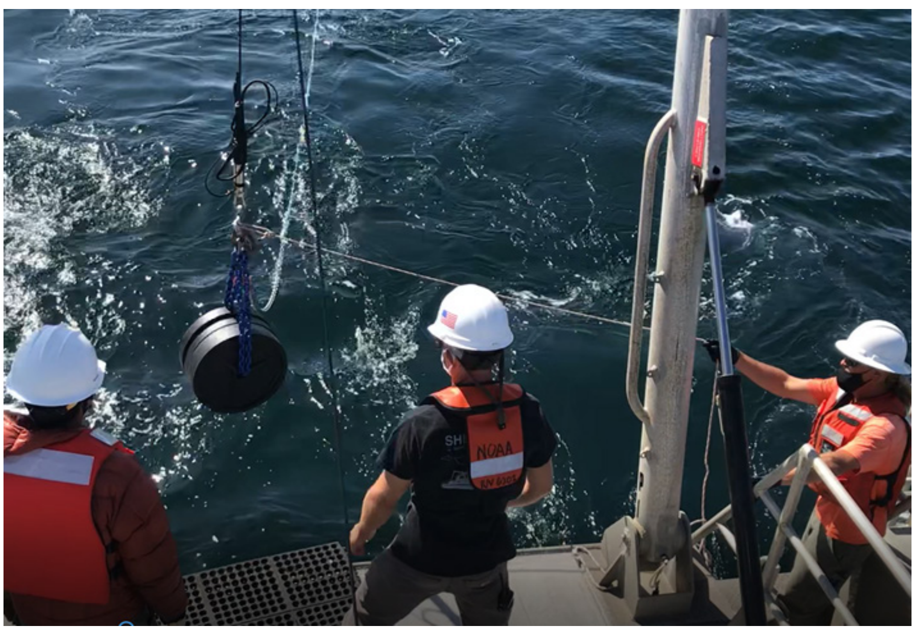

Photo 14. 3/31/2021 Deployment of the Thermistor Chain

Photo 15. 4/21/2021 EdgeTech deck unit used to trigger acoustic releases

Photo 16. 4/21/2021 Thermistor Chain buoys surface after acoustic releases are triggered

Photo 17. 4/21/2021 Recovery of Thermistor Chain

Photo 18. 4/21/2021 Transducer in the water used to trigger acoustic releases

Photo 19. 4/21/2021 NoiseSpotter buoys surface after acoustic releases are triggered

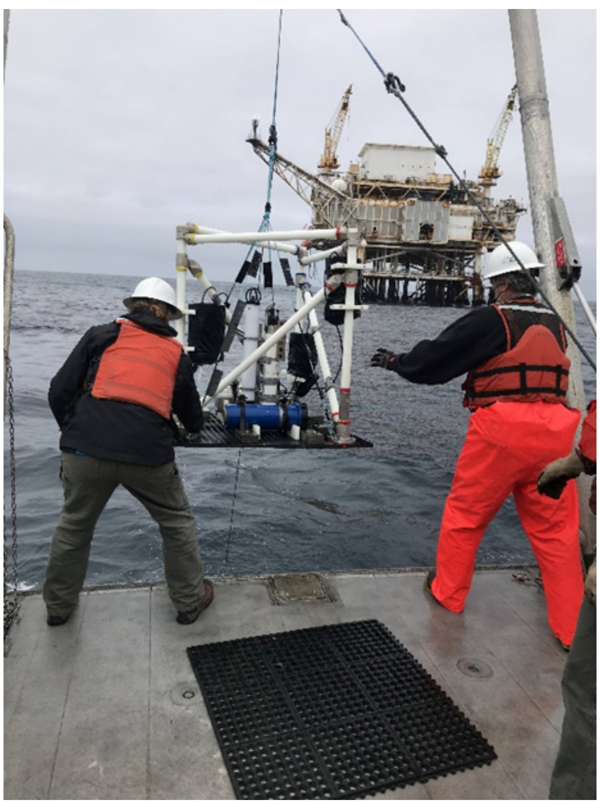

Photo 20. 4/21/2021 Recovery of the NoiseSpotter

Photo 21. 4/21/2021 Recovery of first hydrophone mooring

Photo 22. 4/21/2021 Recovered railroad wheel

Photo 23. 4/21/2021 Unloaded first railroad wheel from vessel

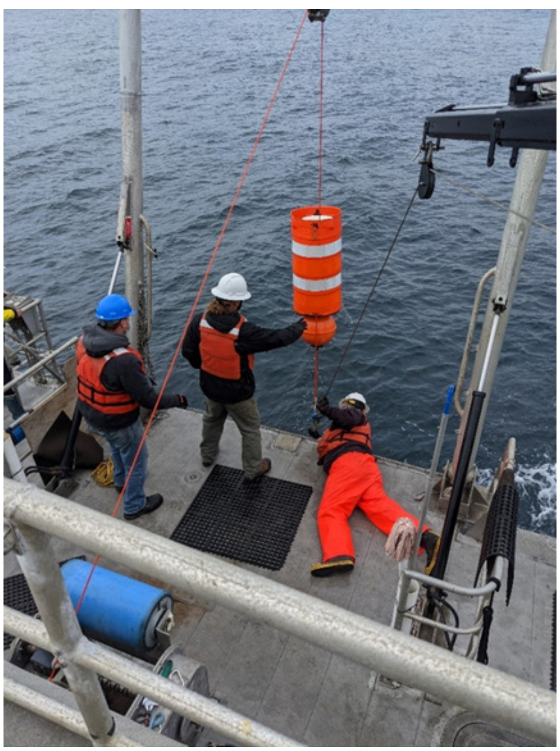

Photo 24. 4/22/2021 Recovery of hydrophone mooring (rope canister shown)

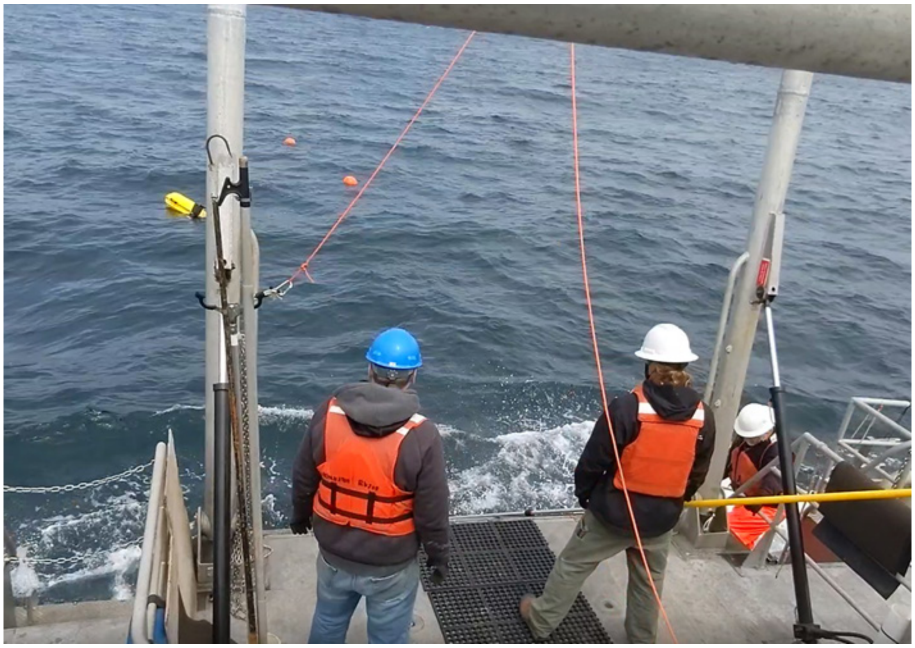

Photo 25. 4/22/2021 Hydrophone mooring buoys surface after acoustic releases are triggered (long mooring with mid-water and bottom hydrophones)

Photo 26. 4/22/2021 Recovery of hydrophone enclosure

Photo 27. 4/22/2021 Recovery of railroad wheel

Photo 28. 4/23/2021 Unloading of railroad wheels onto NOAA truck

Photo 29. 4/23/2021 Railroad wheels loaded on to truck

Photo 30. 4/23/2021 Rope canisters prepared for shipping

Photo 31. 4/23/2021 Buoys prepared for shipping

Photo 32. 4/23/2021 Hydrophone mooring equipment prepared for shipping

Appendix F: Hydrophone - Ocean Instruments Calibration Data

Contents

List of Figures

F.1 Hydrophone - Ocean Instruments Calibration

A critical component to any field program is ensuring that equipment is calibrated so that the measured outputs can be deemed reliable, in combination with the application of the appropriate settings and proper equipment usage. Please find below the calibration certificates from the six SoundTraps used in the study field program showing correct settings and proper usage procedures employed. The calibration certificates are from Ocean Instruments, the manufacturer of the SoundTrap units.

OceanInstruments NZ
Engineering Solutions For Marine Science

Calibration Test Results

Test	Date	17 Sep 2019
	Operator	JA
Device	Model	SoundTrap 300 HF
	Serial No	5353
Source	Model	Center 327
	Serial	130307390
	Frequency	250 Hz
	Coupler	OIC1
	Level	120 dB re. 1 μPa
Reference	Model	B&K 2236
	Serial	2015497
End-to-End Calibration	High Gain	**176.2 dB**
	Low Gain	**189.1 dB**
Calibration Tone	RTI Level @ 1kHz	**135.4 dB re. 1 μPa**

Figure 1. Hydrophone 5353 – Ocean Instruments Calibration

OceanInstruments NZ
Engineering Solutions For Marine Science

Calibration Test Results

Test	Date	17 Sep 2019
	Operator	JA
Device	Model	SoundTrap 300 HF
	Serial No	5356
Source	Model	Center 327
	Serial	130307390
	Frequency	250 Hz
	Coupler	OIC1
	Level	120 dB re. 1 μPa
Reference	Model	B&K 2236
	Serial	2015497
End-to-End Calibration	High Gain	**178.5 dB**
	Low Gain	**189.5 dB**
Calibration Tone	RTI Level @ 1kHz	**137.5 dB re. 1 μPa**

Figure 2. Hydrophone 5356 – Ocean Instruments Calibration

OceanInstruments NZ
Engineering Solutions For Marine Science

Calibration Test Results

Test	Date	17 Sep 2019
	Operator	JA
Device	Model	SoundTrap 300 HF
	Serial No	5362
Source	Model	Center 327
	Serial	130307390
	Frequency	250 Hz
	Coupler	OIC1
	Level	120 dB re. 1 μPa
Reference	Model	B&K 2236
	Serial	2015497
End-to-End Calibration	High Gain	**176.8 dB**
	Low Gain	**189.5 dB**
Calibration Tone	RTI Level @ 1kHz	**135.7 dB re. 1 μPa**

Figure 3. Hydrophone 5362 – Ocean Instruments Calibration

Calibration Test Results

Test	Date	17 Sep 2019
	Operator	JA
Device	Model	SoundTrap 300 HF
	Serial No	5363
Source	Model	Center 327
	Serial	130307390
	Frequency	250 Hz
	Coupler	OIC1
	Level	120 dB re. 1 µPa
Reference	Model	B&K 2236
	Serial	2015497
End-to-End Calibration	High Gain	**176 dB**
	Low Gain	**188.8 dB**
Calibration Tone	RTI Level @ 1kHz	**135.1 dB re. 1 µPa**

Figure 3. Hydrophone 5363 – Ocean Instruments Calibration

OceanInstruments NZ
Engineering Solutions For Marine Science

Calibration Test Results

Test	Date	17 Sep 2019
	Operator	JA
Device	Model	SoundTrap 300 HF
	Serial No	5365
Source	Model	Center 327
	Serial	130307390
	Frequency	250 Hz
	Coupler	OIC1
	Level	120 dB re. 1 μPa
Reference	Model	B&K 2236
	Serial	2015497
End-to-End Calibration	High Gain	**176.4 dB**
	Low Gain	**189.2 dB**
Calibration Tone	RTI Level @ 1kHz	**135.4 dB re. 1 μPa**

Figure 4. Hydrophone 5365 – Ocean Instruments Calibration

Calibration Test Results

Test	Date	17 Sep 2019
	Operator	JA
Device	Model	SoundTrap 300 HF
	Serial No	5366
Source	Model	Center 327
	Serial	130307390
	Frequency	250 Hz
	Coupler	OIC1
	Level	120 dB re. 1 μPa
Reference	Model	B&K 2236
	Serial	2015497
End-to-End Calibration	High Gain	**176.5 dB**
	Low Gain	**189.1 dB**
Calibration Tone	RTI Level @ 1kHz	**135.4 dB re. 1 μPa**

Figure 5. Hydrophone 5366 – Ocean Instruments Calibration

U.S. Department of the Interior (DOI)
DOI protects and manages the Nation's natural resources and cultural heritage; provides scientific and other information about those resources; and honors the Nation's trust responsibilities or special commitments to American Indians, Alaska Natives, and affiliated island communities.

Bureau of Ocean Energy Management (BOEM)
BOEM's mission is to manage development of U.S. Outer Continental Shelf energy and mineral resources in an environmentally and economically responsible way.

BOEM Environmental Studies Program
The mission of the Environmental Studies Program is to provide the information needed to predict, assess, and manage impacts from offshore energy and marine mineral exploration, development, and production activities on human, marine, and coastal environments. The proposal, selection, research, review, collaboration, production, and dissemination of each of BOEM's Environmental Studies follows the DOI Code of Scientific and Scholarly Conduct, in support of a culture of scientific and professional integrity, as set out in the DOI Departmental Manual (305 DM 3).